NSWC/WOL/TR 75-193

12

NSWC TECHNICAL REPORT

WHITE OAK LABORATORY

EMP DESIGN GUIDELINES FOR NAVAL SHIP SYSTEMS

BY
IIT RESEARCH INSTITUTE

22 AUGUST 1975

NAVAL SURFACE WEAPONS CENTER
WHITE OAK LABORATORY
SILVER SPRING, MARYLAND 20910

- Approved for public release; distribution unlimited.

NAVAL SURFACE WEAPONS CENTER
WHITE OAK, SILVER SPRING, MARYLAND 20910

DISCLAIMER NOTICE

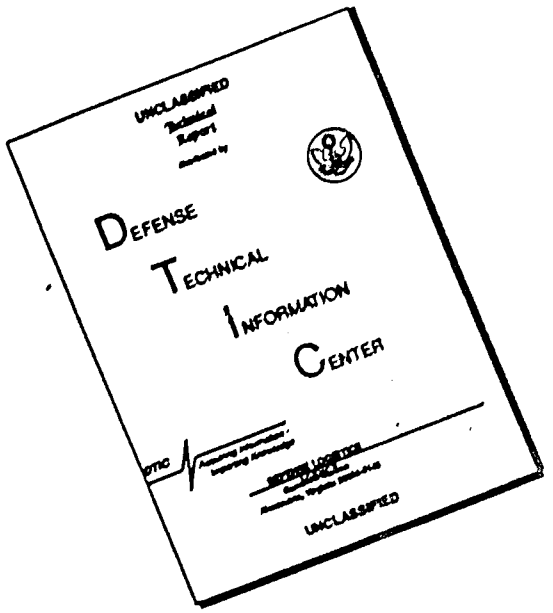

THIS DOCUMENT IS BEST QUALITY AVAILABLE. THE COPY FURNISHED TO DTIC CONTAINED A SIGNIFICANT NUMBER OF PAGES WHICH DO NOT REPRODUCE LEGIBLY.

UNCLASSIFIED
SECURITY CLASSIFICATION OF THIS PAGE (When Data Entered)

(19) REPORT DOCUMENTATION PAGE

READ INSTRUCTIONS BEFORE COMPLETING FORM

(18) 1. REPORT NUMBER: NSWC/WOL TR-75-193

2. GOVT ACCESSION NO.

(9) 3. RECIPIENT'S CATALOG NUMBER: Technical rept.

(6) TITLE (and Subtitle): EMP DESIGN GUIDELINES FOR NAVAL SHIP SYSTEMS.

5. TYPE OF REPORT & PERIOD COVERED

(14) 6. PERFORMING ORG. REPORT NUMBER: IITRI-E6299

7. AUTHOR(s): IIT Research Institute

(15) 8. CONTRACT OR GRANT NUMBER(s): N60921-74-C-0176

9. PERFORMING ORGANIZATION NAME AND ADDRESS:
IIT Research Institute
10 West 35th Street
Chicago, Illinois 60616

10. PROGRAM ELEMENT, PROJECT, TASK AREA & WORK UNIT NUMBERS: 62734N, F34384, ZF34384001, MAT03423020143

11. CONTROLLING OFFICE NAME AND ADDRESS:
Nuclear Weapons Effects Division
Naval Surface Weapons Center
Silver Spring, MD 20910

(11) 12. REPORT DATE: 22 Aug[illegible]75

13. NUMBER OF PAGES: 250

(10) 14. MONITORING AGENCY NAME & ADDRESS (if different from Controlling Office): Kenneth Haag, Yih Shiau, E. W. Weber, Mark Gagner, T. A. Martin

15. SECURITY CLASS. (of this report): UNCLASSIFIED

15a. DECLASSIFICATION/DOWNGRADING SCHEDULE

16. DISTRIBUTION STATEMENT (of this Report)

Approved for public release; distribution unlimited.

(12) 259p.

17. DISTRIBUTION STATEMENT (of the abstract entered in Block 20, if different from Report)

(16) ZF34-384, MAT-034-234/201-43

18. SUPPLEMENTARY NOTES

This work was sponsored by the Naval Surface Weapons Center under task area ZF34384001

(17) ZF34-384-001

19. KEY WORDS (Continue on reverse side if necessary and identify by block number)

Electromagnetic Pulse
HEMP
Hardening Guidelines
Ship Hardening
Electronics Protection
Nuclear Weapons Effects
Nuclear Warfare
Defense

20. ABSTRACT (Continue on reverse side if necessary and identify by block number)

This document presents a methodology which can be applied to hardening ships against a nuclear electromagnetic pulse (EMP). The problem is discussed, a basic protection philosophy is advanced and general requirements and criteria are presented. This is followed by a more detailed discussion of the collection and coupling of EMP energy via antennas, antenna-like structures, apertures, and cables. Then some protection devices are discussed, as well as good construction and installation practices. The applicability of such devices and practices is discussed for ships already in service as well as for those yet to be built.

DD FORM 1 JAN 73 1473 EDITION OF 1 NOV 65 IS OBSOLETE
S/N 0102-014-6601

UNCLASSIFIED
SECURITY CLASSIFICATION OF THIS PAGE (When Data Entered)

175 350

NSWC/WOL/TR 75-193 22 August 1975

EMP DESIGN GUIDELINES FOR NAVAL SHIP SYSTEMS

This document is the first issue of a handbook for incorporating EMP hardening in Navy ships. The material presented is addressed to the ship design community, and is intended to provide an awareness and appreciation of the EMP threat to Naval ships and to give design guidelines and techniques for the hardening of Navy ships to the effects of this threat. When applied to the hardening design of a given ship, these guidelines should be amplified in detail using the results of a continuing technology development program being conducted by the EMP Branch of the Nuclear Weapons Effects Division of the White Oak Laboratory of the Naval Surface Weapons Center.

The guidelines presented in this document were compiled for the Naval Surface Weapons Center by the ITT Research Institute (IITRI) under contract No. N60921-74-C-0176. IITRI staff members making substantial contributions to the preparation of this handbook include Dr. Kenneth Naag, Dr. Yih Shiau, Dr. E. W. Weber, Mark Gagner and T. A. Martin. Important suggestions and technical direction from NSWC were provided by Dr. Robert Haislmaier, Dr. John Malloy, William Emberson and Norman Taslitt, and from IITRI by J. Bridges, I. Mindell, and J. Krstansky.

Comments and suggestions regarding this document are solicited. They should be submitted to:

Commander
Naval Surface Weapons Center
Code WA-502, Rm. 130-108
Silver Spring, MD 20910

John H. Malloy
JOHN H. MALLOY
By direction

TABLE OF CONTENTS

CHAPTER 4

CHAPTER 5

CHAPTER 6

LIST OF FIGURES

LIST OF TABLES

CHAPTER 1

INTRODUCTION

1.1 Statement of Problem

Under the proper circumstances a portion of the energy released during a nuclear detonation can appear as an Electro Magnetic Pulse (hence, EMP) having the same frequencies or wavelengths as those employed by most commercial radio and military system equipments.

Two unique properties of EMP are of crucial significance. Because of its extremely great "damage range", EMP is capable of disabling electrical and electronic systems as far as 2000 miles from the site of the detonation. Thus EMP can cause severe disruption and sometimes damage when other prompt weapon effects such as nuclear radiation effects on electronics, blast, thermal effects, dust, debris and biological effects are all absent. This means that a high-yield nuclear weapon burst above the atmosphere could be used to knock out inadequately designed electrical and electronic systems over a large area of the earth's surface without doing any other significant damage. The second significant property is that the "monopulse transient" nature of the EMP signal is indicative of the spread of EMP energy throughout a broad frequency band. This means that nearly any of the known mechanisms or modes for coupling EMP signals into electrical/electronic equipment will be excited, whether it be an antenna, a cable, an aperture, water pipe, or what have you.

EMP has been recognized as a potential threat to electronic and electrical systems since about 1960. From the Navy's standpoint, a proliferation of factors has greatly increased the significance of this threat:

1. The increasing dependence on electronics in the design of operational and mission critical systems utilized on the Navy ships of today, and

2. The increasing demand and subsequent utilization of miniaturized electronic components (e.g. semiconductor devices) to implement these system designs.

The use of semiconductor or solid-state devices provides the desired advantage of reduced size, space, weight and power requirements which are all highly desirable from the ship designer's point of view. Unfortunately, these devices are also among the most susceptible electronic components to damage by EMP.

The spectrum and waveform of EMP differ from those of any other natural or commonly used man-made sources. The spectrum is broad and extends from extremely low frequencies into the UHF band. The time waveform indicates a higher amplitude and much faster rise time than, for example, the fields generated by a nearby lightning stroke. Since EMP is sufficiently different from any other electromagnetic environment usually encountered, it follows that protection practices and components for non-EMP environments--radio-frequency interference, lightning, radar, etc., will not provide adequate protection against the EMP threat.

This manual provides guidelines and design practices to maximize protection of electrical equipment and systems on ships against the EMP threat. Chapters 1 and 2 discuss the problem from an awareness point of view. The generation of the energy, the collection of the energy, effects on equipment and devices, and basic protection concepts are included in these chapters. Specific design information related to device and system protection for new systems is presented in Chapters 3, 4 and 5. Chapter 6 discusses specific procedures which may be used to improve EMP protection in installed systems.

1.2 EMP Generation and Propagation

When a nuclear device is detonated in the upper atmosphere, gamma rays radiate outward from the point of burst (see Figure 1.1). The gamma rays interact with air molecules in the gamma absorption layer (20-40 km altitude) to produce Compton electrons which initially travel toward the earth's surface. However, they are deflected by the earth's magnetic field causing electromagnetic energy to be radiated towards the surface of the earth.

Compton electrons that move parallel to the geomagnetic field are not deflected, thus, the EMP amplitude is small in two directions along the geomagnetic field line passing through the burst point. The EMP amplitude is a maximum on those rays from the burst point which run perpendicular to the geomagnetic field in the source region. Since the location of enemy bursts relative to the location of Naval vessels cannot be predicted, one should EMP-harden to this maximum environment condition.

Owing to the great height of the source region above the earth's surface in the case of an exoatmospheric burst, the radiated EMP appears over a substantial portion of the earth's surface. Figures 1.2 and 1.3 illustrate the relation between height of burst and EMP coverage of the earth's surface. For example, the distance from a burst point 400 kilometers above the earth's surface to the horizon is 2,250 kilometers or 1,400 miles. Hence, the EMP radiated from such a high-altitude burst will illuminate more than five million square miles of the earth's surface. (Compare this with the three million square mile area of the continental U. S.). This points up one very significant aspect of the EMP protection problem for Navy ships. Since a high altitude burst can occur anywhere about the globe and Naval systems have a world wide distribution, no specific deployment or fleet distribution is relevant when considering the EMP hardening requirements for Naval systems in general.

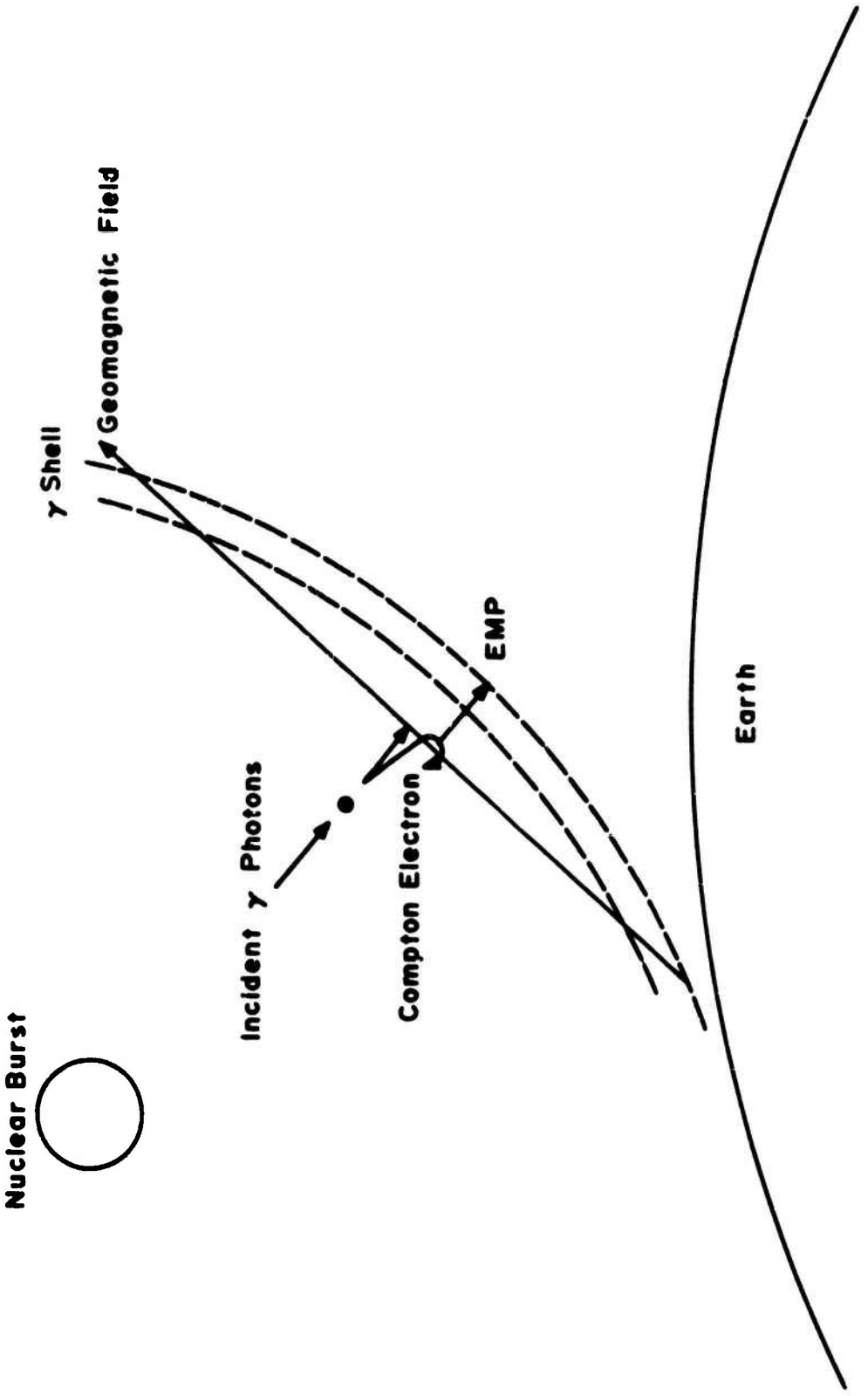

Fig. 1.1 ILLUSTRATION OF EMP GENERATION

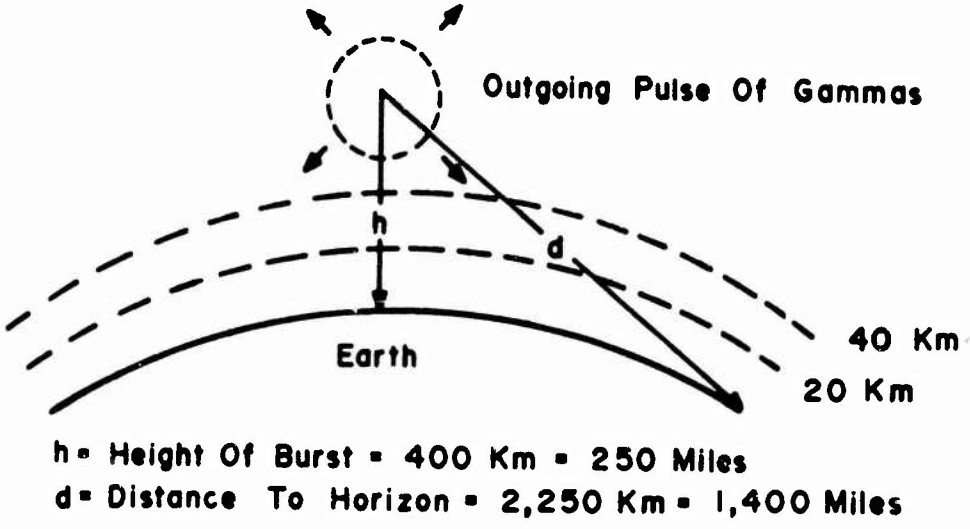

Fig. 1.2 GEOMETRY FOR EMP FROM HIGH-ALTITUDE BURST

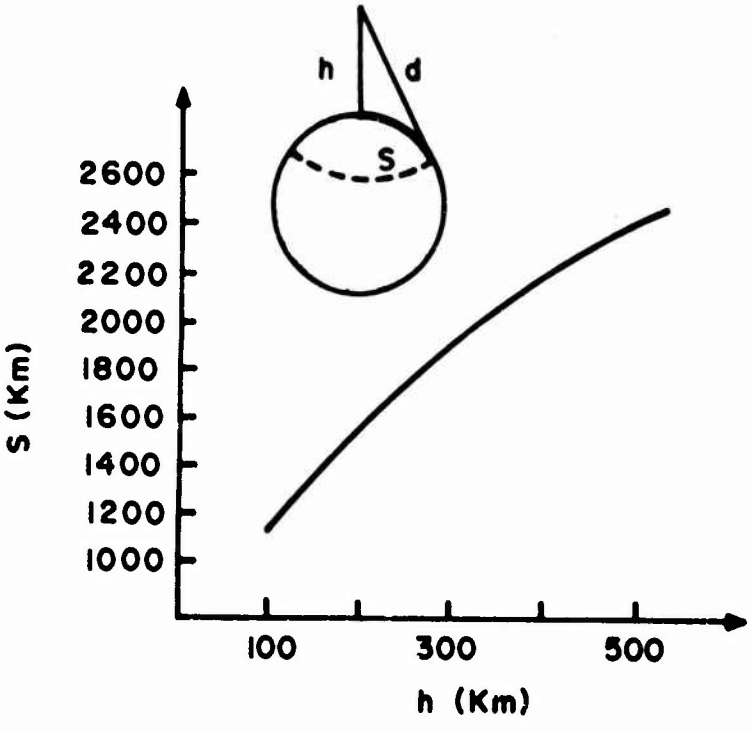

Fig. 1.3 TANGENT RADIUS FOR A HIGH-ALTITUDE BURST

1.3 EMP Waveshape

The far field characteristics of the radiated EMP produced by a single high altitude detonation can have considerable variation in amplitude, waveshape, and propagation characteristics depending upon the weapon yield, the location of the observer, the height of the burst and the orientation of the earth's magnetic field relative to the burst point. One can, however, define a field environment which will not be exceeded by a significant amount, nor is it much greater than the average field environment that Naval ships can be expected to encounter, i.e., it is close to the maximum EMP-environment condition without being too far from the average.

This composite EMP field environment is shown in Figure 1.4 in terms of the incident electric field strength at the surface of the earth. In free space, the EMP field propagates as a plane wave. Therefore, the ratio of the electric and magnetic field strength is a constant (i.e., 377Ω), and orientation or polarization of the EMP field can vary depending on the geographic locations of the burst point relative to the point of observation.

Although the EMP field depicted in Figure 1.4 does not characterize any actual EMP waveform produced by an exoatmospheric nuclear burst, it is nevertheless an extremely useful representation for approximating or estimating EMP effects by analysis. As such it is the characterization that is used throughout this document where analysis is employed to develop specific design guidelines. **For analysis and hardening of Navy platforms and systems, the reader is advised to obtain EMP waveforms from the Nuclear Program Office of the Naval Surface Weapons Center, Silver Spring, Maryland 20910.**

To facilitate the analysis of coupling and/or penetration of the incident EMP on Naval ships it is convenient to represent the waveform given in Figure 1.4 by

$$E(t) = \frac{E_o}{b} \left(e^{-\alpha t} - e^{-\beta t}\right) \qquad (1.1)$$

where:[1, 2]

t = time in seconds

$\alpha = 1.5 \times 10^6 \text{ sec}^{-1}$

$\beta = 2.6 \times 10^8 \text{ sec}^{-1}$

$E_{max}(t) = E(t_1) = E_o = 50{,}000$ volts/meter

t_1 = time to peak or maximum value

b = normalizing factor $= e^{-\alpha t_1} - e^{-\beta t_1}$

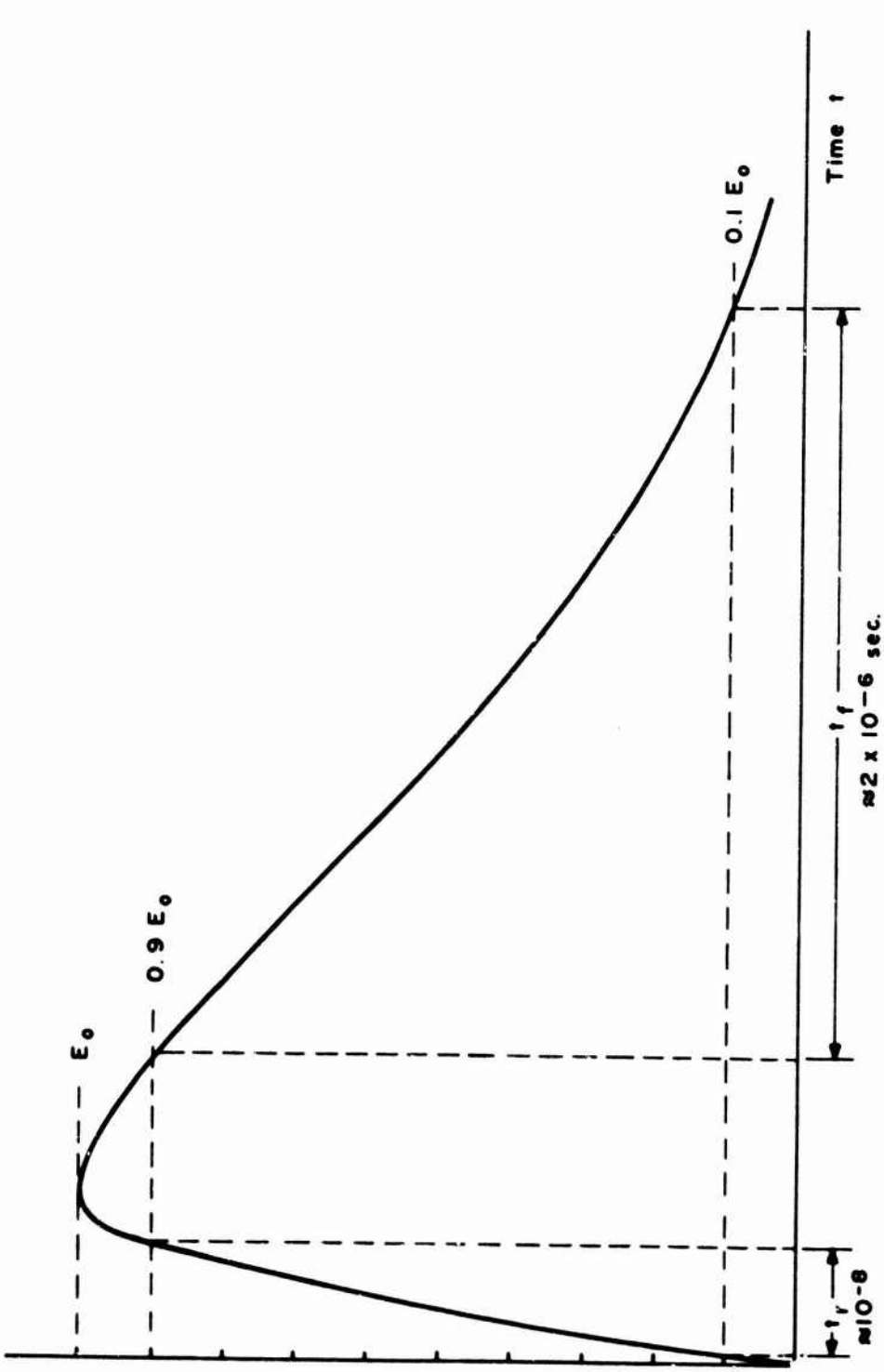

Fig. 1.4 REPRESENTATIVE EMP WAVEFORM FOR HIGH-ALTITUDE BURST (ELECTRIC FIELD)

and the magnetic field intensity is given as

$$H(t) = \frac{E(t)}{\eta_o} \quad \text{(amps/meter)} \tag{1.2}$$

where η_o is the intrinsic impedance (377Ω) of free space.

It is to be noted in this expression that the rise time t_r of the EMP pulse is on the order of 10 ns and the fall time t_f is about 2 μsec (See Figure 1.4).

The EMP amplitude spectrum covers an extremely broad frequency range extending from very low to microwave frequencies. The rate of attenuation of the amplitude spectrum is shown in the plot of Figure 1.5 where the break frequencies are determined by the time constants of the EMP waveform given in Equation (1.1). This plot is obtained from the log-magnitude of the Fourier transform expression for Equation (1.1) which is given by:

$$20 \log |E(j\omega)| = 20 \log \frac{E_o}{b} \left| \frac{(\beta - \alpha)}{(j\omega + \alpha)(j\omega + \beta)} \right| \tag{1.3}$$

$$= 20 \log \frac{E_o (\beta - \alpha)}{b\sqrt{(\omega^2 + \alpha^2)(\omega^2 + \beta^2)}}$$

where

$\omega = 2\pi f$

f = frequency in Hz

It is important to note that the spectrum obtained is almost constant below the MF range. From an equipment standpoint, this means that EMP is difficult to filter and can couple into electronic circuitry over a wide range of frequencies.

1.4 Basic Protection Philosophy

The first and basic principle in the EMP protection of ships is to keep the EMP environment outside the areas or regions containing susceptible electronic/electrical equipments. This requires that these sensitive interior areas be electromagnetically isolated or insulated from the external EMP environment. Techniques for accomplishing this include shielding, the control and/or suppression of field penetrations through this shielding, the control and/or suppression of conducted EMP energy into interior regions, and, where possible, the utilization of less susceptible electronic/electrical equipments.

1.4.1 Environment Reduction (Shielding)

The ideal structure from a shielding standpoint would be a thick walled, highly conductive sphere with no seams, apertures, or cable entries. However, a structure which is intended to serve a useful purpose will require the following variations from the ideal case.

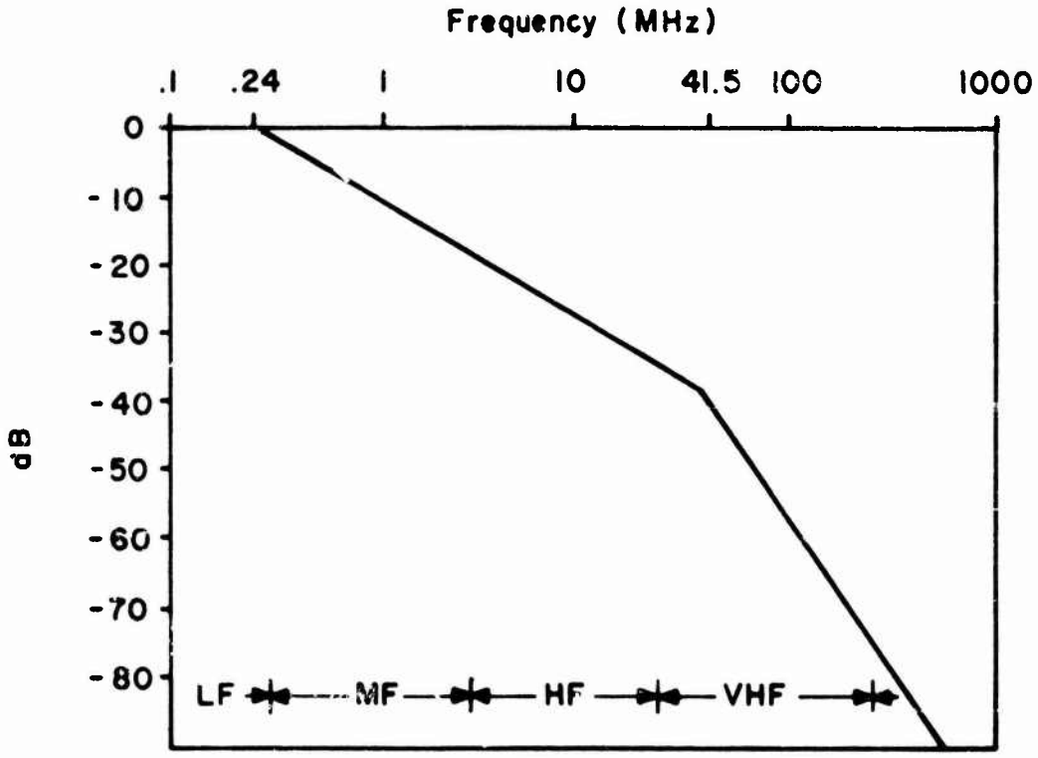

Fig. 1.5 FREQUENCY SPECTRUM OF EMP PULSE

- The shape is influenced by nonelectrical aspects of its use. For example, a ship is designed based on hydrodynamic principles and mission designation.

- Construction must be reasonably economical which usually dictates the thickness and type of material used as well as the need for seams.

- Apertures and doors must be included to provide access to the interior.

- Heating, cooling and ventilation are usually required.

- Any electrical equipment requires cable entries for power and signal transmissions.

The variations from the ideal shielding practice are illustrated in Figure 1.6. Except for the fact that larger dimensions are involved, the shielding problems encountered on a ship are the same as those shown in this figure.

Shielding of interior circuits is provided by the ship's hull and superstructure, by cable shields covering wires connected to the circuits, by compartments internal to the hull and by shielded equipment cabinets enclosing the circuits. The hull and internal compartment shielding integrity is degraded by cable entries, antennas and other apertures. Aperture penetrations can be controlled by the use of waveguides below cutoff (for small holes) and conductive coatings and wire mesh over larger apertures and other dielectric surfaces. Doors, hatches and panels can be sealed with conductive gaskets and spring fingers. Joints and seams in the hull and internal compartments can be controlled by good bonding practices.

Cables can be shielded by flexible braid or by solid conduit. In both cases, connectors used on the cables should maintain shielding integrity by the use of spring fingers and r-f gaskets to circumferentially enclose the shield.

Sensitive electronic circuits are often enclosed in shielded cabinets or enclosures. The seams, joints, vents and access doors in these equipment enclosures should be controlled in the same way as for the ship's hull.

1.4.2 Collection Efficiency Reduction

In addition to direct penetration through shield enclosures, energy may be transmitted to internal areas via conduction on cables and cable shields. Minimizing the conducted energy requires minimization of the collection efficiency. Antennas should be designed to operate in as narrow a frequency band as possible consistent with the requirements of the equipment which is connected to the antennas. Cables which are run above the ship's deck should be routed within solid conduit and/or inside the superstructure to provide additional shielding and hence lessen direct exposure to EMP energy.

Internal cable runs should be routed in a manner which avoids the formation of loops. This requires a single ground point system within any compartment to minimize ground loops.

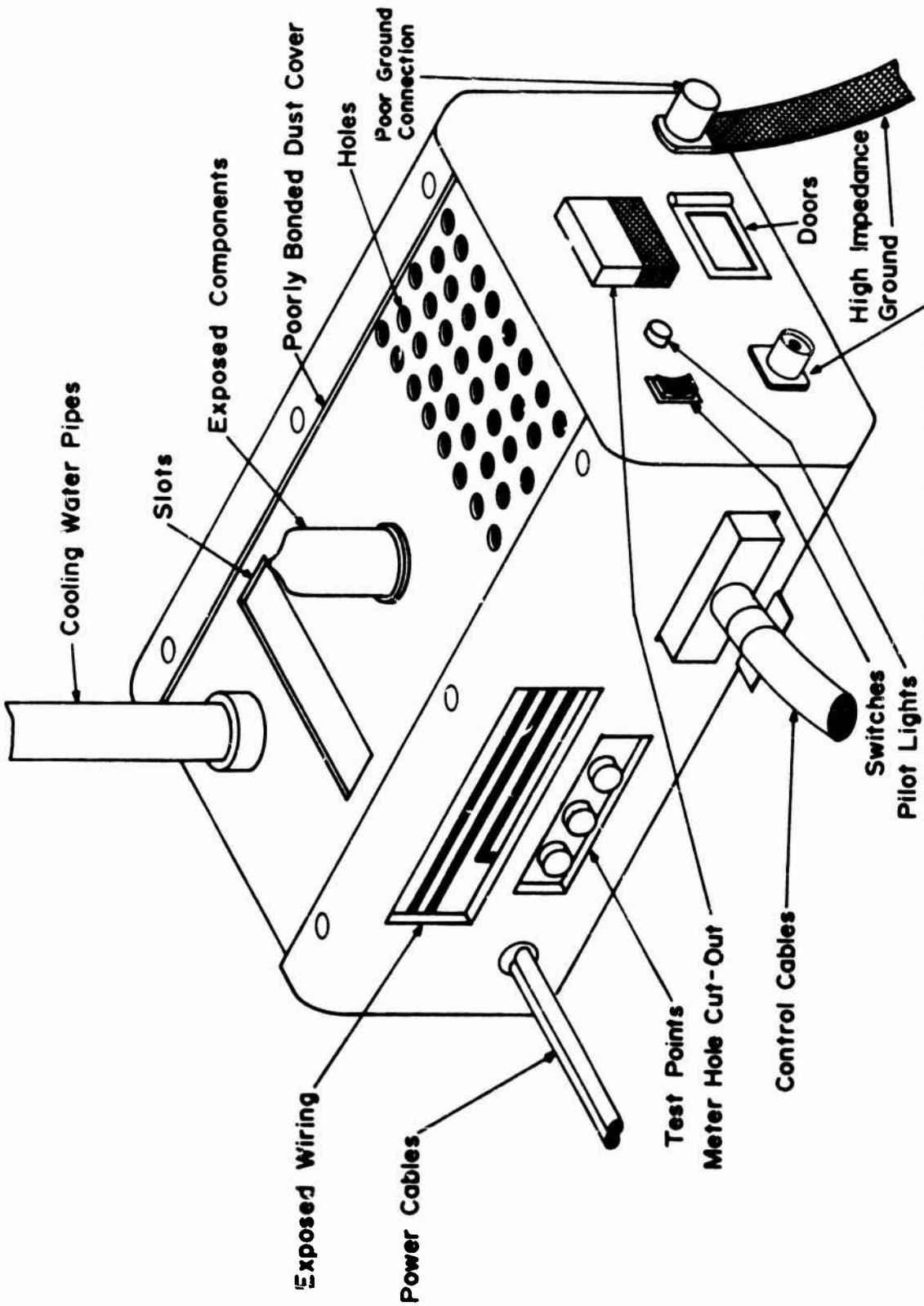

Fig. 1.6 TYPICAL SHIELDING DESIGN PROBLEMS

1.4.3 Circuit Protection Techniques

The main line of defense against EMP energy is provided by shielding and the minimization of collection efficiency. However, it must be recognized that neither of these procedures can be perfect in practice and, therefore, some energy will appear on conductors which are connected to electrical equipment. This energy can result in a disruption of the normal circuit function (transient upset) or may cause permanent damage to components in the equipment.

There are basically three methods which may be employed to reduce the effects caused by transient energy which appears on conductors.

- Reject or dissipate a portion of the energy by inserting filters and/or amplitude limiters between the conductors carrying the energy and the equipment to be protected.

- Choose components which have larger energy damage thresholds. Also, design circuits such that the sensitivity and response time does not exceed the functional requirement of the system.

- Provide a capability for the temporary interuption of information and/or signal processing when an EMP event has occured. This will require prior information regarding the EMP event either by event sensing or early warning devices.

The decision to apply these procedures to a particular piece of equipment, individually or in combination, is based on the characteristics of the expected energy surge (energy level and duration) and on the role which this equipment plays in the success of the mission.

REFERENCES

1. EMP Protection for Emergency Operating Centers, Defense Civil Preparedness Agency, TR-61A, May 1971.

2. DNA EMP Awareness Course Notes, Second Edition, DASA01-69-C-0095, IIT Research Institue, Chicago, Illinois, August 1973.

CHAPTER 2

GENERAL REQUIREMENTS

2.1 System Protection Requirements

EMP protection must be considered from a total system standpoint with completion of the military mission as the primary goal. Determining what to protect involves the classification of equipment and systems according to their mission function and their capability to withstand energy surges. Precise protection methodologies will depend on many factors which include but are not limited to the following:

- expected threat conditions
- reduction of exposure (external cables)
- reduction of penetration (shielding practices)
- reduction of cable interaction (cable run plan)
- reduction of coupling in internal regions (ground plan)
- placement of critical equipment in internal regions which provide greatest natural shielding
- equipment interaction under energy surge conditions
- methods for improving the ability of electronic equipment to withstand energy surges.

The above list is not intended to be all inclusive, but rather to draw attention to the major areas of consideration. Due to the large energy and broad frequency spectrum associated with EMP, protection requirements cannot be met by considering any one item above exclusively. The allocation of protection afforded by each procedure must be determined early in the program for proper cost effectiveness.

2.2 System Hardening Allocation

A systematic approach to the EMP protection problem provides early identification of electrical systems which required special attention. The determination of potentially vulnerable systems is based on the susceptibility of the components or equipments employed in the system and the expected exposure of the system to EMP energy.

The ranking of systems in terms of their susceptibility to EMP energy requires a knowledge of specific equipment to determine its functional type (digital or analog), major subsystems and interfaces, and the fabrication technology (vacuum tube, transistor or integrated circuit). A general guideline for the ranking of Naval systems with respect to their susceptibility to EMP is given in Table 2.1. The less susceptible equipment or components included in the table would be made more susceptible if they were connected to long exposed cable runs, such as intersystem wiring or exposed power or telephone cables.

A second consideration involved in the decision to apply special protection procedures to specific systems is their relative degree of exposure to EMP energy. This is established by the location or distribution and interconnection of systems as determined in the conceptual design phase of development.

In general, systems which are housed in compartments which have no penetrations by cables or other conductors that have been exposed to the EMP and are well below deck would be ranked low in terms of exposure. A high exposure ranking would be given to systems located in the superstructure, particularly if the compartment has large apertures such as windows. Specific information on exposure is available from the Naval Surface Weapons Center (NSWC). This information is obtained from a continuing test program using the EMP Radiation Environment System Simulator (EMPRESS) facility which is located at Solomons Island, Maryland. Monitoring of currents and voltages on cables and field strengths in compartments of a ship which are subjected to the simulated EMP provides an exposure level mapping which is indicative of the threats which will be experienced within ships of similar construction and geometry.

The final criteria for application of protection is the mission criticality of each system. The ranking of most important versus expendable is a value judgment depending on the tactician's view. As an example, the voice communication system may not be vital whereas the Navy Tactical Data System would receive a high criticality rating.

The collection of criteria for additional protection may be presented in tabular form as illustrated in Table 2.2. In this table, both centers and systems are listed to provide a crosscheck and to take into account the fact that some systems can be part of more than one center. A low mission criticality ranking will generally eliminate a center or system from further hardening considerations. However, if EMP exposure is high, the possibility of this system providing energy flow paths to more critical systems must be considered.

A table of this type reveals the specific EMP problem which may exist and, therefore, the most direct corrective measure which may be taken, i.e., high exposure indicates the need for additional shielding while high sensitivity can be lowered using protective devices. In some cases, a potential problem caused by high exposure can be corrected by a simple relocation of equipment if the problem is recognized early enough in the design stage and the relocation does not interfere with construction or tactical requirements.

After deciding which systems need special EMP hardening attention, additional analysis is used to determine the level of protection that is required and the specific procedures which will provide the necessary reduction in energy levels.

Table 2.1

Systems Susceptibility Ranking

Most Susceptible:

Low power, high speed digital computer (upset) either transistorized or vacuum tube

Systems employing transistor or semiconductor rectifiers (either silicon or selenium), such as:

- computers
- transistorized power supplies
- alarm and intercom systems
- life-support system controls
- some telephone equipment which is partially transistorized
- transistorized receivers and transmitters
- transistorized 60 to 400 Hz converters
- transistorized process control systems
- power system controls

Less Susceptible:

All vacuum tube equipment (does not include equipment with semiconductor or selenium rectifiers)

- transmitters
- receivers
- alarm systems
- intercoms
- teletype-telephone
- power supplies

Equipment employing low current switches, relays, meters

- alarms
- life-support systems
- power system controls
- panel indicators
- status boards
- process controls

Hazardous equipment containing

- detonators
- squibs
- explosive mixtures
- rocket fuels

Long power cable runs employing dielectric insulation; equipment associated with high energy storage capacitors or inductors

Least Susceptible:

High-voltage 60 Hz equipment

- transformers
- heavy duty relays
- heaters
- rotary converters
- motors
- lamps
- circuit breakers
- air insulated power cable runs

Table 2.2

Centers and Systems Ranking

	Mission Criticality			EMP Exposure			Sensitivity Ranking		
Centers	High	Medium	Low	High	Medium	Low	High	Medium	Low
Combat Information Center	X					X		X	
Communication Control Center	X				X		X		
etc.									
Systems									
Naval Tactical Data System	X				X		X		
Remote Information Displays		X			X				X

NOTE: Rankings presented in this table are for illustrative purposes only.

2.3 Allowable Degradation

The allowable degradation which may occur in a particular piece of equipment is dependent on the role which that equipment plays in the success of the mission. There are two types of degradation--functional damage and transient operational upset. Functional damage results when the energy content of the EMP transient causes a permanent change in the electrical characteristics of devices or components in the equipment. Operational upset results when the system processes the EMP transient as a normal information signal and produces an erroneous output.

Functional damage is manifested in two forms--parametric change and catastrophic failure. Parametric change refers to changes in the value of resistors, beta or leakage current of transistors, etc., This alteration of parameter value may result in a change in circuit performance. The acceptable level of circuit performance places limits on the allowed change in parameter values. Relating the change in parameter value to the energy contained in the EMP transient by analytical or empirical methods results in a tolerable energy threshold. The establishment of this threshold must include provision for multiple transients as indicated by the threat scenario since the effects of more than one energy surge may be cumulative. When a catastrophic failure occurs, such as a short circuit or open circuit in a component or device, the equipment can no longer function. Failures of this type are also relatable to energy thresholds and cannot be tolerated in mission critical equipment.

Determination of systems whose functions can tolerate operational upset requires an assessment of the equipment in terms of its operational and performance characteristics. This assessment can be done on the basis of response time or update time. For example, consider analog equipment such as an interphone. Typically, the system output is aural, and the system contains no memory. A transient will upset this system, at most, for a time of the same duration as that required for equipment startup after a momentary power dropout. Normal operation will result within milliseconds after transient decay, so that no more than a syllable or two of a verbal message will be lost. Similarly, a single erroneous status update by a digital system used only to drive an instrument display at a low sample rate would entail no serious consequences, since human reaction time will tend to filter incorrect system responses. Upset in either of these systems will not cause adverse system reaction so that neither system has critical functions susceptible to EMP-induced upset.

Redundancy, memory and discrimination may also be used as criteria for evaluating the upset tolerance of systems. For example, consider a subsystem which interfaces with man. In this case, permanent errors, such as isolated language errors in the output of a teleprinter, have little chance of upsetting the meaning of the total text. The same type of error in non-redundant numerical codes could be the cause for upset of critical functions.

When considering time requirements for update of system output, particular attention must be given to stationary nondiscriminatory loads such as electroexplosive devices, ejector solenoids, and other one-shot devices. Many of these devices have operation times which are much shorter than normal update periods.

The case of reset or reload must be considered when screening for upset. If operation and configuration permit equipment to be reset or reloaded as in the case

of a memory scramble, and if it can be shown that the transient perturbation (causing the scramble) produces no concomitant hazardous or catastrophic event, then upset is not a problem and further analysis of the problem is not necessary. However, if a circuit malfunction can cause interference with a mission critical function, then upset is a problem and circuit analysis must be initiated to identify sensitive devices and to analyze their package interface threshold and voltage/current characteristics.

2.4 Equipment Degradation Thresholds

A potential EMP problem can be identified as follows: The energy collected by a particular structure is compared with the minimum energy to damage or upset the components and circuits in question. If the energy collected exceeds the minimum energy required for damage or upset, then a potential problem has been identified.

Devices which may be susceptible to functional damage due to electrical transients are:

1. Active electronic devices (especially high frequency transistors, integrated circuits, and microwave diodes).

2. Passive electrical and electronic components (especially those of very low power or voltage ratings or precision components).

3. Semiconductor diodes and silicon controlled rectifiers (especially those used in power supplies connected to long cable runs).

4. Squibs, detonators, and pyrotechnical devices.

5. Meters, indicators, or relays.

6. Insulated RF and power cables (especially those running near maximum ratings and which are exposed to humidity or abrasion).

Devices or systems which may be susceptible to operational upset due to electrical transients are:

1. Low-power or high-speed digital processing systems.

2. Memory units.

3. Protection or control systems for the distribution of 60 or 400 Hz power.

4. Subsystems employing long integration or recylcing times for synchronization acquisition or signal processing.

Degradation thresholds may be determined analytically or empirically. In order to reduce the scope of the analytical problem, several assumptions are generally made in the analysis. Among these are:

1. Semiconductors are frequenctly more susceptible to damage from a transient pulse than other components, and often are considered to be the only susceptible component.

2. When experimental degradation data are not available, extrapolation of data according to theoretical models can be made.

3. Although a representative waveform is generally used in susceptibility analyses, data bases obtained from square pulses are assumed to be adequate; particularly if the energy content of both is the same.

4. Nonlinear responses such as arcing or leakage are neglected.

5. Synergistic effects are not considered.

The impact of these assumptions upon the accuracy of a given system degradation assessment will vary depending upon the particular system.

The major advantages associated with an analytical approach are:

1. It can be performed early in the program before the circuits and systems are constructed.

2. The exact form of the expected incident voltage or current waveform can be used.

3. Circuits or systems which are found to have low energy failure thresholds may be modified "on paper" and reanalyzed with minimal time and effort.

4. It reduces the empirical testing required by catagorizing those circuits and systems which have borderline failure thresholds.

The major pitfalls in the analytical approach are related to the assumptions that nonlinear responses are known and can be adequately modeled or can be ignored. For devices, reasonable nonlinear models are usually available. However, other nonlinear responses such as would be caused by corrosive interfaces are difficult to predict and to model. In addition, there is the possibility of overlooking energy flow paths in the modeling of complex systems. For these reasons, a testing program should be included in the determination of degradation thresholds. However, the greatest emphasis in the empirical work will be on the circuits and systems which have borderline failure thresholds. Those systems which are predicted to have a wide margin between incident energy and failure threshold should be spot checked experimentally to verify the analytical results.

2.5 Zoning

The protection requirements for a piece of equipment, a subsystem or a system are dependent on its failure threshold, allowable degradation and expected threat level. A systematic approach to providing the necessary protection levels involves the concept of zoning.

Considerations of EM zones within a system nearly always appear overtly in terms of shielding effectiveness. Zone boundaries are generally constrained to coincide with major geometric or structural contours, or with intentionally introduced shields or shielding exclosures. Thus, it is usually the case that zoning considerations do not appear explicitly in an EMP systems analysis. However, there are system cases in which the EM geometries are so intricate that elementary shielding considerations are obviously inadequate. It is then essential to perform a meticulous mapping of the EM zones.

EM zones may be defined in two general ways:

1. Environmental zoning, in which the magnitude and shape of the field pulse is defined within the successive regions from outside progressing inward.

2. Suceptibility zoning, in which the magnitudes and frequency (or time) domains corresponding to the vulnerability thresholds are scaled from inside progressing outward.

In a "good" system, zone boundaries appear as (more-or-less) concentric contours and there is a reasonable coincidence between environmental and susceptibility zones.

Required attenuation of fields in one area is dependent on the whole system shielding plan; for example, the protection provided by the hull determines how well compartments and cables must be shielded. Alternatively, the attainable cable and compartment shielding determines the protection level required from the hull. Overall protection requirements are based on the electronic circuit sensitivity.

All subsystems with similar failure thresholds in the overall system must be shielded to protect against the same external field level. It does no good to harden one subsystem to peak external field of 10^6 V/m, while another subsystem will fail at 10^5 V/m. Also, a subsystem which is not essential to mission completion need not be hardened, however, it is necessary that the subsystem not provide a path for energy to couple into systems which are essential to mission completion.

A system should not be overhardened; i.e., hardened to levels much higher than is required to survive since unnecessary penalties in cost and weight can result. However, it is reasonable to provide some margin of safety. Considering the variations in actual characteristics, in ambient environment, and the uncertainties in manufacture and construction, a margin of safety in the range of 10 to 20 dB is frequently used.

The design and analysis techniques which are used to determine and implement required protection levels are presented in the following chapters of this manual.

2.6 Electromagnetic and Radio Frequency Interference Specifications and Standards

The specifications and operation of all systems and pieces of equipment used on naval ships must meed the applicable standards such as MIL-STD-461/462, and

MIL-STD-1310C(NAVY). However, meeting these standards does not, in itself, guarantee hardening to EMP effects. Radio frequency interference specifications generally fall into two categories, inter- and intra-system specifications and requirements. The inter-system requirements generally have no EMP significance, since these requirements are generally concerned with obtaining data for modeling the low level responses, generally in-band, of equipments for spectrum allocation purposes.

Intra-system requirements are more applicable to equipment EMP protection. These include NACSEM (TEMPEST), lightning, HERO (Hazards of Electromagnetic Radiation to Ordnance), hull noise suppression, and electrical safety. These procedures or requirements will be separately discussed as follows.

2.6.1 Lightning

Protective measures, particularly terminal hardening surge arrestors, as usually applied for lightning protection will provide some unknown measure of EMP protection. The lightning hardening procedures in general, involve identifying the points of likely strikes, either reinforcing the metal to withstand the heavy current and stress effects associated with the stroke or installing a lightning rod and ground and applying heavy duty surge arrestor protection on the cables which are likely to intercept significant fractions of the lightning stroke current. The principal problem arises because of differences in the waveforms of the induced EMP currents with those caused by lightning stroke. The lightning stroke currents have a much slower rise time, a much longer duration, and often a higher energy and coulomb content. Therefore, lightning arrestors are far more robust but do not have the short reaction time required to suppress typical EMP induced transients. Off-the-shelf surge arrestors which can suppress both lightning and EMP surges do not provide sufficient EMP protection for transistorized transceivers. Special hybrid combinations must be devised and specially tailored for each system at hand. Low frequency shielding is frequently employed to protect the more sensitive subsystems and this provides some EMP hardening benefits.

2.6.2 Radio Frequency Interference

In order to control the intra-system compatibility from a radio frequency interference standpoint and emissions from subsystems, two sets of standards and associated laboratory tests are generally implemented. These are MIL-STD-461/462, which consider both emissions and susceptibility of electrical and electronic subsystems, and the NACSEM series, which are designed to assure the control and/or suppression of emissions from secure communications equipment. In general, the various subsystems, drawers, or cabinets are subjected to a series of laboratory tests which measure both the low-level emissions and susceptibilities. Typical exposure limits, however, do not result in injected voltages exceeding 100 volts. The peak powers employed for susceptibility tests are generally below the 100 watt level.

Any concomitant EMP hardening which permits equipment to pass these RFI/NACSEM tests, is primarily dependent on filtering and shielding. In this regard, these tests have the following EMP weaknesses.

- Due to the relatively low signal levels employed in the tests, the inband susceptibility (antenna, front ends, cable terminals) to EMP is not affected by any of the procedures or requirements.

- The ability to withstand energy surges is not determined (specifically with respect to antenna and front end filters and cable terminals).

- The required level of shielding on exposed (topside) cables is not specified.

- A single point ground system within cabinets is encouraged. However, the complete system grounding plan is not considered.

Ordnance pyrotechnical devices, including detonators, exploding bridge wires and squibs, are subject to premature detonation or dudding by the application of unwanted radio frequency energy. Typical controls to assure that this does not occur are embodied in such documents as NAVWEPS-0D030393 and MIL-STD-1385. The procedures generally involve the application of special construction techniques and a design guide in order to meet subsystem and system test exposures to specified field levels. The applicable EMP hardening benefits consists of shielding and filtering, with a possibility of special disconnects, and arming and safety coding systems.

2.6.3 Electrification Safety and Hull Noise

Another problem arises from electrification of portions of the ships superstructure or nearby metallic service equipment such as cranes, hoses, stanchions, life-nets, etc. These pose potential shock hazards to personnel. In addition, the transmitter return currents which flow through the hull may pass through metal-oxide-air interfaces which, in effect, form an electrical nonlinear junction. These nonlinearities convert some of the energy at the fundamental frequency into radio frequency interference appearing in other bands. Control measures to alleviate these problem areas are embodied, for example, in MIL-STD-1310C. In general, these impose constructional requirements or guides to minimize the generation of hull noise or eliminate potential shock hazards.

The principal benefits from an EMP hardening viewpoint is the routing of normally exposed topside cables either within the hull or within a shielded conduit, if topside. The principal EMP deficiency is that EMP induced current can still penetrate into the interior of the hull via the cable shields or armor penetrating from the outside into the interior of a ship or superstructure. While ground straps between the cable shields or armor and the hull may be employed at these penetration points, the length of the ground straps and their constructional features may introduce excessive lead inductance in a grounding circuit, thereby negating the transient suppression. This leads to introduction of transient voltages between the "grounded" cables and other nearby metallic structures both inside and outside the hull and superstructure.

2.6.4 Summary

Table 2.3 summarizes the more important aspects of related radio frequency interference test procedures and EMP hardening requirements. In summary, application of these other requirements does produce some difficulty in quantifying EMP hardening benefits. However, the amount of increase in the EMP hardening is generally insufficient to make any ship reasonably invulnerable to the EMP pickup. This arises because the EMP environment and related pickup currents and voltages are drastically different than the lightning, RFI, EMI, or HERO environments.

In some cases, combining EMP hardening with these other radio frequency interference requirements will produce conflicts and require relaxation of the requirements or the application of special hardening approaches compatible with both procedures. On the other hand, application of EMP protection can upgrade some of the features necessary to counter EMI, RFI, and HERO.

Table 2.3

Summary of EMP Impact of RFI and HERO Requirements

Equipment	Standard	Procedures	EMP Applied Hardening or Benefits	EMP Weaknesses
Electronic/Electrical Subsystems, Drawers and Cabinets, etc.	MIL-STD-461/462 NACSEM 6100	Lab tests for emissions and susceptibility; Max exposure <100 V.	Filtering and Shielding	Inband pickup (antennas) No surge protection. Inadequate terminal protection at penetrations. Inadequate cable shielding.
Complete System	MIL-I-6051C	All modes of system exercised and interference (self-generated)kept below critical levels.	Same as 461/462 but not general	Intrasystem signal and pickup considerably less than EMP pickup
Ordnance Devices-Detonators, EBW, Squib, etc.	NAVWEPS OD 30393	MIL-STD-1385 subsystem test exposures to specified field levels, also construction & design guidelines.	Shielding, filtering, special disconnect	EMP has higher peak power & different waveforms. Terminal protection likely to be insufficient
Ship Superstructure & Interior, Equipment	MIL-STD-1310C	Construction requirements to minimize noise and shock hazards.	Shielding of exterior topside cables	Grounding procedure not always compatible. Bond straps not short enough. Current still penetrates via cables entering compartments.

CHAPTER 3

EMP COLLECTION AND COUPLING

3.1 Introduction

There are two basic mechanisms by which the energy contained in a nuclear electromagnetic pulse may couple into the electronic systems within a ship.

- Direct penetration through the ship's structure
- Collection and transmission by electrical conductors.

Openings and discontinuities in the ship's hull, deck or superstructure such as hatches, doors, portholes, or imperfect seams allow a direct penetration of the energy in the form of free fields which then couple into electronic circuits. The discussion of direct penetration is presented in Chapter 5, "Construction Techniques for EMP Reduction."

Electrical conductors which physically penetrate from exterior (exposed) regions to interior areas of the ship provide a path for EMP energy flow. The segment of the conductor which is directly exposed to the EMP fields collects a portion of the energy in the form of an induced current transient. This current is then transmitted by the conductor to internal areas of the ship where the energy may be radiated and contribute to the interior free field, or it may be directly applied to the terminals of electronic equipment. Examples of conducting energy paths are

- Antennas and their associated feed systems
- Electrical signal and power cables
- Sanitary and fuel system piping.

The purpose of this chapter is to provide analytical tools for the prediction of the amount of energy which will be transmitted to interior regions of the ship via conducting paths and to establish guidelines for cabling practices which will minimize the EMP energy collected by the cables. The techniques which are discussed generally make use of standard engineering practice as follows:

- Approximate the intricate geometry of the physical structure with a model for which analytical procedures are available
- Select appropriate mathematical equations and formulas or reduce the model to an electrical circuit analog

- Utilize numerical or circuit analysis programs on a digital computer to obtain the EMP response as a function of time.

In addition to the foregoing procedure, which results in a time history of the EMP response, methods are presented which provide estimates of certain features of the response, such as peak values and rise times. These methods give approximate results with minimal effort and do not require the use of a digital computer.

3.2 Antennas

The antenna system aboard a Navy ship consists of a large number of individual antennas which are designed to be efficient collectors of electromagnetic energy in specific frequency ranges. The calculation of the energy collected and transferred to the load can be based directly on the antenna specifications if the frequencies contained in the impinging wave are within the design range of the antenna. However, for the broadband frequency spectra contained in the EMP transient, the transfer function calculation requires a knowledge of the antenna geometry. This section presents and illustrates techniques for determining antenna response with respect to the current and voltage waveforms and the energy which appears at the load when the antenna is illuminated by an EMP type waveform.

The material is divided into three major topics. Section 3.2.1 describes several methods which can be used to calculate the EMP response of various antenna systems. It is not possible to determine the magnitude of the voltages and currents induced on all the antenna structures aboard a ship analytically, because of the difficulties in mathematically characterizing the interaction and coupling mechanisms involved in these complex antenna structures. The computation efforts required to determine the EMP response of an antenna depend on the method used and the degree of accuracy required. Consequently, the techniques presented in 3.2.1 vary in rigor and complexity.

Section 3.2.2 gives examples of the application of these techniques/methods to several Navy ship antennas. Since the number of antennas and antenna-like structures on a ship is so great, the emphasis is placed on the most typical structures.

Finally, Section 3.2.3 presents some of the actions which can be taken to protect antenna systems from damage or upset caused by EMP energy collection. The discussion is very brief, and its basic function is to alert and orient the system engineer to general protection guidelines. More specific hardening procedures can be found in Chapter 4, "Protection Techniques and Devices."

3.2.1 General Techniques for Determining Antenna Pickup

This section contains descriptions of five (5) analytical techniques for determining the EMP energy pickup by antennas and, in the last case, by structures which behave like antennas. The first three methods, i.e., the Fourier Transformation Method (FTM), the Lumped Parameter Network Method (LPN) and the Singularity Expansion Method (SEM) are more rigorous than the fourth. They will give more detailed and accurate results, but are more time consuming than the fourth technique--which is based on Landt's method.[1]* The fifth technique is also a rigorous one; however, it is of more limited use to the system engineer of Navy ships. Consequently, its inclusion in this section is primarily for the sake of completeness.

---

*Superscripts refer to numbered references at the end of this chapter.

3.2.1.1 Fourier Transformation Method (FTM)

The solution to the problem of determining the EMP response of a linear antenna system can be obtained by Fourier analysis. In principle, a receiving antenna can always be characterized by a Thevenin equivalent circuit--consisting of a voltage source in series with the antenna impedance as seen by the load connected to the antenna terminals. This is shown schematically in Figure 3.1. In this analysis, two antenna functions, i.e., the antenna impedance and the effective antenna length must be known accurately over the EMP frequency spectrum. The response at the load to an EMP transient is determined from the inverse Fourier transformation of

$$I_L(j\omega) = \frac{-2h_e(j\omega)E_i(j\omega)}{Z_L(j\omega) + Z_a(j\omega)} \tag{3.1}$$

where the following notations are used:

$I_L(j\omega)$ = load current

$h_e(j\omega)$ = effective half length of a cylindrical antenna

$Z_a(j\omega)$ = antenna impedance

$Z_L(j\omega)$ = load impedance

$E_i(j\omega)$ = frequency spectrum of the incident EMP.

Note that the load may be an impedance other than a pure resistance and should include antenna base effects, the connecting transmission line (cable) impedance and the input impedance of the equipment which is connected to the antenna. In most cases, the Fourier integrations would have to be carried out using numerical techniques with the aid of a digital computer.*

3.2.1.2 Lumped Parameter Network Method (LPN)

The lumped parameter network method provides a technique for the analysis of a distributed parameter network (the antenna) connected to a linear or nonlinear load (receiving equipment such as a diode). Like the Fourier transformation method, it utilizes a Thevenin equivalent circuit of the type shown in Figure 3.1 to represent the antenna in terms of its open circuit voltages. Both antenna functions, the antenna impedance and its effective half length, are then approximated by rational network functions that are realizable in terms of an RLC circuit. After the lumped parameter network representation of an antenna is obtained, standard circuit analysis computer codes such as SCEPTRE or NET-2 may be used to

*Electromagnetic computer codes for computing antenna and cable response to EMP that rely on the use of numerical or digital techniques cited here as well as in subsequent sections have been computed and are maintained for customer use by the Electromagnetics and Systems Research Group, Lawrence Livermore Laboratory, Livermore, California 94550. Maintenance of this computer code library is an on-going effort that is funded by the Defense Nuclear Agency under Subtask R990AXEB075, Work Unit 35.

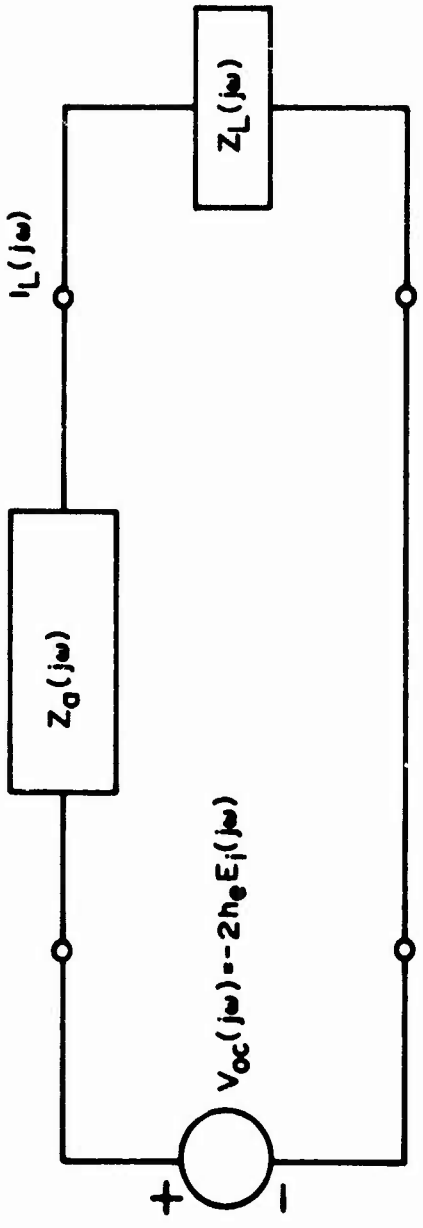

Where: $Z_a(j\omega)$ = Antenna Input Impedance
$2h_e$ = Antenna Effective Length

Fig. 3.1 THEVENIN EQUIVALENT CIRCUIT OF DIPOLE ANTENNA

calculate the transient system response to EMP even for a nonlinear load. The major advantages of the LPN method are:

- it does not require a closed-form analytic description of the excitation;
- it may be used with a linear or nonlinear load.

3.2.1.3 Singularity Expansion Method (SEM)

In classical circuit theory, the time domain solution of a linear circuit excited by an exterior waveform may be determined from the knowledge of the location of any singularities of the transfer function and its corresponding residues. The transient behavior of the circuit is then obtained as a sum of damped sinusoids whose coefficients are determined by the residue theorem.

A new method, namely, the singularity expansion method, has extended this concept to solve electromagnetic boundary value problems. The singularity expansion technique, as applied to general scattering problems by determining the natural frequencies, modes and coupling coefficients which arise from a general three-dimensional body, has been recently formulated by Baum.[2]

Basically, this method involves the determination of the antenna response in terms of singularities in the complex frequency domain which represent the natural frequencies, modes and coupling factors. The antenna response in the time domain is obtained by taking the inverse transform of the terms in the singularity expansion. If the actual incident waveform has singularities in the finite complex frequency plane, the response can generally be split into an object or antenna part containing object singularities (i.e. poles) and a waveform part containing waveform singularities.

Since this is a new approach to the solution of electromagnetic boundary value problems, the full potential of the application of this technique to the EMP collection and coupling problem remains to be exploited.

3.2.1.4 Technique Based on Landt's Method

Use of the Fourier Transformation, Lumped Parameter Network and Singularity Expansion Methods will, in general, require the use of a modern high speed computer and a strong knowledge of EM theory. If the detailed transient characteristics of mission critical antennas or antenna-like structures due to EMP are desired, these analytical methods must be used. However, for system engineers who need a quick, and reasonably accurate, estimate of antenna responses to EMP, a much simpler method is available. This method was developed by Landt[1] to estimate peak currents on various antenna structures for arbitrary input waves.

Background

As formulated by Landt, the peak short circuit current can be obtained by solving the integral

$$I_{sc}(\text{peak}) = h\left(\frac{c\tau}{a}\right) \int_0^{t_2} e(t)\, dt \qquad (3.2)$$

where e(t) is the EMP electric field parallel to the antenna structure. For broadside incidence, the value t_2 is typically chosen as $\ell/2c$, the time that no end reflection is seen at the center of an antenna, where ℓ is the length of the antenna and c is the speed of light.

The function $h(c\tau/a)$ is the impulse response of an infinite wire antenna as shown in Figure 3.2, where "a" is the antenna radius and $\tau = t_2 - t_1/2$, the average time, is chosen midway between the time e(t) reaches its full strength (the rise time, t_1) and the time, t_2, that the integral of Equation (3.2) is terminated. Since the peak current on a wire antenna excited by an EMP usually occurs during the early time response of the structure, the impulse response of the current $h(c\tau/a)$ on an infinite wire antenna is valid on a finite wire antenna, up until the time that the reflection is seen. Consequently, $h(c\tau/a)$, shown in Figure 3.2, is sufficient for calculating the peak current in most cases. Accuracies to within 10% can be obtained, as is demonstrated by several examples that are given in Appendix A.

Polarization

When the electric field $\overline{E}$, of the incident EMP is not parallel to the antenna axis, the term e(t) cos θ is substituted for e(t) in Equation (3.2), where θ is the angle between $\overline{E}$ and the antenna axis.

Modeling of Complex Structures

Landt's method, being limited basically to cylindrical antennas, can be used to estimate the peak EMP currents developed in complex antenna structures by modeling or characterizing these structures as single or composite sets of cylindrical antennas. Missiles, for example, are readily characterized as cylindrical structures having a length and diameter defined by its actual dimensions. For multiple wire antennas, each wire can be modeled and treated separately as a single cylinder to compute the peak currents in each using Equation (3.2). The total antenna response is then determined by simply adding the current contributions from each separate wire.

Loading

To account for antenna loading, Landt gives a formula for computing the peak load current in terms of the peak short circuit current that is computed using Equation (3.2). This approximate formula is given by

$$I_L(\text{peak}) = \frac{G_L}{G_L + G_{eff}} I_{sc}(\text{peak}) \qquad (3.3)$$

where G_L is the admittance (conductance) of the load and G_{eff} is the effective admittance of the cylindrical antenna given by:

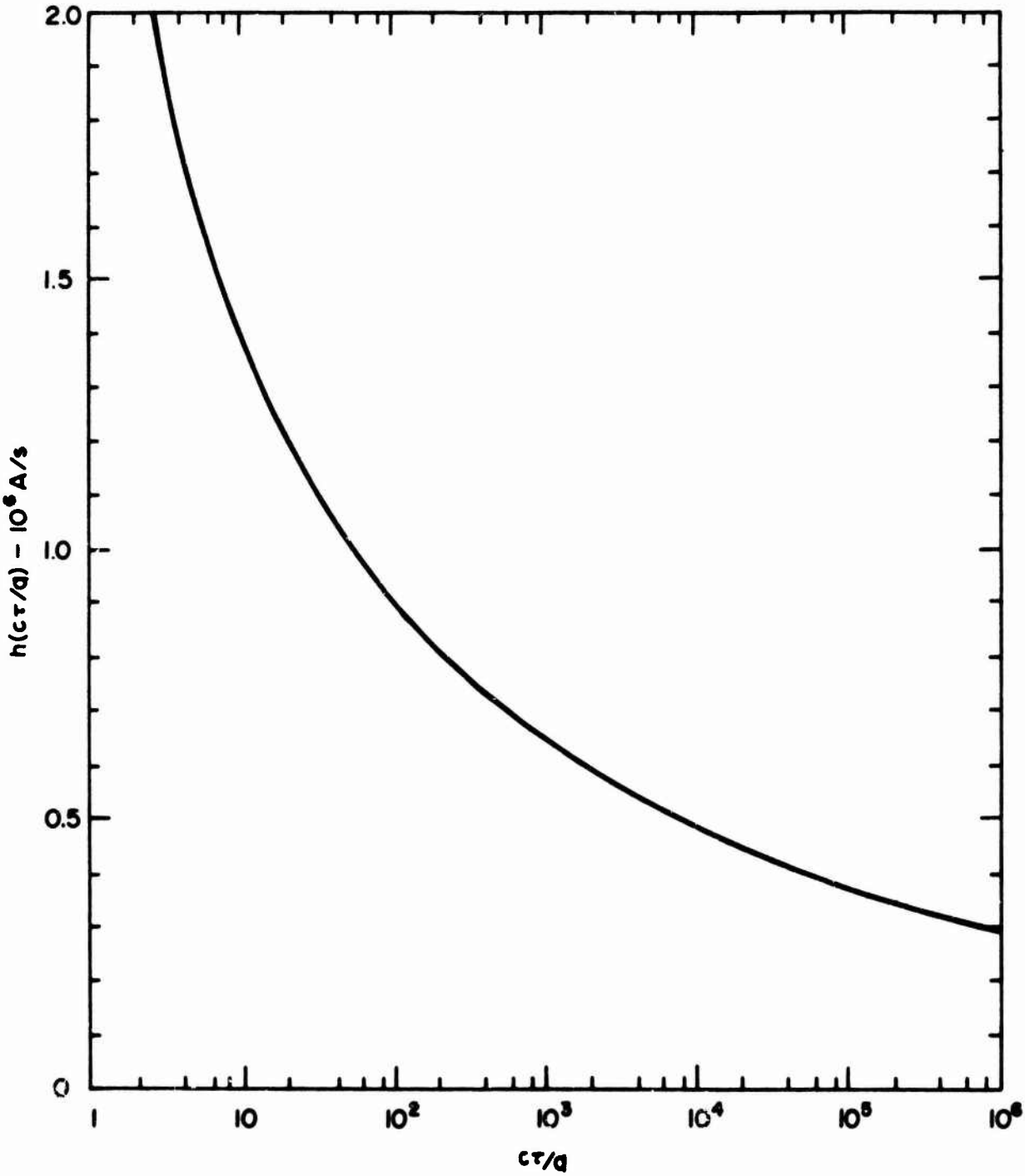

Fig 3.2 IMPULSE RESPONSE OF THE CURRENT ON AN INFINITE WIRE WHEN ILLUMINATED FROM BROADSIDE BY A PLANE WAVE

$$G_{eff} = \frac{I_{sc}(peak)}{c} \int_0^{t_2} e(t)\, dt \qquad (3.4)$$

Estimates of peak currents of select antennas and antenna-like structures using Landt's method can be found in Appendix A.

Advantages and Disadvantages

This approximate method of estimating peak currents has several advantages for the system engineer concerned with the problem of EMP pickup:

- It is relatively simple and easy to use.
- The method does not require excessive computation or the use of a high speed digital computer.
- The user does not require extensive background in EM theory.
- The method can be readily applied to a variety of complex antenna structures and arbitrary EMP waveforms.
- The effects of loading can be considered simultaneously.
- It also provides the EM nonexpert with a feeling for the most extreme problem parameters and/or the effects of varying these parameters.

However, the method also has disadvantages. These are:

- The method can only estimate the peak current. Therefore, for mission-critical antennas, where the details of the transient characteristics (such as the time history of antenna load current) are desired, more exact analytical methods must be used.
- The method is approximate in nature. No exact solution can be obtained. Accuracies to within 10% can be expected if a reasonably good cylindrical approximation of the physical system can be developed.

3.2.1.5 Technique for Analyzing Irregularly Shaped Structures Which Act Like Antennas

A more involved mathematical model and analysis is required for the more complicated structures of appendages to the ship--in which the geometrical configuration is such an irregular shape that neither the cylindrical antenna nor the reflector type of antenna can accurately describe their transient behavior when illuminated by EMP. In general, formulating a solution of Maxwell's equations to such a scattering problem results in integral equations for the current distribution. The current distributions of a perfectly conducting body, as illustrated in Figure 3.3, for example, are governed by the following two well-known equations:

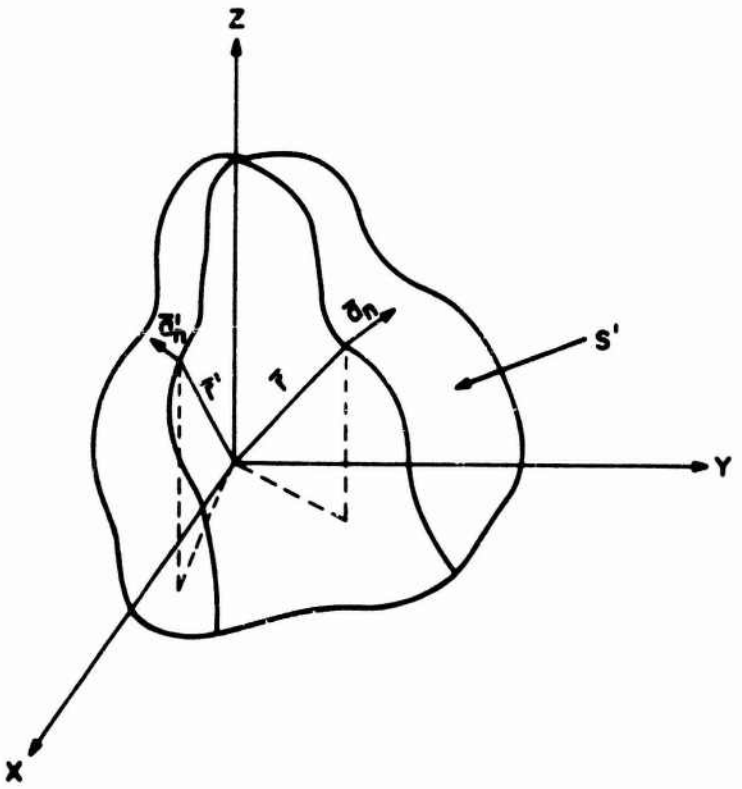

Fig. 3.3 THE GEOMETRY OF ARBITRARY SHAPED ANTENNA-LIKE COLLECTOR

$$E_i(\bar{r}) = jw\mu_o \int_{s'} G(\bar{r},\bar{r}')\, K(\bar{r}')\, dS' \tag{3.5}$$

for the electric-field integral equation and

$$\tfrac{1}{2}K(\bar{r}) = \overline{a_n}(\bar{r}) \times H_i(\bar{r}) + \int_{s'} \overline{a_n}(\bar{r}) \times [\nabla G(\bar{r},\bar{r}') \times K(\bar{r}')]\, ds' \tag{3.6}$$

for the magnetic-field integral equation, where $K(\bar{r})$ is the total surface current distribution on the scattering body illuminated by an incident plane wave, $E_i(\bar{r})$ and $H_i(\bar{r})$ are respectively the incident electric and magnetic fields, and $G(\bar{r},\bar{r}')$ is the three dimensional Green's function given by

$$G(\bar{r},\bar{r}') = \frac{1}{4\pi} \frac{\exp\{-j\beta|\bar{r}-\bar{r}'|\}}{|r-r'|} \tag{3.7}$$

Both position vectors $\bar{r}$ and $\bar{r}'$ refer to points of body revolution. Solutions of these pertinent integral equations are possible with the aid of high speed digital computers.[3,4,5,6] As an example, Figures 3.4 and 3.5 give the current distributions obtained by Mei and Bladel[5] when an incident plane wave is impinging upon a rectangular cylinder.

3.2.2 EMP Pickup of Typical Ship Antennas

Examples of how the previously described modeling and analysis techniques are applied to determine the EMP pickup by the more common types of antennas used on Navy ships are presented in this section. Short dipole/monopole, cylindrical and several types of reflector antennas are included. The analysis techniques described in Section 3.2.1 are used where applicable. Other analyses, which yield more approximate EMP pickup estimates, are discussed for those cases in which rigorous analyses are impossible or highly impractical.

3.2.2.1 Short Dipole/Monopole and Loop Antennas

Antennas, and other cylindrical conducting structures, may be considered as short electric dipoles if their total length is smaller than one-sixth of the minimum EMP wavelength of significance.

As an example, the physical length of an intentional half wave dipole operated at 7 GHz is about 0.0214 meters. The corresponding electrical length, $2h/\lambda$, over a representative EMP frequency range (i.e., from a few hertz to ~ 100 MHz) would be less than 0.0071, where h is the physical half length of the dipole and λ is the minimum EMP wavelength of interest. In view of this relatively small dimension, a short electric dipole model can be utilized. In this case, the EMP pickup and response of the dipole can be characterized in terms of the equivalent circuit representation shown in Figure 3.6 where,

$$C_a = \frac{h}{cZ_o} \tag{3.8}$$

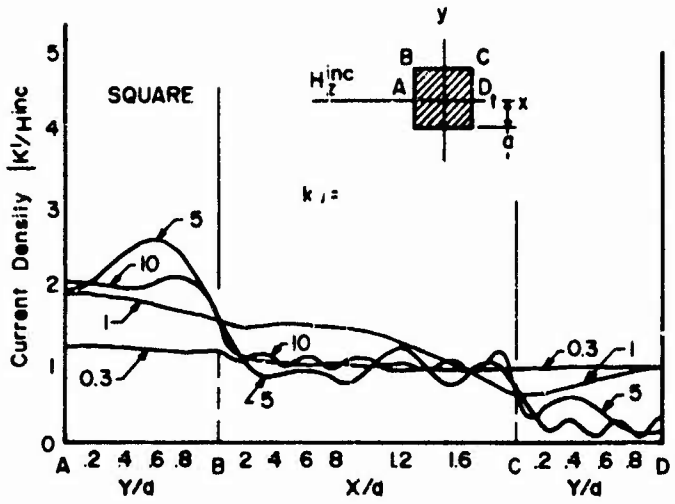

(a)

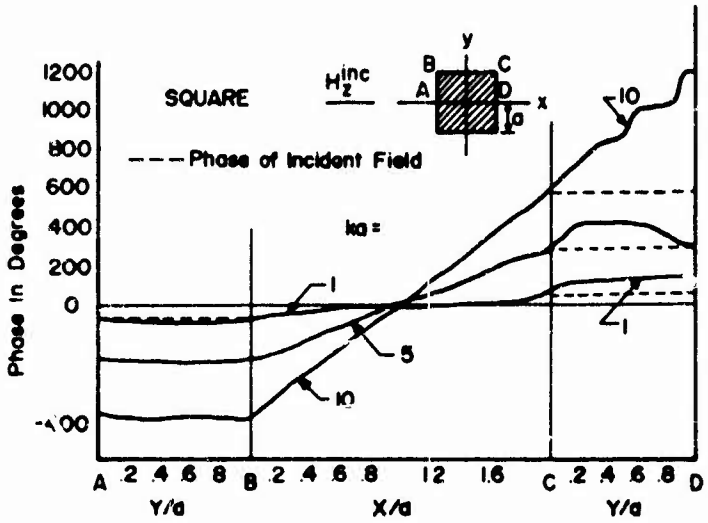

(b)

Fig. 3.4 MAGNITUDE AND PHASE OF SURFACE CURRENT DENSITY ON A SQUARE CYLINDER FOR H-POLARIZED PLANE WAVES

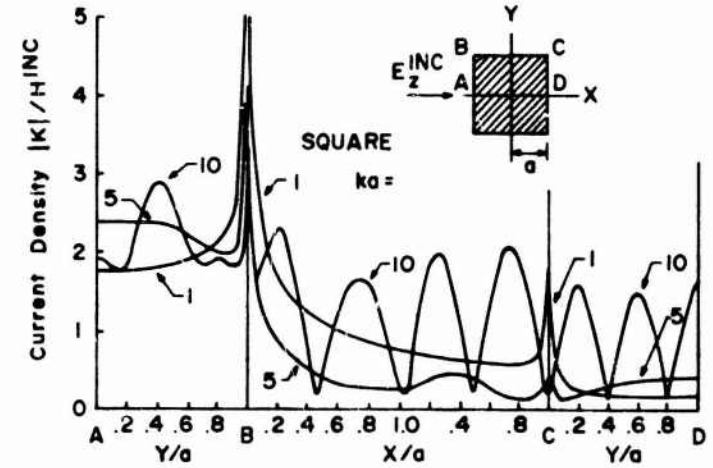

(a)

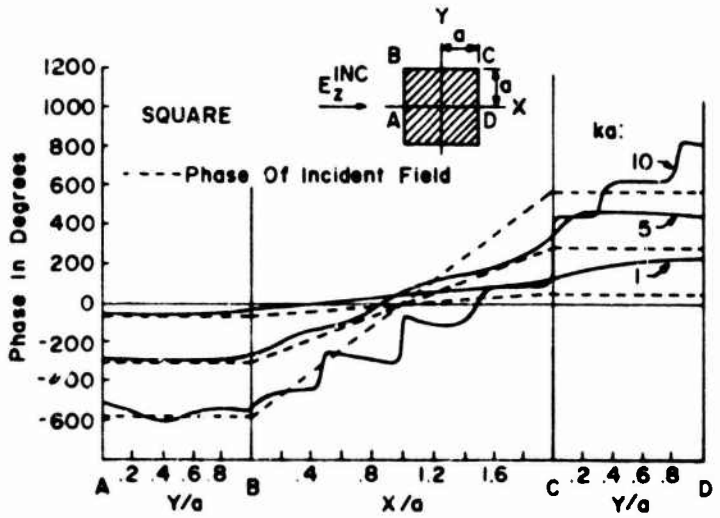

(b)

Fig. 3.5 MAGNITUDE AND PHASE OF SURFACE CURRENT DENSITY ON A SQUARE CYLINDER FOR E-POLARIZED PLANE WAVES

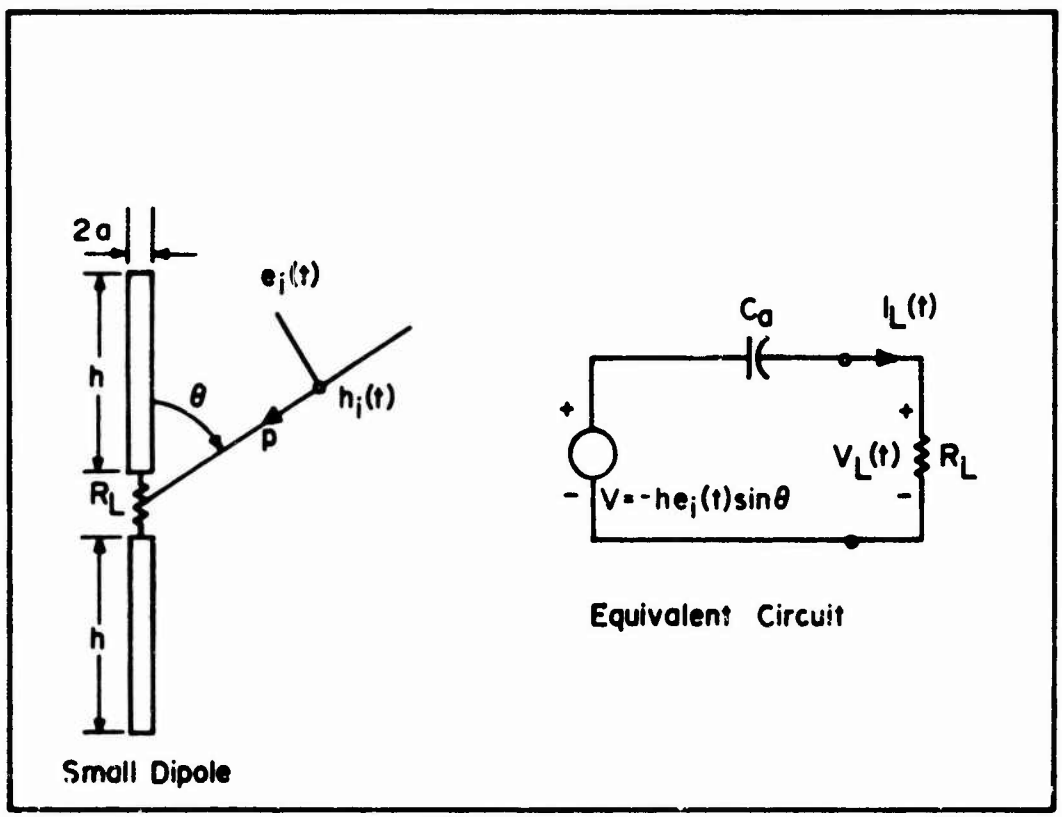

Fig. 3.6 EQUIVALENT CIRCUIT OF A SMALL DIPOLE

where c is the speed of light, and Z_o is the average antenna characteristic impedance given by:

$$Z_o = 60(\Omega - 2)$$

with

$$\Omega = 2 \ln(\frac{2h}{a}) \tag{3.9}$$

in which "a" is the radius of the antenna structure. It is to be noted that this short dipole modeling and analysis is valid under the condition:

$$t_r \geq 4(\frac{h}{c}) \tag{3.10}$$

where t_r is the rise time of the incident EMP. This is consistent with the constraint or condition that the antenna dimension is smaller than one-sixth of the minimum EMP wavelength of interest.

This equivalent circuit representation is also valid for computing the monopole response to EMP by adjusting the circuit parameters of Figure 3.6 as follows:

$$C_a(\text{monopole}) = 2\frac{h}{c} Z_o = 2C_a(\text{dipole})$$

and

$$V(\text{monopole}) = -\frac{h}{2} e_i(t) \sin\theta = \tfrac{1}{2}V(\text{dipole})$$

The equivalent circuit of a small magnetic dipole (loop) is shown in Figure 3.7. This representation is valid for an incident magnetic field $h_i(t)$ under the following conditions:

$$t_r > 4(\frac{R_o}{c}) \tag{3.11}$$

where R is the radius of the loop.

The inductance L_a is given by

$$L_a = \mu_o R \ln[(\frac{8R_o}{a}) - 2] \tag{3.12}$$

where μ_o is the free space permeability, and "a" is the radius of the conducting wire. The factor A in the equation for voltage source given in Figure 3.7 is the area of the loop.

Analysis of the equivalent circuit for the electric and magnetic dipole will give the approximate current and voltage waveforms at the terminals of the antenna. The procedures described are applicable to the extent that an order of magnitude approximation may be obtained from the fast rise time and wide frequency spectrum

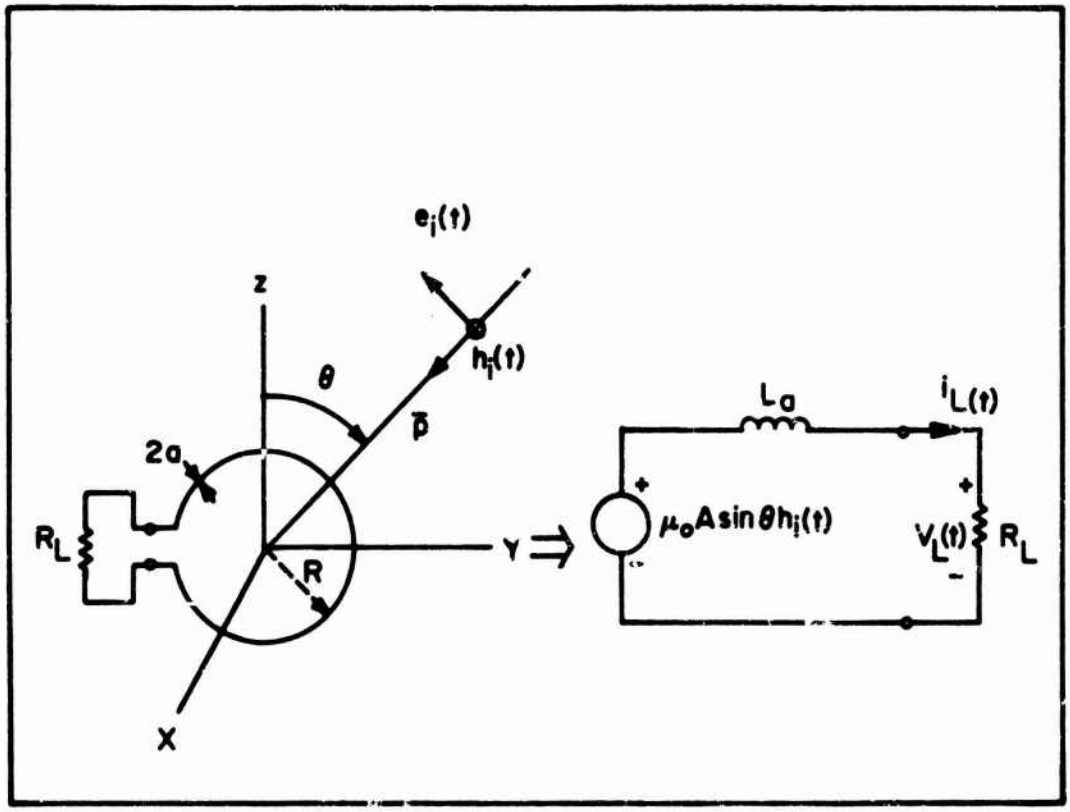

Fig. 3.7 EQUIVALENT CIRCUIT OF A SMALL LOOP

associated with an EMP. To obtain more accurate results, more sophisticated methods and analyses (such as FTM, LPN or SEM) are required.

3.2.2.2 Cylindrical Antennas

If the dimensions of an antenna or other cylindrical conducting structure are large compared to the minimum wavelength in the EMP spectrum, the short dipole model is no longer valid. Instead, the theory of cylindrical antennas may be used.

Expressions for the antenna impedance and effective length of cylindrical antennas are available in the literature.[1] In general, they are functions of the antenna shape factor, Ω, and the electrical half length, βh, where $\beta = \omega/c$, and h is the half length of the antenna. The effective antenna length and impedance over the entire EMP frequency range are determined for low and high frequencies by two well-known theories. For low frequencies, $\beta h \leq 1$, the expression given by King[7] is used. For high frequencies, $\beta h \geq 1$, Wu's theory of long antennas is used. Toulios et al.[8] have extended these theories to the case in which the EMP impinges upon the antenna at any angle of arrival. The effective length of the cylindrical antenna as a function of frequency is then obtained from a spatial Fourier transform of the antenna current distribution in the transmitting mode.[8] The impedance function may be calculated from either the theories presented by King and Wu or from the expression given in the Antenna User's Manual.[9]

A complete characterization of a receiving cylindrical antenna is then possible in the form of a Thevenin equivalent circuit. Using the equivalent circuit of Figure 3.1, either the Fourier transform method or the lumped parameter network method may now be employed to determine the transient EMP response. The transient responses of selected examples are included here for the input trapezoidal shaped pulse of Figure 3.8. Further, a comparison of these transient responses, employing the Fourier transformation method and lumped parameter network method, and using the SCEPTRE computer code, is also given for the purpose of demonstrating the implementation and accuracy of both methods. The examples are:

Transient Response of a 100 Foot Dipole Antenna Using FTM and LPN Methods for a 50 Ohm Load

In this example, a comparison is made in Figure 3.9 between the FTM method and LPN method for calculating the transient response of a 100 foot cylindrical antenna in free space. The antenna parameters are:

h = antenna half length = 50 feet

Ω = shape factor = 20

$E_{i,max}$ = peak amplitude of the incident field = 10 volt/m

ϕ = angle of incidence = 45°

Z_L = load impedance = 50 ohms

The equivalent lumped parameter network of the antenna is shown in Figure 3.10.

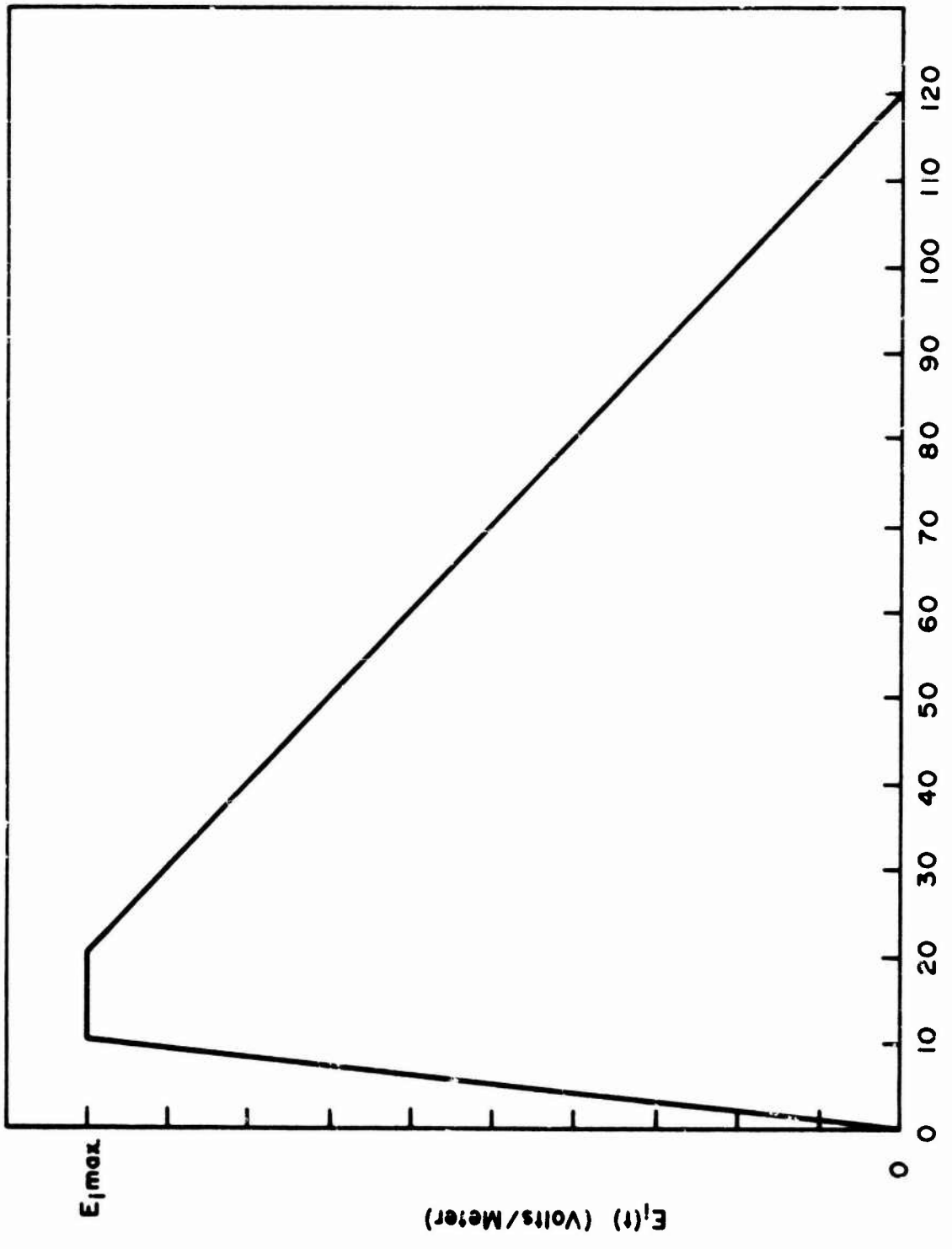

Fig. 3.8 INPUT PULSE SHAPE (INCIDENT ELECTRIC FIELD)

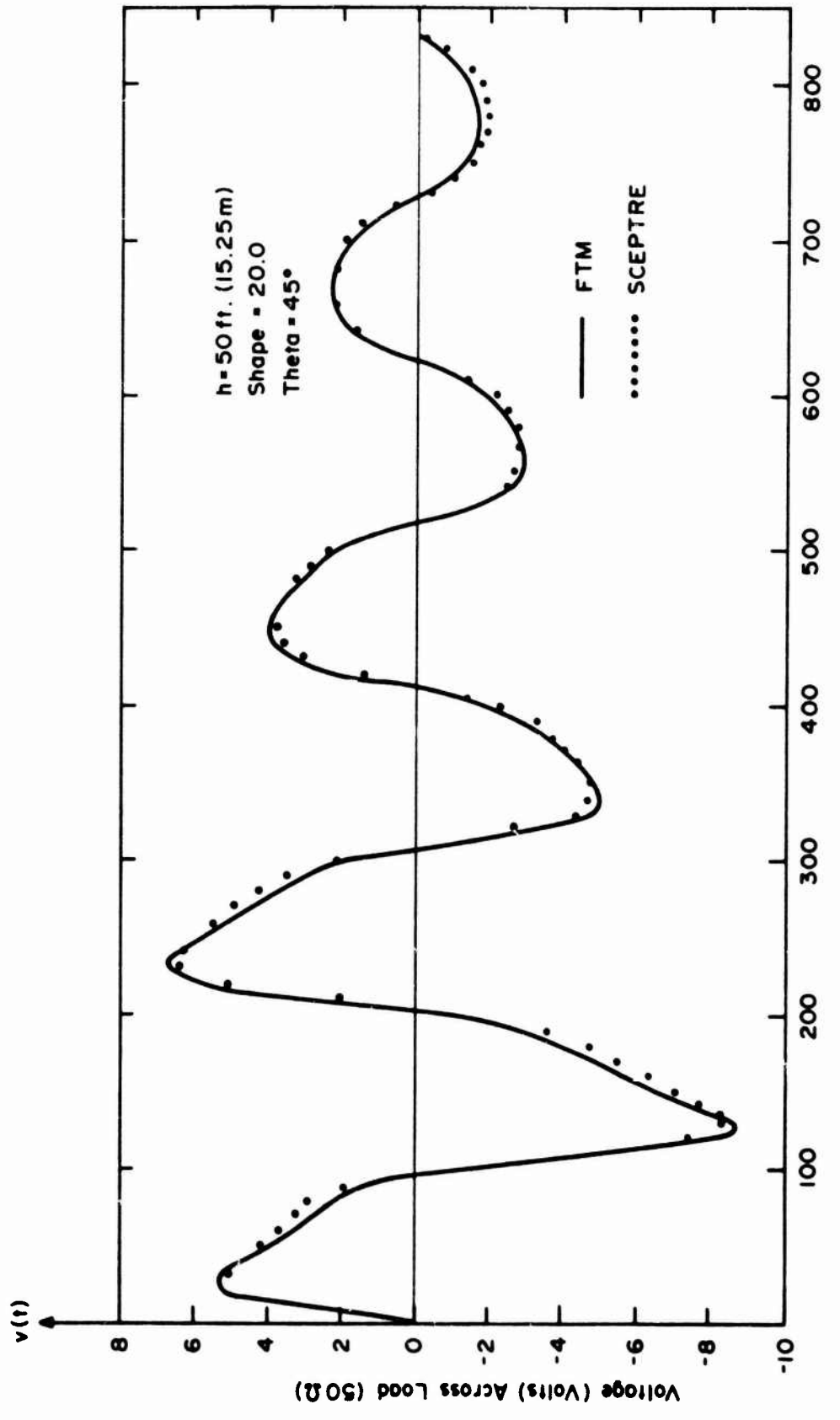

Fig. 3.9 FTM Vs. SCEPTRE ANTENNA WITH 50Ω LOAD

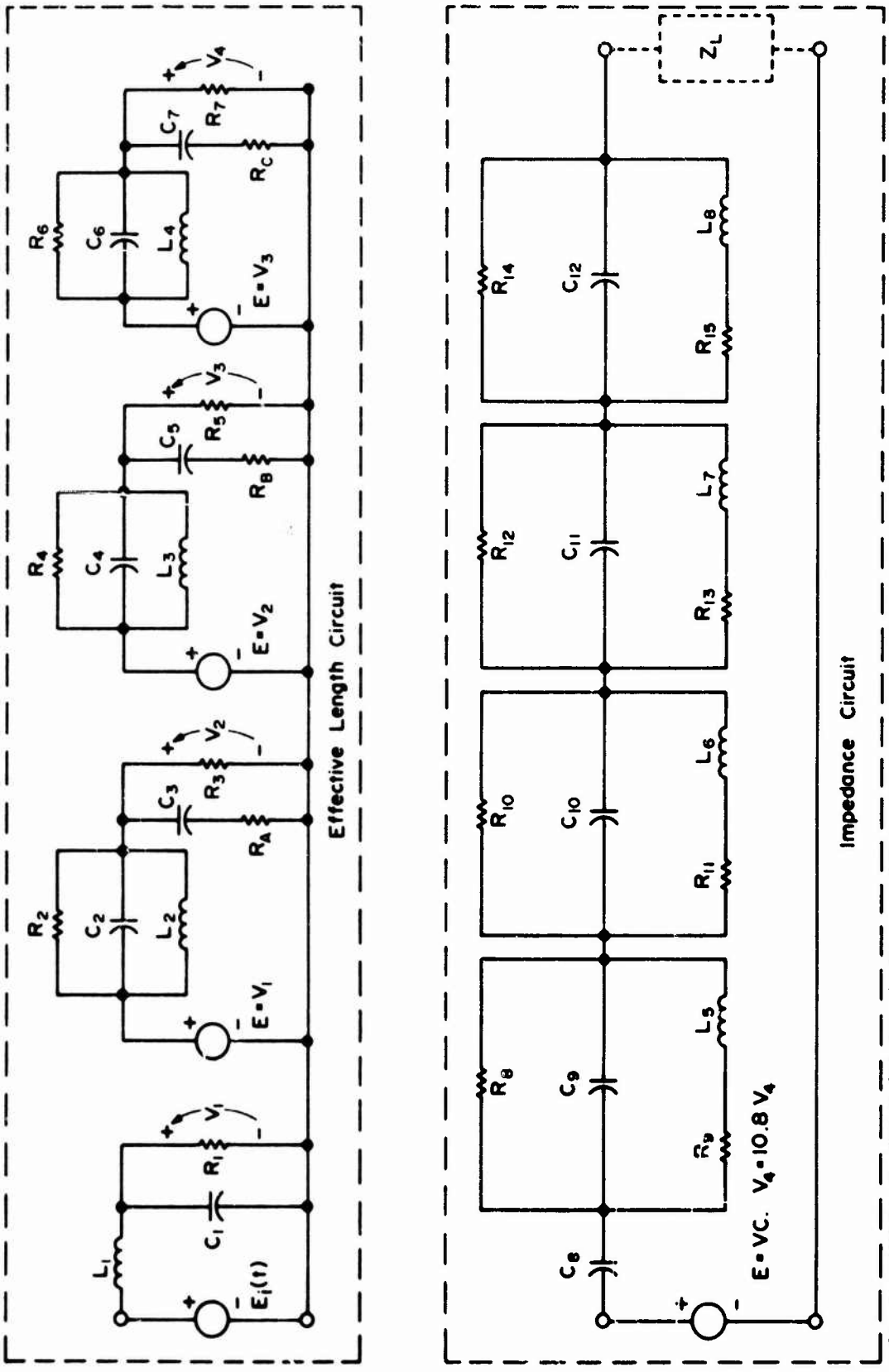

Fig. 3.10 DIPOLE ANTENNA EQUIVALENT CIRCUIT

Transient Response of an 8 Foot Monopole Over a Perfectly Conducting Plane Using FTM and LPN Methods for a 50 Ohm Load

In this example the antenna parameters are:

h = 8 feet

Ω = 15

$E_{i,max}$ = 10 volt/m

ϕ = 45°

Z_L = 50 ohms

Note that the antenna impedance and effective length of a monopole over a perfectly conducting plane is just half those of a dipole in free space. Figure 3.11 shows the results of the analysis using the LPN method when compared to those obtained from the FTM method. The equivalent LPN circuit is presented in Figure 3.12.

Transient Response of an 8 Foot Monopole Over a Perfectly Conducting Plane Using LPN Method for an FET Load

An 8 foot monopole over a perfectly conducting plane is loaded with a field-effect transistor (FET) amplifier. This example demonstrates the implementation of SCEPTRE using a receiving monopole connected to a receiver front end. The model of the FET used and the response waveform are shown in Figures 3.13, 3.14, and 3.15, respectively.

A file of computer programs and their LPN equivalent circuits are available[8,9] for the transient analysis of cylindrical antennas. These include the following antenna configurations:

- Dipole antenna in free space
- Monopole over lossless conducting plane
- Horizontal dipole over lossy plane

3.2.2.3 Reflector Antennas

Depending on the geometric form of the structure, it is possible to classify some conducting or conductive structures aboard the ship, and appendages to the ship as reflector-type antennas. In addition to antennas such as the parabolic dish used for surveillance or tracking radars, other conductive surfaces of revolution of the ship's outer structure or surroundings (such as cylindrical, elliptical, paraboloidal, doubly curved, toroid and/or plane surfaces) could behave like reflector-type receiving antennas when illuminated by an external EMP.

A reflector antenna is an energy collector as well as an energy transmitter. When an electromagnetic plane wave originating from a nuclear blast strikes a reflector-type antenna, surface currents are induced, and some of this energy is

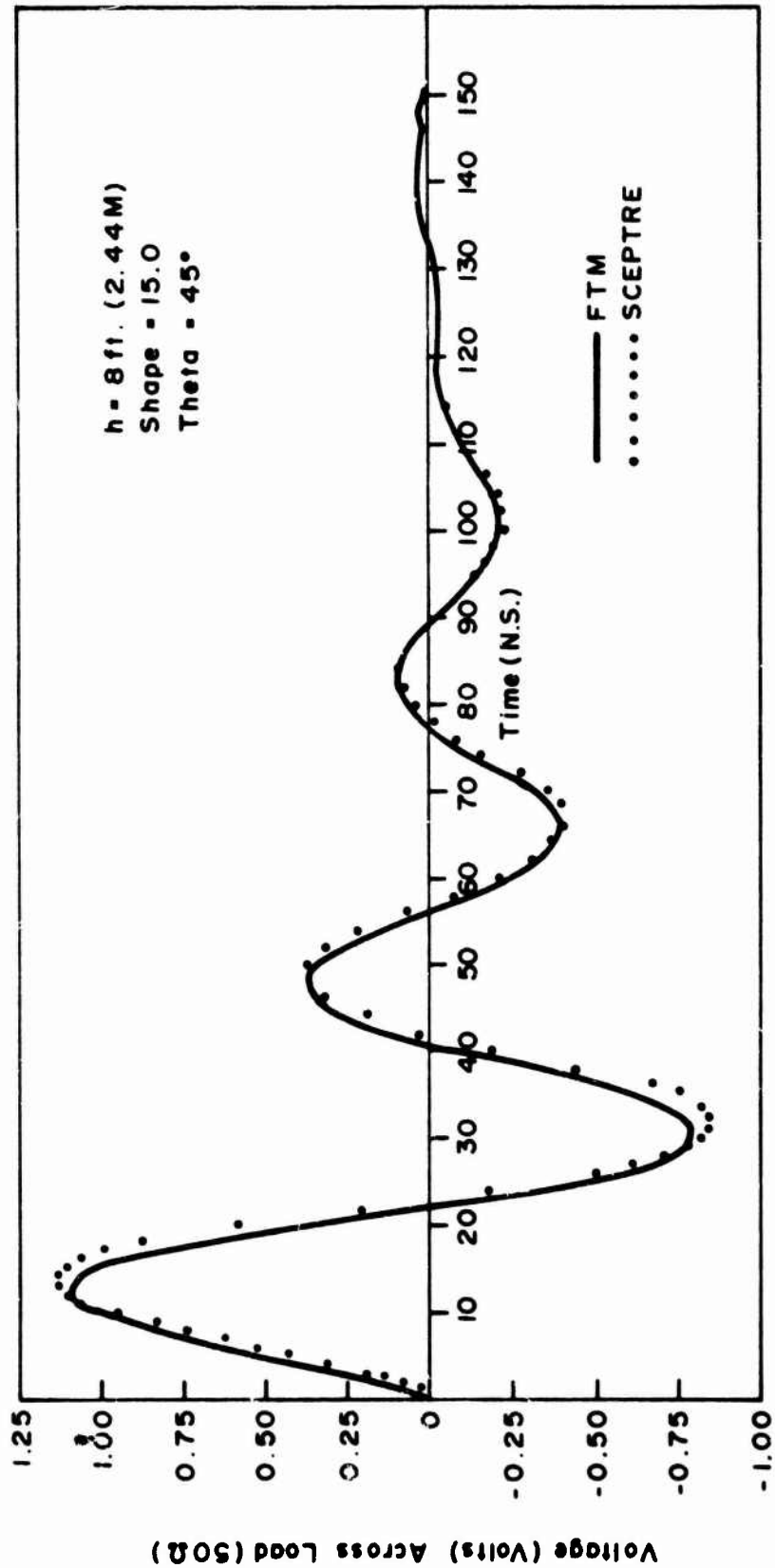

Fig. 3.11 FTM VS. SCEPTRE FOR MONOPOLE ANTENNA WITH 50Ω LOAD

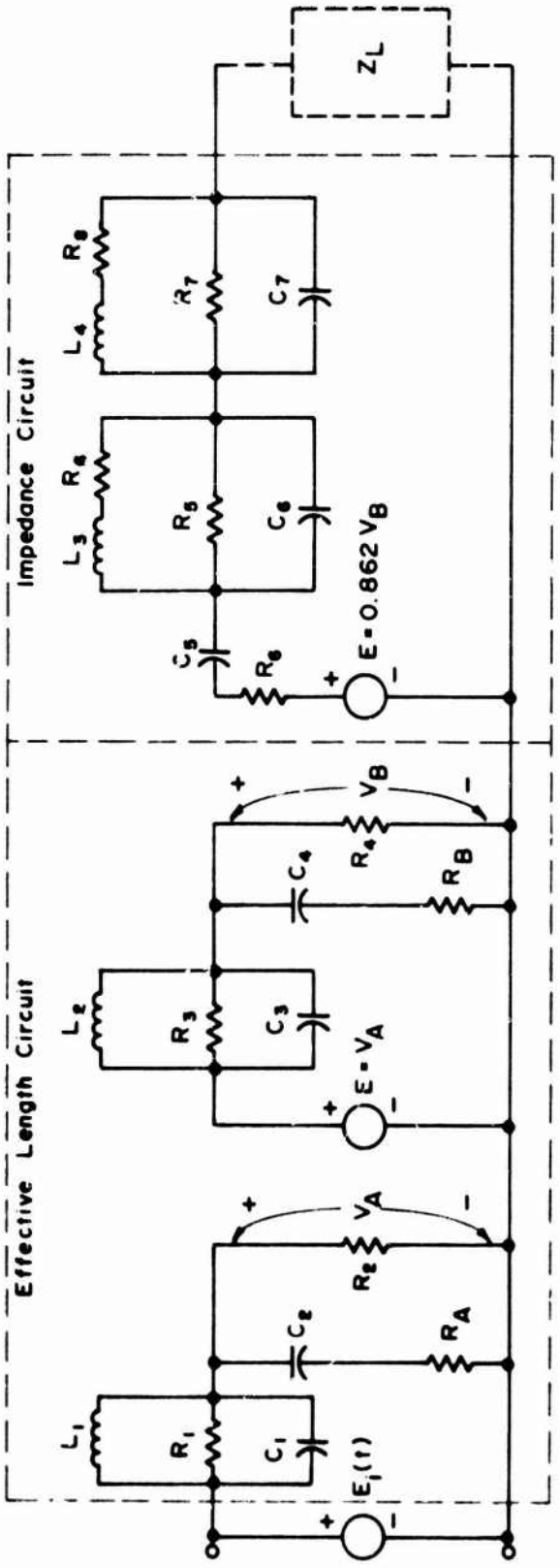

Fig. 3.12 MONOPOLE ANTENNA EQUIVALENT CIRCUIT

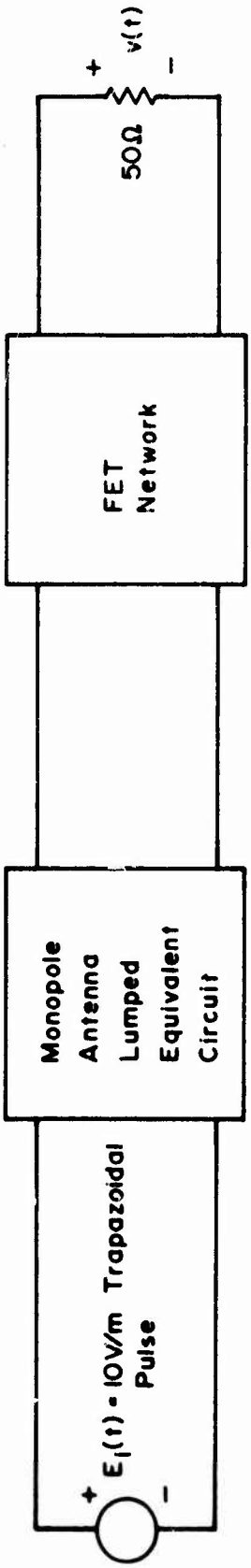

Fig. 3.13 FET-LOADED MONOPOLE ANTENNA

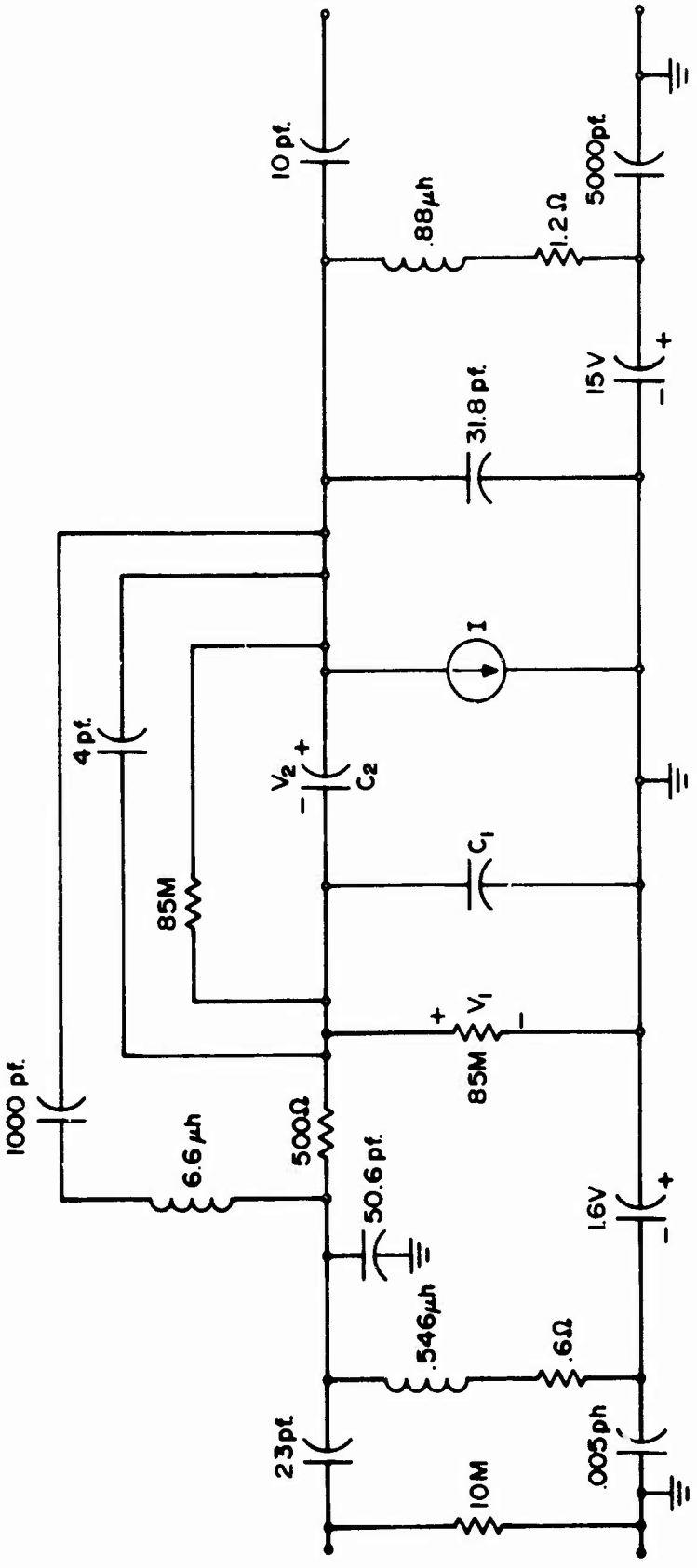

Fig. 3.14 FIELD-EFFECT TRANSISTOR MODEL MOTOROLA NO. MPF 107

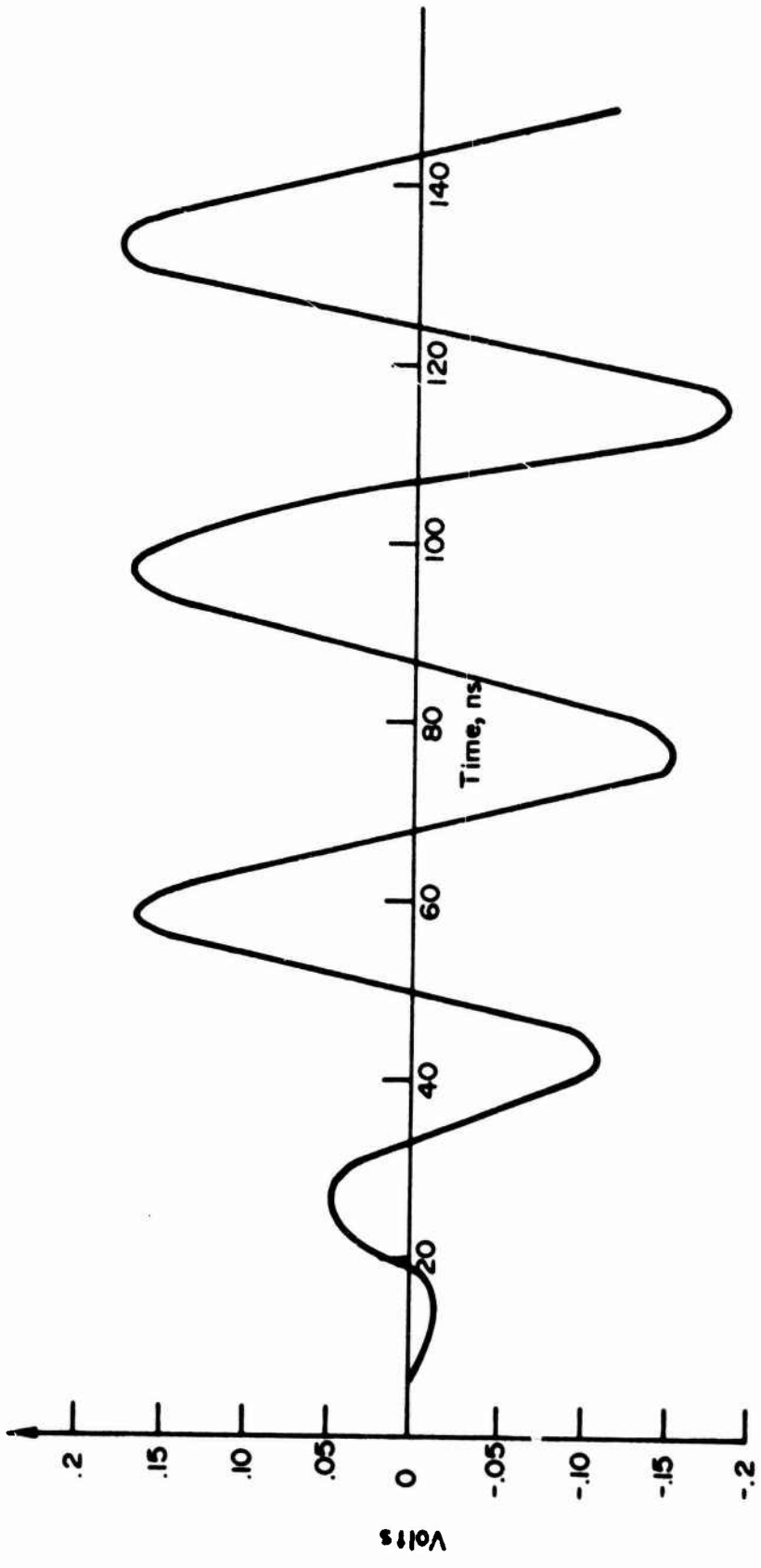

Fig. 3.15 OUTPUT VOLTAGE OF FET LOADED MONOPOLE ANTENNA WITH 10V/m TRAPEZOIDAL PULSE INPUT

collected by the reflector. The remaining portion of the energy could either be reradiated into free space or transmitted, via guided paths, to nearby electronic equipments or other energy collectors, such as a dipole, monopole or cable. The energy transmitted to such collectors may result in strong EMP pickup and interference--causing equipment burn-out, circuit upset or other system malfunctions.

To obtain a meaningful solution to the EMP transient response of a reflector-type antenna, one must determine the surface current distribution on the collector's surface. It is possible in principle to solve the three-dimensional boundary value problem of a reflector antenna exactly. This solution, however, usually involves great mathematical difficulties. From an engineering point of view, there are at least two approaches one can use to estimate the current distribution and thereby simplify the problem.

(1) The first approach is to make an estimate of the current distribution along the collecting structure based on its size and shape relative to the wavelength spectrum of the EMP energy. One must first establish if the collector dimensions are "small" or "large" compared to the wavelength spectrum of the impinging EMP. For very large collecting apertures, that is, the aperture diameter "D" is very large compared to the wavelength (i.e., $D/\lambda >> 1$), experience has shown that the current distribution induced by a plane wave normal to the collector is given by $2\bar{a}_n \times \bar{H}_i$ where $\bar{a}_n$ is the outward unit vector normal to the reflector surface and $\bar{H}_i$ is the incident magnetic field. Under such conditions, the laws of physical optics can be applied whereby the collector/reflector surfaces can be treated as mirrors, focusing lenses, etc., to estimate the energy collected at specific points in space.

For the condition where the collecting aperture dimension "D" is small compared to the wavelength (i.e., the low frequency small aperture situation) other approaches such as the quasistatic approximation or Rayleigh solution may be used to determine the current distribution. It should be pointed out that because the EMP energy is quite broadband, this technique may only be necessary at the low frequency end of the spectrum for a given collector size. As one proceeds to the higher frequencies, the laws of Physical Optics may then be more appropriately applied.

(2) An alternative approach is to identify the actual collector object with a convenient model configuration whose current distribution is known. For example, the current distribution induced on a finite cylindrical reflector could be approximately obtained from that of an infinite cylindrical reflector antenna, if the incident plane wave is properly polarized. This presumption is justified by the work of Kao,[10] in which he shows that for H-polarization (magnetic field parallel to the axis of the cylinder), the induced transverse current distribution on a finite cylinder can be accurately approximated by considering an infinite cylinder, and the induced longitudinal current distribution is small and can be neglected.

A complete and exact analysis of reflector antennas can be made by using techniques which employ the Singularity Expansion method (see Section 3.2.1.3) or by using numerical techniques such as the method of moments[11] to solve the pertinent integral equations. However, these analyses will not be given here. Such an analysis would require extensive analytical or experimental work to obtain the current distribution, which, in turn, is used to obtain the electrical parameters,

such as complex impedance and effective aperture, to characterize the receiving antenna. In many cases, the configurations of reflector antennas are complex, and the antenna impedance and effective aperture are not available in the literature. Therefore, analyses based on engineering approximations are usually employed to obtain an estimate of the collected EMP energy for a reflector antenna. Nevertheless, this estimate can be used to determine the possible degradation of an electronic system that may be either connected to or adjacent to the subject antenna.

3.2.2.3.1 Estimation of Energy Collected by a Reflector Antenna

An approximate energy analysis based on the concept of effective aperture is employed to obtain an estimate of the EMP energy collected by a reflector antenna. This energy could be transmitted to any other energy collector, such as a dipole, connected to the subject reflector. The effective aperture is related to the power gain, G, by

$$A_e(\omega) = \frac{\lambda_G^2}{4\pi} \tag{3.13}$$

where λ is the wavelength.

Listed below are the effective apertures for three types of reflector antennas:

Type	Effective Aperture
large aperture antenna	100% of physical area
pyramidal horn	50% of physical area
parabolic reflector	50-60% of physical area

It is to be noted that the values given in the above table for the effective apertures of collecting antennas have been derived using sinusoidally time-varying fields. However, for the approximate techniques to be presented here, they can be used for the pulsed or transient EMP fields.

For an antenna placed in the field of a linearly polarized sinusoidal EM wave, the power available at the antenna terminals when the load is conjugately matched is given by

$$W = PA_e(\omega) \tag{3.14}$$

where

W = available power (watts)

P = power density of the incident wave (watts/m^2)

$A_e(\omega)$ = effective aperture (m^2)

For an EM pulse, the energy available at the antenna terminals is

$$J_t = \frac{1}{2\pi} \int_{-\infty}^{\infty} A_e(\omega)\, J(\omega)\, d\omega \tag{3.15}$$

where

J_t = available energy (joules)

$J(\omega)$ = energy density spectrum of the pulse (joules/m^2/Hz)

All the available energy will be transferred to the load only when the load impedance presents a conjugate match to the antenna impedance over the frequency range where the excitation has significant components. Such a wide band match is physically unrealizable. To evaluate the system response, an approximation is obtained by assuming a system transfer function of the form:

$$T(\omega) = \begin{cases} A_e(\omega)\, \left(\frac{\omega}{\omega_0+\omega_1}\right)^{2n}; & 0 \leq \omega \leq (\omega_0-\omega_1) \\ A_e(\omega); & (\omega_0-\omega_1) \leq \omega \leq (\omega_0+\omega_1) \\ A_e(\omega)\, \left(\frac{\omega_0+\omega_1}{\omega}\right)^{2n}; & (\omega_0+\omega_1) \leq \omega \end{cases} \tag{3.16}$$

where

ω_0 = center radian frequency

$(\omega_0-\omega_1)$ = lower radian cut-off frequency

$(\omega_1+\omega_1)$ = upper radian cut-off frequency

and the parameter "n" determines the out-of-band attenuation.

Under this assumption, the energy dissipated in the load is:

$$J_t = \frac{1}{2\pi} \int_{-\infty}^{\infty} T(\omega)\, J(\omega)\, d\omega \tag{3.17}$$

The case of n = 1 (6dB/octave) is considered to be extreme and the bandwidth chosen is the tuning range of the system. If additional information is available, a different value of n may be more appropriate.

Assume an incident EMP field of the form:

$$E_i(t) = E_0[\exp(-\alpha t) - \exp(-\beta t)] \tag{3.18}$$

where

E_0 = electric field intensity (volts/m)

$\alpha = 2.0/t_f(\sec^{-1})$

$\beta = 2.0/t_r(\sec^{-1})$

t_f = fall time (sec) of the EMP

t_r = rise time (sec) of the EMP.

The energy density spectrum is then

$$J(\omega) = k\left[\frac{1}{\alpha^2+\omega^2} - \frac{1}{\beta^2+\omega^2}\right] \tag{3.19}$$

where

$$k = (E_{i,max})^2 \left[\frac{(\beta-\alpha)^2}{\beta^2-\alpha^2}\right]$$

For a parabolic dish which has an effective aperture of

$$A_e(\omega) = 0.55\pi\,(\frac{D}{2})^2 \tag{3.20}$$

the in-band energy $[(\omega_0-\omega_1) \leq \omega \leq (\omega_0+\omega_1)]$ dissipated in the load is given by:

$$J_t = 0.55(\frac{D}{2})^2 \left\{\frac{1}{\alpha}(\tan^{-1}[\frac{(\omega_0-\omega_1)}{\alpha}] - \tan^{-1}[\frac{(\omega_0+\omega_1)}{\alpha}]\right.$$

$$\left. - \frac{1}{\beta}\,(\tan^{-1}[\frac{(\omega_0-\omega_1)}{\beta}] - \tan^{-1}[\frac{(\omega_0-\omega_1)}{\beta}])\right\} \tag{3.21}$$

The expression obtained may not result in the greatest degree of energy collection for the actual system, since it assumes infinite rejection of the out-of-band energy. However, it does provide a realistic estimate of the collected in-band energy. This approach represents the best available approximation of the problem at the present time due to the lack of detailed information about the impedance, effective aperture and spurious responses of the system.

3.2.2.3.2 Analysis of EMP Pickup Due to Indirect Coupling of Energy Reradiated from a Reflector Antenna

A portion of the EMP energy collected by a reflector antenna may be reradiated to its own feed antenna system or to adjacent electronic equipments. This coupling mechanism and the resulting EMP energy pickup may be analyzed by considering an antenna system whose configuration consists of a reflector and a feed antenna or a nearby energy collector such as a dipole. A representative configuration of a reflector antenna system is shown in Figure 3.16.

Summarized below are the major steps to achieve the desired objective of determining the EMP response of reflector/feed or energy collector antenna systems:

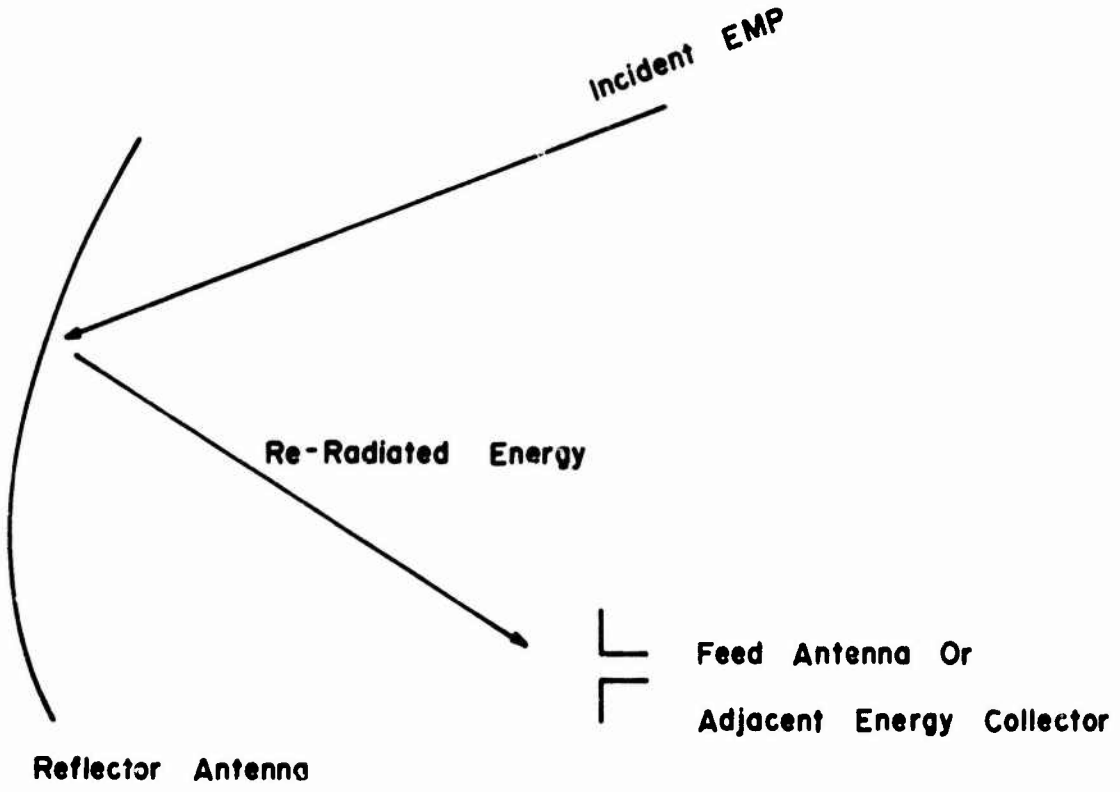

Fig. 3.16 REPRESENTATIVE CONFIGURATION OF A REFLECTOR ANTENNA SYSTEM

- Calculate the surface current distribution on a reflector in the absence of the feed antenna or the adjacent energy collector due to the incident EMP.

- Based on the current distribution, determine the field reradiated by the subject reflector at or near the feed antenna or other antenna collectors.

- Assuming no interaction between the reflector and feed antenna or energy collector, obtain the effective length (or effective aperture) and input impedance as seen at the terminals of the feed antenna or other energy collector such as a dipole, cross-dipole, conical antenna, helical antenna, etc.

- Establish a Thevenin equivalent circuit at the terminals of the feed or collector antenna.

- Use the FTM or LPN method to invert the frequency domain solution to a time domain response due to a high altitude EMP waveform.

The current distribution on the subject reflector may be obtained from either exact analysis or an approximate solution employing the methods described previously, depending on the scope of work and degree of accuracy required. An approximate solution of the EMP response of a simple reflector configuration which consists of a three-dimensional parabolic reflector fed by a dipole or helical antenna has recently been obtained and is available in the literature.[12] Shown in Figure 3.18, for example, is the time history of the load current for a receiving dipole feed antenna when an incident EMP with a waveform of Figure 3.17 impinges upon the parabolic/feed antenna system from the broadside direction. In Figure 3.18, the dotted curve is the result obtained using the physical optics approximation ($2\,\bar{a}_n \times \bar{H}_0$) for the current distribution on the parabolic dish. The solid curve represents the more exact solution obtained from integral equations with the aid of a digital computer. The parabolic dish considered here is 25 feet in diameter, and the feed antenna is a half wave dipole (at 7 GHz) connected to a 50 Ω load impedance.

It should be noted that the response of reflector systems to transient pulses that are currently available in the literature are based on theoretical relations of the type discussed here. Experimental work is in progress to verify these results.

3.2.3 EMP Hardening Techniques for Ship Antennas

The fundamental antenna problem on a ship is to prevent the EMP energy that is collected by the antennas from damaging or upsetting electronic equipment. The calculations which are performed for antennas and antenna-like structures provide information on the peak currents and voltages and the energy which will be collected during an EMP event. This information is then used to determine the need for and level of protection required.

Antennas are connected to receiver and/or transmitter equipment via waveguides or cables. Those systems which are operating in a frequency range for which a waveguide is used in the feed system have minimal vulnerability to EMP, since

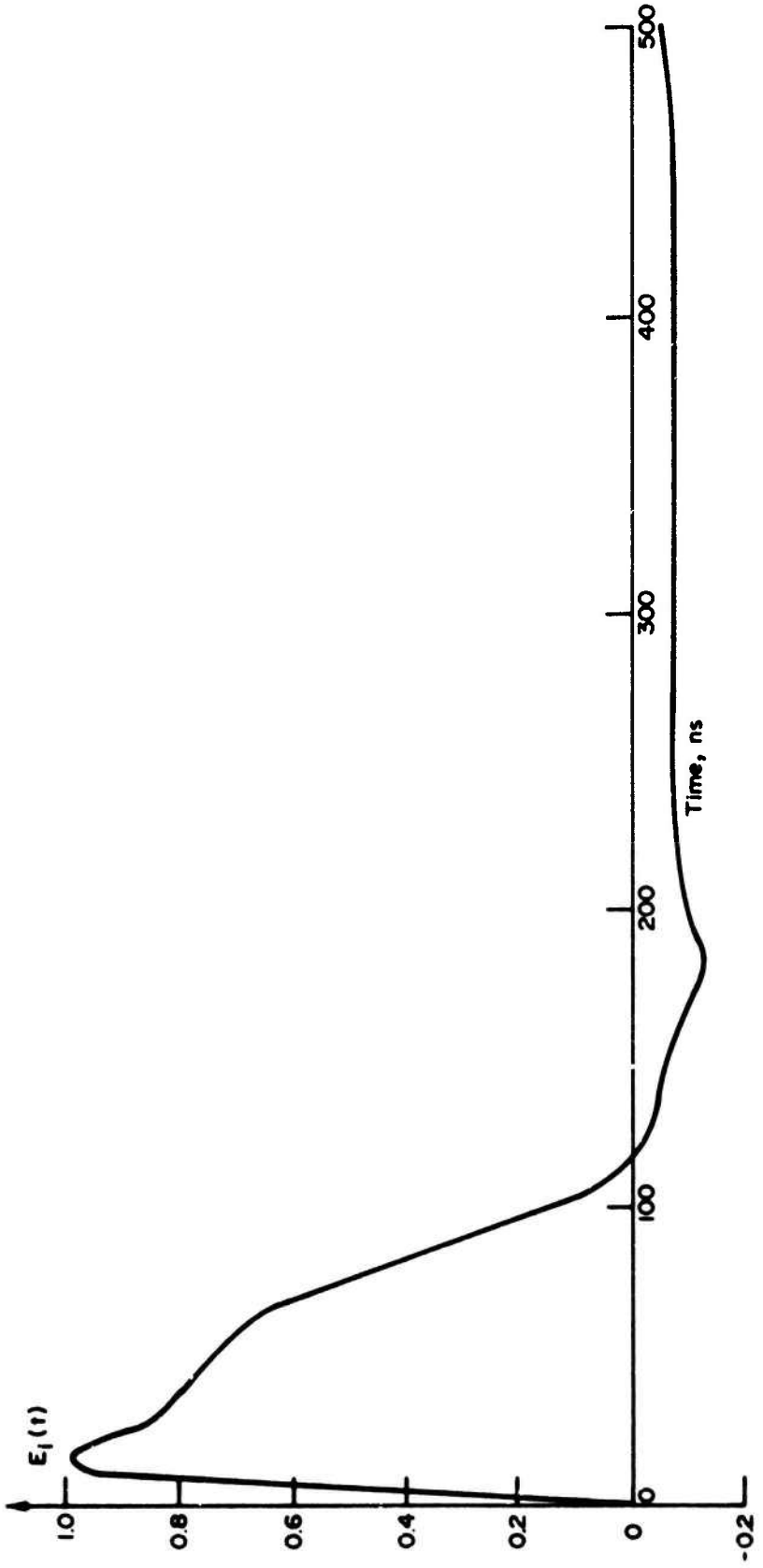

Fig. 3.17 EMP WAVEFORM FOR PARABOLIC/FEED ANTENNA SYSTEM

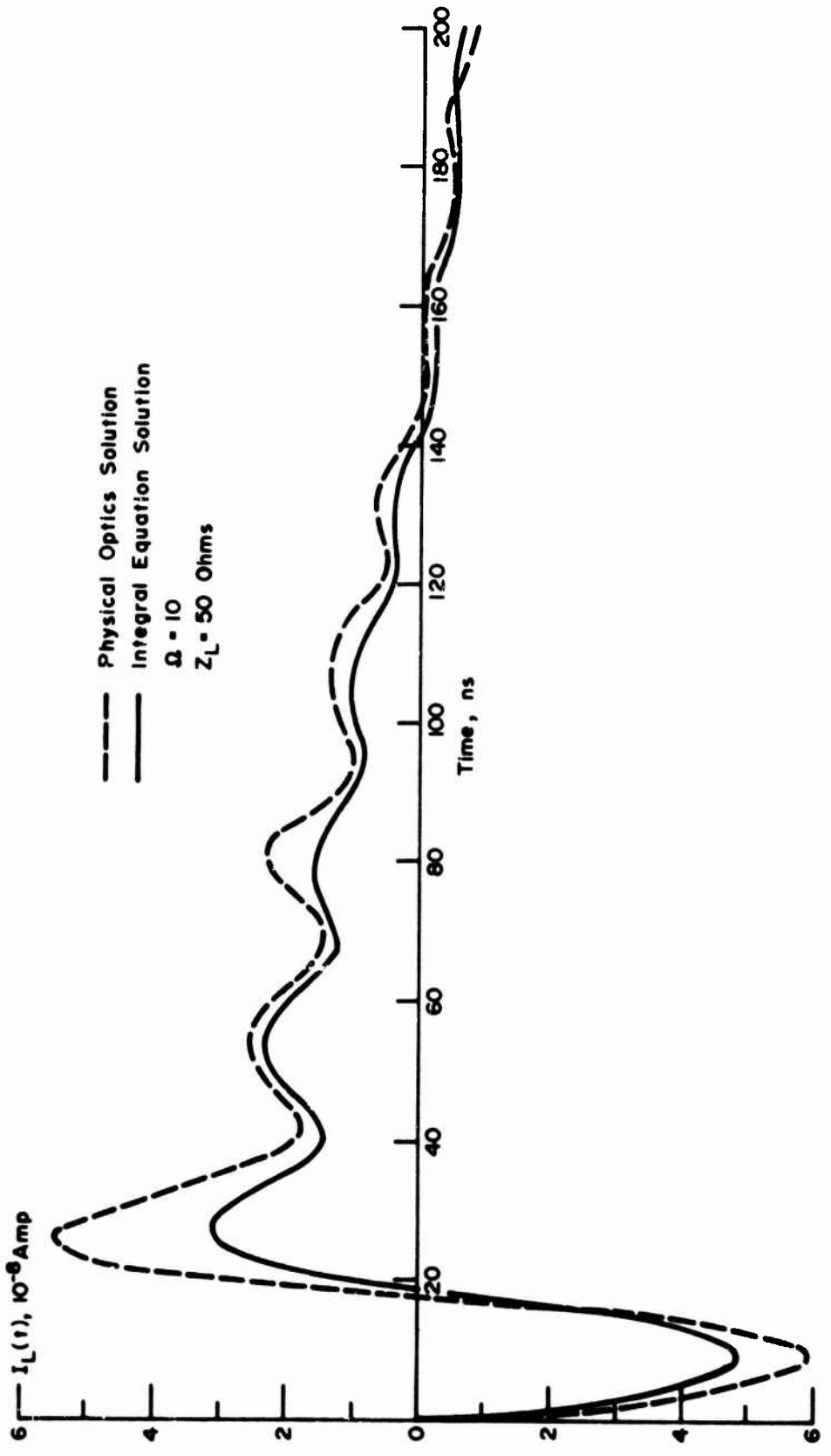

Fig. 3.18 TIME HISTORY OF THE LOAD CURRENT, $I_L(t)$, FOR A RECEIVING DIPOLE FEED ANTENNA IN FREE SPACE

very little EMP energy appears at these frequencies. The waveguide acts as a very effective filter for the lower frequencies which contain the majority of the EMP energy.

Systems which use cable for the antenna feed require filters and/or amplitude limiters, which are discussed in Chapter 4, to keep the transmitted EMP energy below the damage threshold. The data obtained from the antenna calculations establish the characteristics and ratings of the protective device which is used.

One of the simplest measures for preventing the energy which is collected by an antenna from entering the ship is an operational technique. If redundant antennas are available, only one antenna should be used at any one time. The other antennas should be isolated by disconnecting them from the cable connection. An automated switching system, which senses when an antenna is not being used and responds automatically by terminating the antenna at its base, is a very effective way to protect against the effects of EMP.

Antenna-like structures, such as gun turrets, aircraft, missiles, antenna masts, beacon masts, etc., which are in proximity to cables, must be well grounded so that the collected energy is shunted to the ship's hull. The cables must be run close to the structures to minimize the area in any ground loops which are formed.

3.3 Cables

Electromagnetic pulse phenomena will result in transient currents on cables which are exposed to the fields. If the cables are not shielded, the currents will be induced directly on the cable center conductors and conducted to the interior of the ship, where the energy will be applied to the terminals of the equipment served by the cables. For shielded cables, the induced sheath currents will couple some energy to the center or cable core conductor which is then conducted to the terminals of electronic equipment. For both shielded and unshielded cables, the current produced by exposure to the exterior electromagnetic fields will also radiate energy in the interior of the ship, resulting in energy transfer to electronic systems which are not associated with exposed cables.

The understanding of cable coupling mechanisms will aid the system engineer in selecting cables and in designing cable layout geometry to minimize the coupled energy and to choose appropriate protective measures based on the characteristics of the coupled waveform. This section has been prepared primarily to present cable coupling considerations in such a format that desired results and data can be obtained with a minimum of extraneous calculations. Simplified models are developed from which the relative importance of many cable variables can be assessed for their effect on the characteristics of the coupled waveform.

3.3.1 Mechanisms of Cable Pickup

To gain insight into the fundamental characteristics of cable coupling, it is convenient to view the pickup mechanisms for cables in terms of two constituent parts, viz., sheath current and core current pickup. This is necessary due to the large variety of existing cable configurations and the complexities associated with the problem.

3.3.1.1 Sheath (Outer) Current

One way a coupling structure can collect energy from an impinging field is by electric induction. In effect, charges on a conducting surface are separated by the tangential component of the impinging electric field which results in current flow. The overall result is that a voltage source distribution is induced on the wire conductor consisting of incremental (point) voltage generators. The contribution of each point generator to the current at some point on the conductor is determined by its transfer admittance, which is a function of the source and observation points. This concept is illustrated in Figure 3.19.

A coupling structure can also collect energy from an impinging field by magnetic induction. The induced voltage is equal to the negative time rate of change of the enclosed magnetic flux. This concept is illustrated in Figure 3.20.

3.3.1.2 Core (Internal) Current

The mechanisms for producing core currents in cables, as shown in Figure 3.21, generally include electric field penetrations through apertures, as well as the sheath current effects, better known as the transfer impedance mechanism. Recently, other pickup modes such as the so-called "obscure" mode of pickup have also been observed. These mechanisms are briefly discussed in the following paragraphs.

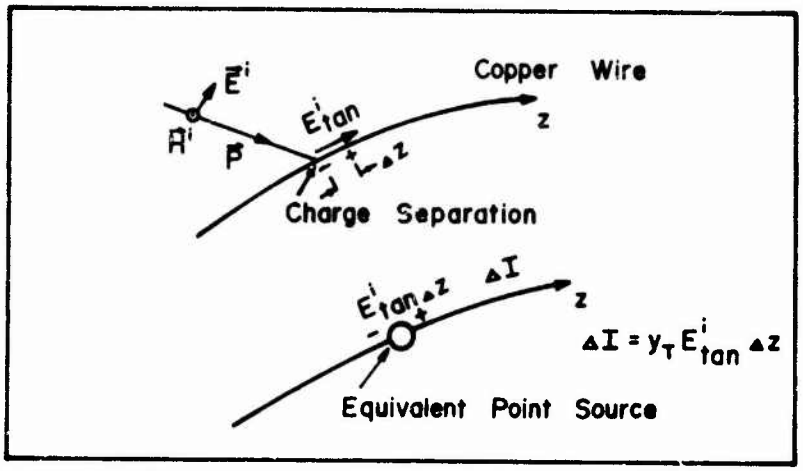

Fig. 3.19 ELECTRIC INDUCTION

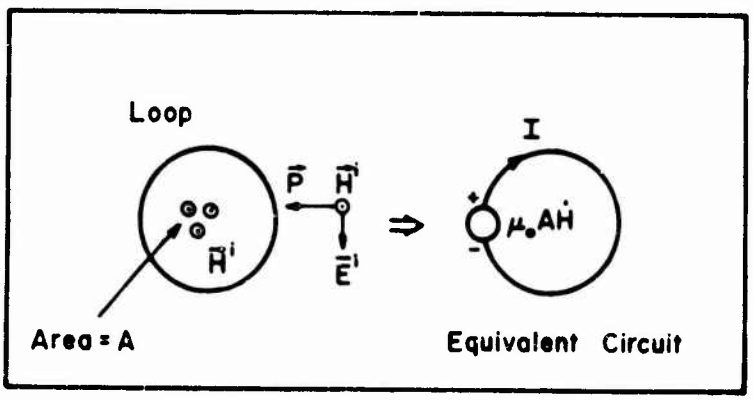

Fig. 3.20 MAGNETIC INDUCTION

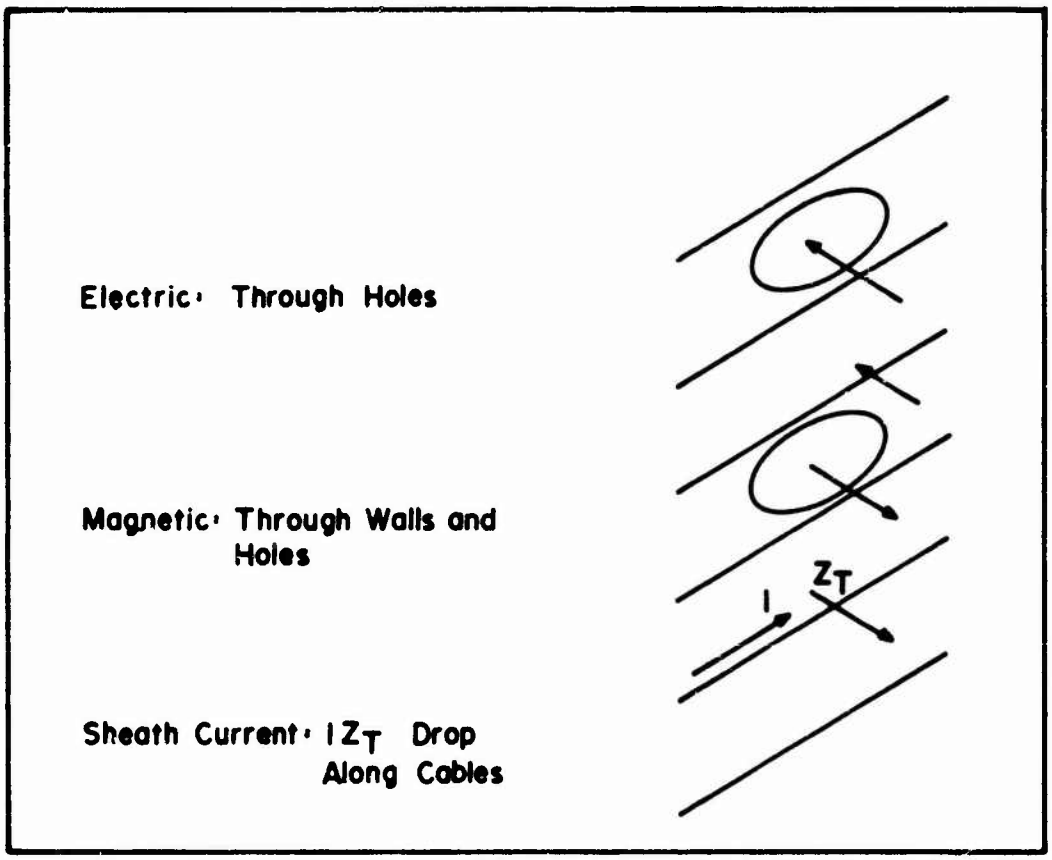

Fig. 3.21 CORE CURRENT PENETRATION MECHANISMS

3.3.1.2.1 Aperture Mode of Pickup

If a cable shield has holes or apertures, these holes or apertures would provide a means for the exterior fields to penetrate into the interior region of the cable where the internal core currents are induced. It is known from electromagnetic diffraction that, for the large aperture or high-frequency limit, a reasonably good description of the aperture effects is obtained by approximating the tangential electric field in the aperture plane by its unperturbed incident wave.

The EMP spectrum, however, covers an extremely broad frequency band extending from very low frequencies to frequencies in the MHz range. Thus, a significant portion of the EMP energy appears in the very low frequency range where the above approximation is no longer valid. When the apertures have dimensions which are small compared to a wavelength, an entirely different mechanism is noticed. This was the small aperture theory suggested by Bethe[13] in which the fields in the neighborhood of the aperture are treated by static or quasi-static methods. To a first order approximation, a small aperture in a conducting wall is equivalent to an electric dipole normal to the aperture and having a strength proportional to the normal component of the external exciting EMP field, plus a magnetic dipole tangential to and in the plane of the aperture and having a strength proportional to the exciting tangential magnetic field. The constants of proportionality are properties that depend upon the aperture shape and size.

For a small circular aperture of radius $r_o \ll \lambda$, the dipole electric moment, $\bar{P}$, and magnetic moment, $\bar{M}$, are related to the incident electromagnetic fields on the surface of the outer shield in the absence of the aperture, by $\bar{P} = -\varepsilon_o \alpha_e (\bar{a}_n \cdot \bar{E}) \bar{a}_n$, and $\bar{M} = -\alpha_m \bar{H}_t$. In these expressions, $\bar{a}_n \cdot \bar{E}$ and H_t are respectively, the normal electric field and tangential magnetic field at the center of the aperture, λ is the EMP wavelength, and ε_o is the free space dielectric constant. The electric polarizability, α_e, is given by $\alpha_e = -2/(3r_o^3)$, and the magnetic polarizability, α_m, is given by $\alpha_m = 4/(3r_o^3)$.

The qualitative description of the electric and magnetic polarizing properties of an aperture is illustrated in Figures 3.22 and 3.23. Figure 3.22a shows the normal electric field of strength $\bar{E}$ at the conducting outside shield of a cable in the absence of an aperture. When an aperture is present on the conducting wall, the electric field lines are distorted, and fringe through the aperture in the manner depicted in Figure 3.22b. This field distribution is essentially that produced by an equivalent electric dipole as indicated in Figure 3.22c. The direction of the dipole is oriented normal to the aperture. Similarly, the tangential magnetic field lines shown in Figure 3.23a will fringe through the aperture. These fringing field lines as shown in Figure 3.23b are equivalent to those produced by a magnetic dipole located in the plane of the aperture in Figure 3.23c.

When the aperture is replaced by equivalent electric and magnetic dipoles, the field penetration into the cable due to these dipoles is computed by assuming that the aperture is now closed by the cable wall (or a conducting wall). The equivalent dipoles correctly account for the fields, and, hence, the energies coupled through the aperture in the outer shield into the inner region of a subject cable. It is also noted that the theory described here is an approximate one, valid only for small apertures. Specifically, r_o, the radius of the aperture, must be smaller than the shortest wavelength of the EMP spectrum.

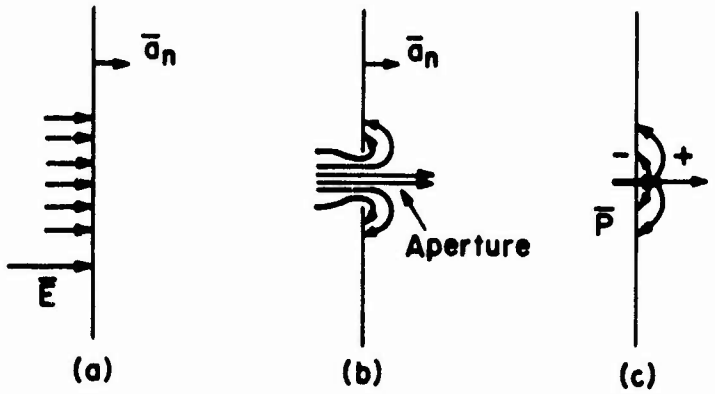

Fig. 3.22 ELECTRIC FIELD PENETRATION THROUGH APERTURE

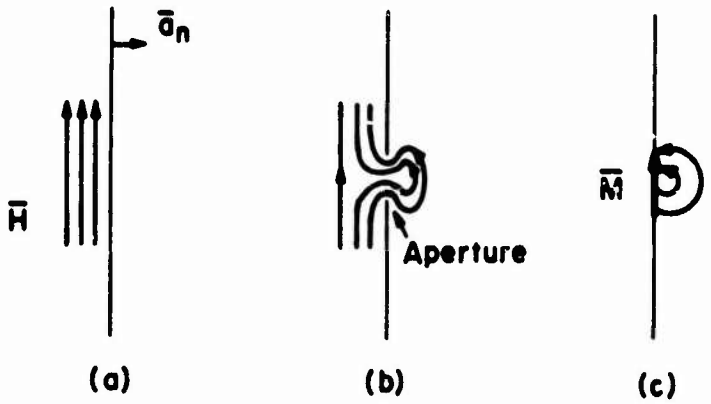

Fig. 3.23 MAGNETIC FIELD PENETRATION THROUGH APERTURE

3.3.1.2.2 Surface Transfer Impedance

When a current flows on the sheath or outer conductor of a cable, a voltage drop per unit length (surface electric field) appears at the inner surface of the outer conductor. In most situations, this is the predominant pickup mechanism by which external electromagnetic energy is coupled into the inner conductor of a subject cable. The external excitations (sheath current) and the inside voltage are related by the transfer impedance, which is defined as the ratio of the voltage appearing on the inside surface of the cable on a per unit length basis to the current flowing on the outside sheath. Hence, the transfer impedance plays a very important role in evaluating the cable performance.

A sheath current $I_S(x)$, flowing on the outer shield of the cable causes an incremental voltage drop, $\Delta V(x)$, to appear across an incremental length, Δx, on the inside surface of the outer sheath as illustrated in Figure 3.24. This voltage is given by $\Delta V(x) = Z_T I_S(x)\Delta x$, where Z_T is the transfer impedance of the cable. The transfer impedance is determined by the construction of the outer shield. Analytical expressions are available for solid-shell cables. For braided cables, the complex geometry of the cable is quite difficult to analyze in detail, and hence, the transfer impedance is most easily determined experimentally.

- Solid Shell Cables

For solid shield cables, it is useful to consider the problem qualitatively. In the very low frequency range, a current flowing on the outer shell of a solid shield cable will experience the dc resistance of the shell. There is very little attenuation due to skin effect. Therefore, at zero or low frequency, the voltage drop appearing on the inside wall of the shell will be the sheath current multiplied by the dc resistance of the shield. The dc resistance is given by

$$R_{dc} \approx \frac{1}{2\pi b\, t\, \sigma} \tag{3.22}$$

for a thin-wall shield, where "σ" is the conductivity of the outer shield, "t" is the thickness of the outer conductor and "b" is the inside radius of the outer conductor. As the frequency increases, less and less sheath current will penetrate the outer shell due to the skin effect absorption. Therefore, the transfer impedance of a solid cable is expected to become smaller.

Schelkunoff[14] has given an approximate expression for the transfer impedance of a solid shell coaxial cable, using the assumption that the thickness of the shell, t, is much smaller than its inner radius. Let "a" be the outer radius of the shell. Then if

$$t = (a-b) \ll b \tag{3.23}$$

is satisfied, the approximate expression for the transfer impedance is

$$Z_T = \frac{\eta}{2\pi\sqrt{ab}\, \sinh \gamma t} \tag{3.24}$$

where η is the intrinsic impedance of the shield and γ is the intrinsic propagation constant of the shield.

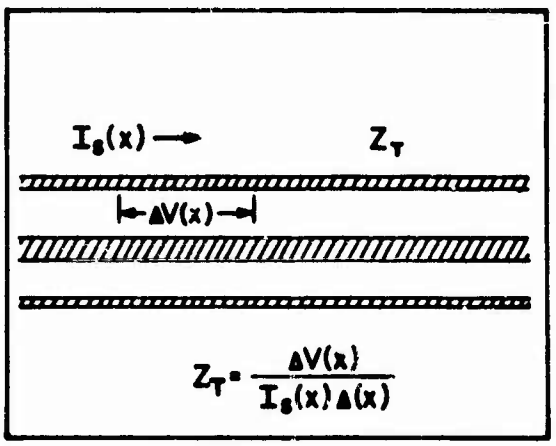

Fig. 3.24 TRANSFER IMPEDANCE DEFINITION

The transfer impedance of a typical solid shell coaxial cable is shown in Figure 3.25. For copper shells, the transfer impedance depends only upon the shield thickness, inner diameter and the square root of frequency.

- Braided Outer Shell

Figure 3.25 also shows the transfer impedance for a typical coaxial cable with a braided outer conductor. At frequencies less than 1 MHz, the behavior tends to follow that of the solid outer conductor, and at zero frequency, the surface transfer impedance is given by the dc resistance of the wires that make up the braid per unit length. Above 2 or 3 MHz, the surface transfer impedance begins increasing with frequency. Kruegel,[15] who investigated braided coaxial lines in great depth, found that this high frequency behavior was strongly influenced by details of the braid construction, e.g., optical covering factor and braid angle. Both factors determined the size and shape of the holes in the braid and, thus, the magnitude of the magnetic fields which can fringe into the interior of the cable. Apparently, it is these fringing fields which determine the high frequency behavior of the cable.

For braided cable, the surface transfer impedance, based on experimental results, is characterized by a resistance and a mutual inductance

$$Z_T = R_{dc} + j\omega M \tag{3.25}$$

where R_{dc} is the dc resistance of the braid per unit length, and M is the leakage mutual inductance of the braid. A typical value of R is 10^{-3} ohms/m and of M is 10^{-10} hy/m. For multiple shields, Kruegel[15] also found that his data confirm the expectation that the shielding effectiveness of multiple braided outer conductors is greater than that of an equivalent single braid. At high frequencies, the leakage mutual inductance is approximately given by:

$$M = \frac{M_1 M_2}{L_S} \tag{3.26}$$

where

M_1M_2 = leakage mutual inductance of individual braids

and

$$L_S = \frac{\mu}{2\pi} \ln \left(\frac{b_2}{b_1}\right) \tag{3.27}$$

where

b_1, b_2 = radii of the two shields

μ = magnetic permeability of the space between the shields.

Several coaxial cable types were investigated experimentally at IIT Research Institute (IITRI)[9] to determine their surface transfer impedances using a triaxial tester. The results for two of the more common cable types are given below:

Cable Type	Resistance (ohms/m)	Inductance (hy/m)
RG-8A/U	4.5×10^{-3}	8.75×10^{-10}
TG-9A/U	3.2×10^{-3}	1.91×10^{-11}

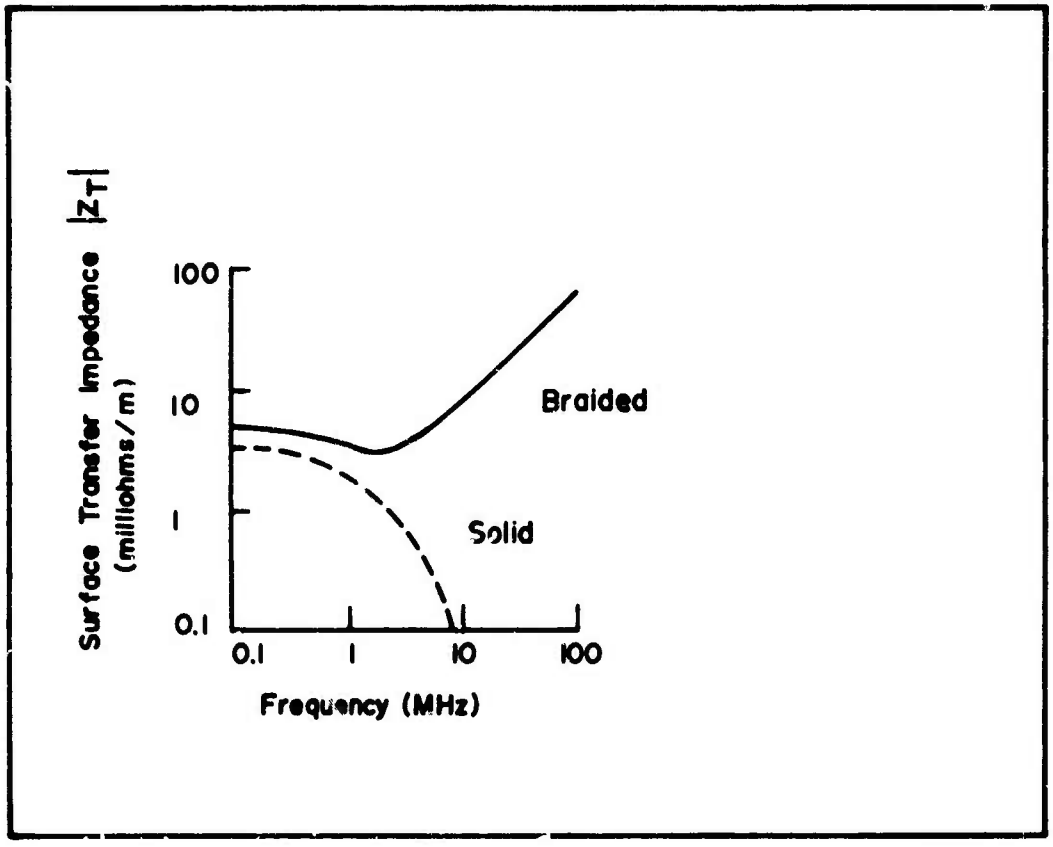

Fig.3.25 TRANSFER IMPEDANCE OF SOLID SHELL AND BRAIDED COAXIAL CABLE

3.3.1.2.3 Obscure Mechanism

The sheath current transfer impedance cable penetration mode has long been exclusively used to determine the vulnerability of important systems employing cable runs. The aperture mode of penetration discussed previously, in special situations, can be very important. Recently, other penetration modes have also been observed. Approximate analyses for several braided cable configurations indicate that the EMP pickup arising from the more obscure penetration modes can be somewhat comparable to the voltage generated by sheath current and obtained from the transfer impedance concept. A qualitative description of the more obscure modes of penetration is given below.

In the case of an electrically short coaxial cable having a braid with a number of apertures which is exposed to an axial electric field, the symmetric properties of the aperture distribution become important. An axial electric field cannot induce any voltage onto the interior region of the cable, if the aperture distribution and all other aspects of symmetry are uniform. However, this may not be true when some asymmetry of the aperture distribution is assumed in a cable run, as shown in Figure 3.26. In this case, more lines of displacement current terminate on the left inner conductor than on the right portion of the inner conductor. The portion of displacement current which penetrates the opening of the left aperture must flow through the load resistor and shunt capacitance of the cable. Thus, the symmetry of the aperture distribution, aperture size and shape, can play a major role in suppressing the axial electric field pickup associated with the electric field penetration mode.

The symmetry of the current distribution or conductivity distribution associated with the outer braid of a coaxial cable is also important. As is illustrated in Figure 3.27, if the current distributions on the outer conductor are completely uniform, and if both conductors are exactly concentric, this coaxial cable will not produce an exterior magnetic field. Conversely, such a symmetrical coaxial cable will not respond to a transverse magnetic field of an external EMP. On the other hand, if there is some mechanism (such as an imperfectly manufactured coaxial cable) which disturbs either the positional symmetry or the symmetry of the current flow, the cable will respond to the external magnetic field of an EMP. These departures in symmetry are considered in terms of displacing the inner conductor away from exact center.

For small separations, the response of the cable to an external magnetic field can be considered in terms of an open wire pair having a separation equal to the eccentricity, Δ, of the center conductor. If the separation is large, some corrections may be desirable to account for the redistribution of the outer sheath current. This is because of the proximity of the inner conductor to the outer conductor. However, such correction factors are usually small and meaningless in view of the other parameter variables normally encountered.

To determine the pickup due to the transverse magnetic field, one can first consider the reduction of the transverse external magnetic field due to the cable shielding and then calculate the penetration effect by using the eccentric displacement and the reduced value of the interior field. The reduction of the transverse magnetic field depends largely on the shielding effectiveness of the outer braid. Very few measurements have been conducted on the shielding effectiveness across the EMP frequency spectrum. For example, the shielding effectiveness of an

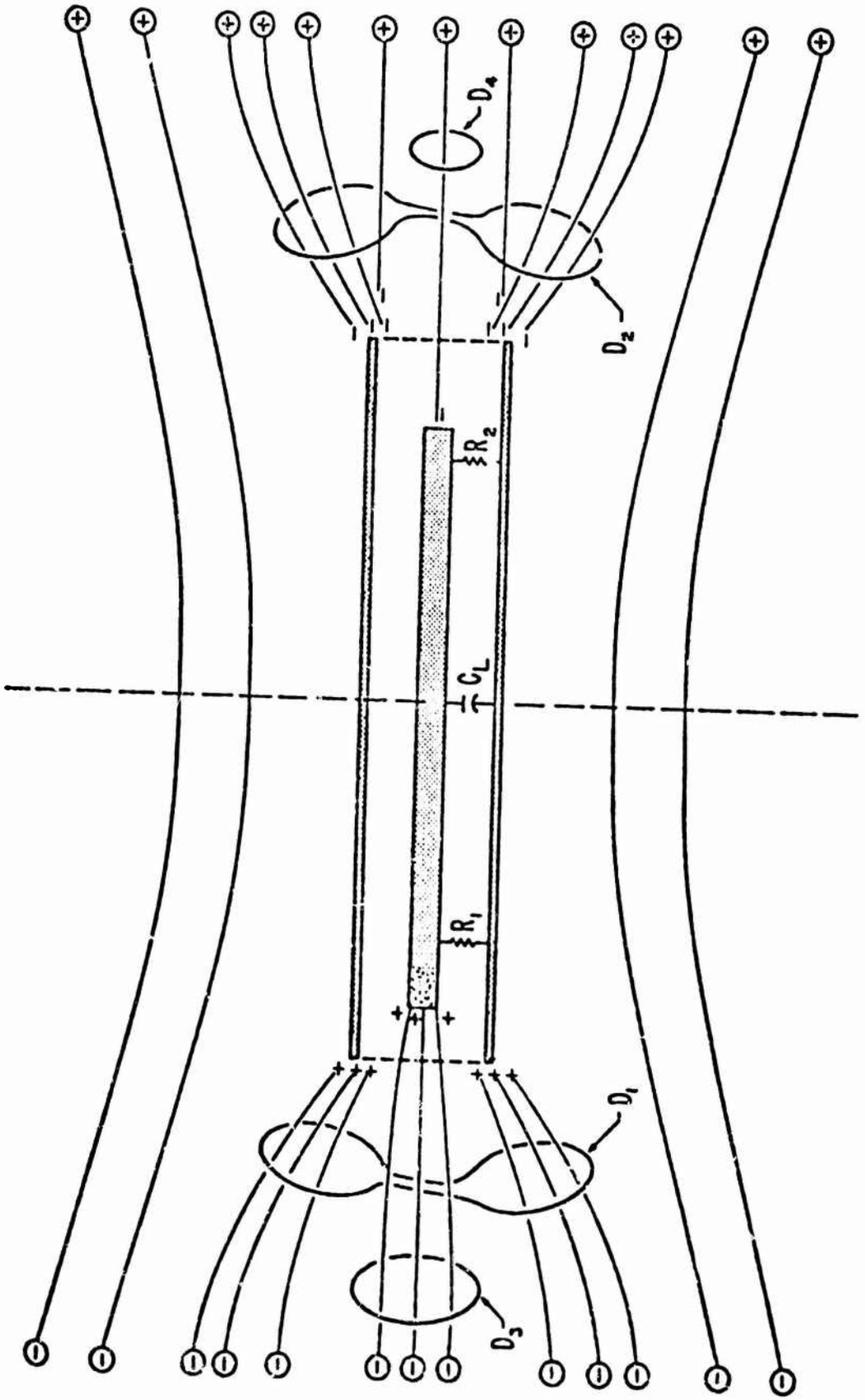

FIGURE 3.26 Asymmetric Electrostatically Shielded Coaxial Cable

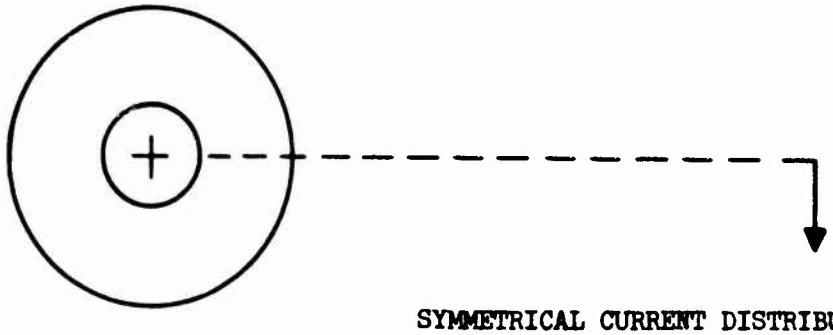

SYMMETRICAL CURRENT DISTRIBUTIONS AND
CONCENTRIC INNER AND OUTER CONDUCTOR
NO EXTERNAL MAGNETIC FIELDS OR TRANSVERSE
MAGNETIC FIELD PICKUP

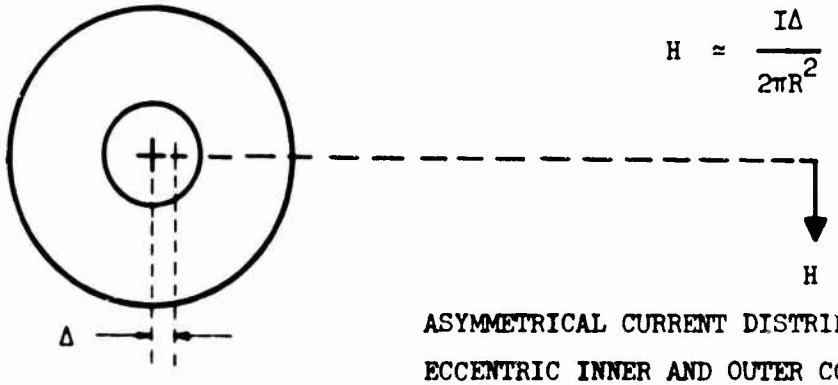

ASYMMETRICAL CURRENT DISTRIBUTION AND/OR
ECCENTRIC INNER AND OUTER CONDUCTOR
PRODUCE EXTERNAL MAGNETIC FIELDS AND
TRANSVERSE MAGNETIC FIELD PICKUP

Figure 3.27 TRANSVERSE MAGNETIC FIELD PICKUP MECHANISMS FOR COAXIAL CABLES

aluminum braided wire which might cover a multiconductor cable apparently does not exceed approximately 10 dB throughout the HF band. On the other hand, a copper braid exhibiting good optical coverage exhibited increasing amounts of shielding effectiveness at the rate of approximately 6 dB per octave from approximately 10 kHz to a maximum of about 40 dB in the middle of the HF band. Solid shields are obviously more effective, since the eddy current flow which contributes largely to the shielding effectiveness is not impaired by corrosion between conductors. In addition, skin effect absorption can also be realized for the thicker wall outer conductors. Thus, reduction of $\dot{B}$ for solid shields might range from 60 to 120 dB.

To assess the impact of this eccentricity displacement, a time rate of change of the exterior magnetic field intensity on the order of 10^{10} amperes per meter-second is of interest from an EMP standpoint. This time rate of change of the exterior field will be reduced by the shielding effectiveness of the outer conductor, either braided or solid.

These factors are assessed and the results are presented in the Table 3.1, which shows the approximate voltage pickup for a one meter section of coaxial cable having an eccentricity displacement of 0.2 or 2.0 centimeters for a transverse $\dot{H}$ of approximately 10^{10} amperes per meter-second. Typical reductions of this exterior $\dot{H}$ are also indicated by the ranges on the left.

Table 3.1 APPROXIMATE VOLTAGE PICKUP

Shield Response Range	$\dot{H}$	Δ = 0.2 cm	Δ = 2 cm
Braid Shields	10^{10} $\frac{\text{Amp}}{\text{m-s}}$	2×10^{1} V/m	2×10^{2} V/m
	10^{8}	2×10^{-1}	2×10^{0}
Solid Shields	10^{6}	2×10^{-3}	2×10^{-2}
	10^{4}	2×10^{-5}	2×10^{-4}
	10^{2}	2×10^{-7}	2×10^{-6}

An eccentricity of approximately 0.2 cm probably represents an upper bound for most of the smaller or intermediate size coaxial cables. As seen in the table, where the outer braid provides only nominal shielding, something on the order of 10 volts per meter length of the cable can be expected with lesser values of pickup as the shielding effectiveness of the outer conductor is increased.

This is by no means an insignificant value when compared to the voltage developed by the sheath current and transfer impedance mechanisms. A typical cable run quite frequently responds with a sheath current on the order of 1000 amperes. Values of transfer impedance in the HF band where the EMP has its maximum spectral

components is in the order of 1 milliohm to 10 milliohms per meter. For these values of transfer impedance, an interior voltage on the order of 1-10 volts per meter is developed via the sheath current transfer impedance mechanisms. The interior voltages associated with the transfer impedance are quite comparable to those developed by the eccentricity pickup mechanism for the transverse magnetic fields.

3.3.2 Analysis of EMP Pickup by Ship's Cabling

The common mode (bulk) current induced in cables by EMP near the conducting surfaces of the ship's outer structure is analyzed in this section as a transmission line problem. Formulas and specific data for external horizontal and vertical cables are presented in two different ways. In Appendix B, precise computer solutions of EMP pickup by ship's cabling is given in terms of such parameters as cable length, orientation, terminating impedance and distance (or height) from the ship's conducting surfaces. In the sections that follow, useful formulas that do not require detailed numerical computations are presented for estimating induced currents, voltages, and energies on cables.

3.3.2.1 Simplified Models for Ship's Cabling

Cabling throughout an all metal ship is almost always routed in close proximity to electrically conductive metal surfaces. Thus, in a majority of EMP coupling problems, the cable can be represented by a transmission line model. In this representation, the cable is considered as one conductor of the transmission line, while the nearby metallic surface is the return path for the current voltage induced by the impinging EMP.

Shown in Figure 3.28 is the simplified model that will be used to analyze the EMP pickup by ship's cabling. This model represents a large number of cables and cable-like structures which are typical of Navy ships. Cables, water pipes, ventilation ducts and cable conduits which are routed externally on or above a metallic surface such as the deck or the superstructure can be treated as a transmission line.

In addition to being representative, this simplified model can be extended to analyze the responses of more complex cable structures by using the general procedure outlined below:

1) Divide the total EMP field into its vector components.

2) Perform the following steps for each field component:

   a) Divide the cable configuration into linear sections;

   b) Determine the EMP pickup for each section;

   c) Superimpose the responses due to individual sections.

3) Superimpose the responses due to the individual field components.

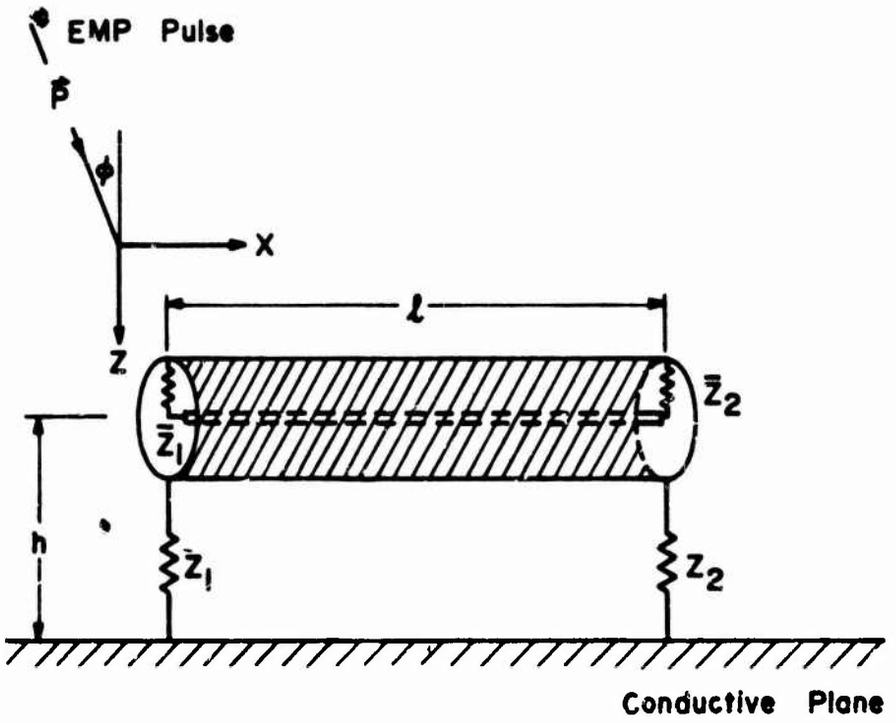

Fig. 3.28 TRANSMISSION LINE MODEL FOR SHIPS' CABLING

For example, the response of a cable loop shown in Figure 3.29 can be obtained by using the cable model of Figure 3.28, if the incident field which impinges upon the cable is replaced by the sum of the actual EMP field and the reflected field from the conductive plane at a height, d, midway between the two-wire cable. Figure 3.30 shows an example of a more complex cable configuration in which the entire cable is divided into separate sections.

In cases where cables are not routed in a straight line, the average height and average spacing can be used as an engineering approximation. Figure 3.31 illustrates a zigzag cable loop and a horizontal cable with an almost random height above the deck of the ship.

The transmission line representation of cable coupling is an important engineering model because: (1) it permits a one-dimensional analysis of the cable pickup mechanism (as contrasted to the two or three-dimensional analysis by classical EM theory); and, (2) it provides solutions that are accurate enough for the majority of engineering applications throughout most of the EMP spectrum and for the greatest number of practical cable configurations found on ships.

It must be noted, however, that when cables are routed vertically aboard a non-metal ship, the transmission line model discussed here is no longer suitable for analyzing the EMP pickup. Instead, the antenna mode of EMP coupling, discussed previously in the antenna sections, may be used to determine the EMP pickup, because a vertical cable with no nearby metallic surface or structure, from electromagnetic viewpoint, would behave as an antenna.

3.3.2.2 Estimation of Sheath Current for Ship's Cabling

Detailed and numerical results characterizing the sheath current induced on ships' cables by EMP are presented in Appendix B, Section B.1. These results were obtained with the aid of a digital computer and are based on accurate theoretical models of the cable coupling problem. This approach provides excellent details of the induced cable transients, and reveals such characteristics as peak current, resonant frequencies, decay time, etc. However, because of the need for a digital computer, and the fact that the parameter values necessary to model the cable coupling problem are not readily available for the myriad of cable configurations found aboard ship, it is of value to consider approximation techniques for this cable pickup problem. In this section, certain engineering approximations are considered which simplify the problem somewhat and which require minimal computational effort. To a great extent, these approximations are obtained by neglecting losses in the cable.

a) Matched Cable

For ships' cabling, the loads Z_1 and Z_2 (see Figure 3.28) could have some impedances due to imperfect grounding or imperfect connections. In the case that Z_1 and Z_2 are matched to the characteristic impedance associated with the conductive plane-cable line, Z_0, it can be shown that the time history of sheath currents may be expressed by the simple relations given by Equations (3.28) and (3.29), given below.

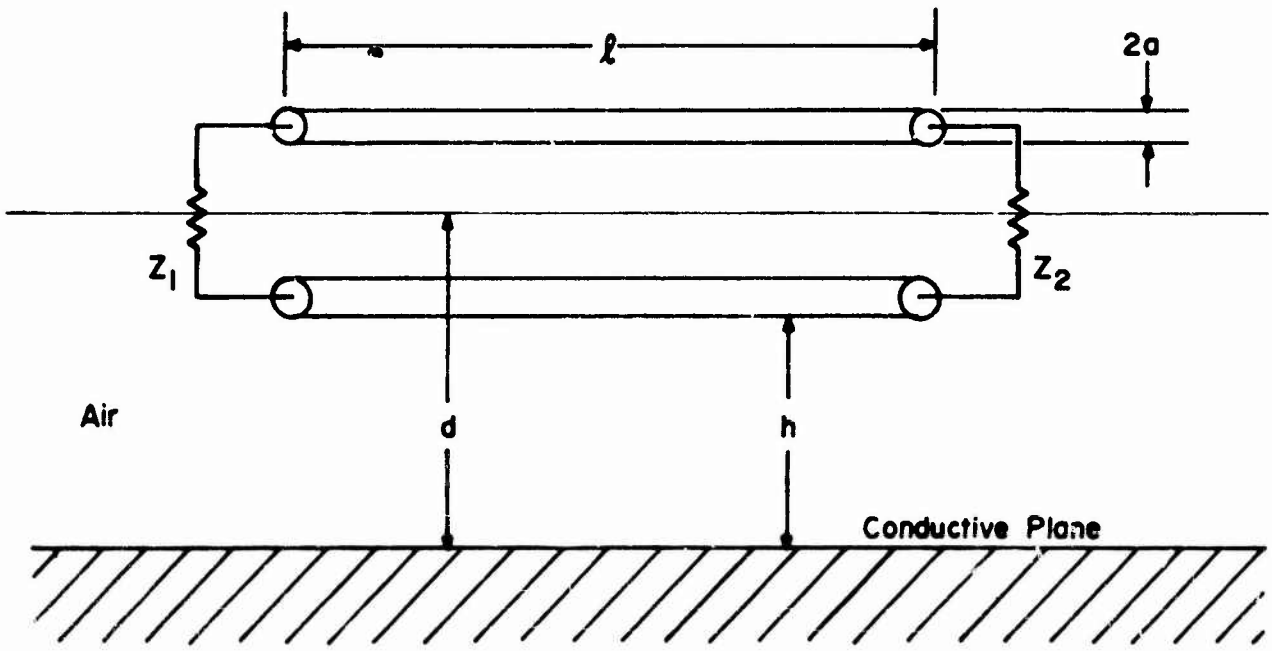

Fig. 3.29 HORIZONTAL CABLE LOOP

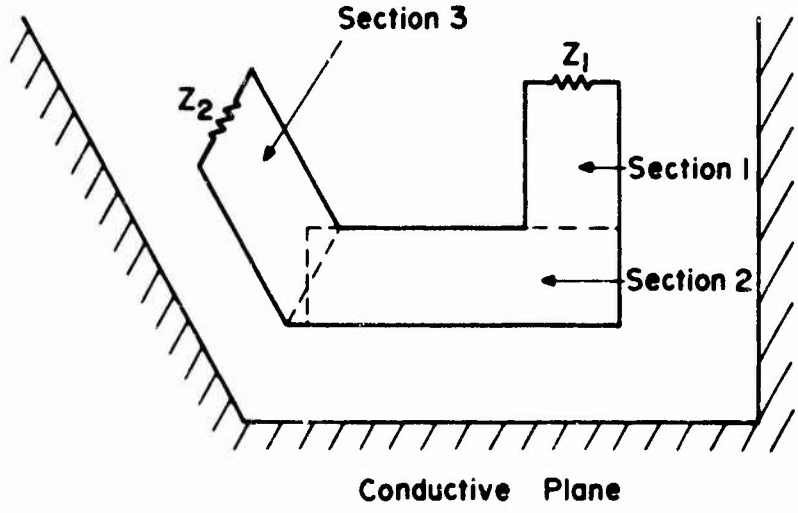

Fig. 3.30 DIVISION OF A CABLE CONFIGURATION INTO SEPARATE SECTIONS

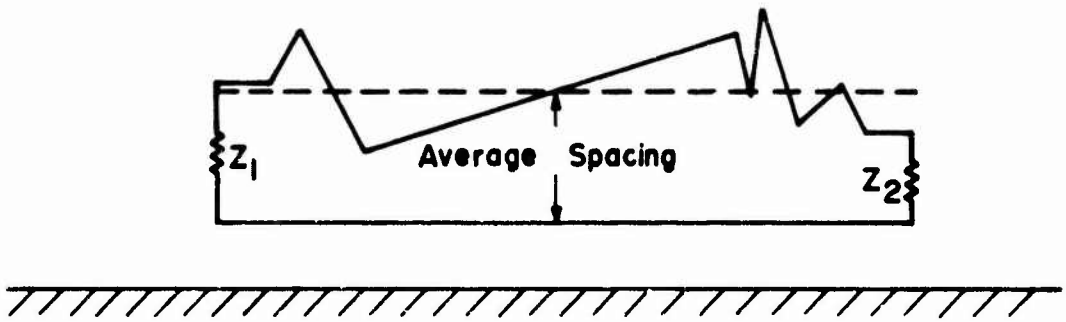

a) Zigzag Cable Loop

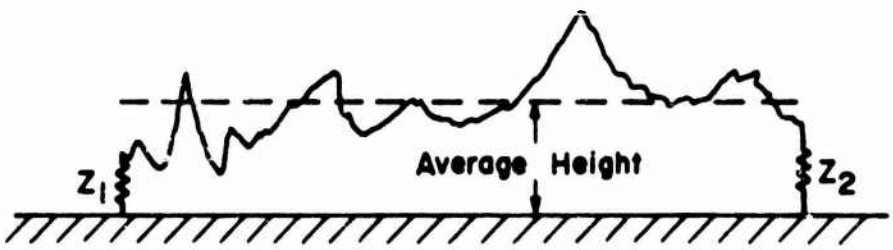

b) A Horizontal Cable With Irregular Height

Fig. 3.31

$$I_s(x=0,t) = -\left(\frac{h}{Z_0}\right)\left[E_i(t) - E_i\left\{t - \frac{(1+\sin\phi)\ell}{c}\right\}\right] \qquad (3.28)$$

at x = 0, and

$$I_s(x=\ell,t) = \left(\frac{h}{Z_0}\right)\left[E_i\left(\frac{t-\ell}{c}\right) - E_i\left(t - \frac{\sin\phi\ \ell}{c}\right)\right] \qquad (3.29)$$

at $x = \ell$, where $E_i(t)$ is the incident EMP electric field, ϕ is its incident angle, and "h" is the height of the cable above the deck.

These two simple expressions provide approximate values for the major characteristics of the desired current response. It can be seen that the maximum peak value of the sheath currents is given by $|I_{s,max}| = h\ E_{i,max}/Z_0$. In the case of an RG-8A/U coaxial cable, the characteristic impedance Z_0 is approximately 203 ohms for h = 15.24 cm. The peak sheath current induced would be about 39 amps for $E_{i,max}$ = 50 kV/m, which compared well with the saturation value in Figure B.4, Appendix B.

It is also apparent, from Equations (3.28) and (3.29), that the pulse duration is $(1+\sin\phi)\ \ell/c$ for the current at x = 0, and is $(1-\sin\phi)\ \ell/c$ for the current at the other end of the cable, i.e., at $x = \ell$. This pulse duration, as indicated, increases for the current at x = 0, as the incident angle ϕ increases. This result also agrees with that obtained in Figure B.5, Appendix B. For the grazing angle of incidence, $\phi = \pi/2$, it is interesting to note that the current at $x = \ell$ (and hence the voltage across Z_2) becomes identically zero. In this case, the current at x = 0 has a peak magnitude $E_{i,max}\ h/Z_0$ with a pulse duration of $2\ell/c$.

Since the voltages across the loads Z_1 and Z_2 are respectively related to the currents by $V(x=0,t) = -Z_0\ I(x=0,t)$, and $V(x=\ell,t) = Z_0\ I(x=\ell,t)$ it can be seen that the response due to a rectangular pulse is as shown in Figure 3.32. Plotted in Figure 3.33 is the corresponding normalized energy, W/W_n, versus angle of arrival for the rectangular pulse, where $W_n = 2h^2\ell|E_i|^2/Z_0c$. Note that for incident waveforms other than a rectangular pulse, an approximation of the incident waveform to a rectangular shape may be made.

It can also be shown that for broadside incidence, $\phi = 0°$, the time history of sheath current at any point along the cable is given by

$$I_s(x=x,t) = \left(\frac{-h}{Z_0}\right)\left[2E_i(t) - E_i\left(t - \frac{x}{c}\right) - E_i\left\{t - \frac{(\ell-x)}{c}\right\}\right] \qquad (3.30)$$

Although this expression is not as simple as Equations (3.28) or (3.29), a system engineer who needs qualitative data can easily perform the calculation on a calculator.

b) Short Circuited Cable

In many cases, cable runs between shielding compartments and superstructures should be grounded for protection purposes. This is a shield shorted-circuit condition. For the case of lossless horizontal cable illuminated by an EMP from the

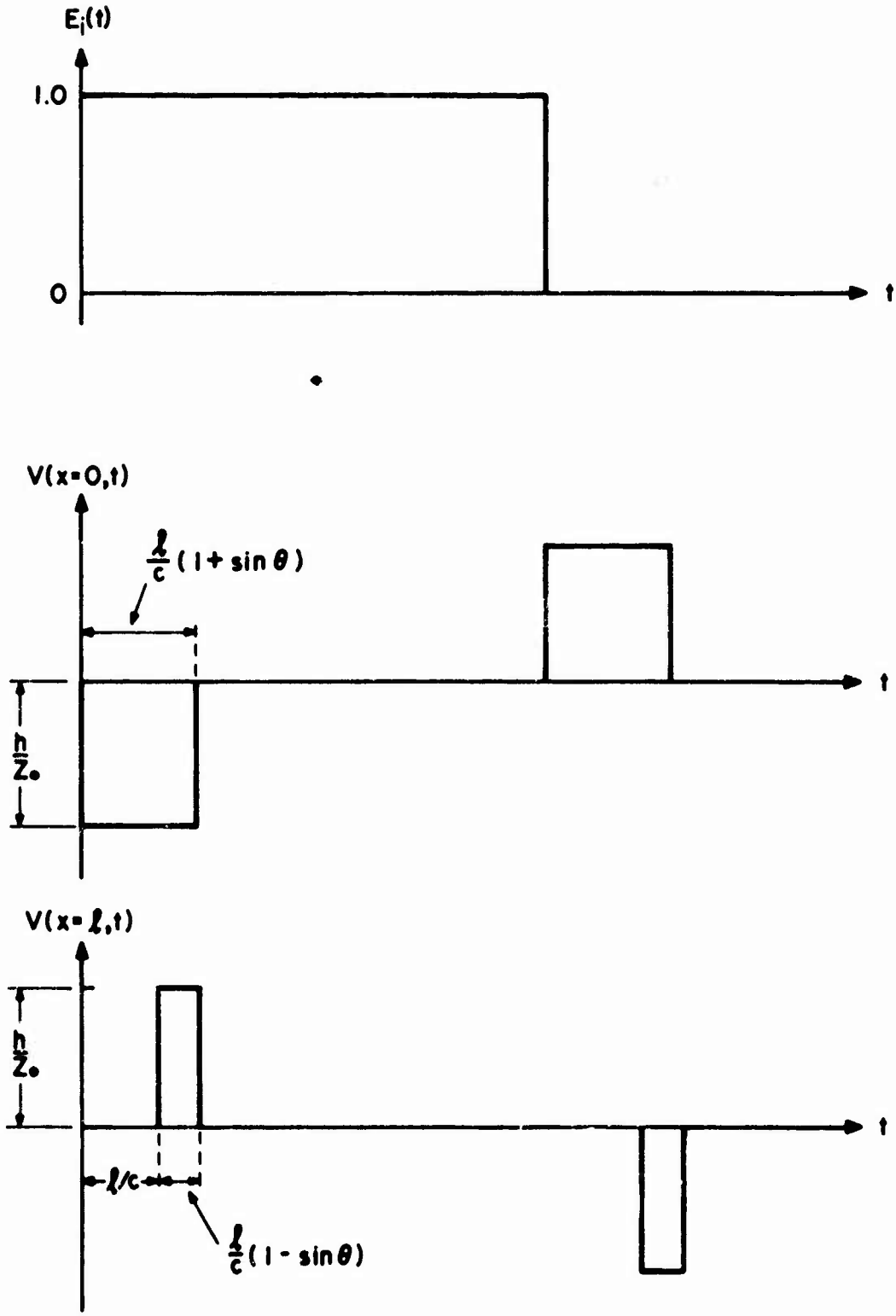

Fig. 3.32 RESPONSE DUE TO A RECTANGULAR PULSE

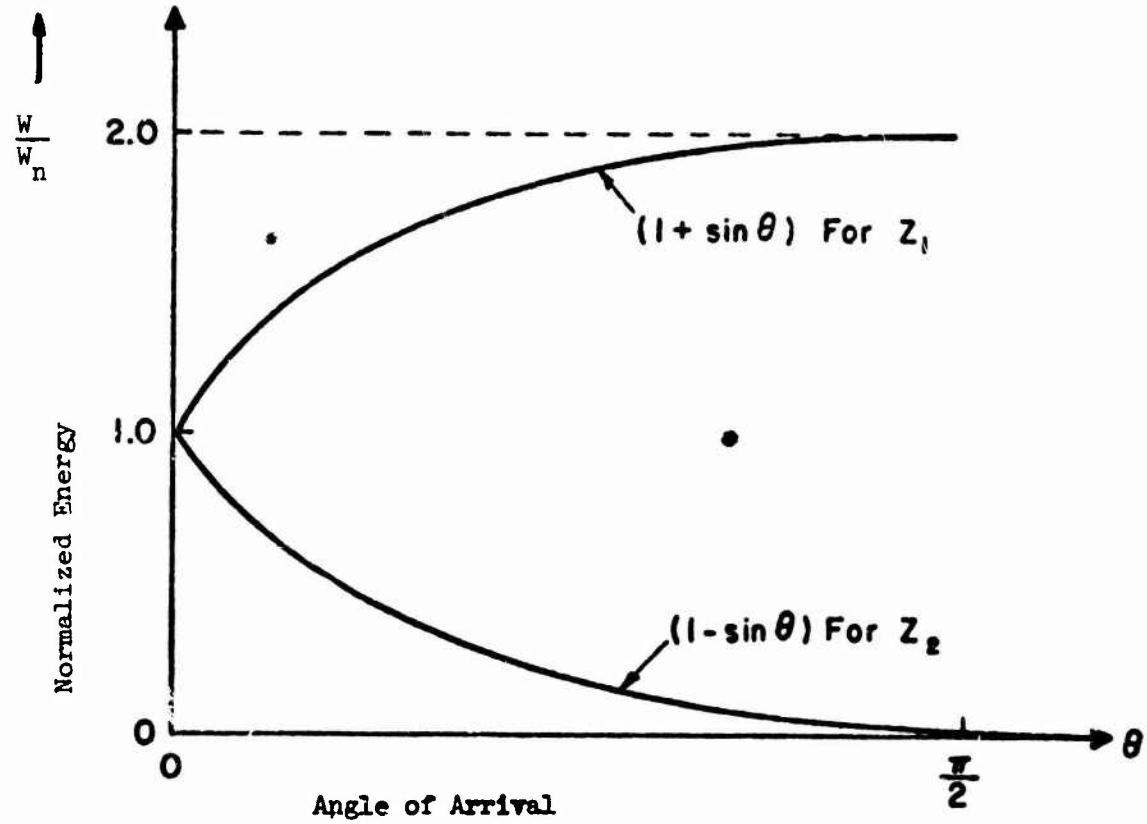

FIGURE 3.33 Normalized Energy Versus Angle of Arrival.

broadside direction, the short circuited sheath current can be expressed approximately by the following simple form:

$$I_s(x=x,t) = (-2h) \frac{E_i(t)}{Z_0} \tag{3.31}$$

Note that Equation (3.31) applies not only to the load currents, but the current at any point along the cable as well. This expression indicates that the sheath current has the same waveform as the incident EMP, but the magnitude of the current is modified by a factor of $(-2h/Z_0)$. Thus, a peak current twice as large as for matched cables can be expected.

To compare the results of the approximate analysis, which neglects losses, to the results of the exact analysis, a plot of the short circuit current obtained from computer calculations is presented is Figure 3.34. Under the same conditions, the normalized peak current is found to be about 1.5 mA from Equation (3.31) (dotted curve) as compared to 1.21 mA from Figure 3.34. It is also clearly seen that, except for the 180° phase shift, the response waveform is exactly the same as that of the incident EMP waveform.

3.3.2.3 Core Current Resulting from Surface Transfer Impedance

Surface transfer impedance phenomena result in a distributed voltage on the inner surface of the cable sheath which produces a current on the cable core conductor by transmission line coupling. Due to the distributed nature of the induced voltage and the phase variation of the EMP transient along the cable length, the calculation of the core current waveform involves the numerical solution of differential and integral equations. A simpler procedure can be used to obtain an estimated value for the peak core current by considering the situation in which all incremental voltage generators are in phase.

Under this condition, it is assumed that the phase distribution of the sheath current is such that the voltage produced by the surface transfer impedance is additive, thus allowing the voltage to be treated as a lumped source. Under transient conditions, the initial traveling wave of core current will be given by:

$$I_c = \frac{V}{Z_c}$$

$$= \frac{I_s Z_T \ell}{Z_c} \tag{3.32}$$

where

I_s = sheath current

Z_T = surface transfer impedance

ℓ = length of exposed cable

Z_c = characteristic impedance of cable

Although this relation is not valid for obtaining a time history of the core current, it is useful for obtaining the approximate peak core current, which is important when considering the type of protection scheme required for the cable.

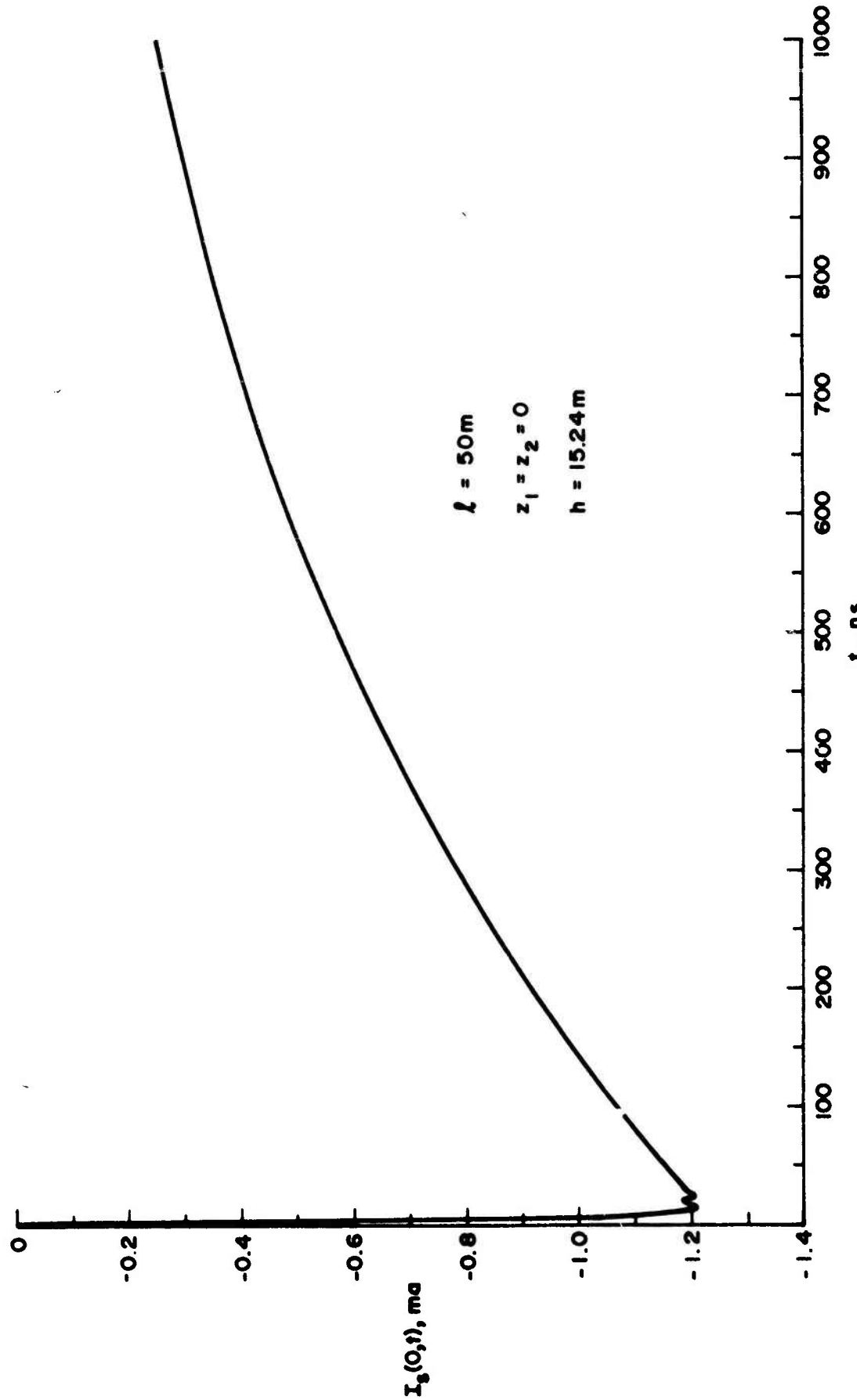

Fig. 3.34 SHEATH CURRENT WAVEFORM FOR SHORT CIRCUIT TERMINATIONS

3.3.2.4 Estimation of Cable Pickup in Terms of Energy

Because of the fact that damage thresholds for a large number of EMP sensitive electronic components are given in terms of energy levels, it is of interest to the EMP hardening engineer to determine EMP pickup by cables in terms of energy. This section is devoted to characterizing EMP pickup in terms of energy--specifically, energy coupled by the conducting element of a cable.

The joule energy delivered to the load may be computed approximately from the time waveform of either the load current or the voltage across the load, as follows:

$$J = R_e \int_0^T I_L^2(t) Z_L dt = \int_0^T \frac{V_L^2(t)}{R_L} dt \qquad (3.33)$$

where R_e denotes the real part, $R_L = R_e(Z_L)$ and Z_L is the load impedance connected to the cable. The load impedance may be an impedance other than a pure resistance. It would include the input impedance of the equipment which is connected to the cable. Note that the load voltages across the loads Z_1 and Z_2 (or $\bar{Z}_1$ and $\bar{Z}_2$) are related to the load currents by $V(x=0,t) = -Z_1\ I(x=0,t)$ and $V(x=\ell,t) = Z_2\ I(x=\ell,t)$. The time, T, of Equation (3.33), in principle, is defined as the time when the waveform decays to zero. As an approximation, however, T could be truncated at the time when the response contributes negligible energy to the cable, compared to that in the period of early rise time. In addition, one could also approximate the time history of the load current (or load voltage) by a much simpler waveshape.

Consider a horizontal cable 50 meters long situated at a height of 15.24 cm above the deck plane of a Navy ship. (The cable is exposed directly to an electromagnetic field with a field intensity of 50 kV/m.) The outer conductor (the shield) is assumed to be shorted at both ends of the cable. If the load impedances, $\bar{Z}_1$ and $\bar{Z}_2$, between the core conductor and the inner shield are both matched, the time history of the load current has a waveform as shown in Figure 3.35, which could be approximated by a simpler waveform of rectangular shape as indicated by the dotted line in the figure. The joule energy delivered to the load, from Equation (3.33) and Figure 3.35 becomes

$$J \approx I_1^2 \bar{Z}_0\ t_1 + I_2^2 \bar{Z}_0\ t_2$$

$$= 61.92 \times 10^{-6} \text{ joules} \qquad (3.34)$$

where $\bar{Z}_1 = \bar{Z}_2 = \bar{Z}_0$ and $\bar{Z}_0 = 50$ ohms. The delivered energy expressed in decibels is about -42.1 dB.

The simplest and perhaps the most primitive way to identify the cable problem area and to determine the potential failure that may be caused by the problem is to compare this collected energy by the load with the minimum damage threshold energy of the most sensitive components which may be connected to the cable as a load.

This approximate method is not meant to replace the more exact solution to obtain the delivered energy by performing the integration of instantaneous power with respect to time numerically, but it is intended to provide an easily obtainable estimate of delivered energy.

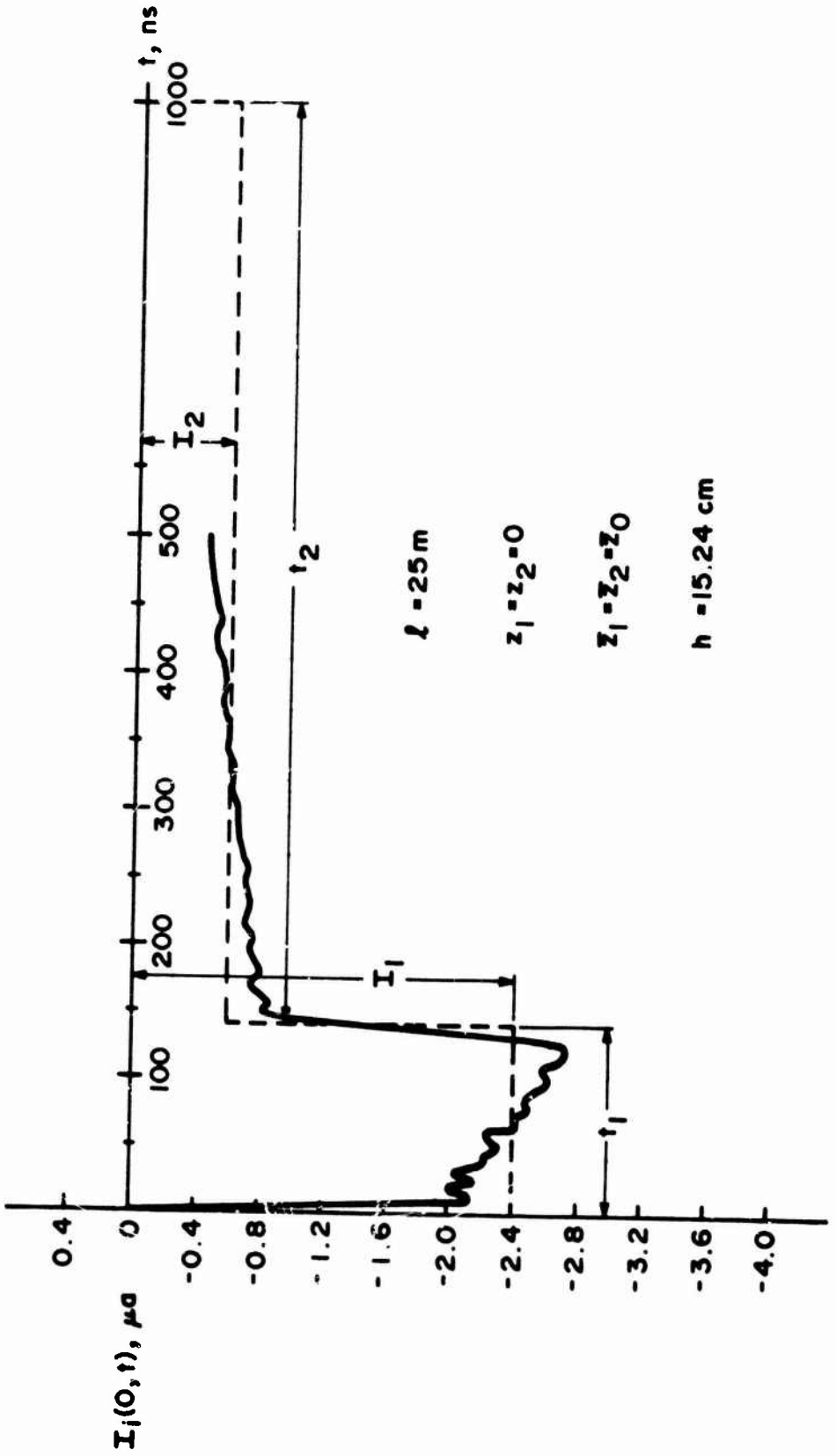

Fig. 3.35 AN APPROXIMATION TO TRANSIENT CORE CURRENT FOR A HORIZONTAL CABLE

3.3.3 EMP Hardening Techniques for Ships' Cabling

3.3.3.1 Cable Shielding

An effective way to reduce the EMP energy pickup on cables is by shielding. This can be accomplished in a number of ways depending on the type of cable, its application, and the requirements and constraints imposed by the ship's construction and equipment layout. In general, the concept of cable shielding means the use of a metallic structure that completely surrounds the cable core of inner conductors. For some cables, this can be achieved by confining them to the interior portions of the ship, thereby taking advantage of the inherent shielding characteristics of the all-metal ship. This approach, however, has certain limitations. The all-metal ship is not an ideal shield because of the large number of apertures, cable and pipe penetrations that permeate its entire interior structure. Hence, to use the ship's structure as a shield for interior cabling, care must be taken to EMP-harden or control these interior apertures and/or penetrations.

More localized techniques for cable shielding include the use of conduit, ducting or cables which are manufactured with solid or braid-type shield. Ducting or conduit, when installed by threaded or welded joints, can provide excellent cable shielding. To insure good electrical conductivity across these joints, all threaded connections should be subject to a torquing specification. In welding, a continuous weld around the entire periphery of the joint should be made. A typical layout of a conduit/ducting system for ships' cabling is shown in Figure 3.36.

Voltages and currents induced on conductors within conduit have complex waveforms. Basically, the voltages and currents depend upon the following factors:

- Surface Current

The currents flowing along the conduit which are produced by the external field environment generate a voltage drop due to the resistance of the conduit. This voltage can be coupled into conductors within the conduit. Rusted and corroded threads will introduce series impedance along the conduit's length, resulting in larger voltages. Therefore, cleanliness and careful assembly are very important in an EMP protection program.

- Dimension and Material

The diameter and wall thickness of the conduit are factors in energy penetrations. In general, there is less coupling into contained conductors within large diameter conduits than into small ones. Induced voltages on conductors within the conduit vary inversely to the square of the conduit wall thickness.

The voltages induced on conductors in conduits are also directly proportional to conduit length. Figure 3.37 shows that the induced voltage increases as the length of conduit runs increases, and dictates that a careful design to minimize the length of conduit runs is necessary.

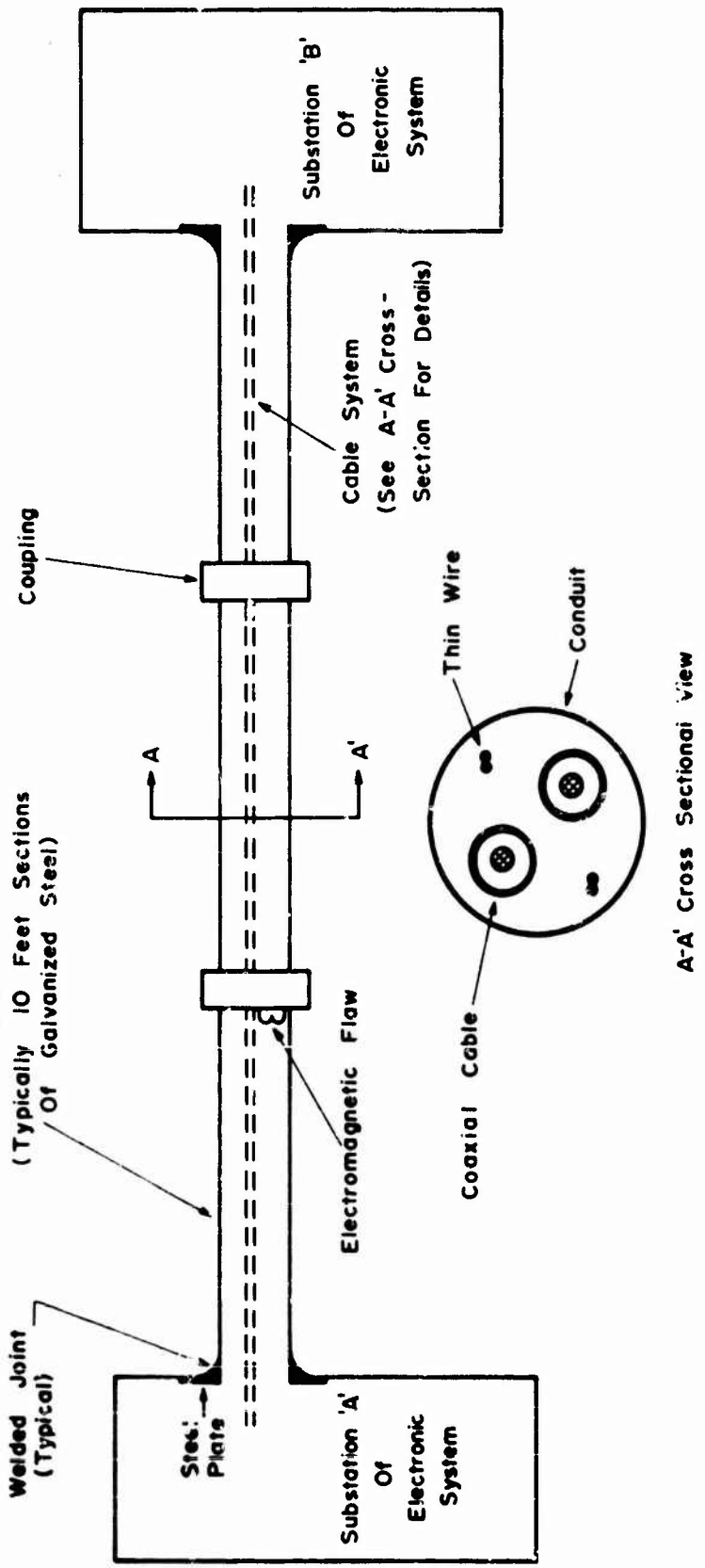

Fig. 3.36 TYPICAL LAYOUT OF CONDUIT/CABLE SYSTEM

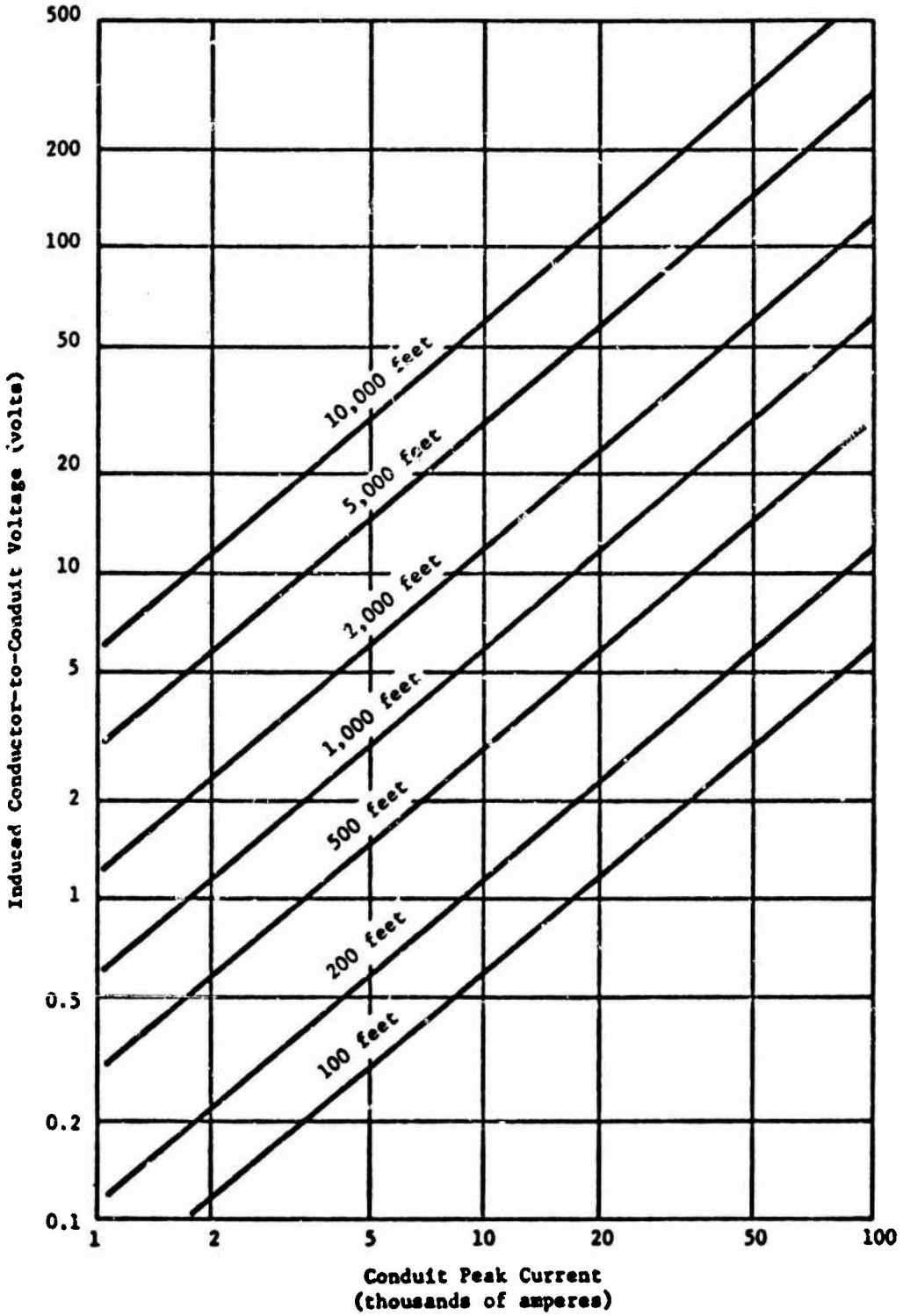

FIGURE 3.37 Conductor voltage vs conduit peak current for varying lengths of standard rigid steel conduit 2 inch trade size or larger with welded joints or threaded couplings (Reference 16).

Also important is the type of conduit material used. Higher magnitudes of induced voltages tend to appear on low permeability conduits, such as those made of aluminum, than on those of high permeability, like steel. Properly installed, galvanized continuous steel conduits with thick walls (typically 1/4 to 3/8 in.) are very effective.

- Number of Couplings

The induced voltage within a conduit is directly proportional to the number of couplings in a conduit run. Assuming that all the joints are constructed to a high standard of workmanship, Figure 3.38 shows the induced voltage inside the conduit versus the external magnetic field. Note that poorly made or loose joints could increase these induced voltages enormously. This suggests that electrically-conducting sealants on threaded couplings or continuous welds at threaded couplings are desirable.

- Bending

The number and kind of bends may influence both the magnitude and waveshape of induced voltages on the inside conductors. As illustrated in Figure 3.39, these induced voltages are directly proportional to the number of bends.

Higher conductor voltages may be induced in severe, short-radius bends than in gradual ones. This is partially the basis for generally avoiding the use of condulets in conduit assembly. Another reason is that the condulet covers may be accidentally removed or omitted, resulting in extremely high flux leakage into the conduit with consequent increases of voltages on the inside conductors.

- Conductors Within the Conduit

Voltages induced on parallel-pair cables are generally higher than on twisted-pair cables because of the greater area presented to the EMP leakage flux. Cables constructed with wound or braided shields within a conduit are effective in reducing the induced voltages, provided such shields are properly grounded. The actual position of conductors within the conduit also affects the induced voltage pickup. However, from a design standpoint, this is hard to control.

A conduit system must give dependable and effective shielding against EMP penetration for the internal conductors of the cable, and it must be bonded to the hull/deck/bulkhead of the ship at entry in such a way as to guarantee that none of the shield current can enter the ship. The conduit should collect all the incident EMP energy and, through carefully controlled grounding practices, disperse this energy on the outer skin of the ship where it will do no harm. Wherever a conduit passes from an external to an internal space it must be circumferentially welded to the hull/deck/bulkhead at the point of entry on the external side. This also applies when a conduit must pass from the outside to an enclosed area in the superstructure.

It should be pointed out here that to insure water tightness of the ship, cables that pass from the external environment to the internal ducting can still be routed through stuffing tubes that terminate internal to the duct.

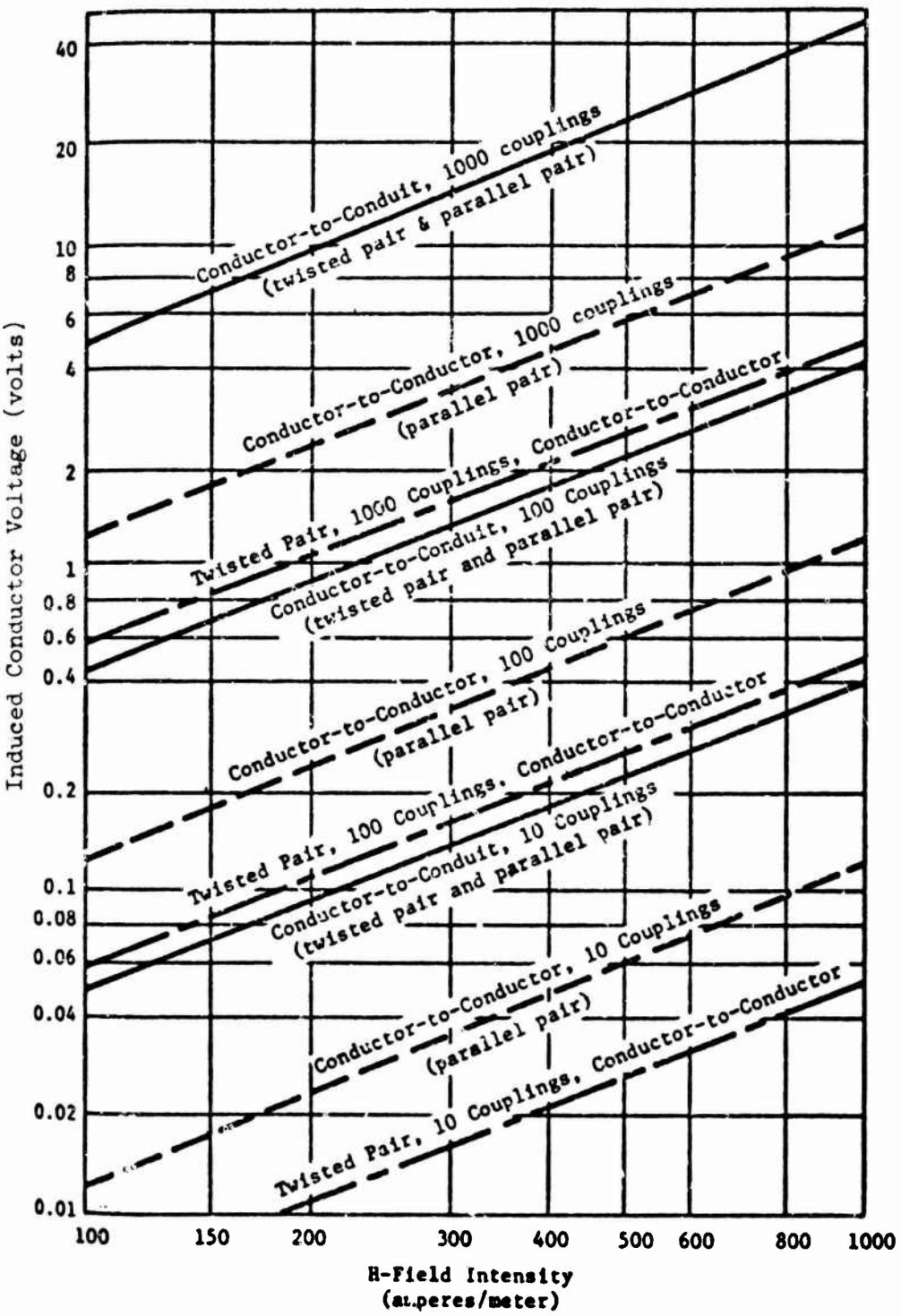

FIGURE 3.38 Conductor voltage vs H-Field intensity for varying number of couplings in standard rigid steel conduit, 2 inch trade size or larger (Reference 16).

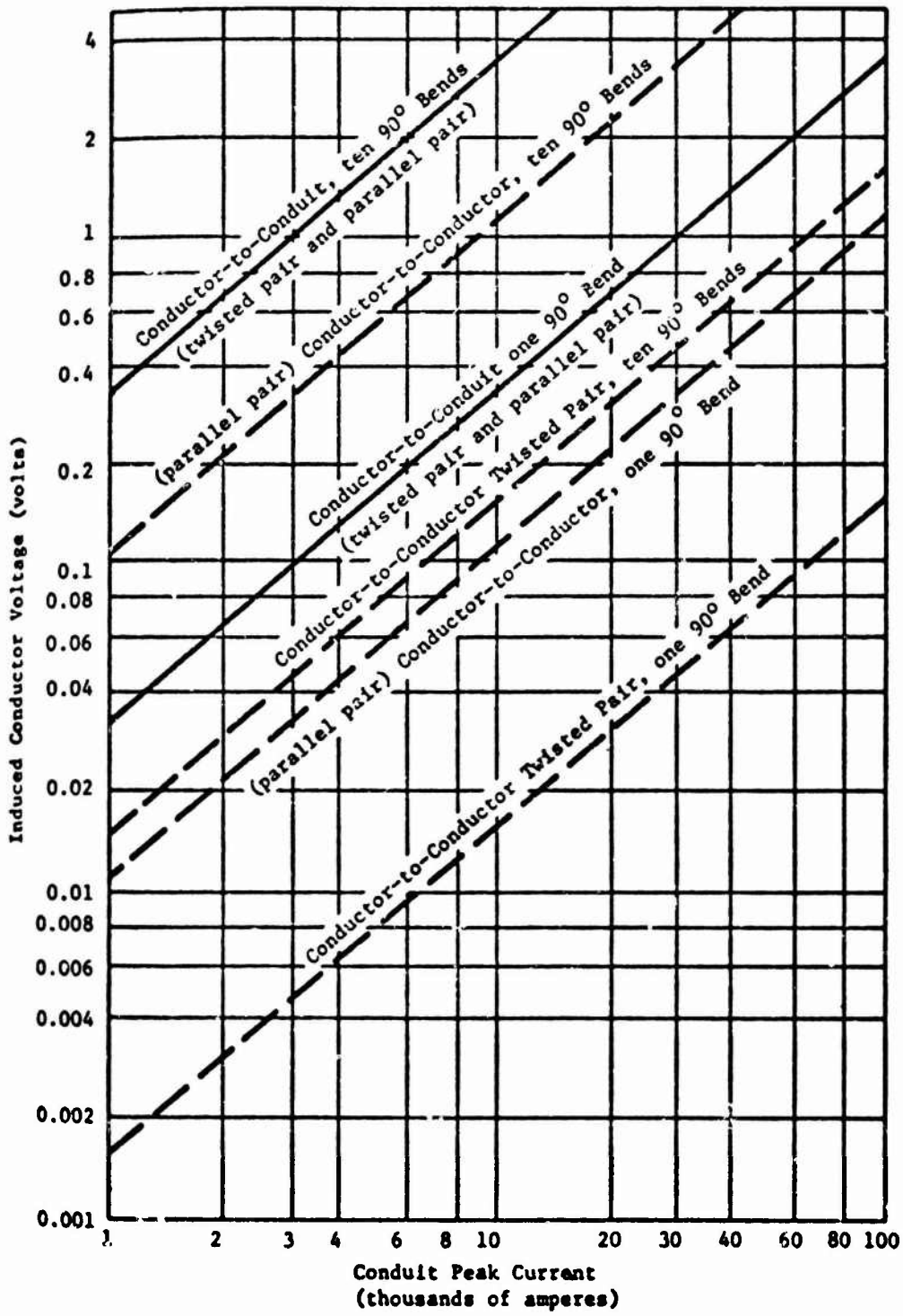

FIGURE 3.39 Induced conductor voltage vs conduit peak current for varying number of bends in standard rigid steel conduit, 2 inch trade size or larger (Reference 16).

It is only necessary to ground all cable sheaths to the outer surface of duct or bulkhead before entering the duct.

Recognizing that all external cables, including those cables that are routed through compartments with windows or portholes and throughout the hangar area, should be in ducts, it is important to note that branch cables from these ducts to permanent equipment in these areas should also be enclosed in ducts or conduit. The branch conduit is to be welded to the main conduit at the point of entry. Connection to the equipment may be accomplished with threaded connectors to provide for easy removal.

In either case, the cable shield/conduit must have good electrical contact with the outer shell of the connector and this shell must provide good electrical contact with the outer skin of the duct.

The cable conduit will prevent the cables from behaving like antennas. If protective devices, such as spark gaps, are not installed at the antenna, the energy picked up will be carried into the duct system. It is imperative that this energy be dissipated before the conduit enters an internal space. To accomplish this, it will be necessary to provide cable vaults. Every cable which comes down the mast in a conduit containing a cable from an unprotected antenna must be filtered and/or surge arrested within the vault to prevent energy from entering the ship.

To aid in running cables and to provide a convenient structure on which to locate entry/exit connectors or branch conduits, metal access boxes may be placed, as needed, along the conduit. To prevent degradation of the duct system, the box should also be constructed of 1/4 inch steel with rounded corners and the conduit should be circumferentially welded to the box. The access cover should be RFI gasketed and bolted shut. The mating surfaces must not be painted and, ideally, the access cover should never be removed at sea. Lastly, the box should be welded to the supporting structure.

3.3.3.2 Cable Routing

Proper considerations of cable routing in a ship could significantly reduce the EMP pickup on system cables. One of the important considerations of cable routing to protect against EMP pickup is the total length of the cable. The less total cable length used in a ship, the less EMP energy coupling. Another important aspect of EMP cable routing is to avoid ground loops. While it is desirable to avoid ground-loops, this can only enhance protection if the cables under consideration are within a shielding enclosure. If the cables are not within a shielded enclosure, these cables will collect substantial current, no matter how they are geometrically arranged. It can be shown that, in certain situations, a straight cable run can collect more current than a loop of comparable dimensions. In general, however, it is best to lay out the cable systems in a radial or tree fashion. Figure 3.40 illustrates these wiring systems. The purpose of such wiring configurations is to avoid forming ground loops which would provide additional pickup.

Cable runs in a ship usually take the shortest or most convenient route; consequently, a cable might pass through a mission critical area (though it serves no function in that area). As a result, higher fields are produced in such areas due to the additional coupling. Therefore, it is suggested that

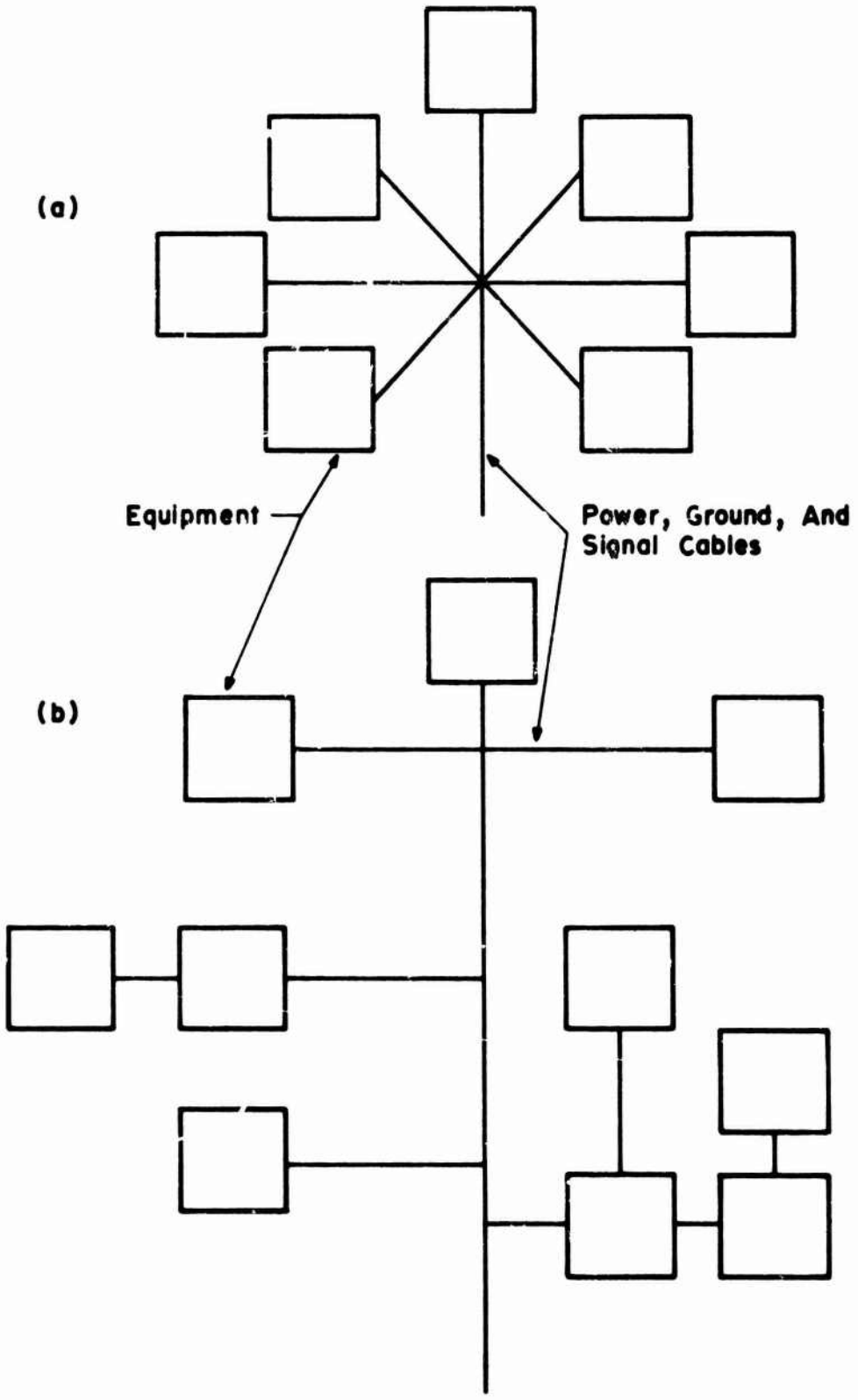

Fig. 3.40 RADIAL (a) AND "TREE" (b) WIRING SYSTEMS USED TO REDUCE EMP SUSCEPTIBILITY

all cables which are not terminated or serve no purpose in these shielding areas should be routed around the shielded areas. In addition, cable bundles should be grouped or zoned in terms of their specific power and signal transmission functions. Power cables, control cables and RF communication cables, for example, should be grouped in separate bundles or conduits. The distance spacings between them should be adequate to keep their interaction or coupling to a minimum.

3.3.3.3 Penetration Treatment

EMP energy may penetrate from exterior to interior regions of a ship via the induced sheath currents on cables. If the outer sheath is not properly bonded to the bulkhead, the sheath current will not be entirely dissipated on the skin of the ship. As a result, currents will penetrate into the interior region of the shielding compartment. This current will reradiate EMP energy which, in turn, could be coupled to other cables or sensitive electronic equipment within the compartment. Therefore, the effects of cable penetration could, in principle, couple EMP energy into all portions of a Navy ship.

Two techniques to avoid such EMP energy penetration are to use only a single point entry and to bond the cable shielding at the point of penetration.

- Single Point Entry

Preferably, all cables that terminate within a shielded space should enter/exit via a cable vault of "EMP Entry/Exit" room, with a single point entry. Shown in Figure 3.11 is a sketch of a typical shielding shelter showing a hypothetical single point entry. In this "EMP Entry/Exit" room, all the protective devices and/or techniques (such as grounding, isolation, limiters, filters, etc.) necessary to reduce EMP penetrations into the hardened area via these cables, ducts, etc., would be housed. The bulkhead defining the outer wall, where the cables and pipes will enter, should be 1/4 inch or thicker steel. Conduits or steel pipes penetrating this bulkhead should be welded circumferentially on the outer surface. Any cables not in conduit should have the insulation stripped off at the entry point, and the shield is to be shorted to the bulkhead.

- Bonding of Cable Shielding at Point of Penetration

All cables which must penetrate the compartment shield must be properly terminated and protected at the points of entry. If single point entry proves impractical, more than one entry/exit vault may be considered. This might not significantly decrease the protection integrity due to the thickness of steel normally used for the interior bulkhead. Unshielded cables should be shielded and/or be in ducts before penetration. The bulkhead should have sufficient area so no penetration of cables will occur within about 5 feet of the nearest edge. The entrance should be continuously welded around its perimeter to the shielding compartment. For an illustration of these EMP penetration protection techniques, the reader is referred to Figure 5.3 in Chapter 5 of this book.

Reduction in coupling due to penetrations can also be accomplished by grounding the shield of cables directly to the bulkhead at the point of entry.

All incoming cables such as power cables and data lines should be routed

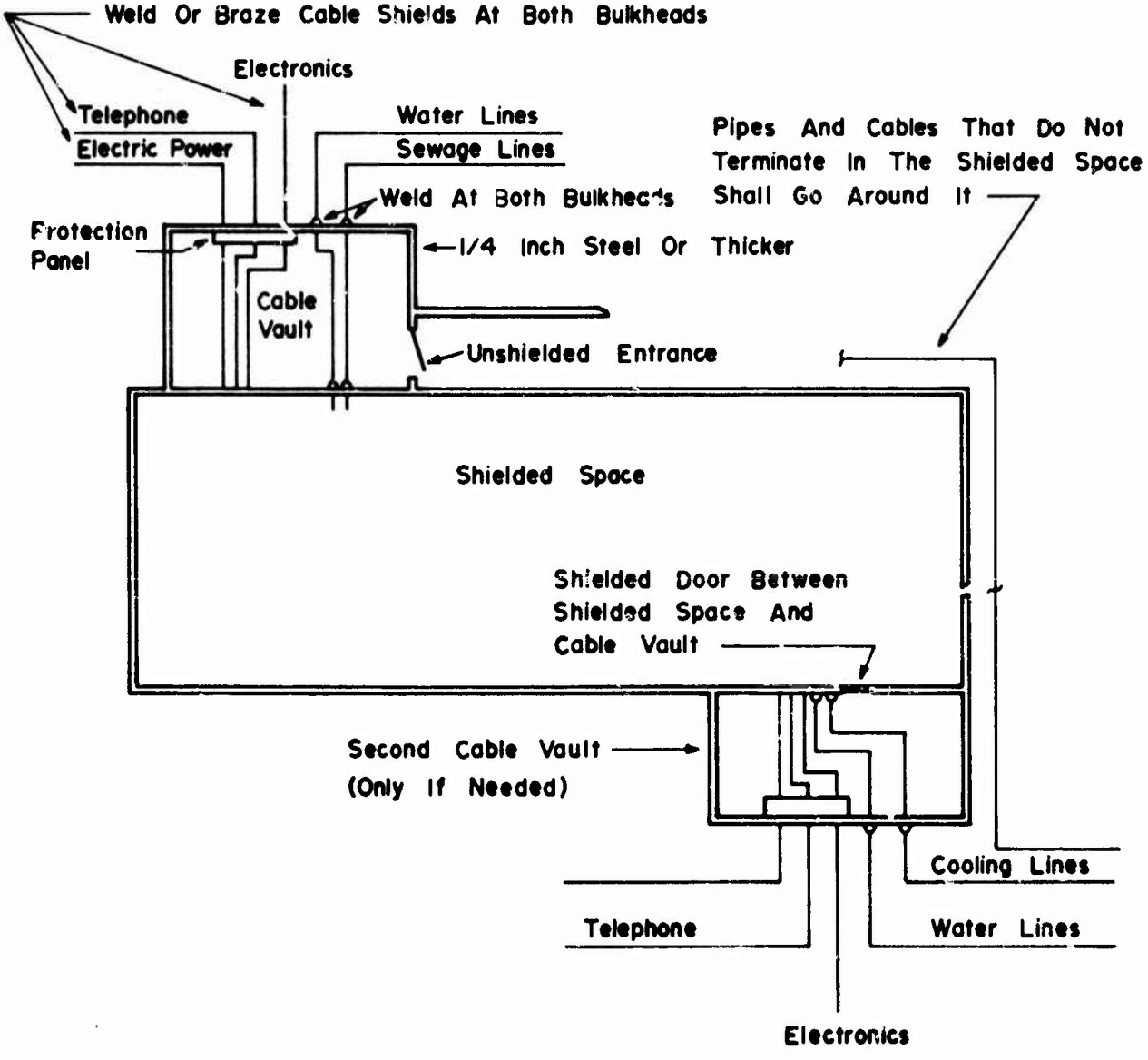

Fig. 3.41 ILLUSTRATION OF SINGLE POINT ENTRY

in such a way that, at the penetration point, protective devices can be mounted on the bulkhead. Protection may be in the form of either filters or surge arrestors. (Details of protection devices are discussed in Chapter 4.)

3.3.3.4 Supplemental Protection Practices for Transmission Systems

For the EMP hardening of a Navy ship, the problems associated with energy pickup on cables is of major concern. Previous sections have discussed the reduction of EMP energy transmission on cables to interior regions utilizing proper grounding of cable shields and protection devices. This section will deal with the reduction of energy pickup on information transmission channels.

- Carrier System

It is known that an EMP pulse is quite broadband, containing a large amount of energy in the low frequency region of the spectrum. The use of a carrier system at a frequency well above the frequency range of the EMP spectrum for the internal transmission of information would result in a rejection of the induced EMP energy. In addition, carrier systems also have the advantages of permitting floating, balanced conductors, narrow band-pass filtering and transformer isolation.

- Non-Conducting Transmission Links

One of the most effective ways to reduce the collected EMP energy is to use a transmission system which does not respond to the EMP pulse. One such system is a dish antenna with a waveguide used for the transmission link. Other types of transmission links which would be quite suitable for intership data transmission are microwave links, laser transmission links, dielectric waveguide and fiber optics.

The microwave and laser systems require line-of-sight transmission and could be used between deck and superstructure. The dielectric waveguide and fiber optic systems would be used for inter- and intra-compartmental data transmission. All of these transmission links would require some additional electronic equipment for transmission and reception of the signals. However, the cost of the additional equipment may be less than the cost required to achieve required protection levels using conventional transmission links.

- Damping Schemes

EMP propagation along the direction of a cable could induce a traveling wave type of voltage buildup. One way to circumvent this difficulty is to ground the sheath. Another way to alter and suppress the transmission of fields along a cable is to change the transmission impedance. It is known that any change in the transmission impedance will produce reflections and reduce transmitted energy. Thus, the insertion of perpendicular conducting baffles can suppress pulse interferences in a cable system.

Similarly, anything which can be done to enhance the fields in a lossy material will increase pulse attenuation effects. This may be accomplished by introducing a ferrite ring around a cable. By locating the lossy ferrite at the base of a baffle, an ultimate degree of feasible attenuation can be achieved.

- Twisting and Shielding

One of the favored approaches for hardening cable is the use of twisted wire cable to minimize the "B-dot" pickup. This twisted wire cable must also be shielded to minimize the E pickup effects. The inside voltages induced by sheath currents are minimized by the use of balanced terminations which, in effect, are not connected to the external sheath. This is shown in Figure 3.42.

- Terminations

It should be pointed out that terminations and splices also can play a significant role in increasing the coupling effects associated with long cable runs. In the case of a balanced pair within a cylindrical shield, the cable must be terminated both for the balanced and common mode terminations. It is good practice to consider multilayer shields and common mode (phantom) circuits as independent energy transmission lines and to terminate them accordingly.

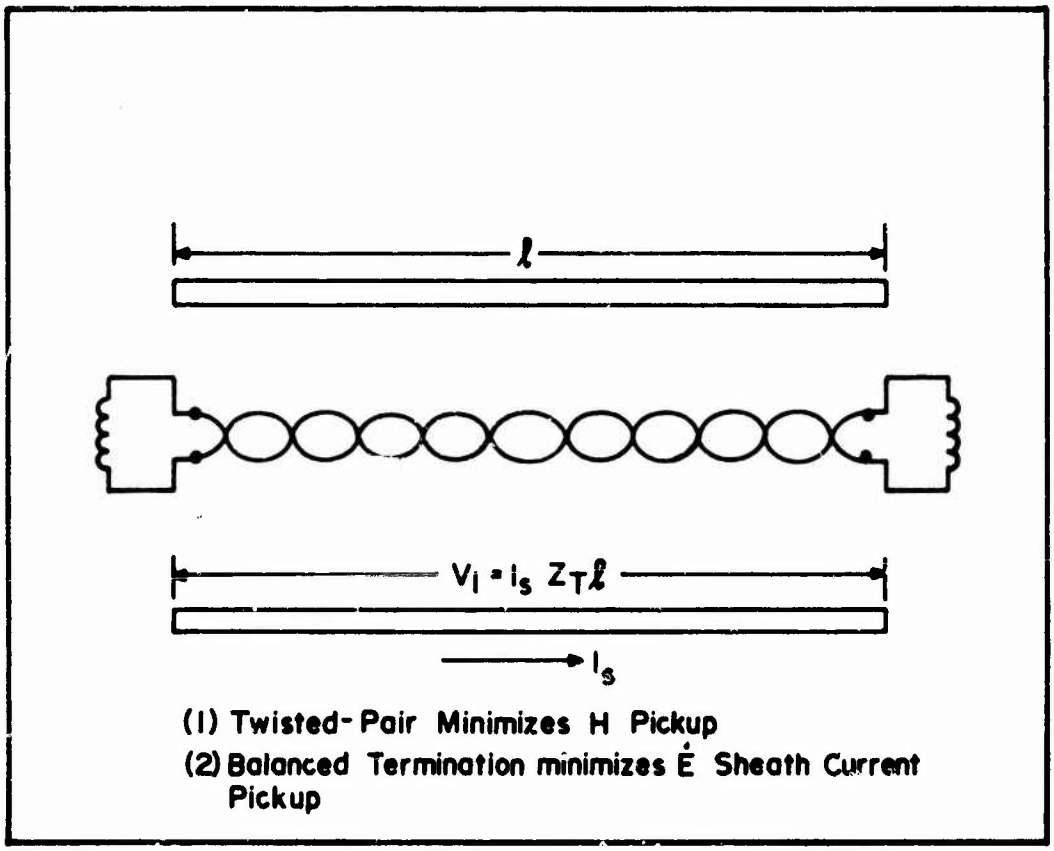

Fig. 3.42 MINIMIZATION OF PICKUP

REFERENCES

1. Landt, J.A., "Peak Current Estimates: Cylinders in Free Space with Extensions to Other Structures", EMP Protection Engineering and Management Note, PEM-32, July 1974.

2. Baum, Carl E., "On the Singularity Expansion Method for the Solution of Electromagnetic Interaction Problems", Interaction Notes, Note 88, December 1971.

3. Tsai, L.L., Wilton, D.R., Harrison, M.G., and Wright, E.H., "A Comparison of Geometrical Theory of Diffraction and Integral Equation Formulation for Analysis of Reflector Antennas", IEEE Trans. Antennas and Propagations, Vol. AP-20, No. 6, pp. 705-712, November 1972.

4. Richmond, J.H., "Scattering by a Dielectric Cylinder of Arbitrary Cross Section Shape", IEEE Trans. Antennas and Propagations, Vol. AP-13, No. 3, pp. 334-341, May 1965.

5. Mei, K.K., and Bladel, T.G.V., "Scattering by Perfectly Conducting Rectangular Cylinders", IEEE Trans. Antennas and Propagations, Vol. AP-11, No. 2, pp. 185-192, March 1963.

6. Sancer, M.I., and Varvatsis, A.D., "Calculation of the Induced Surface Current Density on a Perfectly Conducting Body of Revolution", Interaction Note, Note 101, April 1972.

7. King, R.W.P., The Theory of Linear Antennas, Harvard University Press, 1956.

8. Toulios, P.P., et al., Effects of EMP Environment on Military Systems, Technical Report No. E6114, Under USAMERDC Contract No. DAAK02-68-C-0377, IIT Research Institute, Chicago, Illinois.

9. Toulios, P.P., and Kaurs, A.R., Antenna User's Manual for Linear Antennas in an EMP Environment, Volumes I and II, Technical Report No. E6239, Under Contract No. DAAG39-72-C-0192, IIT Research Institute, Chicago, Illinois.

10. Kao, C.C., "Electromagnetic Scattering from a Finite Tubular Cylinder: Numerical Solutions", Radio Science, Volume 5, No. 3, pp. 617-624, March 1970.

11. Harrington, R.F., Field Computation by Moment Method, The Macmillan Company, New York, 1968.

12. Toulios, P.P., and Shiau, Y., EMP Response of Parabolic Reflector Antenna, Technical Report No. E6276, Under Contract, Subtask R99QAXEB075, No. DAAG390-73-C-0189, IIT Research Institute, Chicago, Illinois.

13. Bethe, H.A., "Theory of Diffraction by Small Holes", Phy. Rev., Vol. 66, pp. 163-182, October 1944.

14. Schelkunoff, S.A., Electromagnetic Waves, D. Van Nostrand, Chapter 8, p. 278, 1943.

15. Krugel, L., "Abschirmwirkung von Ausseuleitern Flexibler Koaxialкable", Telefunken-Zeitung, Vol. 29, pp. 256-266, December 1956.

16. "EMP Protection for Emergency Operating Centers", Defense Civil Preparedness Agency, Protection Engineering and Management Note, PEM-8.

CHAPTER 4

PROTECTION TECHNIQUES AND DEVICES

4.1 Introduction

In general, protection techniques involve methods which reduce the probability of performance degradation of electrical equipment due to the EMP energy which is collected by the ship. These techniques fall into four basic categories.

- Reduction of collected and transmitted energy by construction and installation techniques.
- Increasing failure threshold of circuits by design and component selection.
- Modifying circuit function to reduce susceptibility.
- Reduction of incident energy on equipment using protection devices.

The reduction of collected and transmitted energy involves the concepts of antennas, shielding, zoning, and cable considerations. Methods for dealing with these areas of protection are discussed in other chapters of this manual. Circuit modification and design are beyond the scope of the Ship Design Guidelines. The emphasis in this chapter is, therefore, on the last category.

Protection devices reduce the EMP transient energy transmitted to the equipment by reflecting and/or dissipating a portion of the energy which is incident on the protection device as indicated in Figure 4.1. The device changes both the shape and frequency content of the transient pulse, P_t, that is transmitted to the equipment. The analysis and prediction of the effectiveness of the protection device is performed in either the frequency domain or in the time domain depending on the characteristics of the device. For linear devices, a frequency domain analysis is used while nonlinear devices require a time domain analysis.

The two major types of protection devices considered in this chapter are filters and surge arrestors. Filters are used to limit the frequency spectrum of the interfering pulse, while surge arrestors limit the amplitude. Both are used extensively for EMP protection.

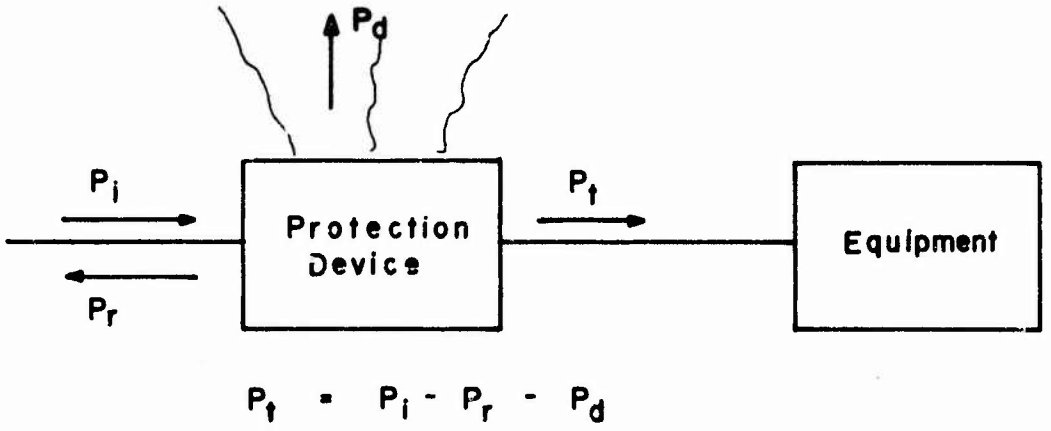

Fig. 4.1 ENERGY BALANCE FOR PROTECTION DEVICE

Filters are used when the equipment to which cables are attached makes use of only a small part of the spectrum of the interfering signal. Therefore, these devices prevent energy outside of the range of interest from entering the equipment.

Surge arrestors limit the amount of energy entering the equipment by dissipating some of the energy contained in the interfering signal in the surge arresting device. The net effect of this is the limiting of the voltage levels on the cables attached to the equipment.

The choice of type of device to be used is dictated by a number of factors. Some of these are:

- frequency spectrum of the information carried on the cables
- amplitude requirements of the information carried on the cables
- susceptibility and vulnerability of the equipment attached to the cables to the interfering pulse
- size, weight, and installation space
- cost (initial and maintenance).

In the discussion that follows, these factors are considered for each type of device. Filters (spectral limiting devices) are considered in the next section.

4.2 Spectral Limiters (Filters)

If a piece of equipment has cables entering it that carry voltages whose spectral content is a small portion of the EMP spectrum, the EMP signal entering the equipment can be significantly reduced by using a filter. In order to specify

an appropriate filter, several pieces of information are required. These are:

a) the desired spectrum of the signal that is to pass through the filter

b) the spectrum of the EMP signal appearing on the cable

c) the required amount of attenuation of the EMP signal

d) the terminating impedances of the filter.

The purpose of this section is to describe available filter types and to discuss their application.

Spectral limiting involves the use of a frequency domain filter whose transfer characteristic is a function of frequency and, ideally, is independent of amplitude. The analysis is performed using Fourier or Laplace transform procedures. The basic steps in the analysis are:

a) transform the expected EMP waveform from the time domain to the frequency domain

b) determine the transfer characteristic of the filter

c) multiply the pulse spectral function by the filter transfer function

d) transform the results of c) to the time domain to obtain the waveshape at the output of the filter.

These steps are shown in flow diagram in Figure 4.2

This procedure is directly applicable to the model system shown in Figure 4.3 where the transfer function of the filter is specified for particular values of source and load resistance. However, this simplified resistor representation of source and load is usually valid only over the relatively narrow range of frequencies which contains the normal information signals. For the wide band frequency spectrum associated with EMP energy, the source and load impedances normally required the inclusion of reactive elements for accurate representation. When this modification is made, the circuit representation of the filter must be used to obtain the proper transfer function of the circuit.

Filters may be classified in a number of ways such as:

- frequency range (audio, HF, etc.)
- frequency characteristic (low pass, band pass, etc.)
- type of elements used (RC, LC, crystal, etc.)
- application (power line, receiver input, power supply, etc.)

For purposes of discussion in relation to EMP, it is useful to consider the broad categories of nondissipative and dissipative filters. These classifications refer

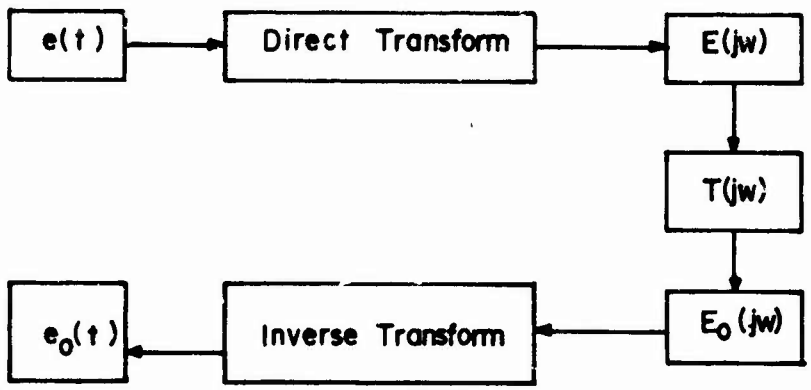

Fig. 4.2 TRANSFORM ANALYSIS FLOW DIAGRAM

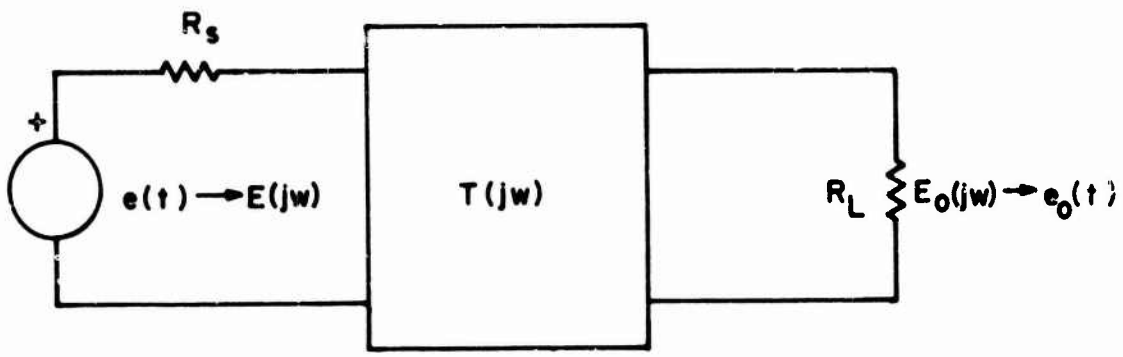

Fig. 4.3 MODEL SYSTEM FOR SPECTRAL LIMITING ANALYSIS

to the physical means by which the filter controls the frequency range of the transmitted energy.

4.2.1 Nondissipative Filters

Nondissipative or reflective filters are made up of inductors and/or capacitors in the lumped element or of tuning stubs in the case of distributed parameter systems. The design and performance of the filter is strongly affected by the source and load impedance. The specifications for the filter usually give a range of frequencies over which energy is to be transferred with little or no attenuation (the passband) and the minimum attenuation of energy in the frequency range outside the passband (the stopband). The source and load impedances are also specified and are often given as pure resistances.

Physically, the filter behaves as a frequency dependent impedance transformer. For frequencies in the passband, the input impedance of the filter approximately matches the source resistance and maximum power is transferred to the filter. Since the filter is lossless, any power accepted by the filter is transferred to the load. For stopband frequencies, the input impedance of the filter is reactive and reflection takes place at the input terminals of the filter.

The fact that nondissipative filter action is a reflective process is, in general, a disadvantage as related to EMP protection for two basic reasons:

a) Energy which is reflected will appear elsewhere in the system and must be dissipated by other elements of the system.

b) Reflections often result in larger peak amplitudes of voltage or current than would otherwise occur. These larger amplitudes could result in arc over in the filter components. This arcing provides a path for energy flow to the equipment which is being protected and also could result in damage to the filter such that energy in the passband would not be transferred by the filter following the EMP event.

Another disadvantage of nondissipative lumped parameter filters is that the interconnection and layout often results in parasitic inductance and capacitance which may cause spurious responses not predicted by the analytical design. These responses could allow large amounts of EMP energy to reach the protected equipment.

Two basic types of lumped parameter nondissipative filters, the Π-filter and the T-filter, are illustrated in Figures 4.4 and 4.5. The low-pass Π-filters may not adequately protect against EMP because high voltages can develop across the input capacitor and cause degradation or failure when the capacitor resonates with an inductive source[1]*. Since T-filters are not susceptible to these high voltages, they are often used for EMP hardening. However, with a T-filter, more power can possibly be delivered to the load. In Figure 4.6, if the source and load capacitances resonate with inductances L_1 and L_2, respectively, the voltage across R_L is greater than it would be without the filter.

*Superscripts refer to numbered references at the end of the chapter.

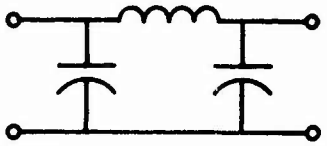

Fig. 4.4 LOW-PASS π-FILTER

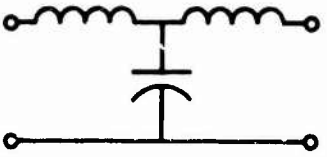

Fig. 4.5 LOW-PASS T-FILTER

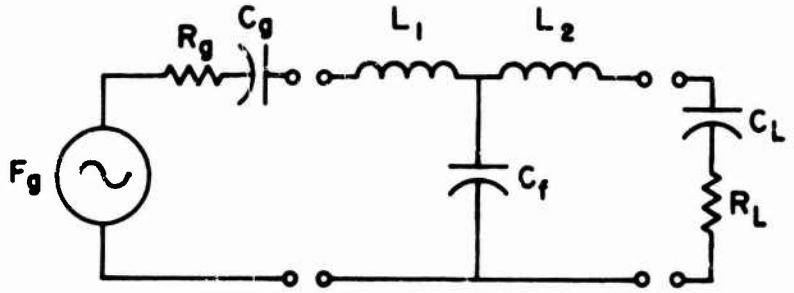

Fig. 4.6 LOSSLESS T-SECTION FILTER

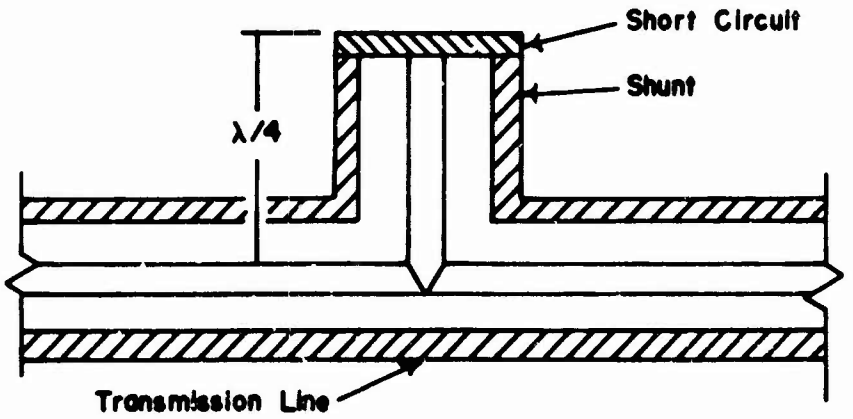

Fig. 4.7 CROSS SECTION OF QUARTER WAVE SHUNT

A distributed parameter nondissipative filter is the quarter wave shunt. It consists of a shorted transmission line which is connected in parallel with the signal transmission line as illustrated in Figure 4.7. The shorted line appears as an open circuit (no shunting effect) to frequencies for which the line's length is an odd number of quarter wavelengths. For other frequencies, the line appears as a shunt reactance and will produce reflections due to mismatch. Such a filter is practical only at the higher frequencies where a quarter wavelength is a reasonable length.

4.2.2 Dissipative Filters

A dissipative filter includes elements which dissipate energy in the stopband range of frequencies. Unfortunately, all stopband frequency energy is not dissipated within the filter since mismatches result in the stopband and some energy is reflected. However, the reflected energy and, hence, the peak voltage and current transients are generally less in the dissipative filter than in the nondissipative filter.

Probably the most familiar lumped element lossy filters are the RC networks illustrated in Figure 4.8. To obtain a larger attenuation in the stopband, the LCR filters shown in Figure 4.9 may be used. The characteristics of the lumped element dissipative filters are subject to the same degradations as mentioned in Section 4.2.1 (spurious responses due to stray inductance and capacitance and the possibility of resonances with source and load reactance).

For protection applications which require a low pass filter, it is recommended that a lossy material filter may be used. These commercially available devices consist of materials that encircle the conductor lead that is wired to the device or equipment which is to be protected. The energy is inductively coupled into the material and is dissipated there. Two advantages associated with these filters are:

a) simple construction and therefore minimal parasitics and associated spurious responses,

b) the attenuation characteristics are not critically related to source and load impedances as in the case of reflective filters.

The major disadvantage is that lossy material filters are inherently low pass devices.

A ferrite bead, which is a small ferrite torroid whose equivalent circuit is a series RL circuit in the conductor around which it is placed, is used in one type of dissipative lossy material filter. Figure 4.10 shows a ferrite core (bead) placed around a wire and the first order equivalent circuit. The resistance and reactance are functions of frequency. Figures 4.11 and 4.12 illustrate the variations of the resistive impedance and reactive impedance as a function of frequency for various types of cores. As shown in these figures, the individual cores are relatively low impedance elements. Sometimes more attenuation can be obtained by using many cores on a given conductor. However, this may result in an impedance reduction at certain frequencies, as illustrated in Figure 4.13. In this figure, 30 beads are more effective above 20 MHz than are 300 beads.[2]

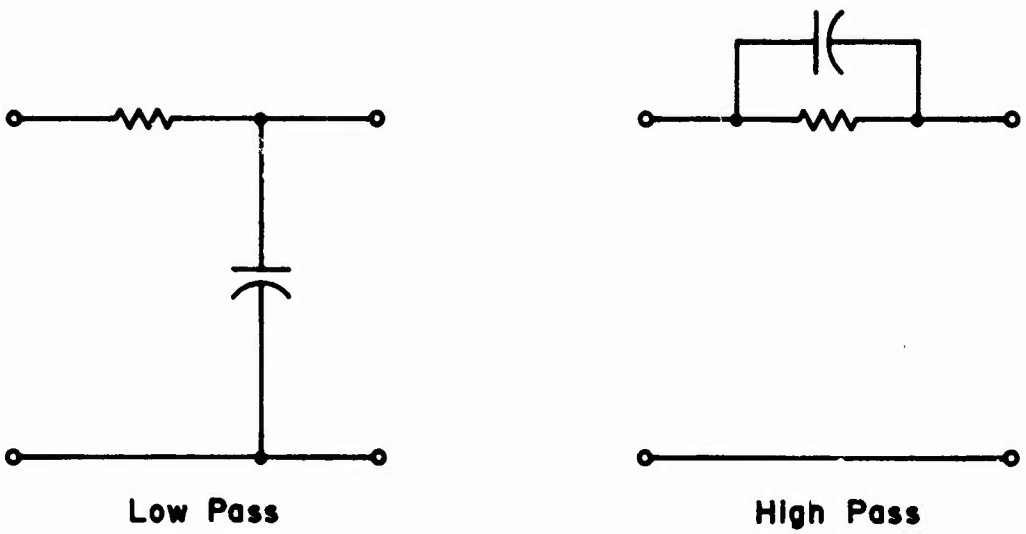

Fig. 4.8 SIMPLE LOSSY FILTERS

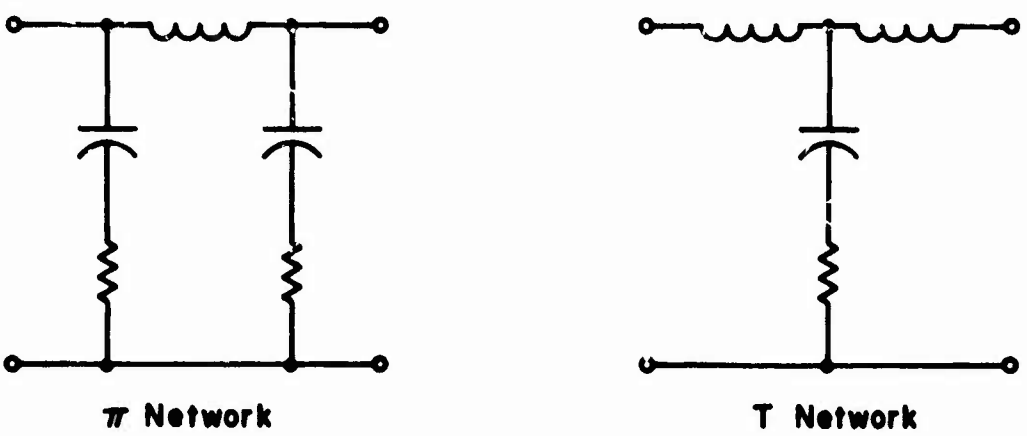

Fig. 4.9 TWO TYPES OF LCR FILTERS

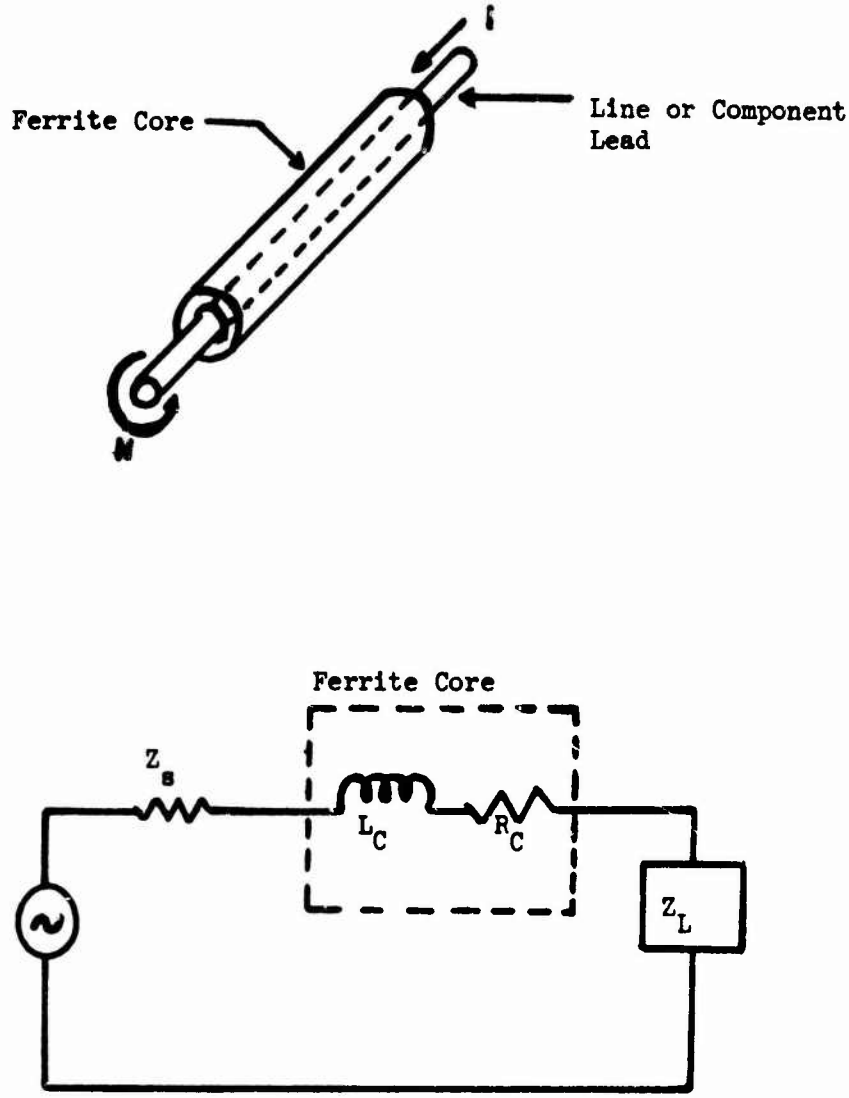

FIGURE 4.10 Ferrite Core and Equivalent Circuit

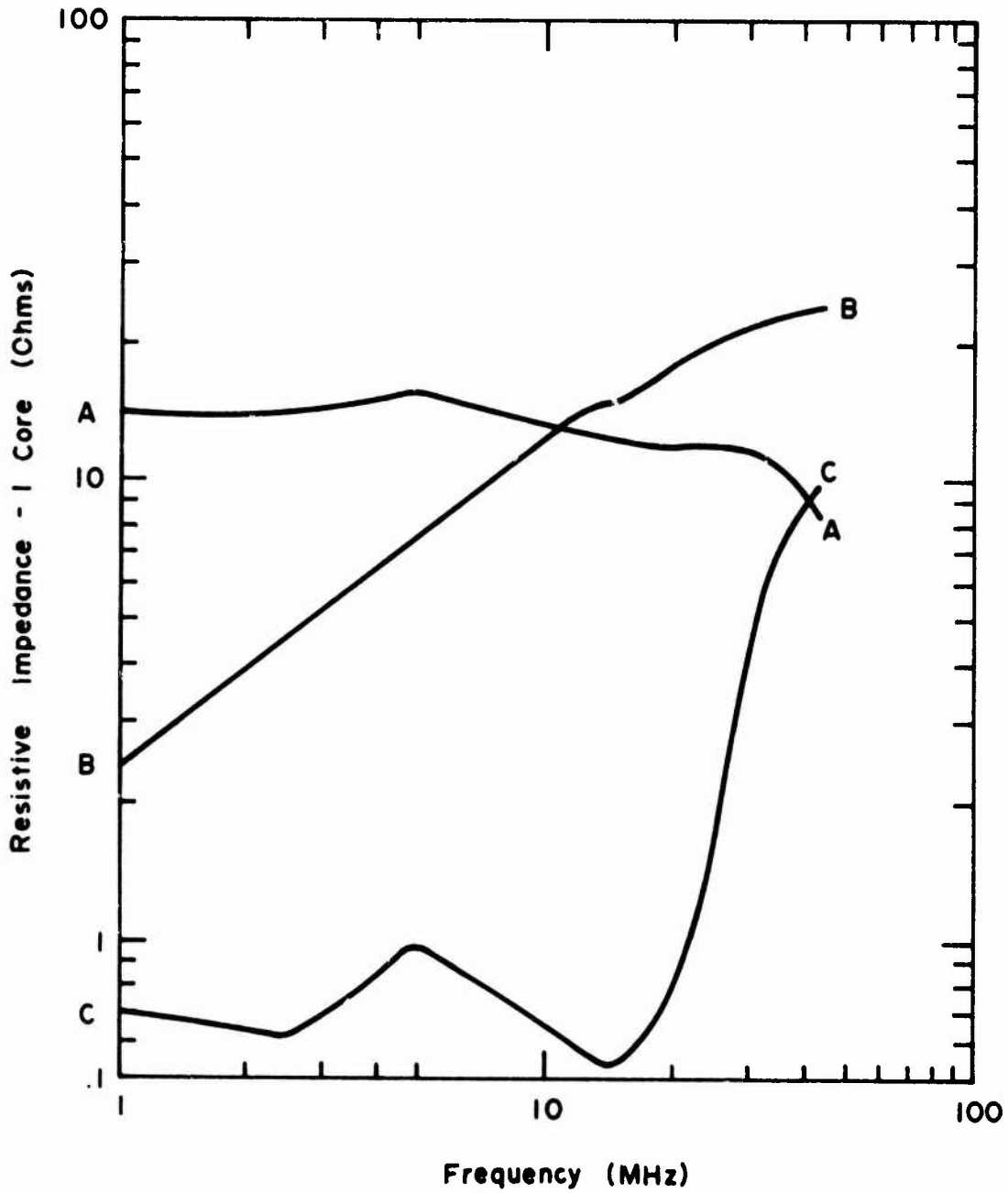

A - Indiana General Type 06

B - Ferroxcube Type 4A6

C - Indiana General Type QI

Fig. 4.11 RESISTIVE IMPEDANCE PER CORE OF VARIOUS FERRITE CORES. (REF. 2)

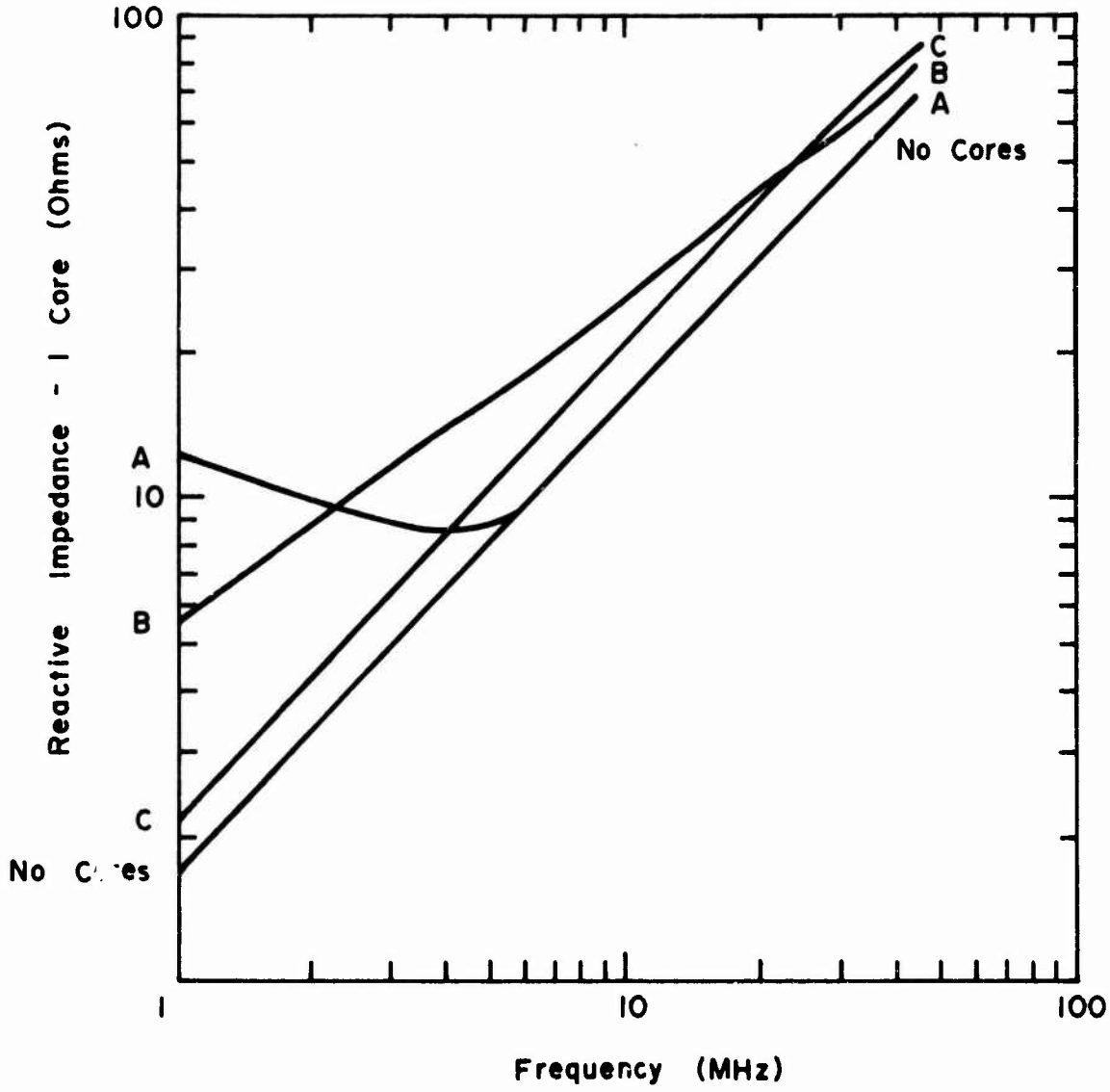

A - Indiana General Type 06

B - Ferroxcube Type 4A6

C - Indiana General Type Q1

Fig. 4.12 REACTIVE IMPEDANCE PER CORE FOR VARIOUS FERRITE CORES (REF.2)

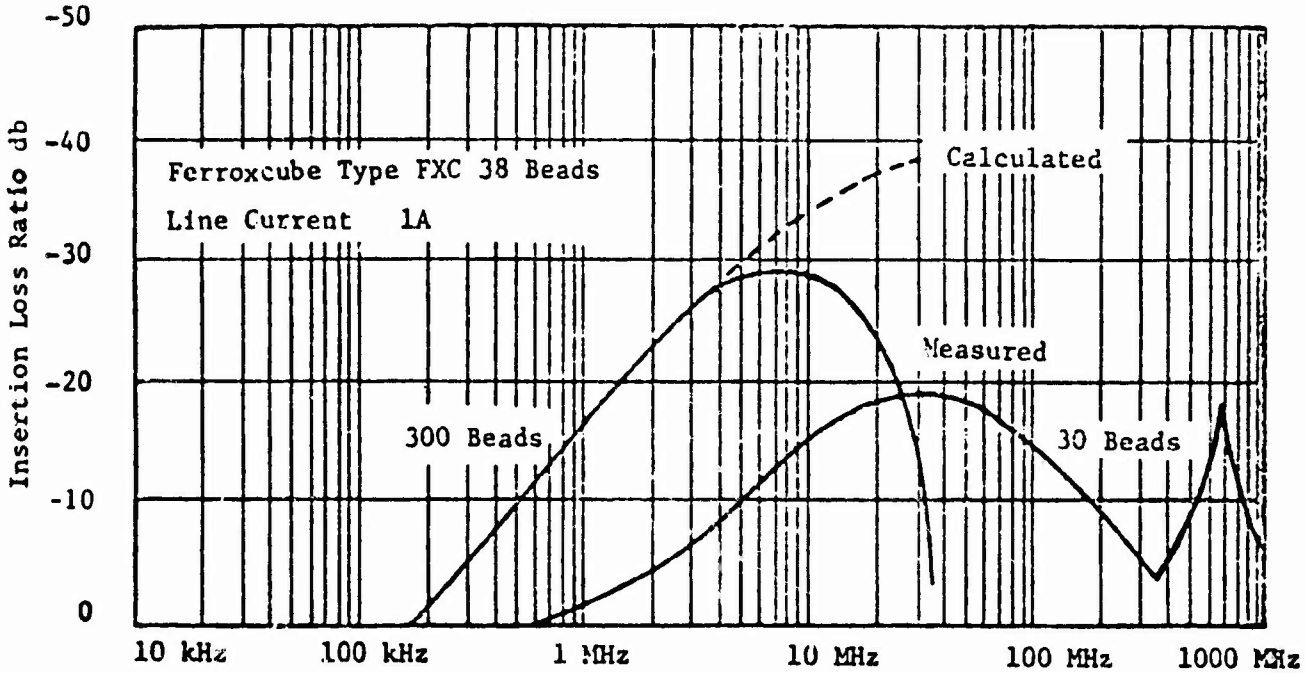

Figure 4.13 INSERTION-LOSS RATIO OF 30 BEADS STRUNG ON A LINE IS VERY FREQUENCY-DEPENDENT (Ref. 2)

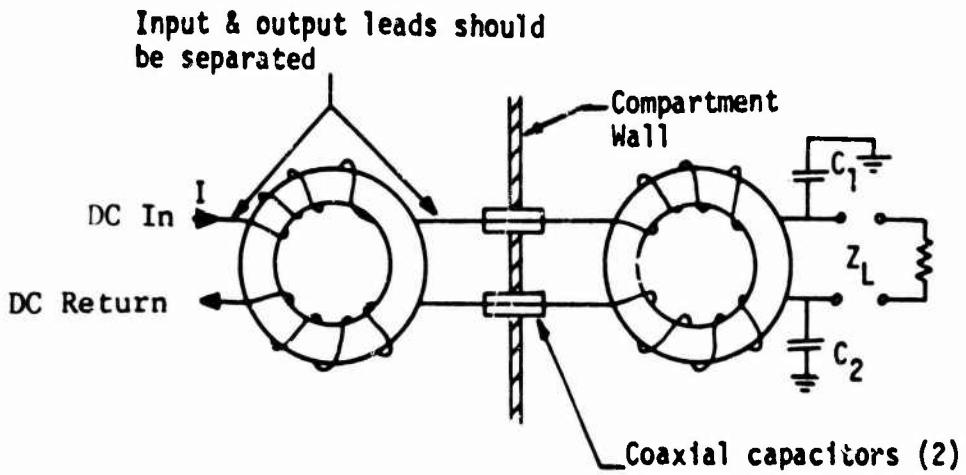

Figure 4.14 FERRITE CORES DESIGNED TO NULLIFY EFFECTS OF HIGH DC CURRENTS (Ref. 3)

Core saturation at high currents, which should be considered in the use of ferrite beads, varies from material to material; therefore, manufacturers' data on individual materials must be consulted.

An effective way of nullifying the saturation effects of cores in a DC power line is illustrated in Figure 4.14. Here, ferrite torroids are installed in a DC power line as EMP filters. The high-side and low-side windings are wound in opposite directions; thus the DC flux, which is reduced almost to zero, does not saturate the core. The coaxial capacitors and C_1 and C_2 short out the AC components. Thus, the AC current in each winding on the torroid is different, and normal filter action takes place. As noted in Figure 4.14, input and output leads should be separated to prevent arcing between them. In DC power circuits, the filter resistance is important, but because ferrites have such high permeabilities, only a few turns are needed and, therefore, filters can be made with large wire, which minimizes the DC resistance.[3]

Lossy material filters are available in forms other than the ferrite bead. Figure 4.15 illustrates one construction which is commercially available and shows a comparison of loss filter and reflective (i.e., reactive) filter responses. Of significance in this comparison is the lack of spurious responses in the lossy filter characteristics.[4]

Filter pin connectors provide a means for incorporating filters into the system with minimal increase in space and weight. These filters are designed as an integral part of the connector, and therefore, do not require special housing or circuit space. They come in circular, miniaturized and subminiaturized rectangular shapes, can accomodate up to 61 contact arrangements, and are available in Π, LC, CL, and capacitor configurations shown in Figure 4.16. As indicated, ferrite beads can be used to provide dissipative filtering.

Figure 4.17 shows typical insertion loss test results obtained as per MIL-STD-220 on contacts in a filter pin connector. Since not many EMP hardness data are available for filter pin connectors, systems qualification tests must be conducted.[5]

When designing filters for operation in the audio frequency range, one finds that the large component values required lead to large physical size and weight. To avoid this difficulty, an active filter design is often used. Such circuits are quite satisfactory for operation with the normal signal levels in the system. However, these filters provide little EMP protection since the semiconductors and integrated circuits used in the circuits are generally as susceptible to damage as are the components in the equipments one is trying to protect.

4.2.3 Applications

A number of systems employ filters for reasons other than EMP hardening. A few examples are:

a) low pass power line filters at equipment inputs for reduction of voltage spikes and surges.

b) filters on control and information leads of audio and video equipment for noise reduction. These may be low pass or band-pass filters depending on the frequency range of the desired signal.

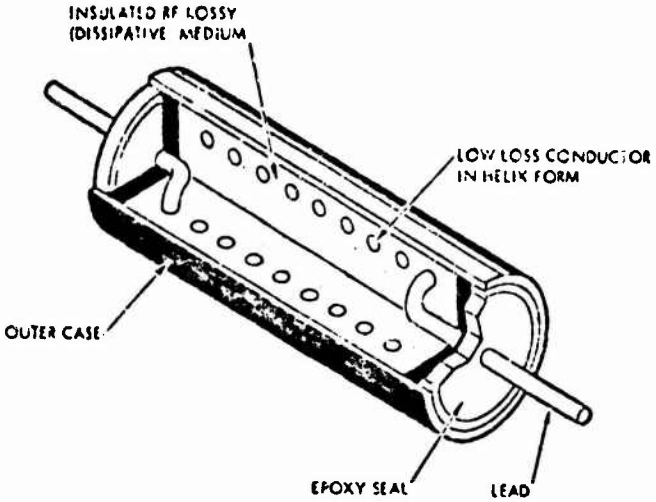

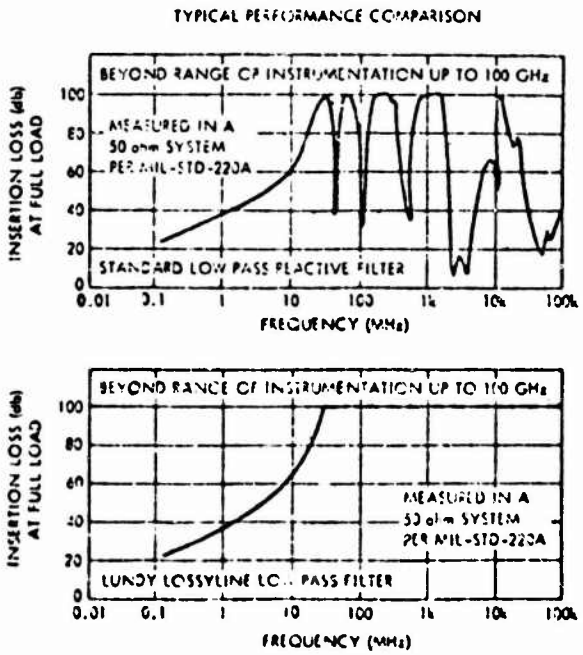

Figure 4.15 DISSIPATIVE FILTER (Ref. 4)

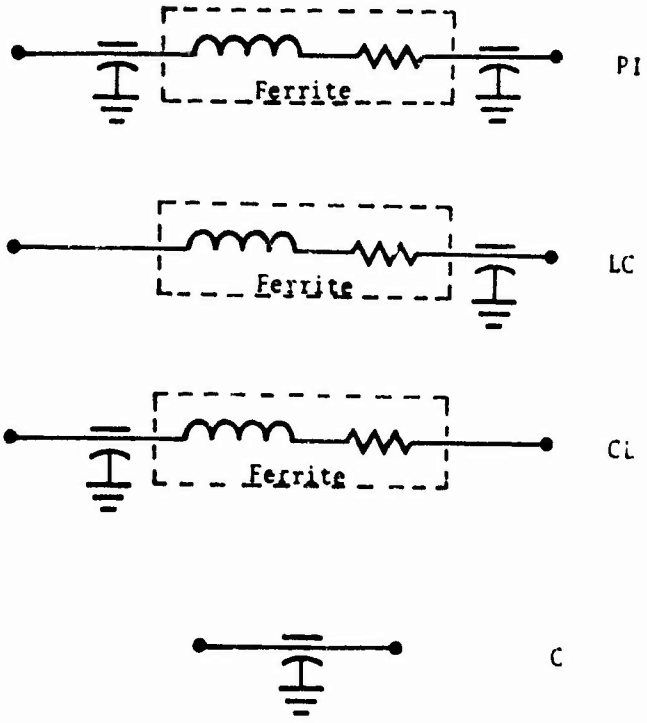

Figure 4.16 SCHEMATICS FOR FILTER PIN CONFIGURATIONS (Ref. 5)

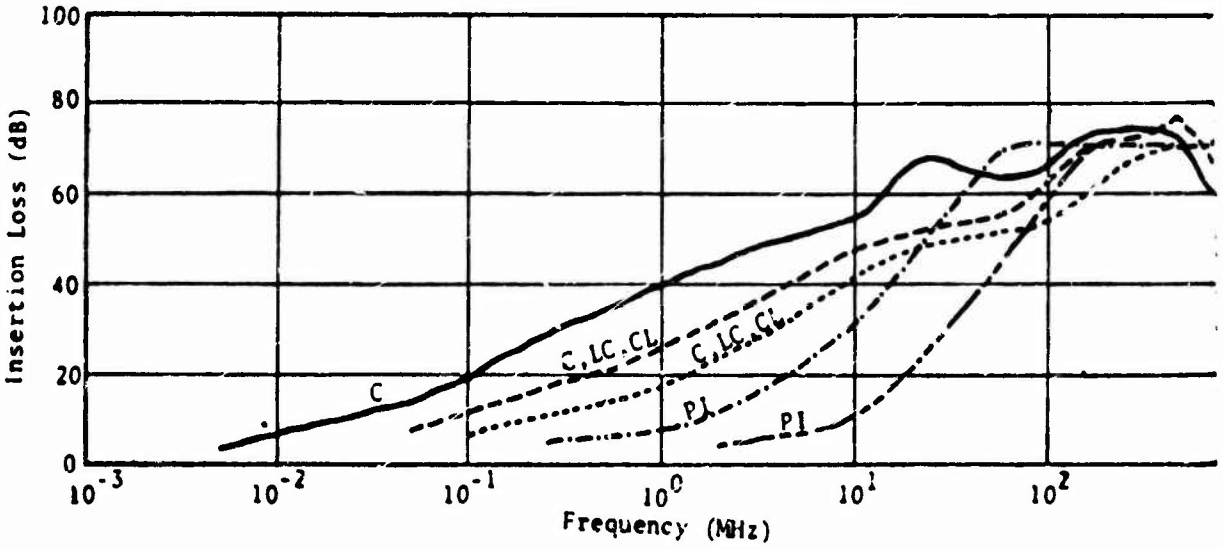

Figure 4.17 TYPICAL INSERTION LOSS TEST RESULTS AS PER MIL-STD-220 ON FILTER CONTACTS IN A FILTER PIN CONNECTOR MATED WITH A STANDARD NON-FILTER CONNECTOR (Ref. 5)

c) bandpass filters at the input of communication receivers for noise reduction and channel selection.

d) cryptographic installations.

These filters may not provide substantial EMP protection since the normal specifications would not provide for the large levels of voltage and current which could be experienced in an EMP environment. Therefore, breakdown and/or damage of these filter components could occur.

The decision to use a protective device is based on a comparison of the expected incident energy and failure threshold for the device or equipment being considered. The type of protective device to be used (spectral limiting, amplitude limiting or a combination of the two) is based on the following considerations:

- Normal signal levels associated with the equipment.
- Frequency range of the normal information or power signals.

Two examples of signal level considerations which would require the use of filters for EMP protection are the very low level signals associated with sensitive receiver inputs and the high level voltages (near cable breakdown rating) associated with transmitter outputs. Since amplitude limiting devices are not very effective for reducing voltage levels to less than approximately three volts, spectral limiting must be used to protect receiver inputs where normal levels are in the millivolt or microvolt range. When normal signal levels are near cable breakdown ratings, amplitude limiting will not be effective, since the limiting action will likely occur at a voltage above the cable rating. In this case, the filter would be placed at the antenna input to protect the cable.

Fortunately, the frequency range of the information signal in equipment which operates with low level or high level signals is often relatively narrow. Therefore, bandpass filtering will be effective in these situations providing the filter elements are chosen with EMP level stresses in mind.

Frequency range considerations are related to the amount of EMP energy which will be passed by the filter. Obviously, the filter must pass energy in the frequency range that the normal signal appears. Therefore, the use of a filter may not result in much protection for wide band, low frequency devices such as video amplifiers since very little EMP energy would be stopped by the filter. In general, systems which operate in a narrow frequency band and/or at high frequencies are candidates for EMP protection via spectral limiting.

The initial decision regarding the use of a filter for protection is based on the EMP energy contained in the passband frequency range of the filter. This value of energy is obtained by transforming the expected transient waveshape from the time domain to the frequency domain using the Fourier transform integral.

$$V(j\omega) = \int_0^\infty v(t)e^{-j\omega t}dt \qquad (4.1)$$

The lower limit on the integral is zero to conform with the assumption that the transient starts at t = 0. The energy contained in the spectrum between the limits $0 \leq \omega \leq \omega_c$ is obtained from the integral;

$$W = \frac{1}{\Pi}\int_{0}^{\omega_c} |V(j\omega)|^2 \, d\omega \qquad (4.2)$$

Where W is normalized with respect to the load resistance, i.e., actual energy is equal to W divided by the load resistance. The total energy in the spectrum is determined by letting ω_c approach infinity.

Table 4.1 summarizes the results of these calculations for three types of waveshapes--the single exponential, the double exponential and the damped sinusoid. The energy equations are plotted as a fraction of total energy in Figures 4.18, 19, and 20. The curves of W/W_T represent the fraction of total energy contained in the region $0 \leq \omega \leq \omega_c$ (see Table 4.1) and are useful for determining the energy delivered or passed to the load when using low pass filter designs. For high pass filter designs the $1 - W/W_T$ curves, which represent the fraction of total energy contained in the region $\omega_c \leq \omega \leq \infty$, would be used. Bandpass applications may use either set of curves depending on the frequency range of the passband.

As an example of the use of these curves, consider the damped sinusoid shown in Figure 4.21 as representing the EMP-induced current input to a critical circuit. The damping factor and ring frequency can be determined from this waveform by using the relationships

$$a = \frac{1}{t_2 - t_1} \ln \frac{I_2}{I_1} \qquad (4.3)$$

$$\omega_0 = \frac{2\Pi}{T} = \frac{2\Pi}{t_2 - t_1} \qquad (4.4)$$

where (t_1, I_1) and (t_2, I_2) are the coordinates of successive peaks on the waveform. For this curve they have values of

$$t_1 = 8 \text{ nsec}, \quad I_1 = 315\text{A}, \quad t_2 = 35 \text{ nsec}, \quad I_2 = 80\text{A}$$

which result in $a = 50 \times 10^6$ and $\omega_0 = 233 \times 10^6$.

As can be seen in Table 4.1, the total energy for the damped sinusoid depends on the magnitude V_0 (or in this case I_0) of the input waveform. To determine I_0, and thus the total energy in the damped sinusoid, the following expression can be used:

$$I_0 = I_1 e^{at_1} = 470 \text{ A} \qquad (4.5)$$

Inserting those parameter values (i.e., a, ω_0 and I_0) into the expression for W_T given in Table 4.1, a value of .053 joules is obtained for the total energy that would be dissipated in a 50 ohm load.

If the EMP energy collector is connected to a system or load in which the normal information signals are contained in the frequency range above 50 megahertz, one could use a high pass filter to reduce the transient energy incident on the load.

	Time Domain	Frequency Domain	Energy $0 \le \omega < \omega_c$ (W)	Total Energy (W_T)
Simple Exponential		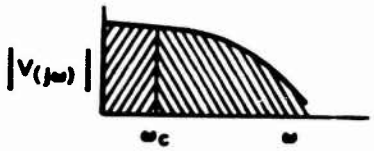	$\frac{V_o^2}{\pi a} \operatorname{Tan}^{-1} \frac{\omega_c}{a}$	$\frac{V_o^2}{2a}$
	$V = V_o e^{-at}$	$V_{(j\omega)} = \frac{V_o}{a + j\omega}$		
Double Exponential		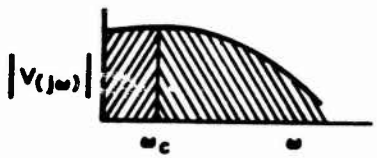	$\frac{V_o^2 (b-a)}{\pi (b+a)} \left[\frac{1}{a} \operatorname{Tan}^{-1} \frac{\omega_c}{a} - \frac{1}{b} \operatorname{Tan}^{-1} \frac{\omega_c}{b} \right]$	$\frac{V_o^2 (b-a)^2}{2ab (b+a)}$
	$V = V_o (e^{-at} - e^{-bt})$	$V_{(j\omega)} = \frac{V_o (b-a)}{(a-j\omega)(b+j\omega)}$		
Damped Sinusoid		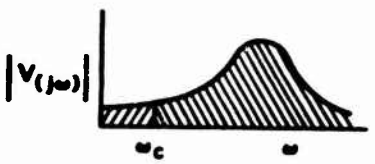	$\frac{V_o^2 \omega_o}{4\pi a (a^2+\omega_o^2)} \left[\omega_o \operatorname{Tan}^{-1} \frac{2a\omega_c}{a^2+\omega_o^2-\omega_c^2} - \frac{a}{2} \ln \frac{(a^2+\omega_o^2-\omega_c\omega_o)^2 + \omega_c^2 a^2}{(a^2+\omega_o^2+\omega_c\omega_o)^2 + \omega_c^2 a^2} \right]$	$\frac{V_o^2 \omega_o^2}{4a(a^2+\omega_o^2)}$
	$V = V_o e^{-at} \sin \omega_o t$	$V_{(j\omega)} = \frac{V_o \omega_o}{-\omega^2 + j2a\omega + a^2 + \omega_o^2}$		

Table 4.1 SUMMARY OF ENERGY RELATIONS FOR EMP WAVESHAPES

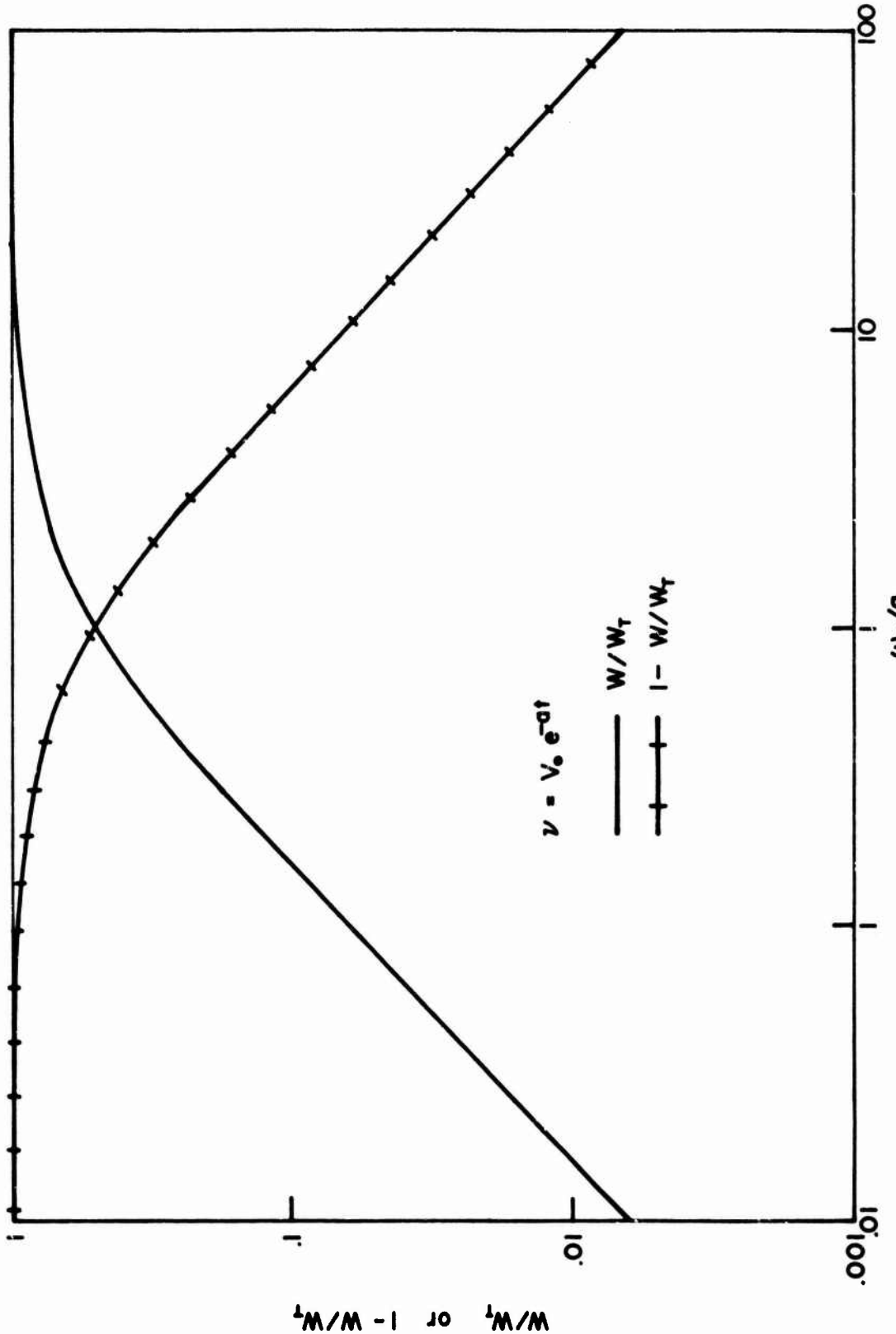

Fig. 4.18 FRACTION OF TOTAL ENERGY CONTAINED IN RANGE $0 \leq \omega \leq \omega_c$ FOR SINGLE EXPONENTIAL PULSE

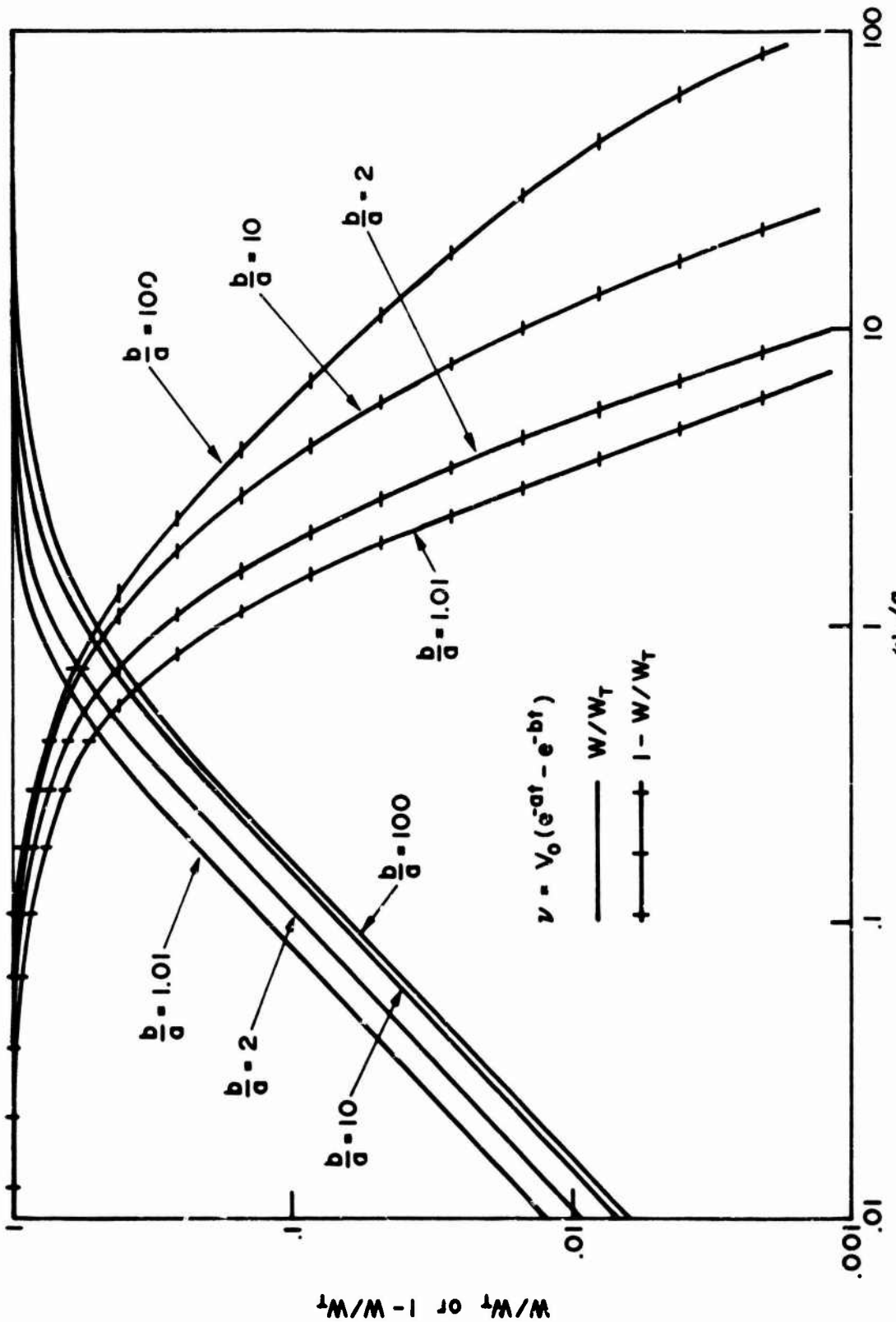

Fig. 4.19 FRACTION OF TOTAL ENERGY CONTAINED IN RANGE $0 \le \omega \le \omega_c$ FOR DOUBLE EXPONENTIAL PULSE

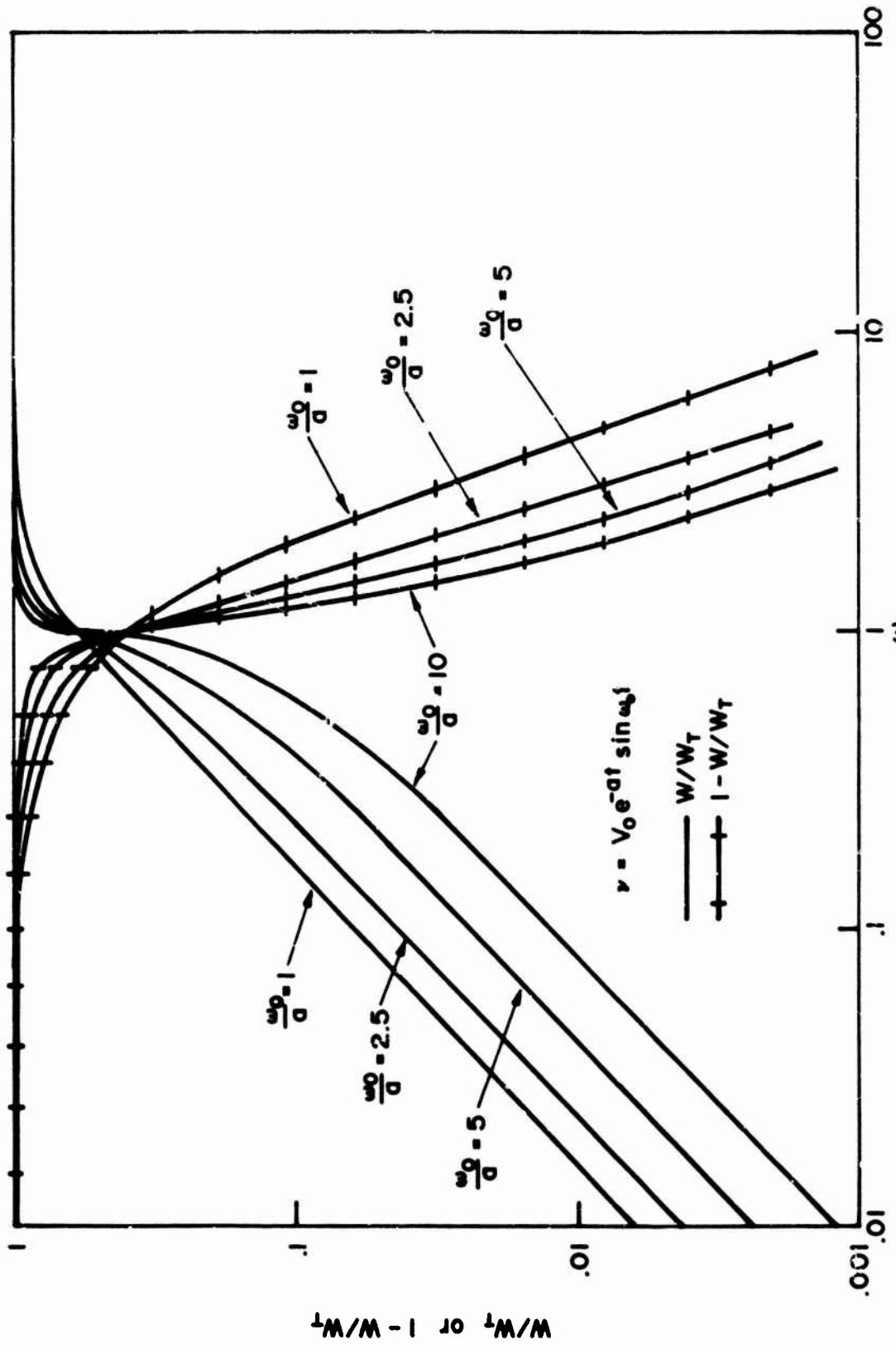

Fig. 4.20 FRACTION OF TOTAL ENERGY CONTAINED IN RANGE $0 \le \omega \le \omega_c$ FOR DAMPED SINUSOID

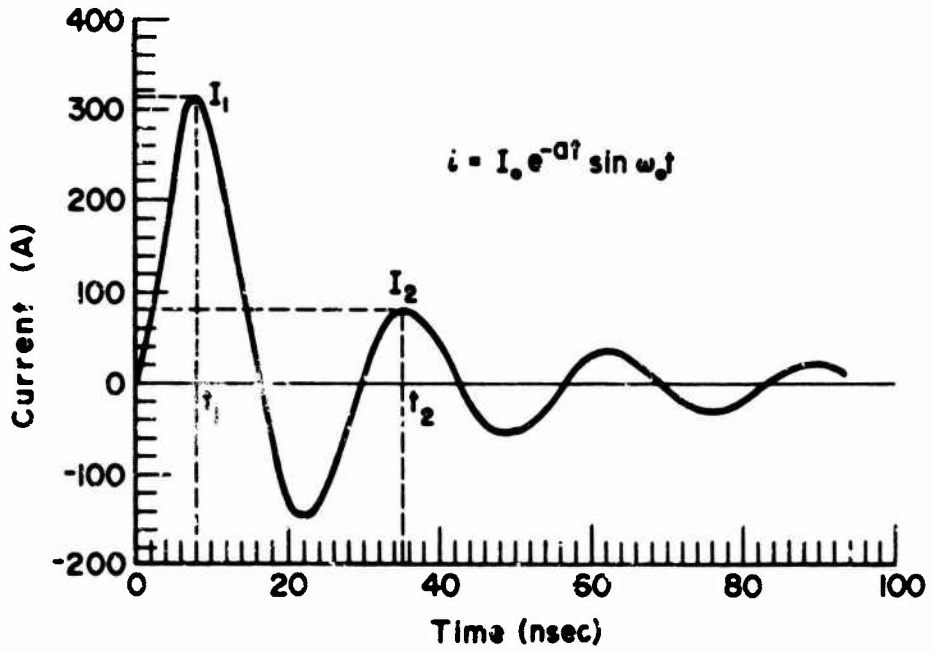

Fig. 4.21 WAVEFORM FOR EXAMPLE CALCULATION

A quick estimate of the amount of energy passed by the filter is obtained by assuming an ideal filter and using Figure 4.20 with $\omega_0/a = 4.65 \simeq 5$ and $\omega_c/\omega_0 = 50 \times 2\Pi/233 = 1.35$. This gives a value of $1 - W/W_T = 0.75$ for the fraction of the total EMP input energy that will be passed to the load through the high-pass filter; 0.75 x .053 = .004 joule is delivered to the load. Comparison of this value with the amount of energy required to produce damage or upset to the circuit will determine whether or not a filter will provide the necessary level of protection.

It must be kept in mind that this procedure provides order of magnitude results since ideal filter characteristics are assumed. Therefore, if the decision is made to use a filter, analysis and/or tests of the entire system must be made with the filter included to take into account the finite slope of the filter characteristic in the stopband and to determine if energy is redistributed in the frequency domain due to the mismatch which results in the stopband region of the filter.

When a filter is used for EMP protection, it is essential that the filter operate as predicted from analysis, i.e., no spurious responses. Generally, a simple filter in terms of number of components minimizes the parasitics and unintended loops and, therefore, minimizes the probability of spurious responses. As mentioned earlier, a dissipative filter is normally superior to a nondissipative filter in terms of the likelihood of spurious responses.

4.2.4 Installation Practice

The construction and installation of a protective device is as critical as its design. Since the filter acts as a controlled energy barrier, its input and output connections must be isolated from one another. A good filter (or other protective device) is usually constructed in three electromagnetic sections as shown in Figure 4.22.[6]

Most frequently, filters and limiters operate "against ground"; that is, the "return" side of the protective element is well bonded internally to the filter case. Good filter design and adjustment takes into account whatever mutual coupling may exist between input and output within the central component compartment. This convention comes from the customary circuit practice of using "case" as the reference mode in small and medium size system elements, both for single-ended and balanced systems.

Obviously, the same care in isolation is required in installation since most of the device's value is lost if the protected equipment can "see" the input side of the filter. Figure 4.23 illustrates the correct installation practice. It is important that the filter case make a tight peripheral contact so that there is no hairline aperture and so that the common reference impedance is nearly zero.[6] Poor installation practices can largely negate the effects of a filter. This is especially true if the line being filtered has a shield with a sheath current flowing on it. If a filter is just inserted in the line with the case grounded (or ungrounded) the sheath current could flow over the filter case and on to the sheath of the line on the output side of the filter. This situation cannot happen if the correct practice shown in Figure 4.23 is followed.

If commercial power line low pass filters are to be used, it is important to specify that no fuses be present in series with the shunt capacitors. Some power line filters normally have these fuses present - especially in epoxy potted filters-

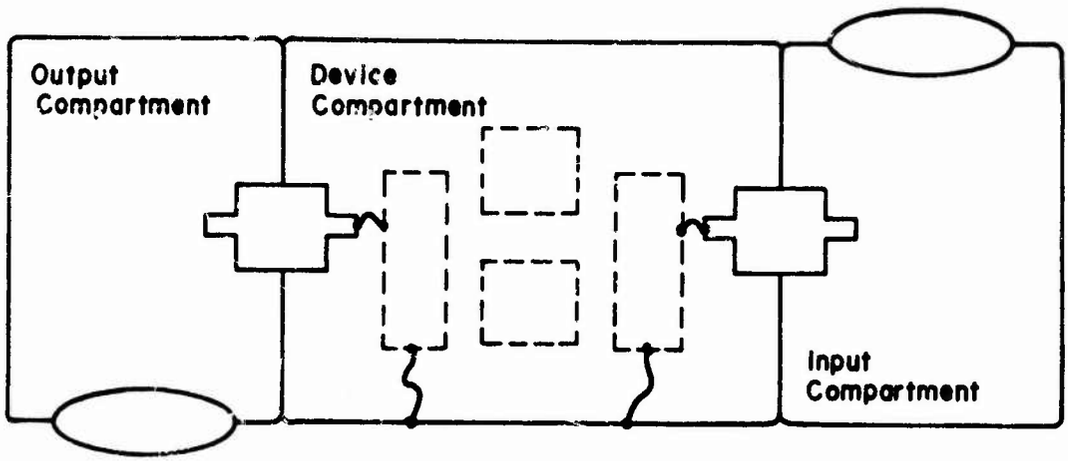

Fig. 4.22 DEVICE CONSTRUCTION (Ref. 6)

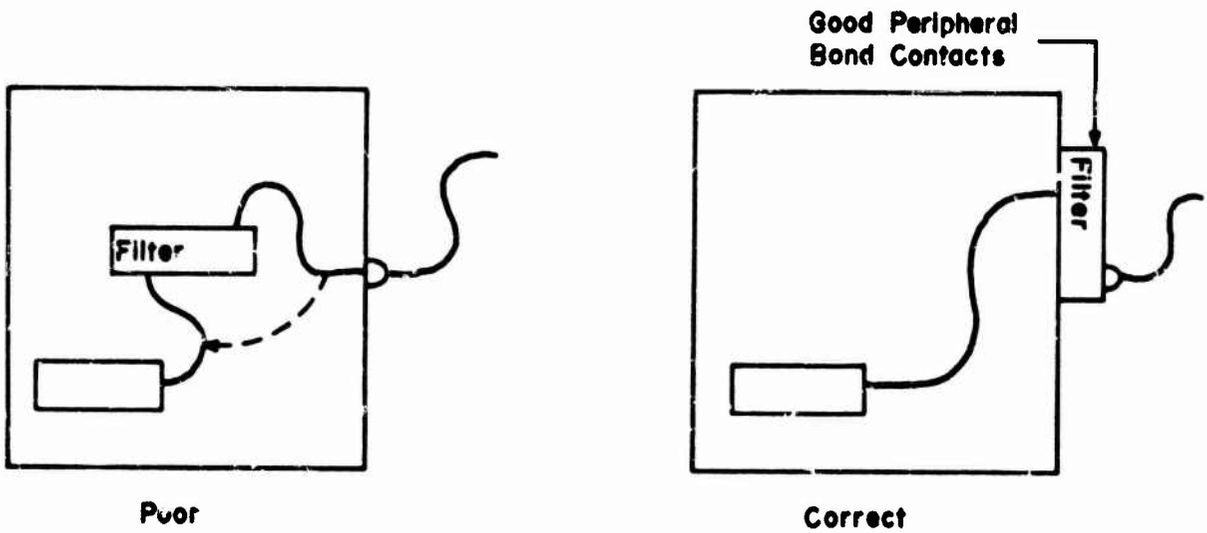

Fig. 4.23 DEVICE INSTALLATION (Ref.6)

to prevent an explosion in case a power line surge shorts a capacitor. It is possible for these fuses to blow without giving any indication, thus the filter action can be negated without anyone being aware of it. It is far better to specify a power line filter filled with transformer oil and no fuses, rather than the smaller potted type.

4.3 Amplitude Limiting

The impedance of an amplitude limiting device is a function of the current through it or the voltage across it. Devices placed in series such as a circuit breaker or fuse change from a low impedance to a high impedance when the current through them exceeds the rated value. Devices placed in parallel such as spark gaps or semiconductor junctions change from a high impedance to a low impedance when the voltage across them exceeds the rated value. Obviously, an amplitude limiting device is nonlinear and therefore a time domain analysis must be used to predict waveshapes and energy levels which will impinge on the protected equipment.

Since amplitude limiting devices produce large impedance changes when they operate, a portion of the energy which impinges on them is reflected due to impedance mismatch. As mentioned in the section on filters, this energy must be dissipated somewhere in the system.

An illustration of the difficulties which can occur if one does not consider the entire system when using amplitude limiting for protection is given in Figure 4.24. In the ideal case, the device simply clips off the top portion of the transient and the energy associated with the rejected portion is dissipated elsewhere. However, in the actual case, the rejected energy may "bounce again" in the system producing an elongated pulse as shown in Figure 4.24. This results in (1) larger amounts of energy being dissipated in the device and protected equipment increasing the probability of damage, and (2) a longer period of time during which the equipment is not operable.

To summarize, amplitude limiting for EMP protection can be a useful technique. However, to intelligently utilize amplitude limiting, one must be aware of the system characteristics, the operating modes of the available protection devices and any parasitics associated with the devices

4.3.1 Devices

The various types of amplitude limiting devices can be categorized as:

- Mechanical
- Dielectric breakdown
- Semiconductor junction
- Nonlinear resistance material

There are many device types which fall into each of these categories. However, the basic electrical characteristics which are of importance in selecting a device for transient protection are related to the mechanism by which limiting is achieved. The nomenclature given to these characteristics varies among manufacturers. In this manual the following terms will be used.

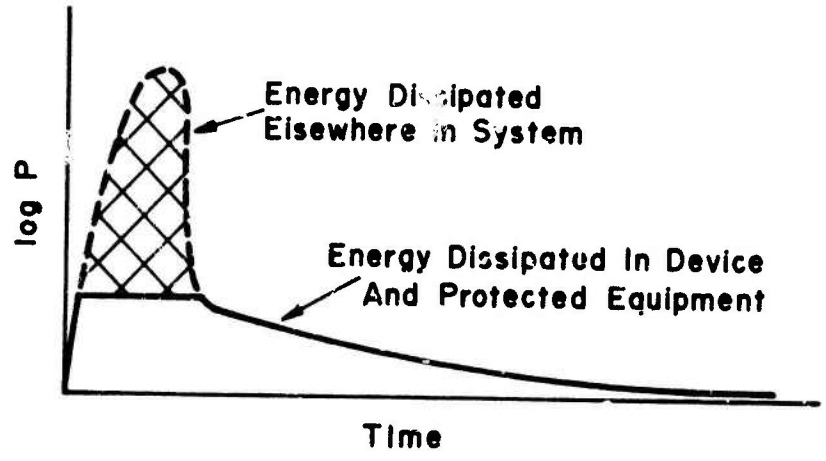

a) Ideal Case

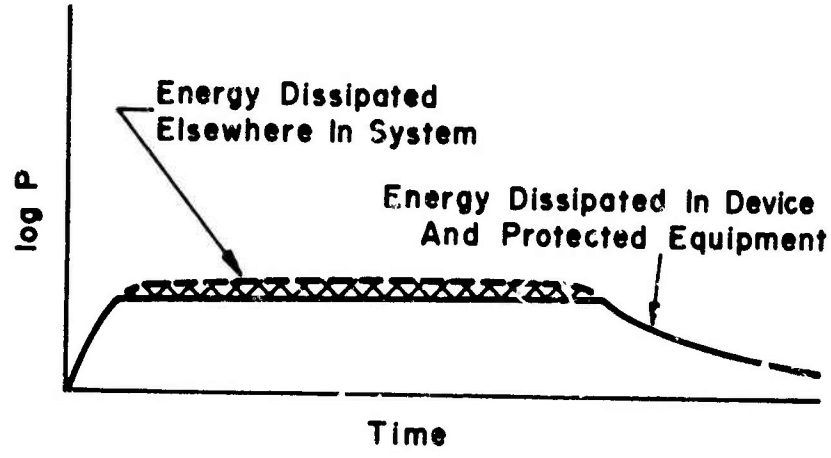

b) Actual Case

Fig. 4.24 AMPLITUDE LIMITED TRANSIENTS

- Static breakdown voltage -- the voltage at which the device begins to conduct when subjected to a very slowly rising DC voltage. The static breakdown voltage must be greater than the normal operating voltage of the circuit in which the device is used.

- Surge breakdown voltage -- the voltage at which the device begins to conduct when subjected to a rapidly rising voltage transient. This value may be dependent on the rate of rise of the applied voltage.

- Clamping or arc voltage -- the voltage which is maintained across the device after breakdown has occurred. This value is generally dependent on the current which is flowing through the device and is normally given for a specific value of current.

- Extinguishing voltage -- the value of voltage at which the device changes from a conducting to a nonconducting state. This voltage may be a function of the current through the device.

- Surge current -- current which flows through the device during the time which the transient is applied. The surge current rating of a device is dependent on both the peak value of the current and the waveform since these quantities determine the energy which the device must dissipate.

- Follow current -- the current from the system power source which flows through the device during and after the transient which has produced breakdown in the device. This rating is of importance for devices which do not extinguish immediately after the transient has subsided.

- Leakage current -- the current which flows through the device when it is in its nonconducting state. The value is sometimes specified in terms of an insulation resistance instead of a leakage current. This rating is used to determine the effect which the device will have on a system during normal operation.

- Shunt capacitance -- parasitic capacitance which appears across the terminals of the device. The size of this capacitance determines the degradation which will result if the device is used in a high frequency system.

- Polarity -- refers to the symmetry of the device's voltage versus current characteristic. A bipolar device has a symmetrical characteristic whereas a unipolar device has an unsymmetrical characteristic. Bipolar devices may be used in either ac or dc circuits. Unipolar devices may be used directly in dc circuits but must be used in combination with other unipolar or bipolar devices in ac circuits.

4.3.1.1 Mechanical Devices

Mechanical devices include fuses, circuit breakers, and relays. Fuses and circuit breakers are placed in series with a line and are actuated by current sensing. Relay contacts may be placed in series or in parallel and hence may be used to stop current by opening or to shunt current by closing. A relay may be actuated by sensing of voltage or current depending on the connection of the relay coil.

Mechanical devices will not provide primary EMP protection due to their slow response times. In addition, the manual replacement or reset of fuses and circuit breakers after they have operated would result in relatively long periods of time during which equipment is not operational. Since relays can be connected in a self resetting configuration, they may be useful in a hybrid scheme for automatically resetting a fast acting device such as a spark gap. An application of this type is discussed in Section 4.3.2.

4.3.1.2 Dielectric Breakdown Devices[7]

Dielectric breakdown devices (often called spark gaps) utilize two or more electrodes separated by a dielectric which is usually gas. The voltage versus current characteristic has the general shape shown in Figure 4.25. As can be seen from the figure, this is a bipolar device. The value of the static breakdown voltage is controlled by the type of gas used, the pressure of the gas, and the spacing of the electrodes. The static breakdown voltage for commercially available devices is generally greater than 90 volts.

The surge breakdown voltage is dependent on the rate of rise of the applied transient voltage. The manufacturer presents this information in curves of the type shown in Figure 4.26. These curves provide the user with the value of the surge breakdown voltage as a function of the rate of rise of the transient and the device type. For example, a device type corresponding to curve D_2 would break down at voltage C in time A when subjected to a transient having a rate of rise given by curve B. Use of this information and a plot of the expected transient waveform allows one to determine the energy and peak voltage which will impinge on the load before the spark gap responds.

After breakdown has occurred, operation of the spark gap moves across the V-I characteristic of Figure 4.25 along the curve labeled "turn on". Generally, the current which results from an EMP transient is sufficient to produce operation in the arc region of the spark gap characteristic. This arc voltage is to some extent a function of current and remains across the device until the combination of voltage applied and current available falls into the extinguishing region of the characteristic.

In ac systems, the spark gap will extinguish at the first zero crossing of the ac voltage following the transient. However, in dc systems, extinguishing of the gap may be a problem if the normal system voltage is greater than the arc voltage. In such a case, the current through the device due to the system voltage must be limited.

Figure 4.27 illustrates the relationship which exists between system characteristics and the device characteristic. To ensure that the device will extinguish, the system characteristic must be entirely within the extinguishing region of the

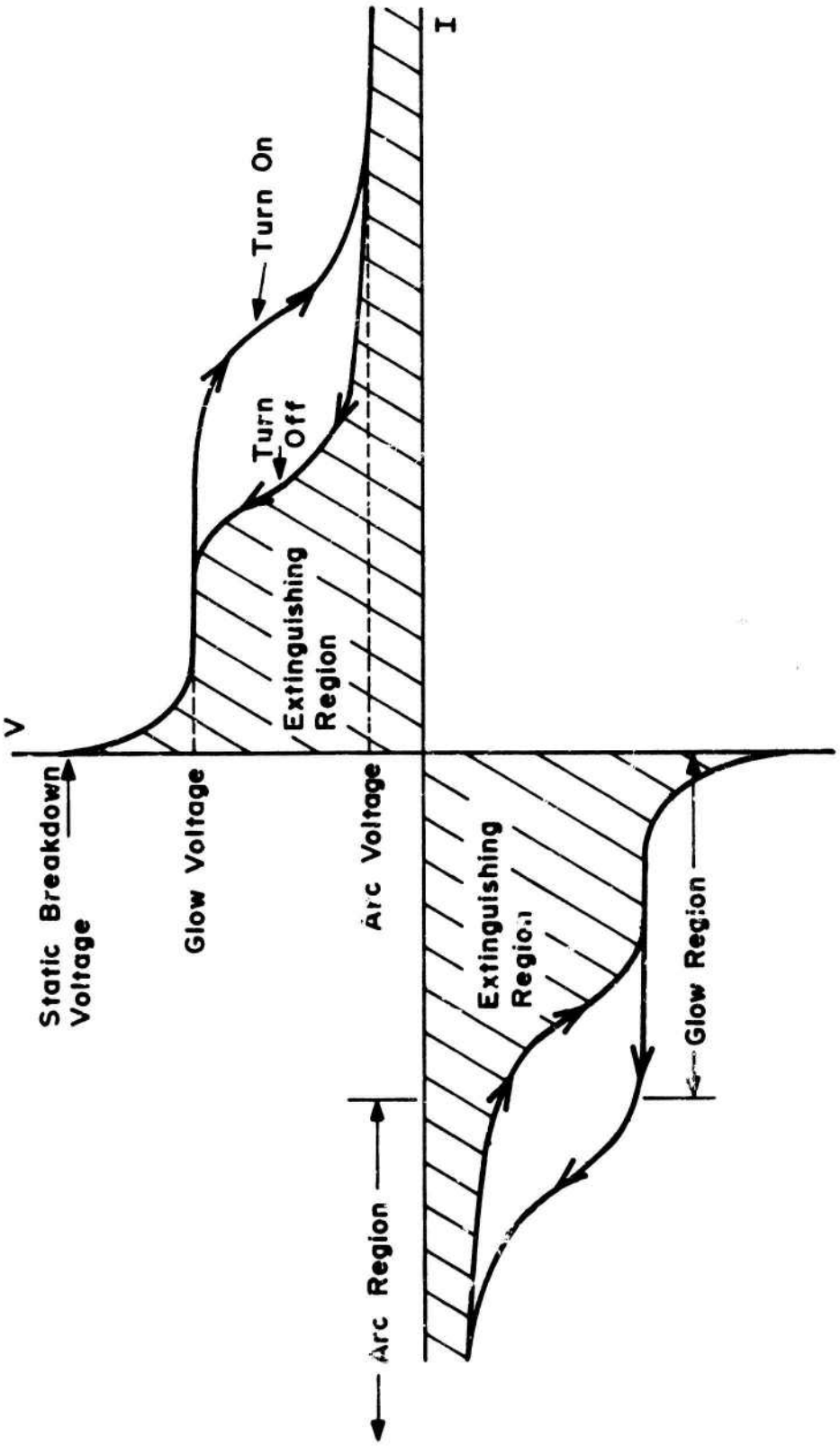

Fig. 4.25 TYPICAL V-I CHARACTERISTIC OF A SPARK GAP

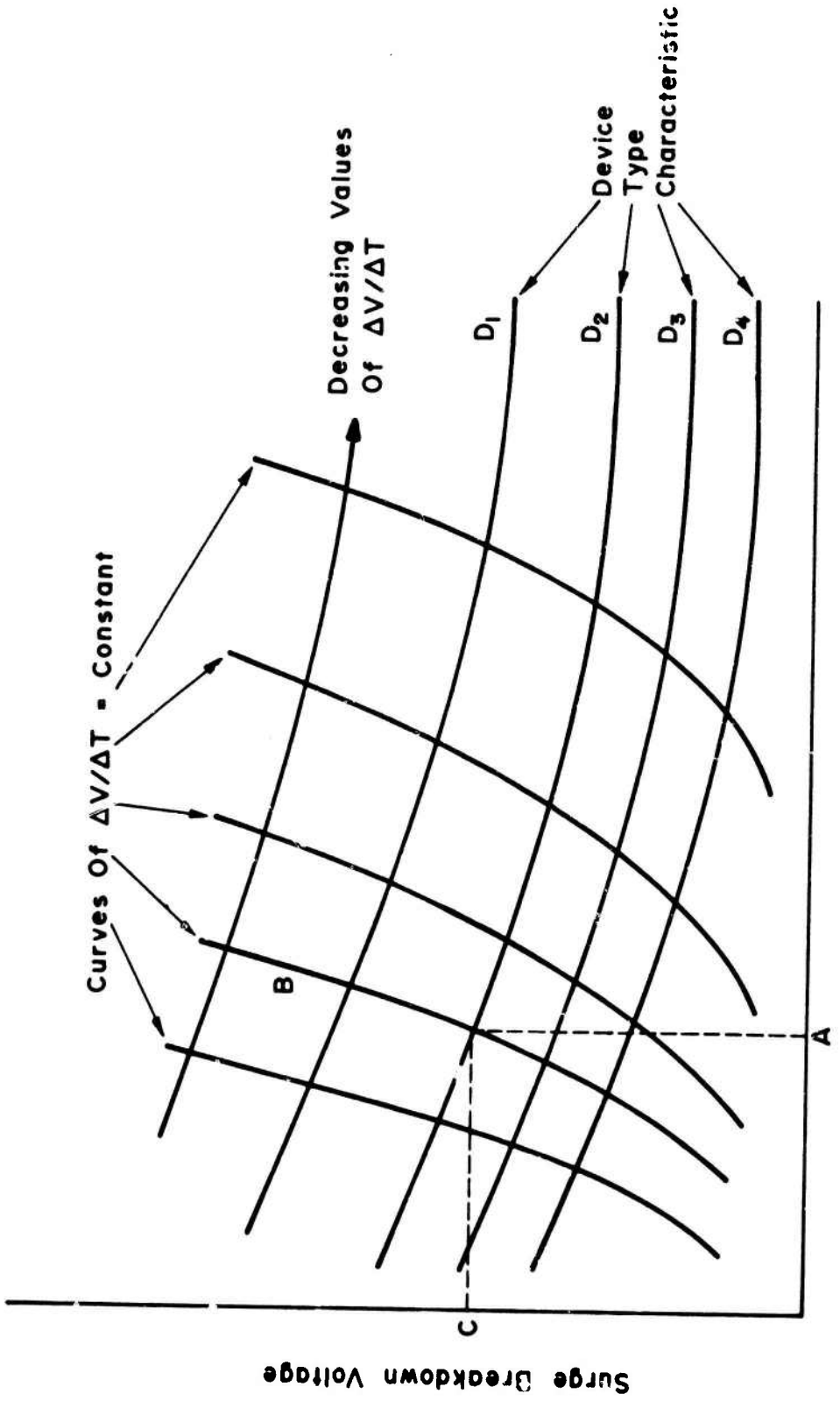

Fig. 4.26 SURGE VOLTAGE CHARACTERISTICS OF SPARK GAPS

device characteristic. Therefore, the system associated with case A would not extinguish while extinguishing would be achieved in the case B system.

Use of a spark gap for protection in the case A system of Figure 4.27 would require the insertion of a resistor in series with the spark gap. The size of the resistor would be such that the short circuit current available at the terminals of the spark gap is reduced to a value which places the combined resistor and system characteristic within the extinguishing region of the device characteristic. Placement of a resistor in series with the spark gap does have a detrimental effect on transient protection as shown in Figure 4.28. The device surge current produces a voltage drop across the resistor and results in a larger transient voltage in the system than would be present if the resistor were not used. If the manufacturer does not supply the actual characteristic of the device, he will specify the combination of system voltage and maximum short circuit current for which extinguishing will occur.

The current capacity of a spark gap is broken down into two categories -- 1) surge current and 2) follow current. The flow of current through the device causes heating of the electrodes. This heating, if excessive can inhibit extinguishing or may damage the device. Since the time which the EMP transient is present is relatively short, the peak surge current rating may be 100,000 amperes or more.

Assuming that the device is applied properly, follow current is not a problem in a dc system since extinguishing will occur immediately after the transient has subsided. However, in ac systems, extinguishing is normally accomplished by the zero crossing of the system voltage. In this case, current will continue to flow through the device from the time of the transient until the first zero crossing occurs.

The follow current is shown in Figure 4.29. The time during which follow current flow is considerably longer than the time during which the transient appears. For this reason, the follow current rating is generally at least an order of magnitude less than the surge current rating.

It must be kept in mind that follow current comes from the system power source. Therefore, any fast acting fuses or circuit breakers could be actuated by this current resulting in unnecessary down time for the protected equipment.

Spark gaps have minimal leakage currents since their insulation resistance is on the order of a thousand megohms. The shunt capacitance is generally less than 3 picofarads and may be a fraction of a picofarad. Therefore, they may be used to protect equipment which operates in the tens of megahertz region without appreciably affecting normal system performance.

4.3.1.3 Semiconductor Junctions

All semiconductor junctions (diodes) exhibit a current versus voltage characteristic similar to that illustrated in Figure 4.30. When used individually, the devices may be applied only in unipolar or dc systems due to their asymmetrical characteristic.

If a forward or positive voltage is applied to the device, current conduction begins for very small voltages and increases exponentially with increasing voltage. This continuous change in voltage as current changes is a disadvantage when using

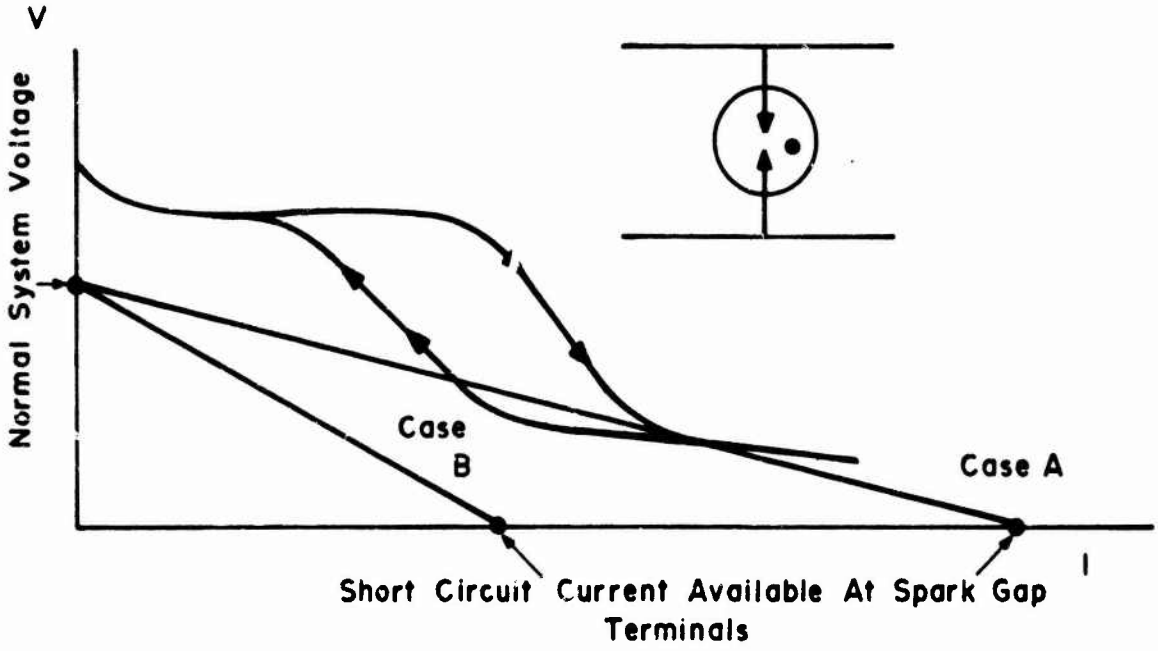

Fig. 4.27 RELATION BETWEEN DEVICE CHARACTERISTIC AND SYSTEM CHARACTERISTIC

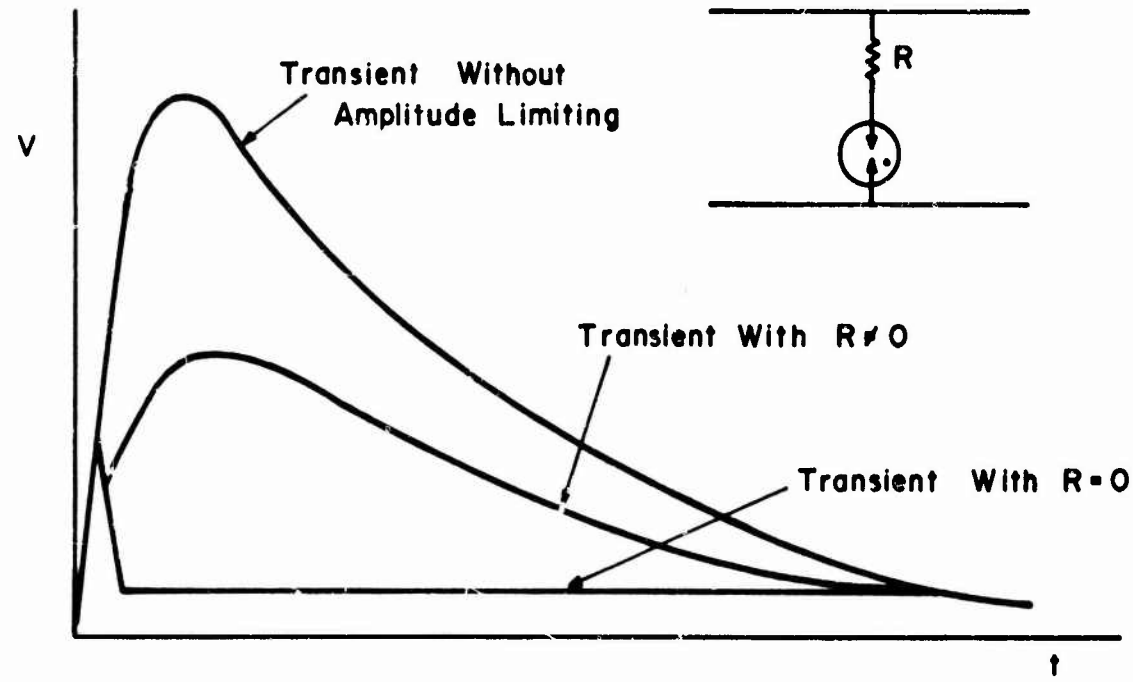

Fig. 4.28 EFFECT OF SERIES RESISTOR ON TRANSIENT SUPPRESSION

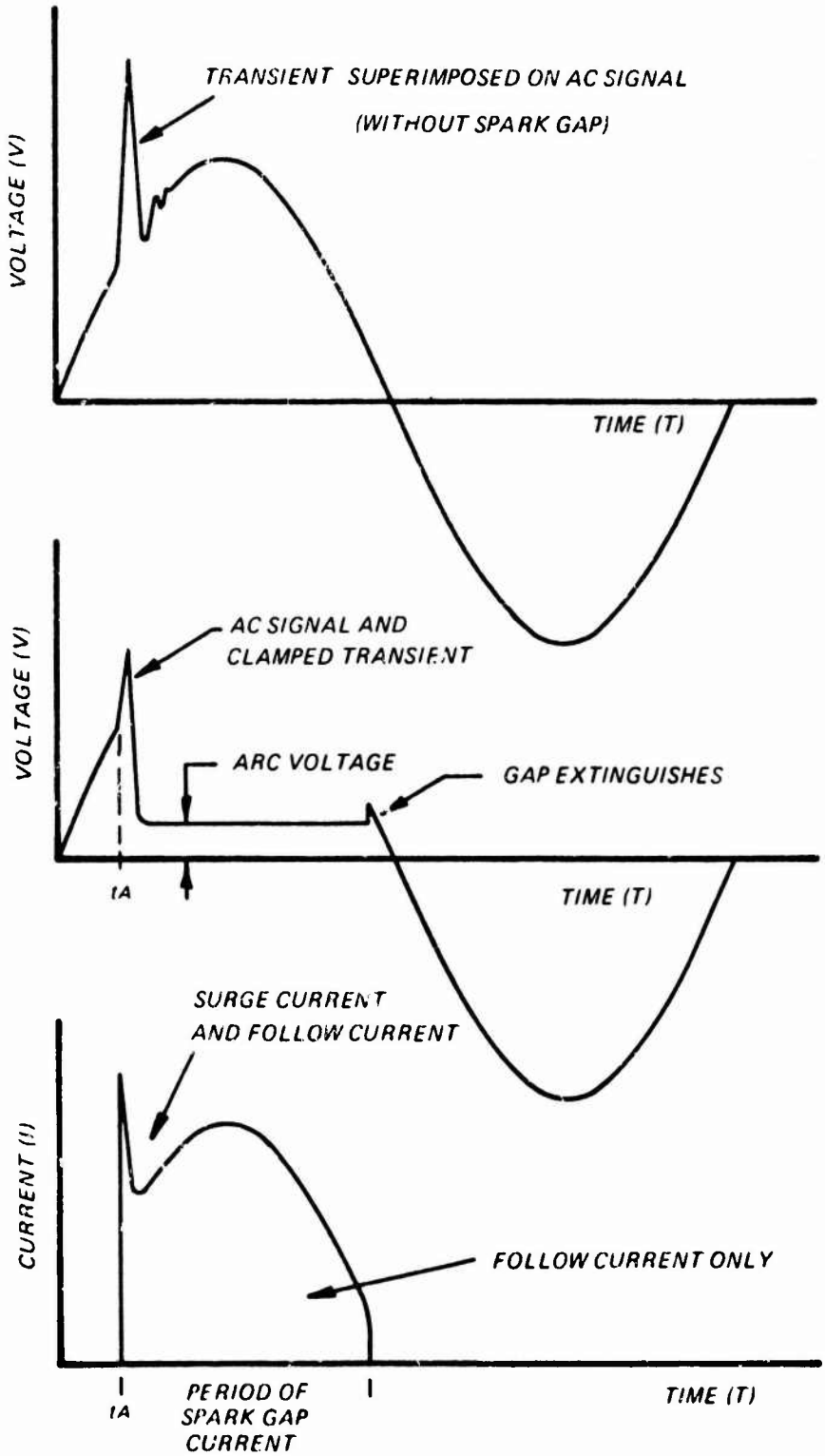

Figure 4.29 FOLLOW CURRENT

the device for EMP protection for two reasons -- 1) a considerable variation in the relative value of the clamping voltage for various peak currents results and 2) the continuous nonlinearity can produce distortion and intermodulation in the normal information signal. However, the forward mode of operation of the semiconductor junction is the only way one can achieve protection by amplitude limiting for voltage levels between one and three volts.

If a reverse or negative voltage is applied to the junction, current remains almost constant at a relatively small value until the breakdown voltage is reached. At this value of voltage the device changes from a nonconducting to a conducting state with $\Delta V/\Delta I$ having a value which ranges between a few ohms and a few hundred ohms depending on the power and voltage rating of the device. Diodes which are intended for operation in their reverse mode have a relatively sharp transition from the nonconducting to the conducting state and are referred to as zener, breakdown, or regulating diodes.

The static breakdown voltage is not a meaningful term when using a diode in its forward conduction mode since a continuous change in current results as the voltage is increased. For reverse operation, the static breakdown voltage is normally called the zener or breakdown voltage by the manufacturer and may have a value ranging between 3 and 200 volts with a tolerance of $\pm 5\%$, $\pm 10\%$, or $\pm 20\%$.

The surge breakdown voltage of a zener diode is not dependent on the rate of rise of the applied voltage and is the same as the static breakdown voltage. The response time is theoretically on the order of 10^{-12} seconds and values on the order of 10^{-9} seconds (correspondence from General Semiconductor Industries, Inc.) have been measured.

The clamping voltage of a zener diode is a function of the current flowing through it. For small currents, the relation between a change in voltage and a change in current is linear. However, as the current becomes large, the $\Delta V/\Delta I$ relation becomes nonlinear. This is easily seen in Figure 4.31. Normally curves showing the nonlinear region of the breakdown characteristic are not available. Therefore, this information must be specifically requested or measurements must be made on sample devices.

Some diodes such as the TransZorb* are manufactured specifically for transient protection. For these devices the manufacturer specifies the maximum clamping voltage which will result when the maximum allowed surge current is flowing.

The extinguishing voltage of a zener diode is the same as its breakdown voltage. Therefore, the diode will return to its nonconducting state when the transient voltage has decreased below the breakdown voltage.

The surge current rating for EMP type transients applied to a diode is generally not available unless the device is specifically intended for transient suppression. For forward voltage operation, the manufacturer specifies a surge current rating which is based on conduction for a half cycle of a power system sinusoid. For reverse voltage operation in the breakdown region, surge power curves of the type illustrated in Figure 4.32 may be given. The surge current rating is obtained by dividing the zener voltage into the surge power rating. It should be noted that the pulse width specified on these curves is considerably longer than the usual EMP

*General Semiconductor tradename.

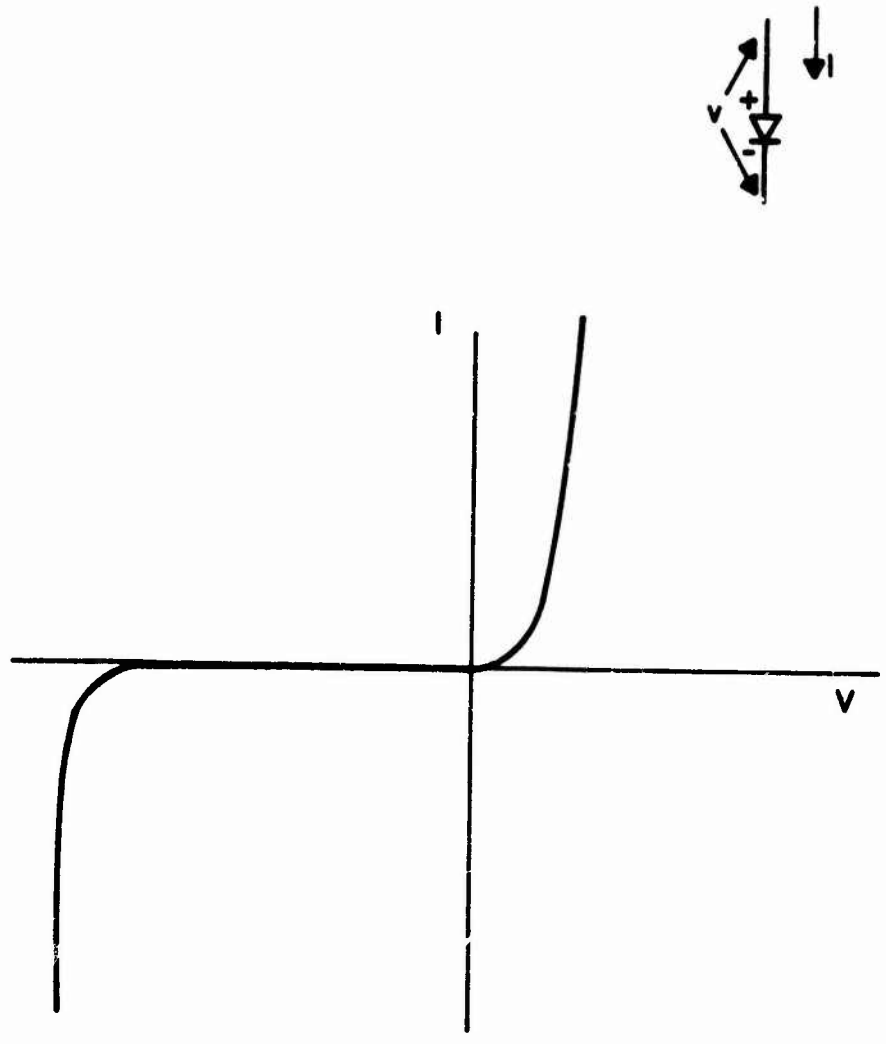

Fig. 4.30 TYPICAL SEMICONDUCTOR I-V CHARACTERISTIC

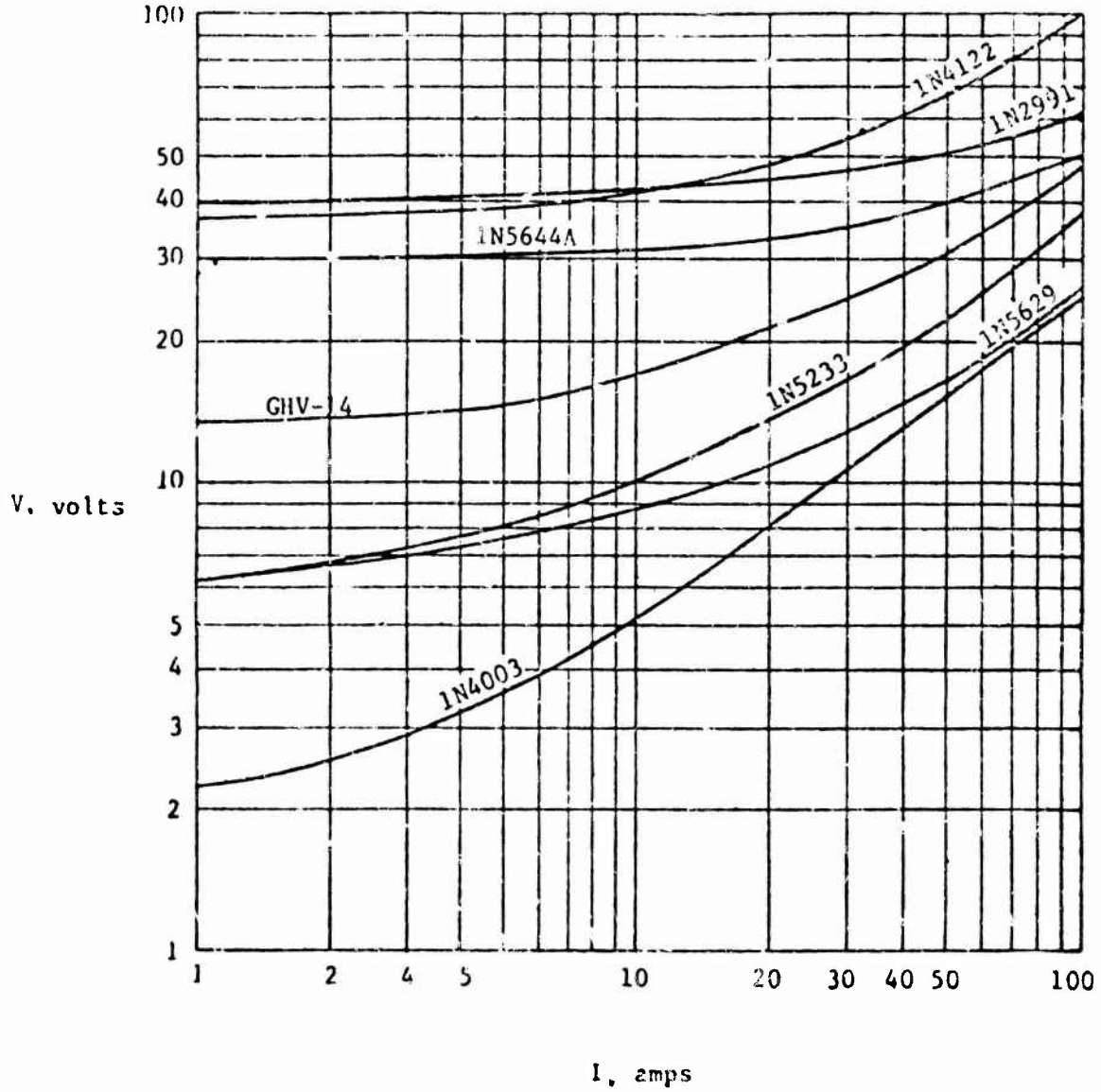

Figure 4.31 V-I CHARACTERISTIC CURVES FOR SOME ZENER DIODES, TRANSZORBS™ AND A 1N4003 RECTIFIER (Ref. 8)

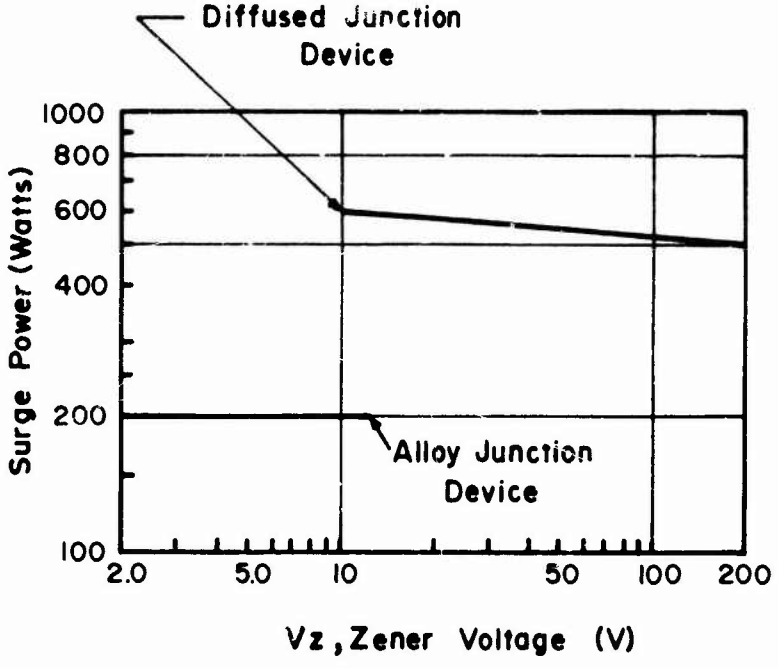

Square Wave Pulse
Pulse Width = 0.01 ms
Duty Cycle = 0%
T_L = 20°C ± 2°C at $\frac{3}{8}$"

Fig. 4.32 ZENER DIODE SURGE POWER CURVE

transient time and that allowable surge current increases as pulse width decreases. The thermal failure model equations may be used to estimate the surge current capabilities when this information is not available from the manufacturer or has not been determined experimentally.

Since the extinguishing voltage and the breakdown voltage are the same for a diode, follow current does not occur after transient breakdown of the device.

The leakage current has little meaning when the diode is operated in the forward voltage mode since current increases continuously with applied voltage. For reverse voltage operation, the leakage current is specified as a maximum value for a given reverse voltage (usually near the breakdown voltage) and a given ambient temperature.

The shunt capacitance information is generally provided only for reverse voltage operation. Since the capacitance is a function of the voltage, this information is often presented in curve form. An insertion loss specification is sometimes given in lieu of shunt capacitance information for devices which are intended for use as transient suppressors.

It is usually the case that the leakage current and the shunt capacitance associated with a semiconductor junction increase as the power rating increases and the breakdown voltage rating decreases.

4.3.1.4 Nonlinear Resistance Material (Varistors)

A nonlinear resistor obeys the current-voltage relationship

$$I = (|V|/K)^N \tag{4.6}$$

where K is a constant dependent on geometry and type of material used and I has the same sign as V, i.e., this is a bipolar device. A family of curves for increasing values of N is plotted in Figure 4.33. Note that as N increases, the characteristic asymptotically approaches an abrupt transition from a nonconducting to a conducting state at V equal to K.

Varistors can be made out of many materials such as silicon carbide, selenium, zinc oxide, and bismuth oxide. The GE tradename for its metal oxide varistor is MOV. MOV's have a fast response time and a relatively large value of N. Other varistor types are slower but have higher energy handling capabilities.

Figure 4.34 shows the V-I characteristics of several types of varistors. A linear resistor and a zener diode characteristic are included in the figure for comparison.

The V-I characteristics of some varistors and dielectric breakdown devices are presented in Figure 4.35.

One advantage associated with varistors is the ability to fabricate a large variety of geometrical shapes. This eases the packaging and installation problem as shown in Figure 4.36 and 4.37 where a varistor is included as an integral part of a cable structure.

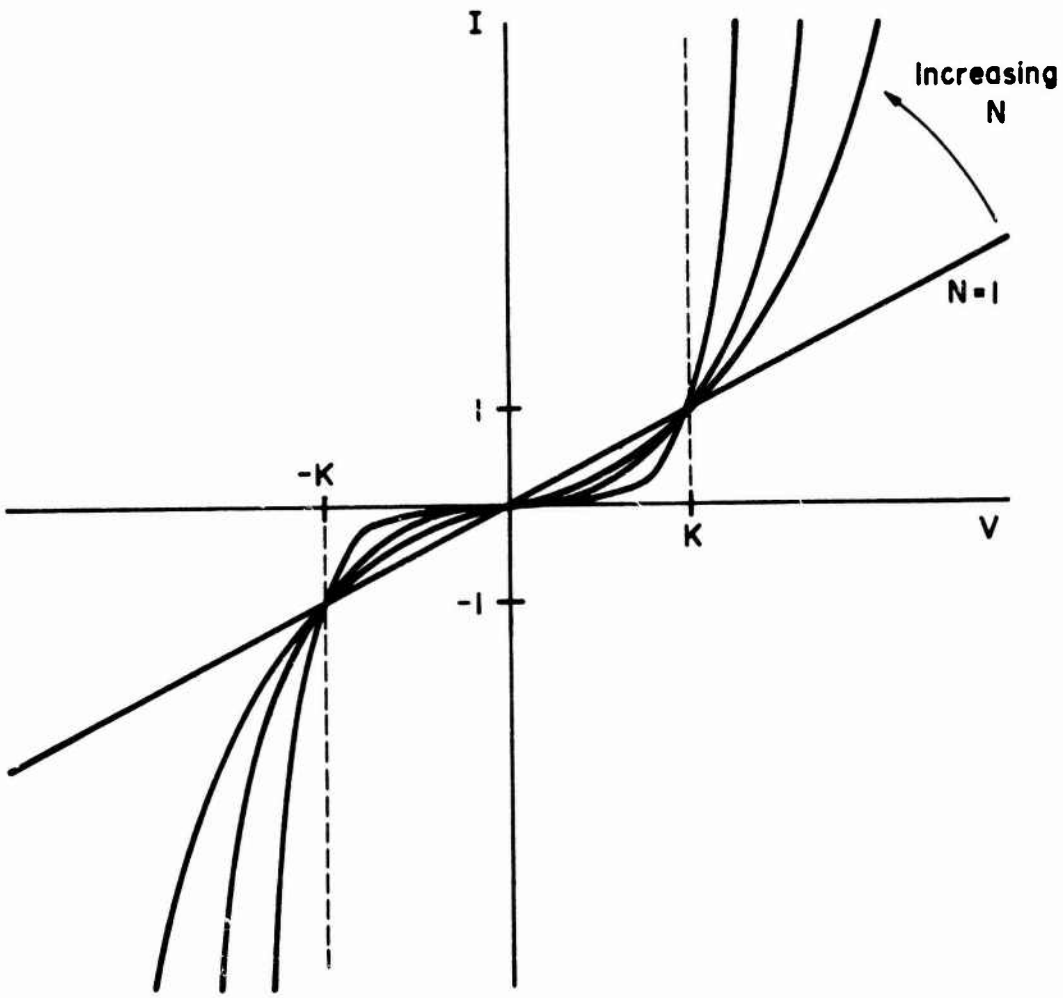

Fig. 4.33 PLOT OF NONLINEAR RESISTOR EQUATION

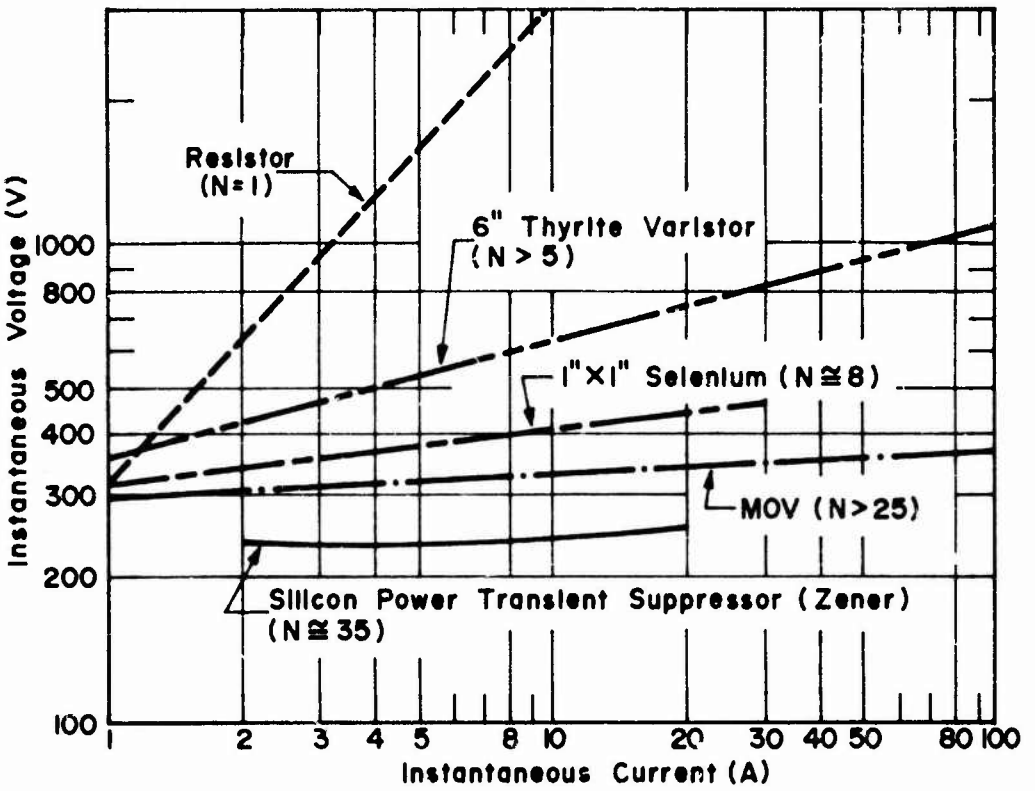

a) Comparison Of Amplitude Limiter Characteristics

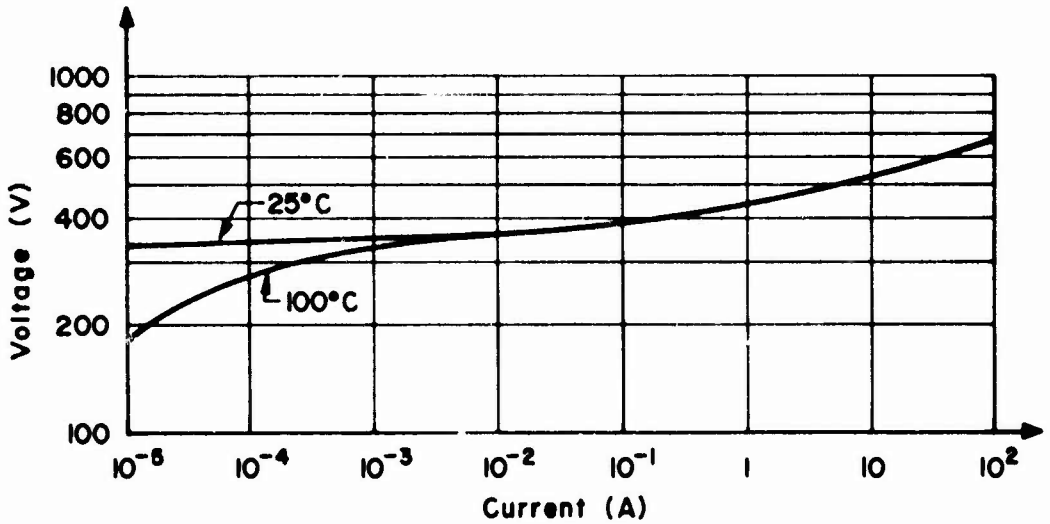

b) Typical GE-MOV* V-I Characteristics

* Trademark Of The General Electric Company

Fig. 4.34 AMPLITUDE LIMITER V-I CHARACTERISTICS (REF. 2)

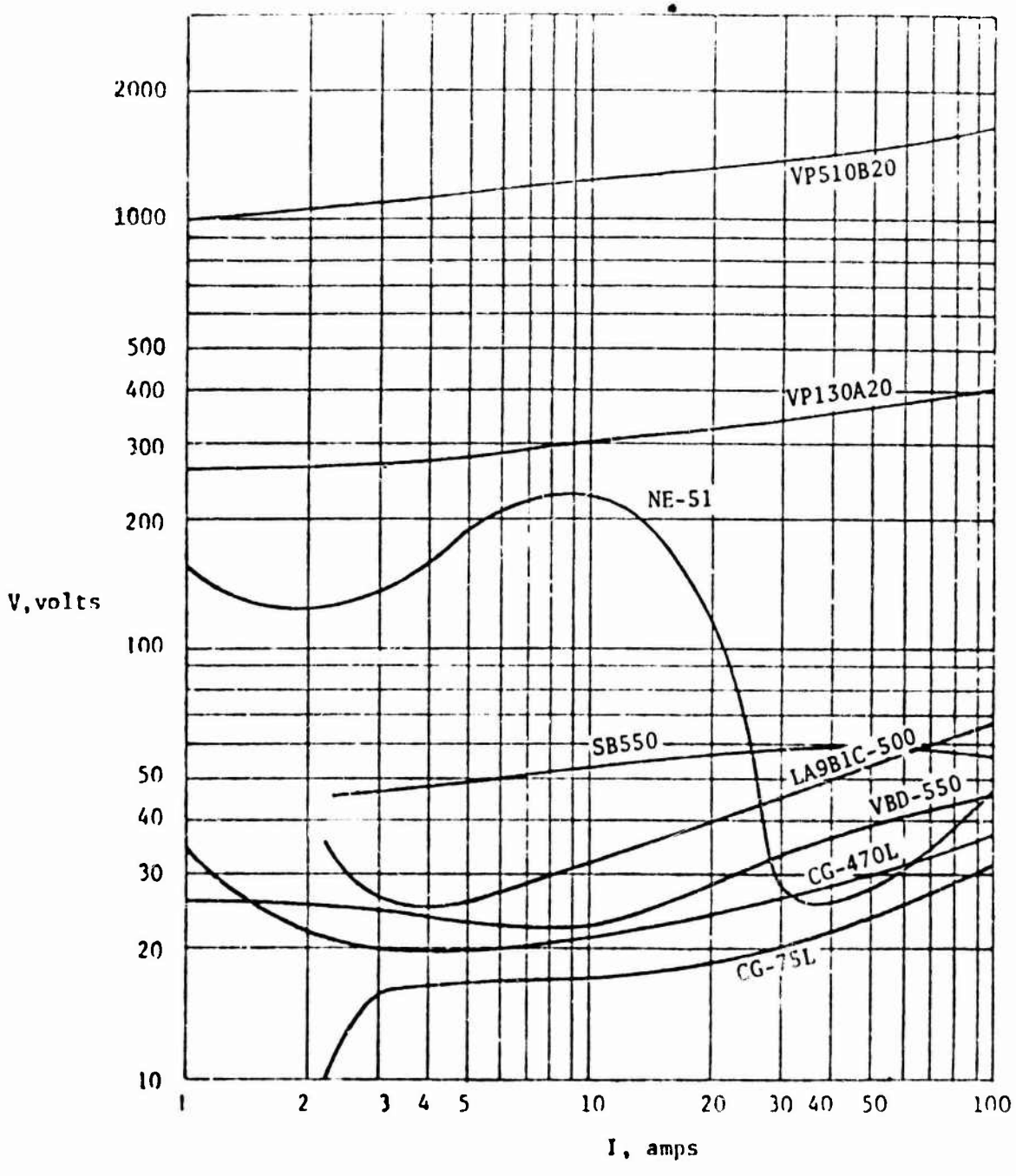

Figure 4.35 V-I CHARACTERISTIC CURVES FOR SOME MOVs AND DIELECTRIC BREAKDOWN TPDs (Ref. 8)

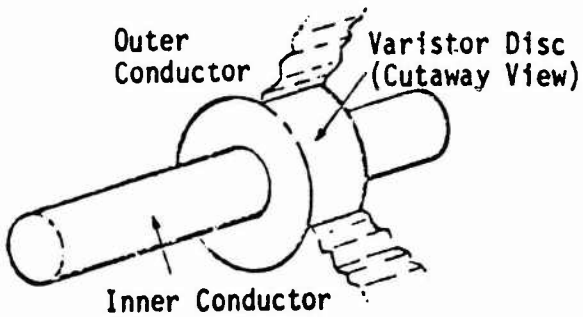

Figure 4.36 VARISTOR PROTECTIVE DEVICE (Ref. 10)

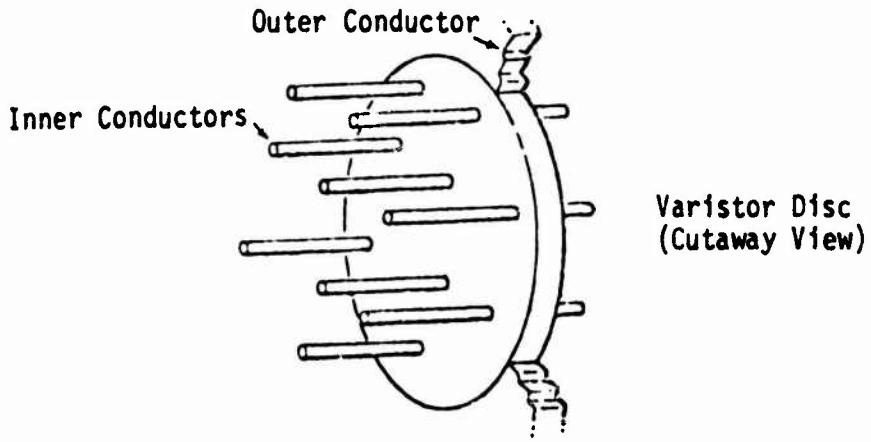

Figure 4.37 ALTERNATE GEOMETRY FOR VARISTOR PROTECTION (Ref. 9)

As in the case of the diode operated in its forward voltage mode, the nonlinear characteristic of a varistor could result in distortion or intermodulation of the normal signal in the system in which it is employed.

The varistor effectively responds instaneously to voltage surges and, therefore, the static breakdown voltage and the surge breakdown voltage are the same. However, due to the continuous change in voltage with current (especially for devices with small N), breakdown is defined as the voltage which produces a specific value of current flow through the device. This continuous change in voltage with current also results in a clamping voltage that is dependent on the peak current which exists during the transient pulse.

The extinguishing voltage is the same as the breakdown voltage. Hence, follow current is not a problem when using the varistor for transient protection.

There are two types of permanent damage which may result from the flow of surge current through an amplitude limiting device.

- Catastrophic failure -- Surge current amplitudes less than some critical value produce very little change in the device characteristic, i.e., small changes in the value of the breakdown voltage and the leakage current. When the critical value is exceeded, an abrupt change in the device characteristic occurs resulting in a large reduction of the breakdown voltage. Spark gaps and breakdown diodes are amplitude limiting devices which exhibit this type of damage.

- Gradual performance degradation -- Increasing the energy content of the surge current results in a continuous change in the device characteristic (usually an increase in the leakage current). The damage is dependent on the level of the surge current and on the number of times which the device is subjected to the transient. Varistors exhibit this type of damage.

Figures 4.38 and 4.39 show the effects of single energy surges on MOV characteristics. The cumulative effect of multiple pulses is illustrated in Figure 4.40. Both single pulse and multiple pulse surges result in larger values of leakage current.

The determination of when failure has occurred and, hence, the maximum allowable current, is dependent on the type of voltage which normally appears on the conductor to which the device is connected. If only dc voltage is present, failure is dependent on the value of leakage current (dc current drain from the line) which produces a degradation in system performance. For lines which carry ac voltage, the increase in slope of the characteristic represents a decrease in the effective ac shunting resistance associated with the device. For this case, the maximum ac current drain which will not effect system performance determines the allowable change in device characteristic. When dc and ac voltages are normally present, both the increase in leakage current and the decrease in ac resistance must be considered when determining the maximum allowable surge current.

The shunt capacitance associated with an MOV increases as the cross-sectional area increases and as the length decreases. The power handling capability is

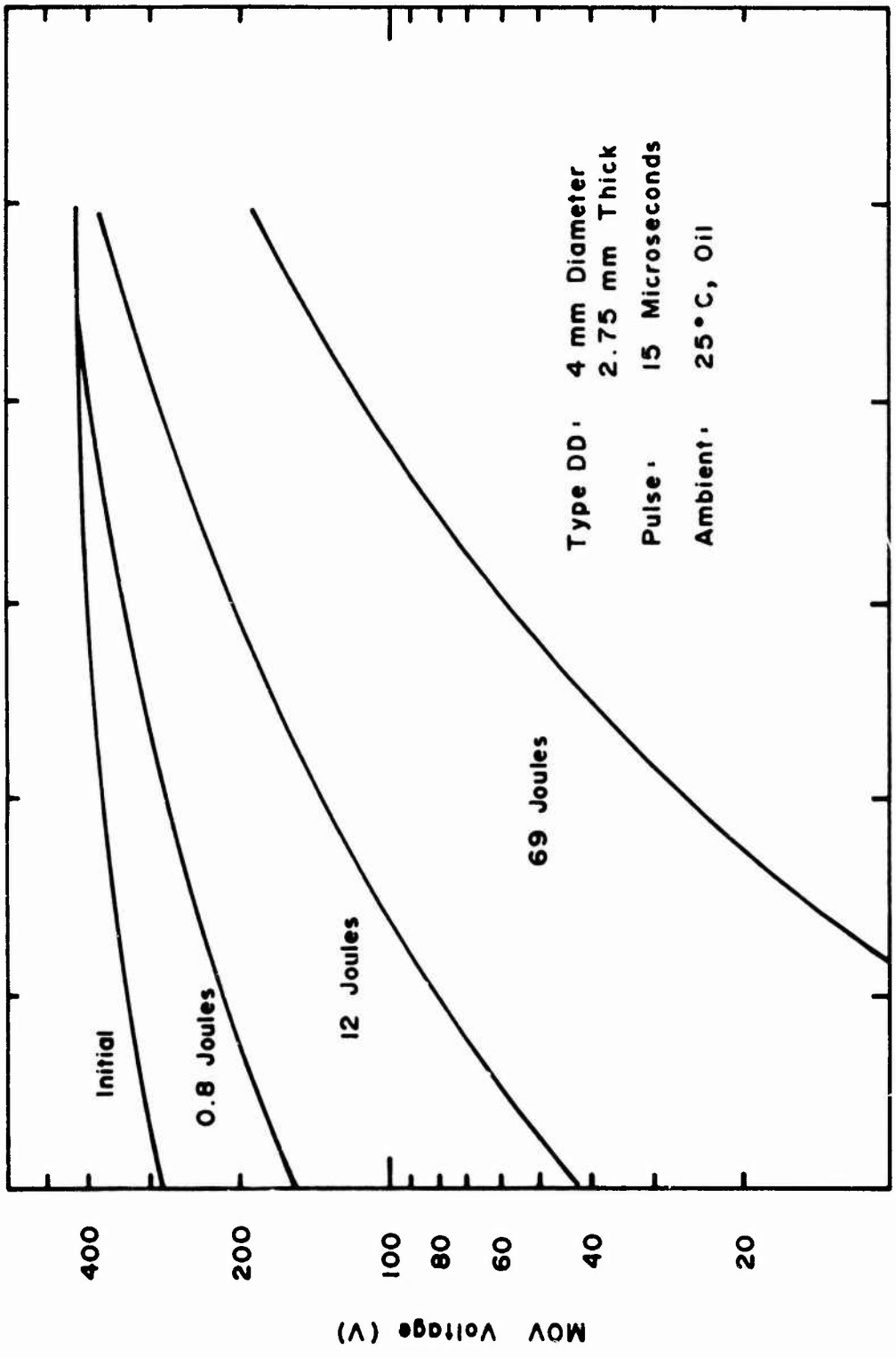

Fig. 4.38 TYPICAL PULSE ENERGY DEGRADATION OF GE-MOV™ CHARACTERISTICS (REF. 10)

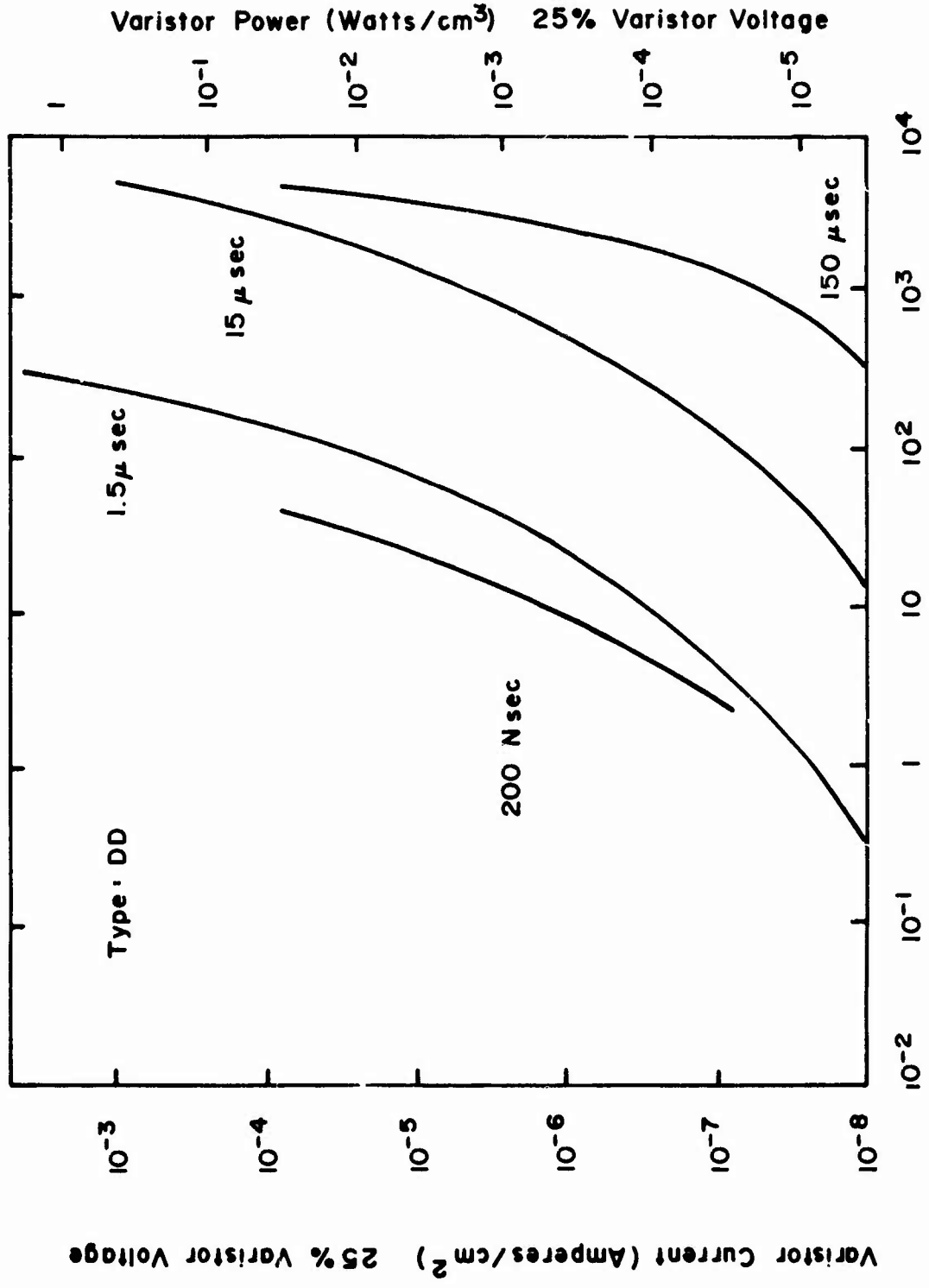

Fig. 4.39 TYPICAL ENERGY – TIME DAMAGE CHARACTERISTIC OF THE TYPE DD GE-MOV™ VARISTOR MATERIAL (REF. 10)

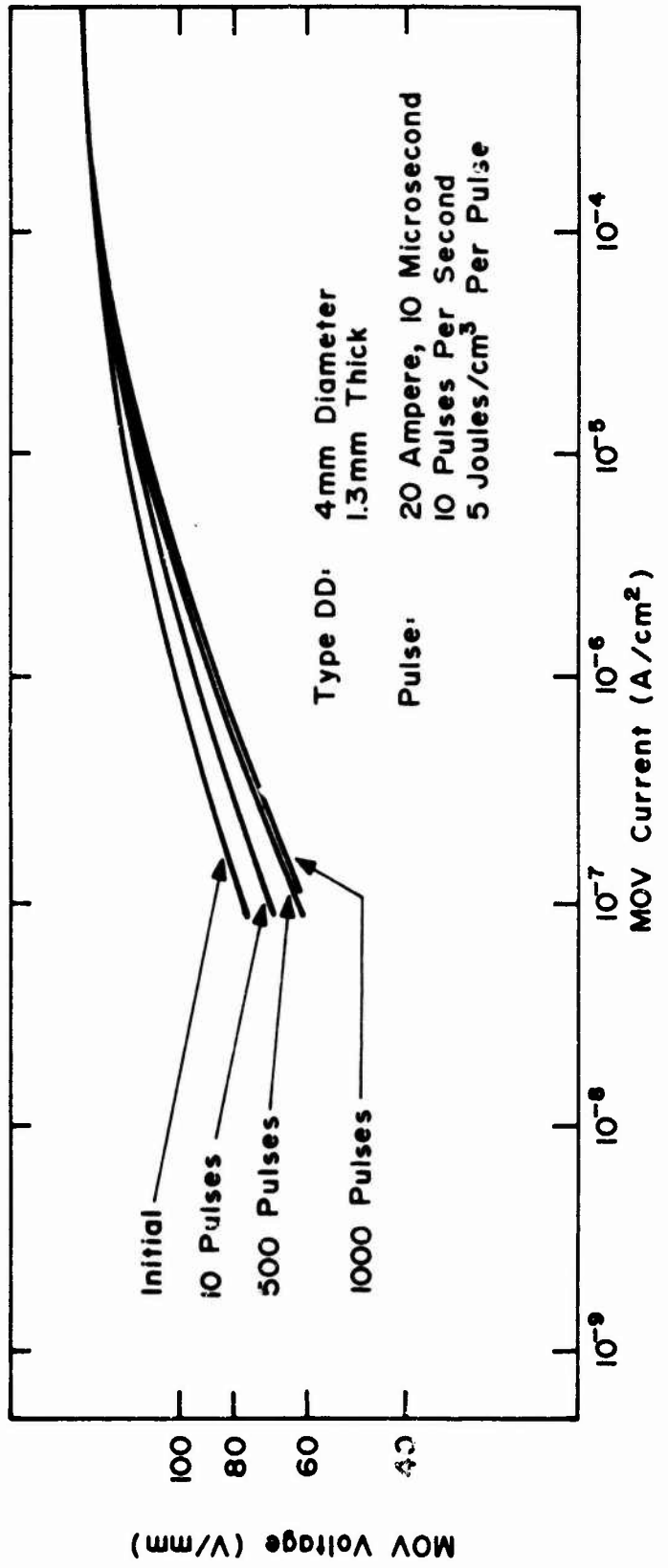

Fig. 4.40 GE-MOV™ HIGH POWER STRESS STABILITY (REF. 10)

proportional to cross-sectional area and the breakdown voltage rating is proportional to length. Therefore, shunt capacitance of the device increases with increasing power rating and with decreasing voltage rating.

4.3.2 Applications

An amplitude limiting device is normally employed to prevent component damage due to transient surges. The breakdown voltage of the device, however, must be greater than any instantaneous voltage that may normally appear on the lines which are protected by the device. Therefore, during the time which the transient is present, unless special design techniques are used, a circuit upset will likely occur due to the abnormal voltage at the circuit terminals. The importance of this temporary upset is dependent on the function of the circuit and length of time over which it occurs.

As previously mentioned, amplitude limiting devices produce large impedance changes when they operate which results in energy reflection due to impedance mismatch. This reflected energy must be dissipated and could increase system threat at other locations. Therefore, the most desirable application of amplitude limiting is an external location such as receiver antennas and external cabling where reflection of incident energy does not present a large problem.

When choosing a device for amplitude limiting, one must consider characteristics such as breakdown voltage, power rating, shunt capacitance, etc., which were discussed in the previous section. Table 4.2 provides a general comparison of the properties of the three basic types of amplitude limiting devices. Some of the low ratings given to spark gaps and zener diodes can be improved by using more than one device as illustrated in Figures 4.41 and 4.42.

When a diode is operated in the forward voltage mode with a small current flow, the junction capacitance is very small. In Figure 4.41 a), the current through the forward diode will be the small leakage current of the zener diode. Since this is a series connection, the total capacitance will be less than the small capacitance associated with the forward diode.

The total breakdown voltage in the connection of Figure 4.41 b) will be the sum of the breakdown voltages of the individual diodes. In part c) of this figure, diode 1 limits the voltage when V is positive and diode 2 limits the voltage when V is negative. The breakdown voltages of diodes 1 and 2 would be chosen somewhat larger than the normal positive and negative voltages in the system.

It should be noted that symmetrical bipolar limiting is not always desirable. For instance in dc power systems or in systems which employ unipolar signals (such as logic systems), a single zener diode with its associated asymetrical characteristic would provide more protection against transients with bipolar waveforms than a device or combination of devices which had a symmetrical limiting characteristic.

Figure 4.42 a) shows a hybrid connection utilizing a spark gap and a zener diode. The zener diode will respond almost instantaneously to a transient and will limit the voltage until the spark gap has fired. After breakdown of the spark gap has occurred it will operate in the arc region and the majority of the energy in the transient will be handled by the gap. To produce breakdown in the spark gap, the breakdown voltage of the zener diode must be greater than the static breakdown voltage of the spark gap.

Table 4.2

COMPARISON CHART OF COMMON PROTECTION DEVICES
DESIGNED FOR USE IN EMP APPLICATIONS (REF. 7)

	Ability to Divert large surge currents >500 AMP	Fast Response to rapid transient voltage rises	Minimum capacitance (minimum insertion loss)	Maximum Insulation Resistance	Ability to protect at low voltage levels <50 Volts
Gas filled Spark Gaps	1	3	1	1	3
Zener Diodes	3	1	3	2	1
Varistors	2	2	2	3	2

1 = most favorable

3 = least favorable

	Ability to protect at high voltage levels >400 Volts	Ability to extinguish on DC systems	Freedom from susceptibility to radiation effects	Capable of Bi-polar operation	Linearity (no cross modulation to voltage level of protection	No temperature dependence
Gas filled Spark Gaps	1	3	1	1	1	1
Zener Diodes	3	2	3	3	2	3
Varistors	2	1	2	1	3	2

1 = most favorable

3 = least favorable

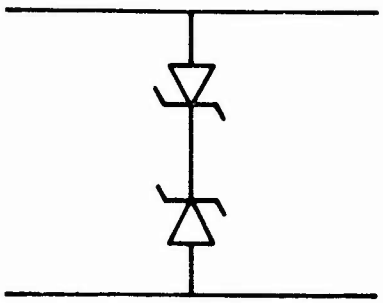

a) Reduction Of Shunt Capacitance

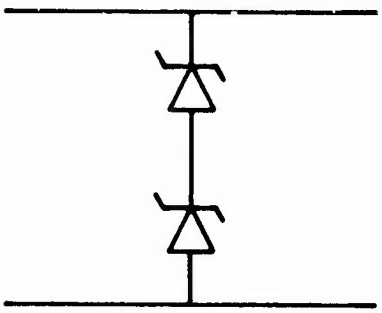

b) Increase In Breakdown Voltage

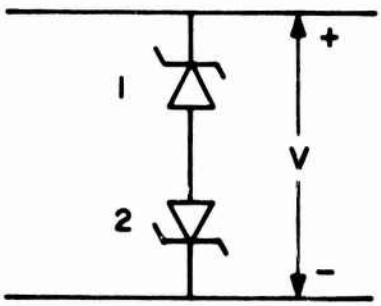

c) Bipolar Operation

Fig. 4.41 CONNECTIONS TO IMPROVE ZENER DIODE CHARACTERISTICS

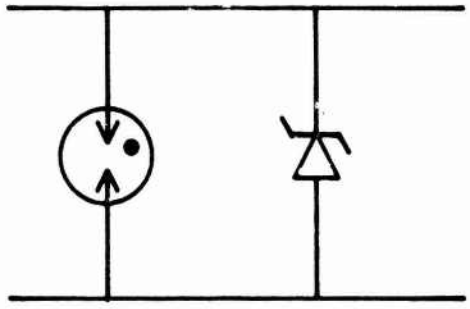

c) Reduce Response Time

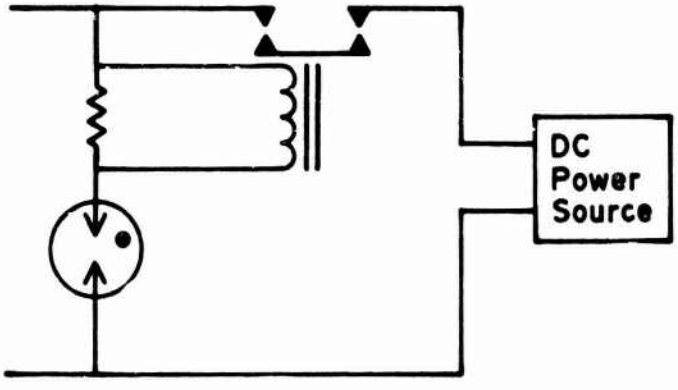

b) Extinguish In DC System

Fig. 4.42 CONNECTIONS TO IMPROVE SPARK GAP CHARACTERISTICS

Extinguishing in a dc system is a major problem when using spark gaps. A possible solution is shown in Figure 4.42(b). The follow current which results after the gap breakdown will produce a voltage across the small series resistor. This voltage will energize a relay which disconnects the gap from the power source and allows the gap to extinguish. When the gap has extinguished, the relay will no longer be energized and normal system operation resumes.

Amplitude limiting and spectral limiting may be used in combination as illustrated in Figure 4.43. In this connection scheme, the amplitude limiter provides the dual functions of reduction of transmitted energy and reduction of voltage stresses on the filter components.

4.3.3 Installation Practice

To contain the radiated field which results from the switching action and large surge current in amplitude limiting, the device must be mounted in a well grounded, shielded enclosure. In addition, the length of leads used to connect the device to the protected circuit must be kept short since lead inductance can result in a significant voltage.

Voltage overshoot due to lead inductance is illustrated in Figures 4.44 through 4.48. Figure 4.44 shows an EMP type transient applied to a 50Ω load before amplitude limiting is employed. Figures 4.45 through 4.47 show the effect of increasing lead lengths when an amplitude limiting device is used. It is easily seen that the peak value of voltage increases and that the length of time during which the overshoot occurs also increases as the lead length is increased. The transient voltage across the leads is shown in Figure 4.48. If one were to raise these curves by 200 volts, a near reproduction of the traces in Figure 4.46 and 4.47 would result, indicating that lead inductance is the major factor which contributed to the overshoot.

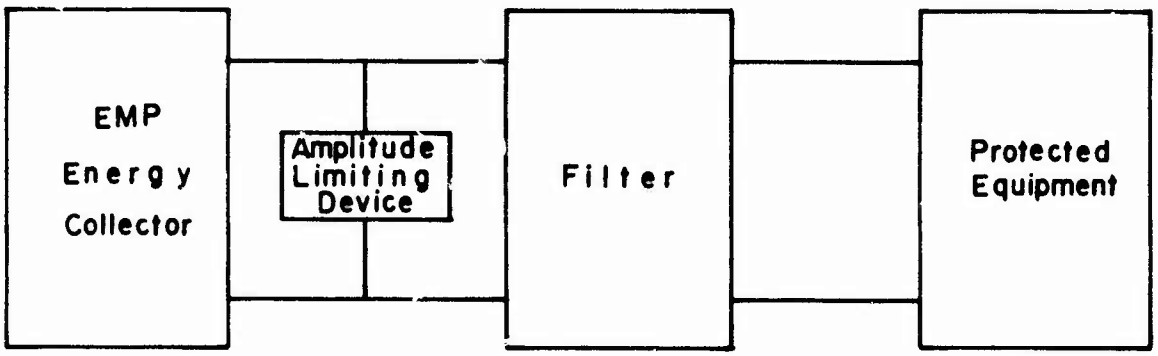

Fig. 4.43 COMBINED AMPLITUDE AND SPECTRAL LIMITING

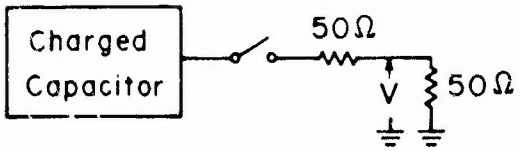

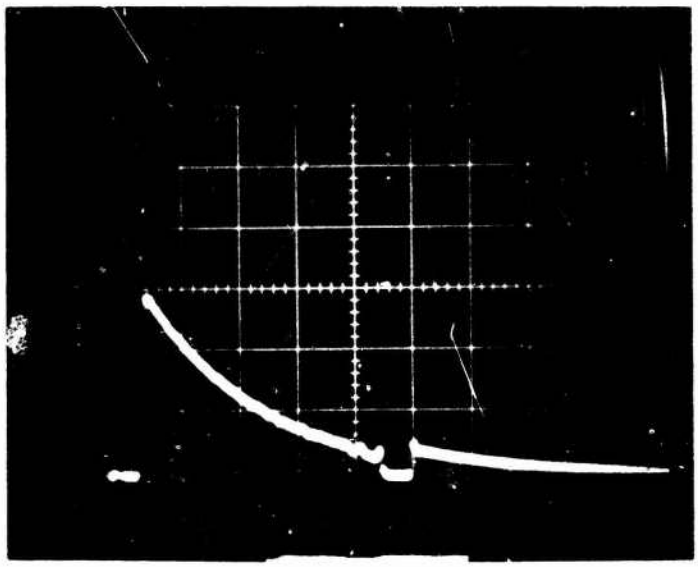

Hor = .2 μsec/Div.
Vert = 200 V/Div.

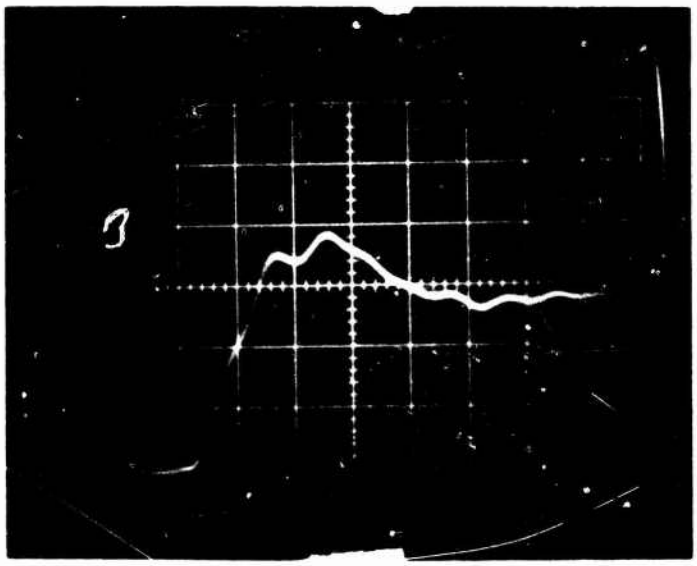

Hor = 5 nsec/Div.
Vert = 200 V/Div.

Fig. 4.44 EMP TEST WAVEFORM

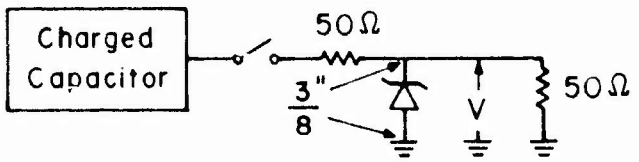

Trans Zorb
IN5665A
Breakdown Voltage
200 V

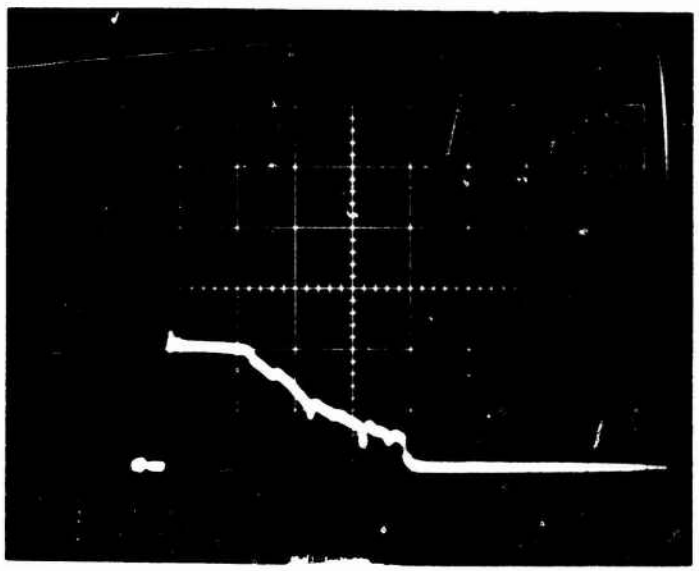

Hor = .2 μsec/Div.
Vert = 100 V/Div.

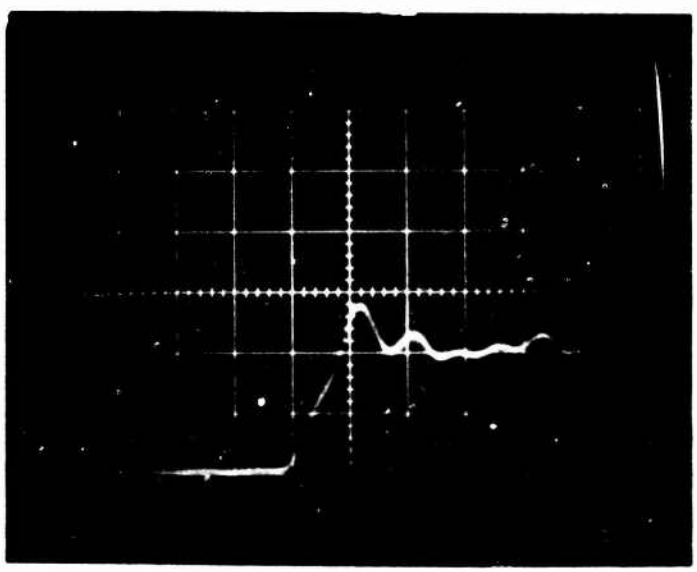

Hor = 5 nsec/Div.
Vert = 100 V/Div.

Fig. 4.45 AMPLITUDE LIMITING WITH SHORT LEADS

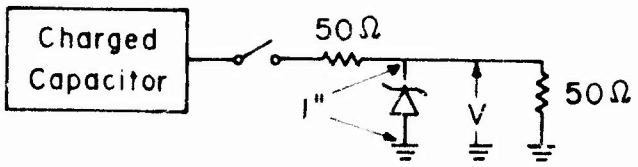

Trans Zorb
IN5665A
Breakdown Voltage
200 V

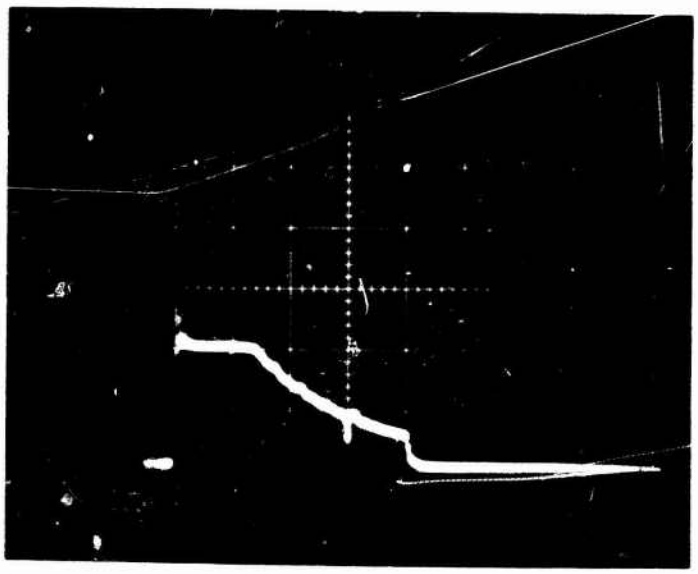

Hor = .2 μsec/Div.
Vert = 100 V/Div.

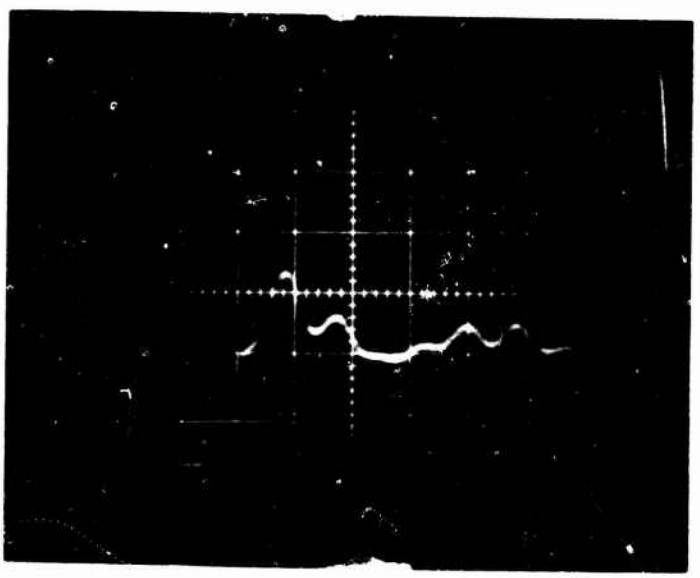

Hor = 5 nsec/Div.
Vert = 100 V/Div.

Fig. 4.46 AMPLITUDE LIMITING WITH A TOTAL DEVICE LEAD LENGTH OF 2 INCHES

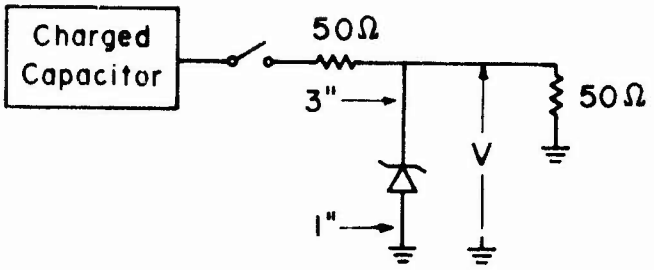

Trans Zorb
IN5665A
Breakdown Voltage
200 V

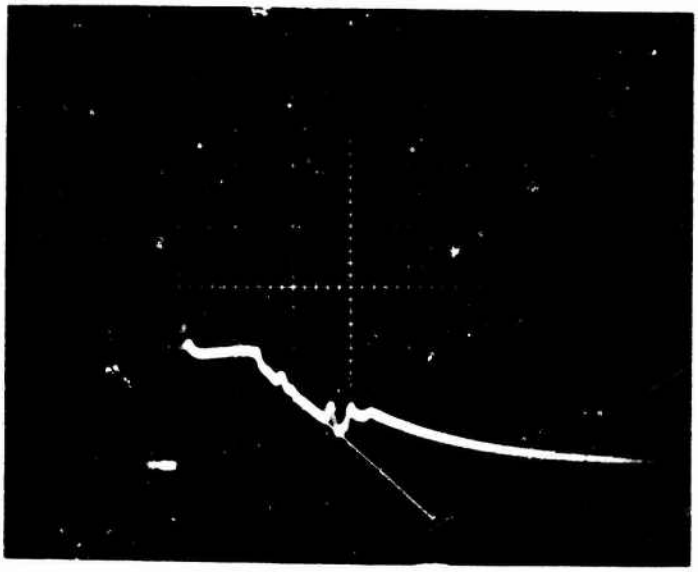

Hor = .2 μsec/Div.
Vert = 100 V/Div.

Hor = 5 nsec/Div.
Vert = 100 V/Div.

Fig. 4.47 AMPLITUDE LIMITING WITH A TOTAL DEVICE LEAD LENGTH OF 4 INCHES

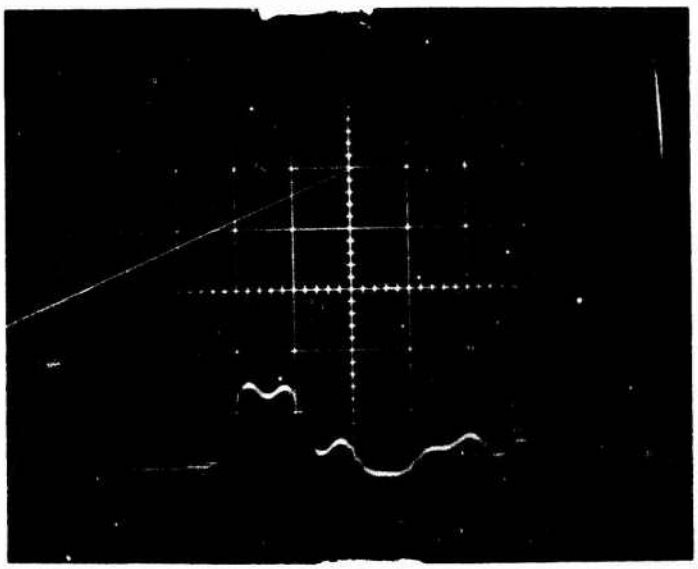

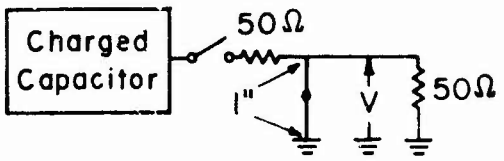

Hor = 5 nsec / Div.
Vert = 100 V / Div.

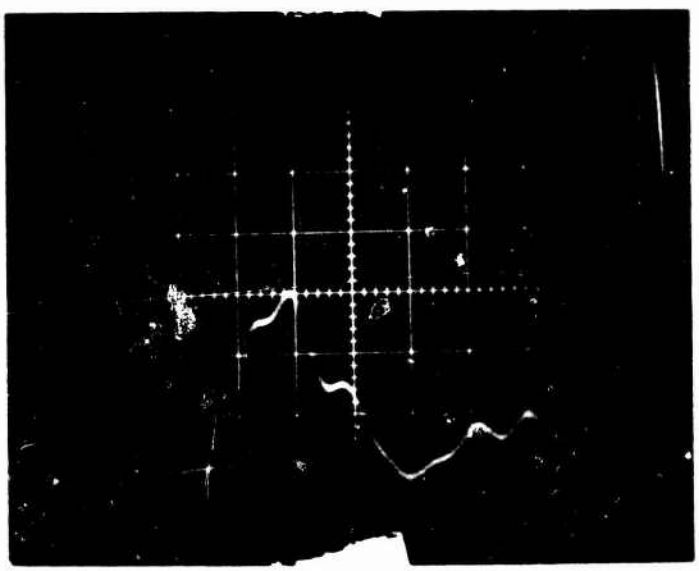

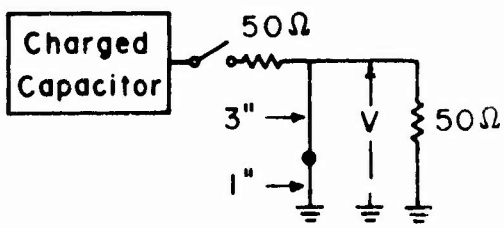

Hor = 5 nsec / Div.
Vert = 100 V / Div.

Fig. 4.48 TRANSIENT VOLTAGE DEVELOPED ACROSS LEAD LENGTHS

REFERENCES

1. Bridges, J.E., and Emberson, W.C., EMP Preferred Test Procedures (Selected Electronic Parts), Draft Number 2, DNA001-72-C-0084, IIT Research Institute, July 1973.

2. EMP Damage Hardening Guidelines, AFWL Contract No. F29601-72-C-0028, The Boeing Company, November 1972.

3. Perala, R.A., and Ezell, T.F., Engineering Design Guidelines for EMP Hardening of Naval Missiles and Airplanes, NOL Contract No. N60921-73-C-0033, Mission Research Corporation, December 1973.

4. "Lossy Transmission Line Filters", Lundy Electronics and Systems, Inc., Glen Head, New York.

5. Morgan, E.G., and Erb, J.C., et al., Design Guidelines for EMP Hardening of Aeronautical Systems, C72-451/201, Autonetics, April 1972.

6. DNA EMP Awareness Course Notes, Second Edition, DASA-01-69-C-0095, IIT Research Institute, August 1973.

7. Hart, W., and Higgins, D., A Guide to the Use of Spark Gaps for Electromagnetic Pulse (EMP) Protection, Joslyn Electronic Systems, 1973.

8. EMP Electronic Design Handbook, AFWL Contract No. F29601-72-C-0028, April 1973.

9. Electromagnetic Pulse Handbook for Missiles and Aircraft in Flight, SC-M-710346, Contract No. DOAF(29-601)-64-4457 and FY7617-71-10270, Sandia Laboratories, September 1972.

10. Tasca, D.M., and Peden, J.C., "Characteristics and Applications of Metal Oxide Varistors for EMP Hardening", Paper presented at DNA EMP Seminar - "Subsystem and Component Susceptibility", IIT Research Institute, May 14-16, 1974.

CHAPTER 5

CONSTRUCTION TECHNIQUES FOR EMP REDUCTION

5.1 Introduction

The all metal construction of ships, using thick steel sheet and the continuous welding of all seams, would provide the near ideal EMP shield were it not for the myriad of apertures, cables, pipes, and other such penetrations throughout the metal structure that are necessary to make the ship functional. Furthermore, the internal network of metal "box-type" compartments or rooms within the interior of the ship's structure makes for even greater shielding against EMP. These metal "boxes", however, also contain many apertures and penetrations which degrade the basic shielding properties of this internal configuration of all-metal enclosures. Hence, from the standpoint of EMP protection, shielding of all metal ships is primarily a matter of controlling and/or properly treating these apertures and penetrations to exploit the inherent shielding characteristics of the ship's structure. This will, of course, include deciding to what extent shielding is necessary, selecting or locating the area(s) within the ship that are to be shielded and controlling all apertures and penetrations through those shielded areas.

In the sections that follow, a shielding philosophy for ships is adopted that is based on the premise that at least one EMP-free environment must be established within the ship to protect certain EMP-sensitive and mission-critical electronic equipments from exposure to the EMP fields. This EMP-free environment consists of an all-metal shielded enclosure together with penetration control techniques designed to maintain the basic shielding characteristics of the all-metal enclosure. The number of EMP-free zones required will depend on the type of ship, its mission, the amount of EMP-susceptible equipment it employs, and the distribution of these equipments throughout the ship. Hence, those EMP-free zones can consist of a select number of shielded compartments or rooms within the ship or of the entire ship's interior. The advantage of this approach is that:

- EMP-sensitive equipments within each of these zones do not have to be individually hardened.
- The addition of new equipment or retrofitting is less expensive since the equipments to be placed within the zone need not be individually hardened.

It is apparent that not all sensitive equipment can be contained within the zone, and treatment of this type of equipment is also considered.

The chapter contains five main sections. The first is the Introduction, the second deals with the EMP-free zone philosophy. The third section discusses shielding construction practices. Section four describes the Grounding Plan needed to implement the EMP-free zone approach, and Section five summarizes the shielding guideline.

5.2 Systems Geometry/Configuration

From a systems point of view, the ship itself can be looked upon as a "protective device" since the metal decks and bulkheads can provide substantial reduction of electromagnetic fields in internal spaces. Use of the correct construction techniques can enhance the shielding provided by the ship's structure and thereby reduce or eliminate the need for shielding on an individual equipment basis.

For shielding purposes, all systems may be considered as being either distributed, compact, or a combination thereof. The distinction between these configurations is somewhat difficult, and changes from ship to ship. Basically, a system is considered to be compact if it is practical to locate the entire system within a shielded compartment or a suite of contiguous shielded compartments. A system is considered to be distributed if, because of function or dispersion of system elements, it is not practical to shield the entire volume occupied or serviced by the system. An example of a distributed system is a radar system--the function of radar is just not compatible with the concept of compactness. The system will not work with the antenna in a shielded room. Other examples of distributed systems are the electric power or lighting systems. Such systems could only be considered compact if the entire ship were tightly shielded. In short, the distributed system is characterized by the existence of system elements and/or interconnections that are exposed to direct or poorly attenuated EMP.

5.2.1 Large Distributed Systems

In general, the distributed system must be hardened on the basis of the individual equipment, since each subsystem and/or cable will present a unique combination of pickup and sensitivity. If hardening is to be done on distributed system elements, as shown in Figure 5.1a, it is best accomplished by utilizing the protective techniques outlined in Chapter 4, together with shielding and techniques covered in the remaining chapters of this report.

If this approach were applied to large electronic systems, the hardening effort can become quite expensive. This is especially true of those systems containing many sensitive units interconnected by cables, such as the data processing and storage systems finding ever increasing use on modern warships. Under such circumstances it is usually best to partition the system, locating all possible susceptible equipment in a compact, shielded space and hardening all equipment which must remain distributed on an individual basis. Figure 5.1b gives an example of system partitioning for a hypothetical system.

Let us assume that the radar antenna is mounted atop the superstructure and that the receiver/repeater must be located nearby, within the superstructure. Furthermore, one can assume that the other subsystems are located below decks,

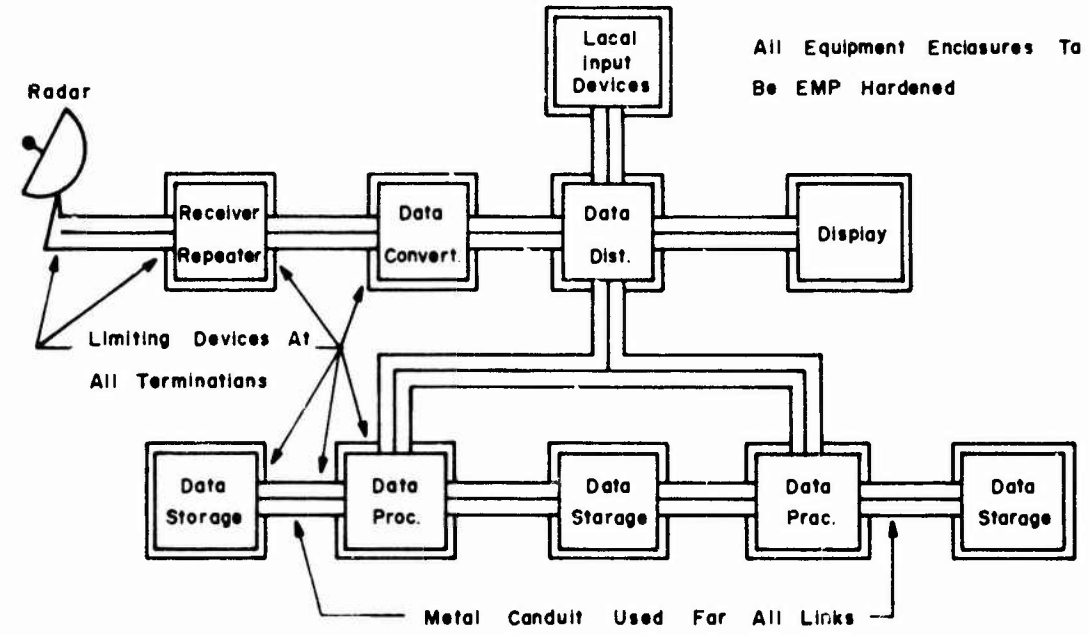

a) Totally Distributed System Protection Scheme

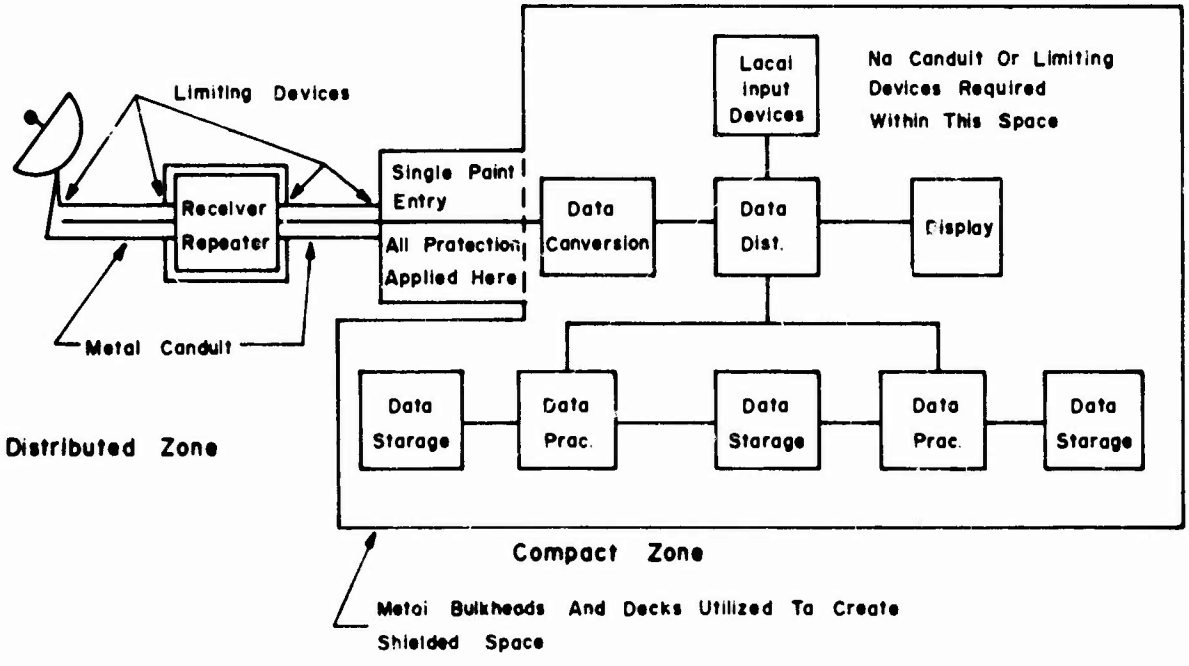

b) Partitioned System Protection Scheme

Fig. 5.1 EXAMPLE OF SYSTEM PARTITIONING

perhaps in scattered locations. Note that the receiver/repeater must be housed in a hardened cabinet and the cables connecting it with other subsystems should be protected by metal conduit as well as by limiting devices. The other subsystems, located below decks, will benefit from the partial shielding provided by the ship's structure, since as much as 60 to 80 dB of shielding may be present in well buried compartments. Digital equipment is very sensitive to operational upset and damage, and the shielding provided by a conventionally constructed buried compartment may not be adequate. For such equipment, rigorous structural hardening must be applied, otherwise each unit must be hardened individually.

In the partitioned system approach the inherent structural shielding of the ship is utilized to create a shielded space. The contained subsystems should be grouped as close together as is practical to reduce the size and cost of the hardened area. Any units which may not conveniently take advantage of such structural shielding due to constraints of function or location must be hardened individually. In Figure 5.1b we see such an example. The receiver/repeater and its interconnecting cables must still be hardened. All other units, however, have been gathered into a hardened, contiguous suite of compartments. In this area no shielded cabinets are required and no conduit or limiting devices are needed on the myriad of internal interconnections. The techniques necessary to provide such a hardened area will be discussed in the following sections of this chapter.

Finally, since many trade-offs are involved in determining where the systems can and should be partitioned, the ship and systems designers must work together to arrive at the most cost-effective compromise.

5.2.2 Compact Systems

Compact systems, in most instances, are those systems that employ semiconductor and integrated circuit devices which are most susceptible to EMP. Fortunately, however, their compactness enables the ship designer to locate them in specific EMP-free zones.

It is to be noted that modifying the shielding to provide an EMP-free zone will increase the cost of the ship. There will be significant savings, however, on all electronic equipment protected by the shielding. Thus, there will be savings on every new and/or replacement system throughout the life of the ship as well as during initial outfitting. Considering these various factors, the most cost-effective approach to shielding compact systems is, generally, to locate the system in a hardened area.

Such a hardened area is depicted in Figure 5.2. To take advantage of the structural shielding already provided by the ship, it is best to locate this area approximately amid ships. As will be shown, the major EMP penetration of a shielded enclosure is due to shield discontinuities, apertures and cable penetrations. However, the continuously welded seams presently used in ships' construction provide excellent shield continuity and allow very little direct EMP penetration. Thus, the major breaches in the shielding integrity of a ship compartment are due to apertures and cables.

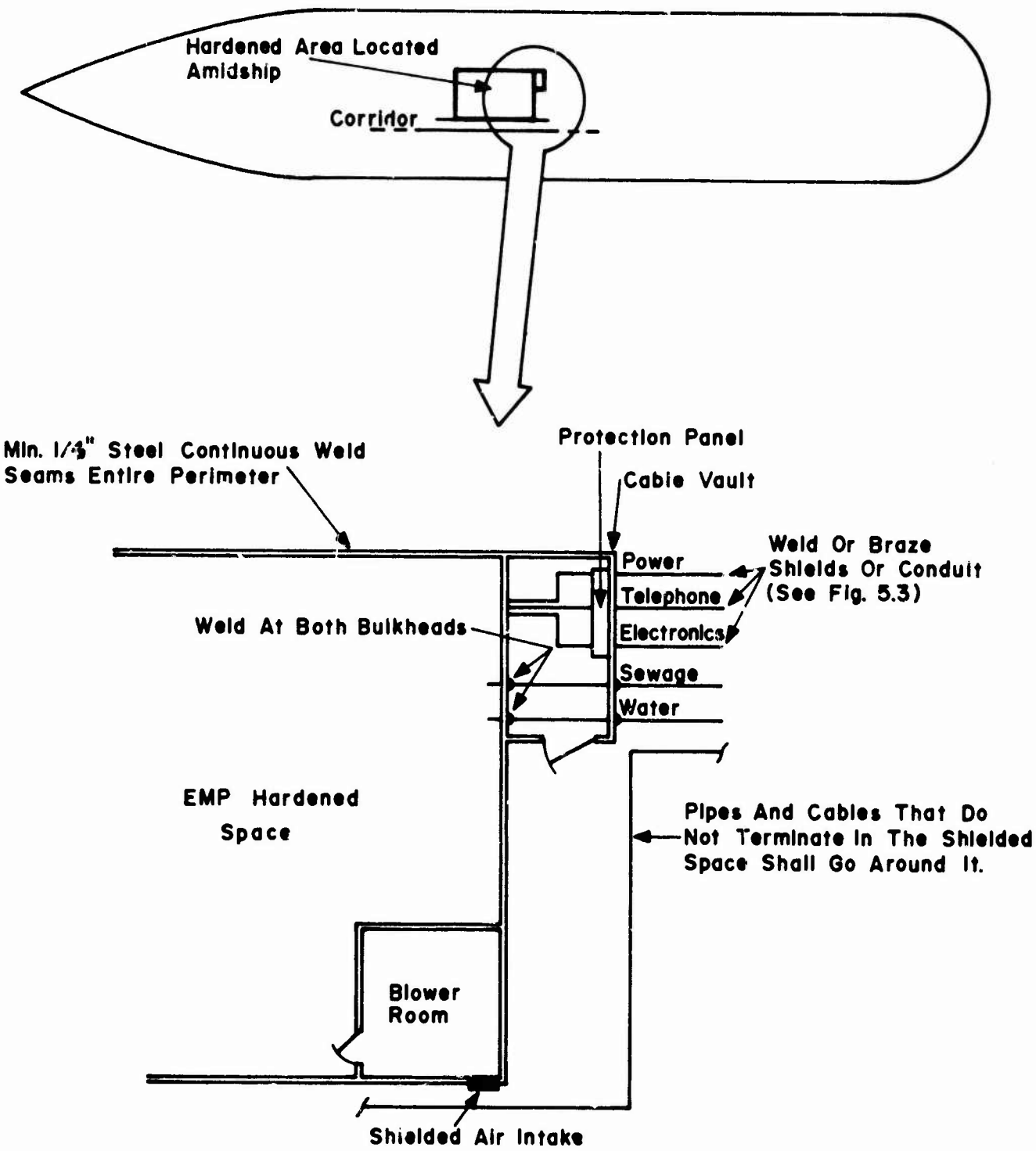

Fig. 5.2 TYPICAL EMP HARDENED SPACE

Only as many apertures as are absolutely necessary should penetrate the hardened area. No ducts venting to the outside of the ship should penetrate the area, as these ducts may possibly act as waveguides which carry portions of the external EMP field into the shielded area. This will require that ventilation for the hardened space be drawn from an adjacent corridor and exhausted in the same manner. These vents must be hardened as shown in Section 5.3.4. Any ducts which do not service the shielded space may not enter it, but must be routed around. The walls and decks defining the boundaries of this enclosure should be a minimum of 1/4" steel and continuously welded at all seams. Ideally, there should be only one entry, and this should be hardened as shown in Section 5.3.4. Bear in mind that an open door is a hole; and having a single entry provides one less aperture and eliminates a "short-cut" through the shielded zone.

Cables and cable-like structures that do not terminate within the shielded compartment should be routed around it. Those cables/pipes which service the shielded space should enter via a single point entry at a cable vault/cabinet. Within the cable vault, all cables entering or leaving the shielded space must be protected with protective devices, as already described in Chapter 4. The purpose of this action is to dissipate any excess energy that may appear on the cable conductors before they enter the shielded space itself. Because large amounts of energy may be released within the cable vault in the event of an EMP, it is recommended that there be no access door between the cable vault and the shielded space. Where the cables, conduits and other cable-like structures penetrate the outer wall of the cable vault, they should be circumferentially welded, as shown in Figure 5.3 (Class A bond per MIL-STD-131C-C). This is to dissipate any current being carried on the cable shield/conduit before it enters the cable vault. It is best to dissipate as much energy as far away from the sensitive equipment as possible.

5.3 Shield Construction

Metallic materials or structures illuminated by electromagnetic energy reflect part of the incident energy and absorb some of the rest. These two properties, if exploited correctly, can be used to protect or shield sensitive electronic equipments from the direct and damaging exposure to EMP radiation. In general, the most effective EMP shield would be a uniform all-metal enclosure having no apertures, seams, penetrations, corners, or similar discontinuities which tend to break the metal or geometric continuity of the enclosure. This requirement suggests that the ideal shield is either an infinite metal plate, a spherical metal shell or some similarly closed surface of revolution. Although, neither of these configurations are ever constructed, they do serve a useful purpose in providing an analytical basis for defining and establishing fundamental shielding concepts. Thus derived, these concepts can be useful in the analysis, design and development of the more practical shield configurations.

5.3.1 Shielding Effectiveness

For comparative purposes, it is convenient to rate a shield design in terms of "shielding effectiveness". This figure of merit takes on the character of a transfer function that relates the output to the input of an electromagnetic field impinging on the shield. "Output" in the sense is taken as the amplitude-frequency characteristics of the electromagnetic (EM) field inside the shield

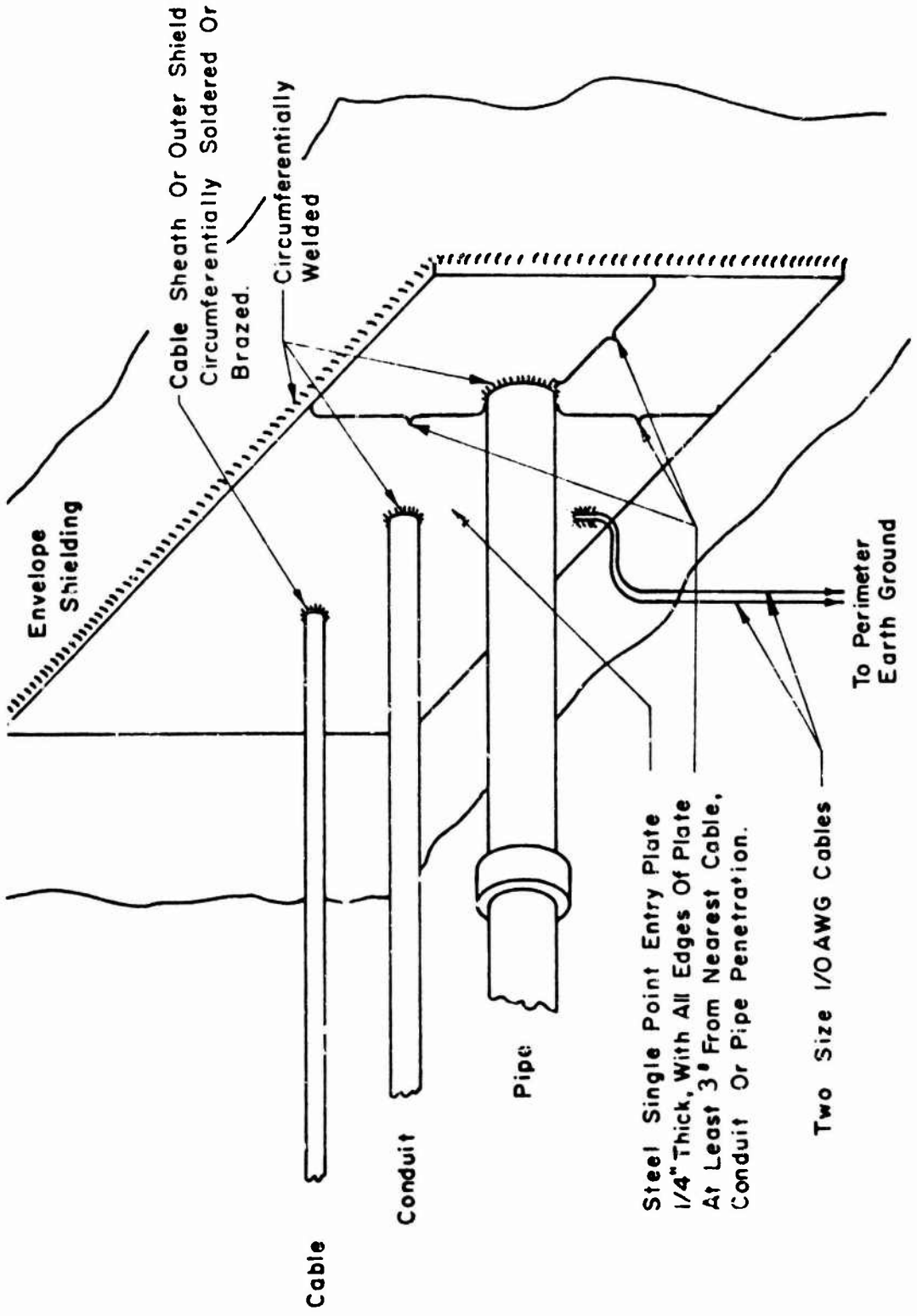

Figure 5.3 SINGLE-POINT ENTRY PLATE SHOWING RIGID CABLE CONDUIT AND PIPE SHIELDING PENETRATIONS

and "input" is the amplitude-frequency characteristic of the external field. Because of the fact that a metal shield will, in general, respond differently to the electric and magnetic components of the EM field, it is necessary to define two such transfer functions of the form:

$$T_E(\omega) \equiv \frac{E_{in}(\omega)}{E_{ex}(\omega)} \tag{5.1}$$

and

$$T_H(\omega) \equiv \frac{H_{in}(\omega)}{H_{ex}(\omega)} \tag{5.2}$$

where, $E_{ex}(\omega)$ and $H_{ex}(\omega)$ are the transformed (Fourier) external electric and magnetic fields, respectively; and $E_{in}(\omega)$ and $H_{in}(\omega)$ are the corresponding internal fields. For spherical, cylindrical and parallel plate shield enclosures, and for frequencies greater than a few Hertz, King[1]* has shown the transfer function for magnetic field shielding to be:

$$T_H(\omega) = \frac{1}{\cos(k_2 d) - \frac{k_2 b}{2} \sin(k_2 d)}$$

where

$\omega = 2\pi f$

f = frequency of incident field

$k = (\mu_0/\mu) k_2 b$

$k_2 = \sqrt{-j\omega\mu\sigma} = \frac{\sqrt{-j2}}{\delta}$

$\delta = 1/\sqrt{\pi f \mu \sigma}$ = skin depth of material

d = thickness of enclosure walls

μ_0 = permeability of free space

μ = permeability of enclosure walls

σ = conductivity of enclosure walls

the factor "b" in Equation 5.3 is a geometric variable that characterizes the different enclosure geometries as follows:

* Superscripts refer to numbered references at the end of this chapter.

b = the separation distance between plates for large area parallel plate shields

b = the radius for cylindrical enclosures

b = 2/3 the radius for spherical enclosures

At high frequencies, where the wall thickness is greater than the skin depth (i.e., d>δ) Equation 5.3 reduces to:

$$T_H(\omega) = \frac{2\sqrt{2}\,\delta e^{-d/\delta}}{b} \tag{5.4}$$

and at low frequencies, where (d<δ), the magnetic field shielding becomes:

$$T_H(\omega) = \left|\frac{1}{\frac{j\omega d\sigma\mu b}{2}+1}\right| \tag{5.5}$$

The transfer function[1] for electric field shielding is given by:

$$T_E(\omega) = \frac{2\,(k_1 b)^2}{k \sin k_2 d} \tag{5.6}$$

where

$k_1 = 2\pi/\lambda$

λ = wave length of impinging field

At high frequencies where d>δ, Equation 5.6 can be expressed as

$$T_E(\omega) = \frac{9\,\omega\varepsilon_o b e^{-d/\delta}}{\sqrt{2}\;\sigma\delta} \tag{5.7}$$

where

$\varepsilon_o = 10^{-9}/36\pi$ farads/meter

for low frequencies where d<δ, the electric field shielding becomes:

$$T_E(\omega) = \frac{9\omega\varepsilon_o b}{4\sigma d} \tag{5.8}$$

With the exception of the constant "b", the shielding transfer functions are the same for spherical enclosures, cylindrical enclosures, and parallel plates. Since the form of the transfer function is not affected by the geometry of the structure, these equations may be used to find the fields inside rectangular and cubic enclosures. It must be remembered that these results are not valid near corners or apertures, and that the shielding is degraded by penetrations. These effects will be discussed later in this chapter.

In applying these transfer functions to cubic and rectangular enclosures, it is necessary to select the correct value for the constant "b". This is done on the basis of similarity. A cubic structure most closely resembles a sphere, so b would be set equal to 1/2 the width. A structure in which the length and width are much greater than the height is similar to a parallel plate structure and b would be set equal to the height. Conservative practice is to model all structures as spheres in which the diameter is equal to the smallest dimension of the shielding enclosure.

Miller and Bridges[2] have shown that shielding problems can be modeled as equivalent electric circuit analogs. In particular the low frequency magnetic field shielding effectiveness is given as:

$$T_H(\omega) = \frac{R_s}{R_s + j\omega L_s} \tag{5.9}$$

where R_s and L_s are the resistance and inductance respectively in the equivalent RL circuit, and

$$R_s = \frac{2\pi}{3d\sigma} \tag{5.10}$$

$$L_s = \frac{\pi\mu b}{3} \tag{5.11}$$

In the high frequency case

$$\left|\frac{H_i(\omega)}{H_o(\omega)}\right| = \frac{R_s\sqrt{2}\,d}{\omega L_s \delta}\, 2e^{-d/\delta} \tag{5.12}$$

Miller and Bridges have further shown that if 5.10 and 5.11 are substituted in these equations, the rigorous high and low frequency expressions of 5.5 and 5.4 will result. In order to determine the energy picked up by circuit loops within the shielded enclosure, it is desirable to be able to calculate an approximate value for the peak internal magnetic field strength. This has been shown to be

$$H_{in(max)} = \frac{R_s}{L_s}\int_{T_2}^{T_1} H_o(t)dt \quad \text{for } T_2 - T_1 < L_s/R_s \tag{5.13}$$

where $T_2 - T_1$ = approximate duration of the external magnetic field.

This function will be used in a later chapter for loop pickup calculations.

Figures 5.4 and 5.5 illustrate the electric and magnetic field shielding effectiveness of an ideal structure. This enclosure is an aluminum sphere 36 inches in diameter and 1/16 inch thick.

Notice that at no point is there less than 200 dB of electric field attenuation but that, at low frequencies, there is little or no magnetic field shielding. In below-deck areas of a ship, however, the steel hull and decks will provide a substantial increase in magnetic shielding, due to the greater permeability of iron.

It is apparent that, if a ship were such an ideal enclosure, the direct EMP penetration to the interior would be negligible. A ship, by necessity, is not an ideal shield. The walls have seams and are penetrated by apertures such as hatches, windows and air ducts. These items are discontinuities in the shielding structure and represent shielding defects. Each of these discontinuities will degrade the actual shielding effectiveness from the ideal levels given by Equations 5.4, 5.5, 5.7 and 5.8.

Thus, to determine the actual shielding effectiveness of a structure, a detailed analysis must account for each aperture, seam, cable penetration and any other shield discontinuity. It should be apparent that such a detailed analysis is not feasible for a structure as large and complex as a ship--although studies have been made concerning aircraft and missiles[3, 4].

An alternative, and much simpler approach, is available. As we have demonstrated, the direct penetration of EMP energy through the steel walls of the ship is insignificant. The threat arises from the presence of shielding discontinuities created by the many apertures and penetrations needed to make the ship functional. This being the case, the ship designer need only concern himself with taking appropriate measures to reduce the penetration of EMP through the many discontinuities that prevail throughout the ship's structure.

5.3.2 Typical Shielding Parameters for Various Materials and Thicknesses

As can be seen in the formula presented in the previous section, shielding effectiveness, is a function of skin depth. This means that shielding effectiveness depends upon the electrical and magnetic properties used to construct the enclosure.

Figure 5.6 plots skin depth versus frequency, for several non-ferrous materials and the approximate skin depth for steel. The relative permeability for the non-ferrous materials is 1, and their skin depth is a function of conductivity only. The permeability of steel, however, is a strong function of frequency, as illustrated in Figure 5.7. The relative permeability of steel is over 1000 in the 100 kHz region and falls rapidly with increasing frequency, thereby producing the non-linear skin depth versus frequency curve in Figure 5.6. It should be noted that the skin depth of steel is less than the skin depth of copper over the entire frequency range of interest.

Table 5.1 lists the relative permeability and relative conductivity for several metals at 150 kHz. These parameters, coupled with the equations presented in Section 5.2.1, allow the designer to calculate shielding effectiveness for ideal structures of his own choosing.

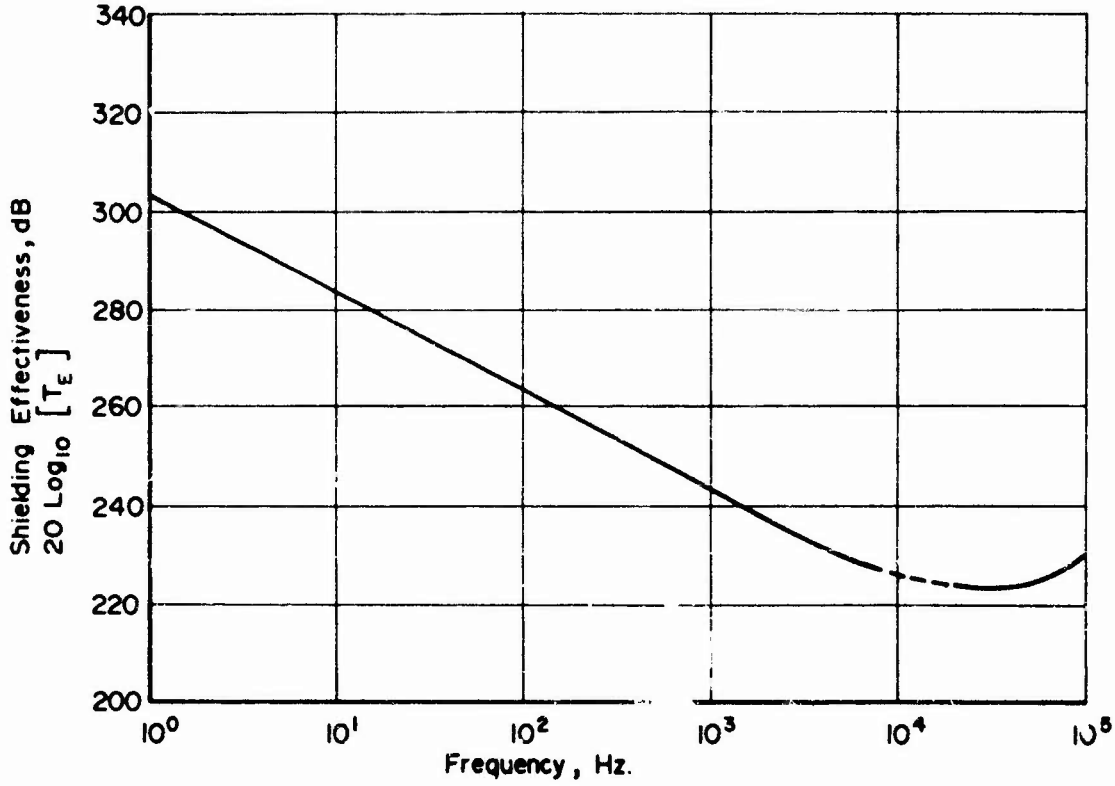

Fig. 5.4 ELECTRIC FIELD SHIELDING EFFECTIVENESS FOR 18 INCH RADIUS ALUMINUM SPHERE, 1/16" INCH THICK (REF. 2)

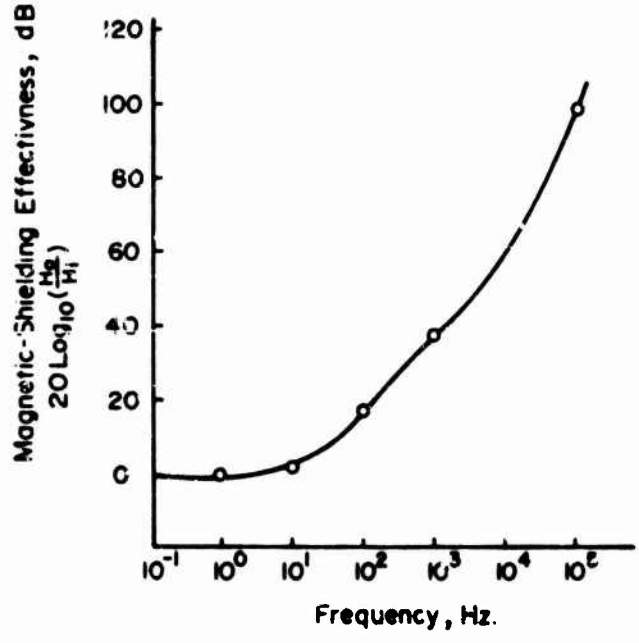

Fig. 5.5 MAGNETIC-FIELD SHIELDING EFFECTIVENESS FOR 18 INCH RADIUS ALUMINUM SPHERE, 1/16 INCH THICK (REF. 2)

METAL	RELATIVE CONDUCTIVITY, G_R	RELATIVE PERMEABILITY,* μ_R
Silver	1.05	1
Copper, annealed	1.00	1
Copper, hard drawn	0.97	1
Gold	0.70	1
Aluminum	0.61	1
Magnesium	0.38	1
Zinc	0.29	1
Brass	0.26	1
Cadmium	0.23	1
Nickel	0.20	1
Phosphor-Bronze	0.18	1
Iron	0.17	1,000
Tin	0.15	1
Steel, SAE 1045	0.10	1,000
Beryllium	0.10	1
Lead	0.08	1
Hypernick	0.06	80,000
Monel	0.04	1
Mu-Metal	0.03	80,000
Permalloy	0.03	80,000
Steel, 18-8 Stainless	0.02	1,000

*Obtainabl only if the incident field does not saturate the metal.

$$\mu_R = \mu/\mu_0$$

$$\mu_0 = 4\pi \times 10^{-7} \text{ Weber/Amp-m}$$

Table 5.1 RELATIVE CONDUCTIVITY AND RELATIVE PERMEABILITY FOR METALS AT 150 kHz (REF. 4)

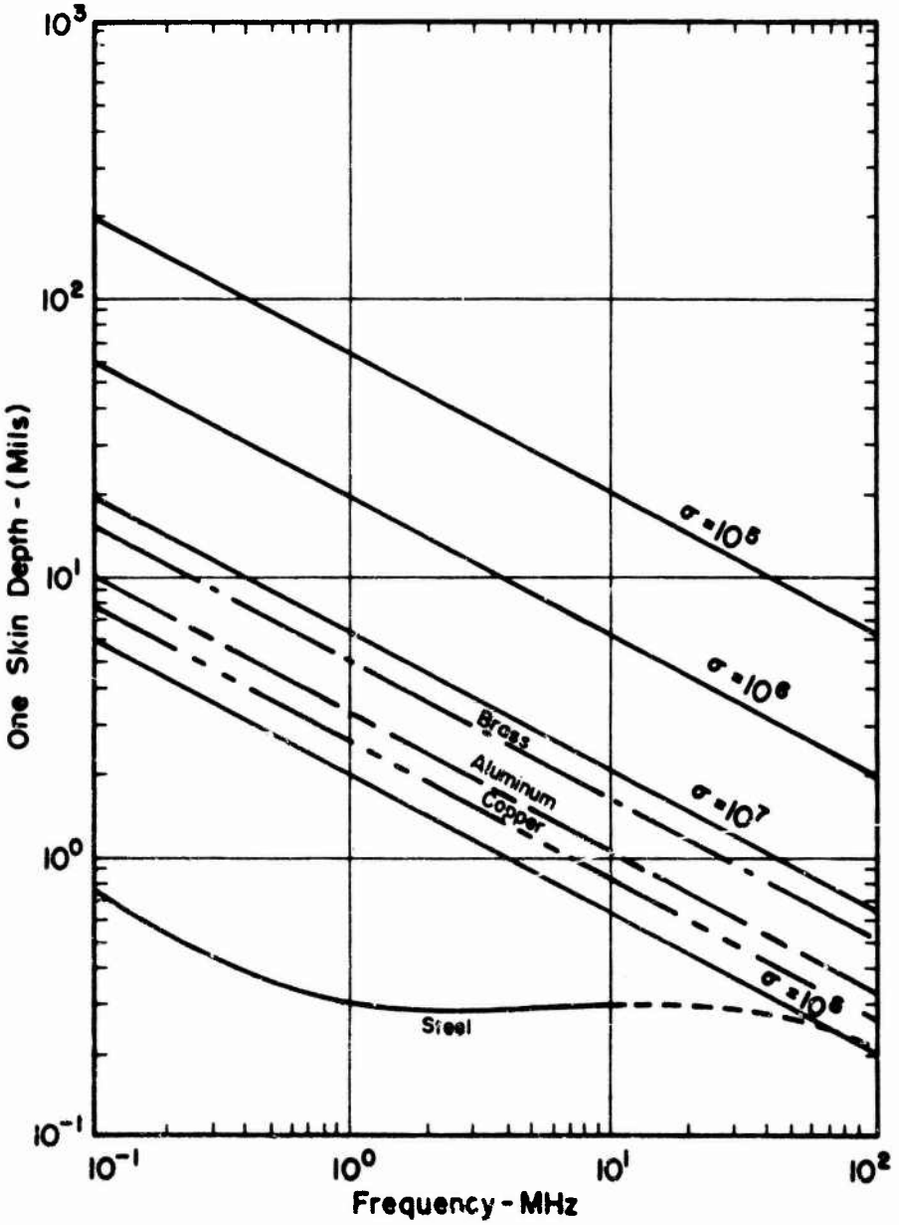

Fig. 5.6 ONE SKIN DEPTH OF SELECTED MATERIALS AND CONDUCTIVITIES (REF. 5)

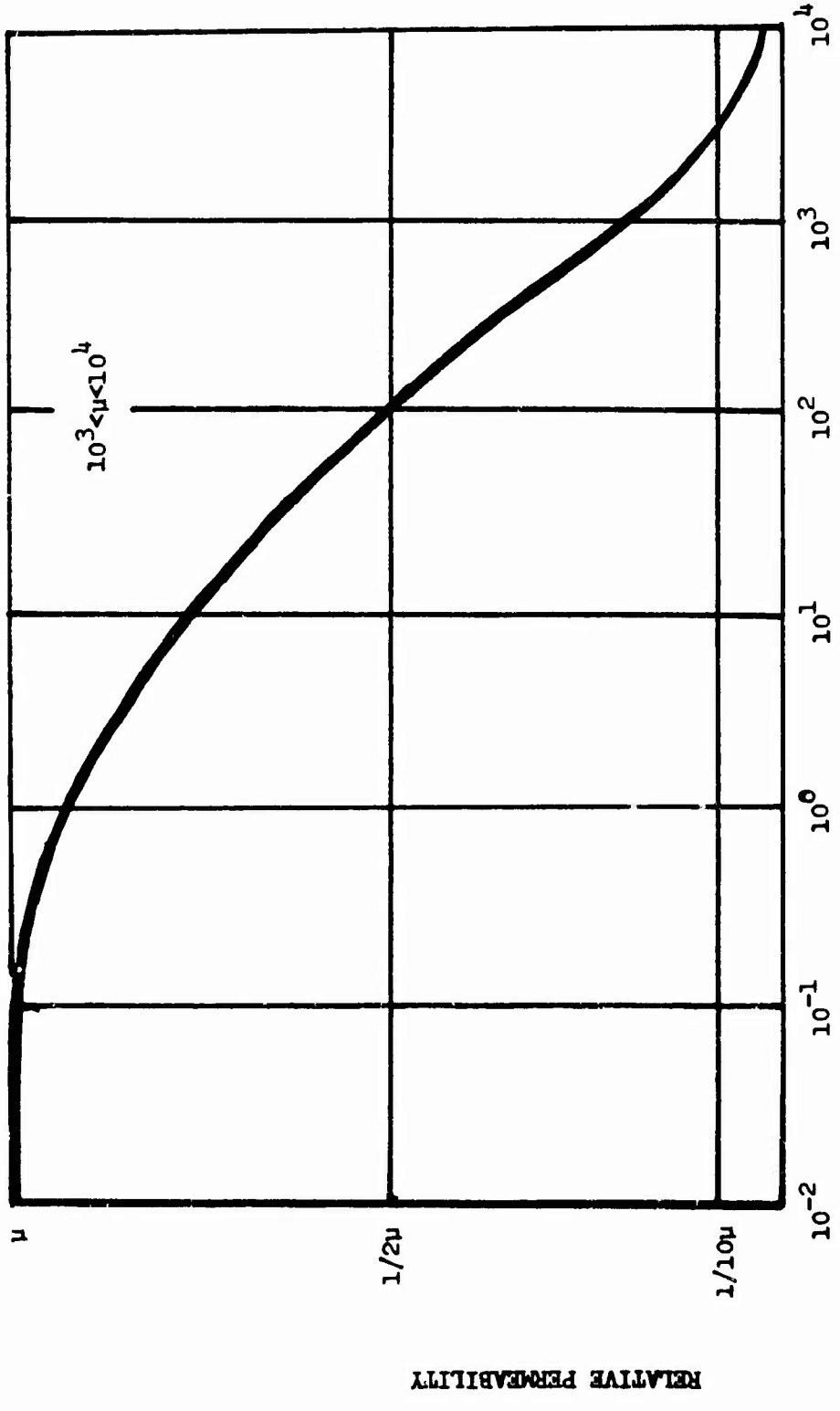

FIGURE 5.7 Typical Variation of Relative Permeability of Iron with Frequency. (Ref. 6)

To further simplify any analysis regarding steel structures, Figure 5.8 illustrates the minimum shielding effectiveness which can be obtained from steel walls of several thicknesses.

In general, the designer may safely assume 40 dB per shielding surface, except in the vicinity of apertures. For example, if there are two decks between the shielded compartment and the surface of the ship, about 80 dB of attenuation may be expected if there are no apertures in the decks in the vicinity of the shielded area.

5.3.3 Seams

As previously mentioned, the shielding effectiveness for ideal boxes and spheres is quite large. We know, however, that in real structures the discontinuities seriously degrade the shielding. The effects of seams are of concern to the designer because of their extensive use in Naval construction. Figure 5.9 shows qualitatively the effect of a low conductivity seam on the effectiveness of the shield. Generally, there are two mechanisms by which EMP penetrates a seam.

The first is direct penetration. This occurs when there are gaps in the seam, such as when two plates are bolted together. These gaps act as slits or perforations in the shield and may be viewed as small apertures. This problem exists on older steel ships bearing aluminum superstructures, since the means of bonding was by riveting or bolting. Figure 5.10 shows such an assembly. The Navy has, however, recently adopted the explosive bonding technique for joining dissimilar metals. Jolliff[8] has shown that this technique provides excellent shield continuity at the bond.

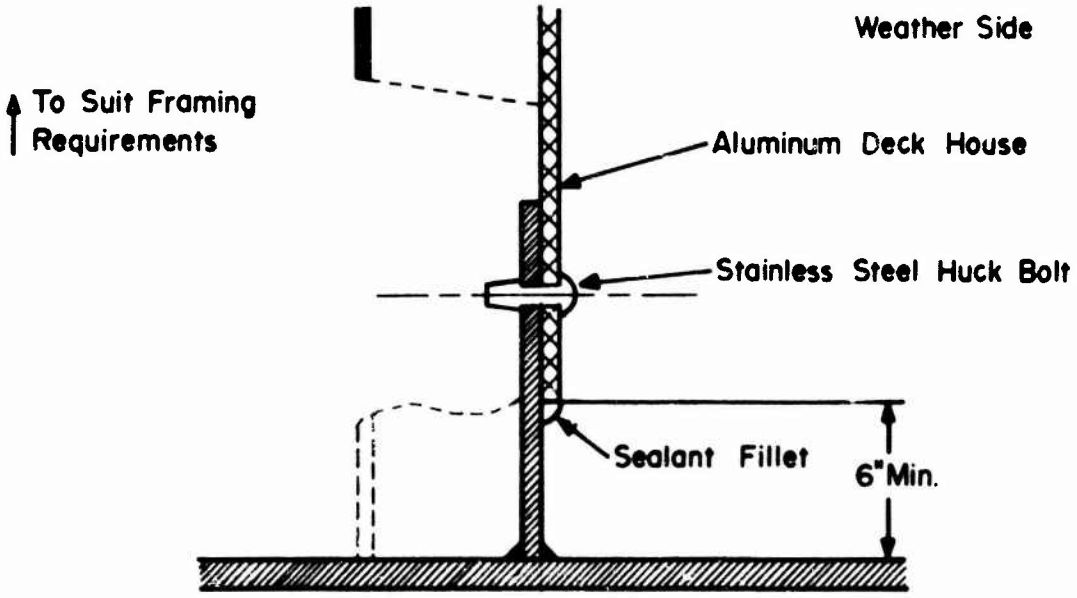

Fig. 5.10 ALUMINUM DECKHOUSE JOINT DETAIL

The second means of EMP penetration is via low conductivity welds. In this case, the EMP induced currents on the skin of the ship produce voltage drops across the high resistance seams.

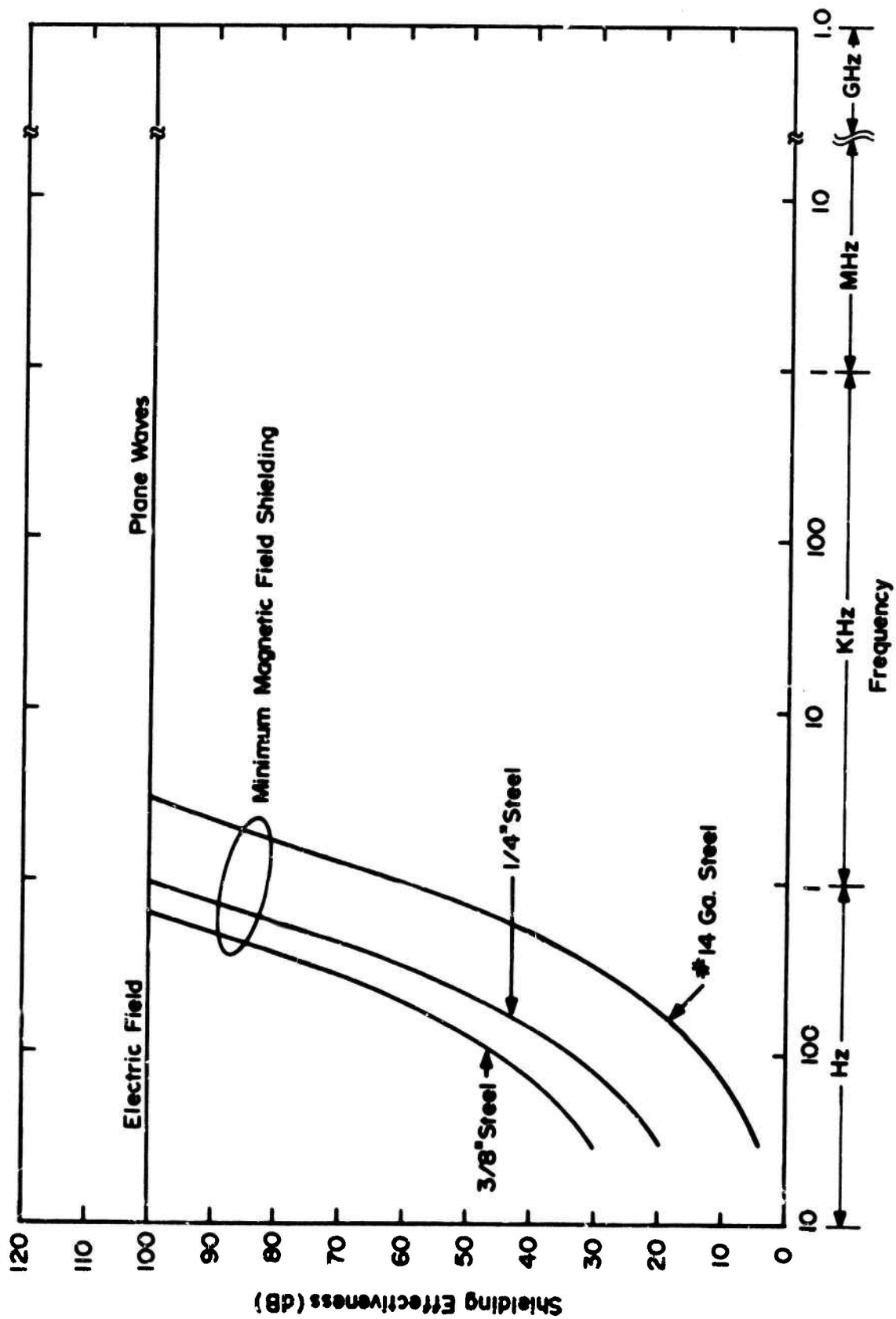

Fig. 5.8 MINIMUM SHIELDING EFFECTIVENESS OF LOW CARBON STEEL WALLS (REF. 7)

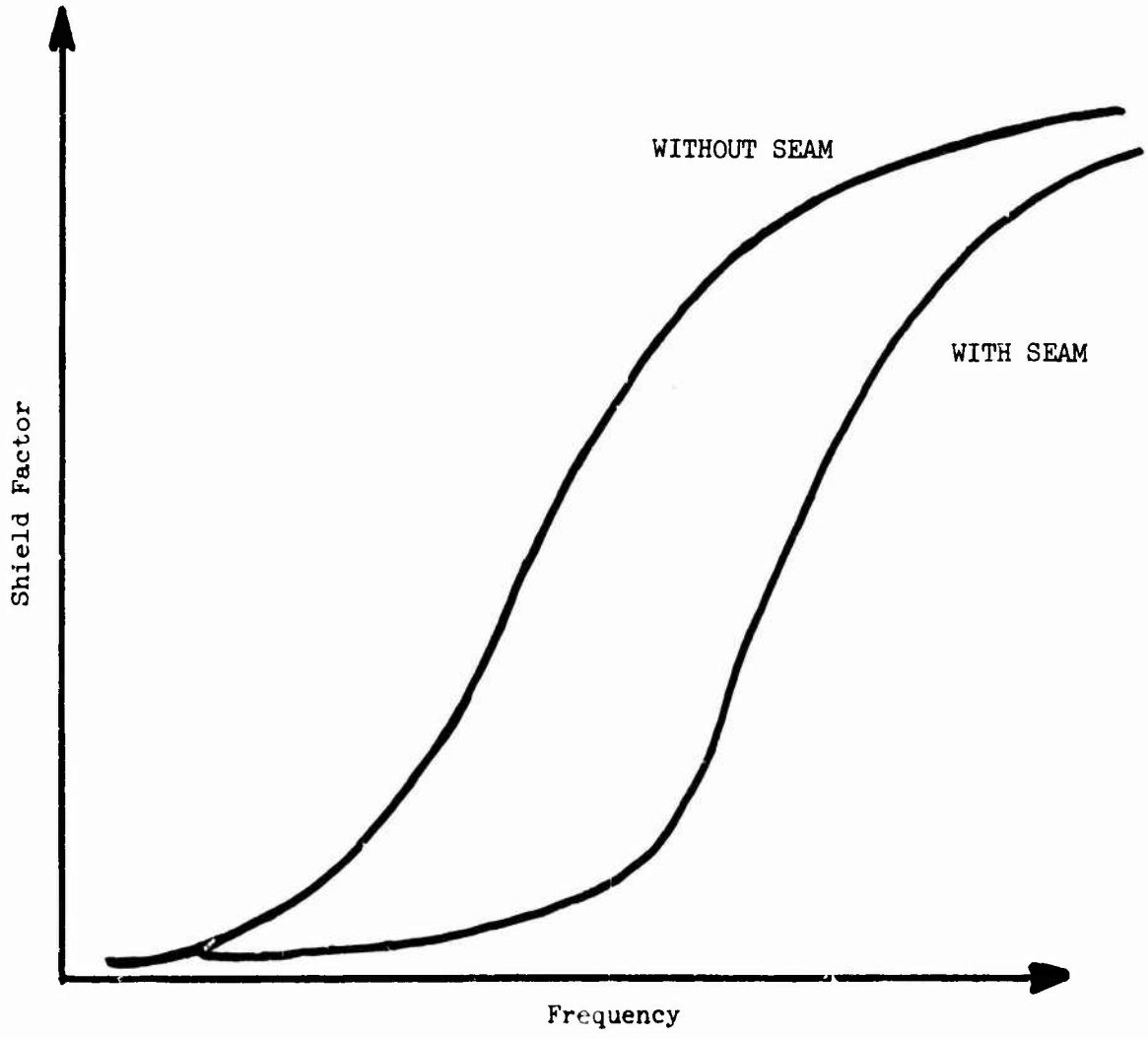

Figure 5.9 COMPARISON OF SHIELD FACTORS OF TWO ENCLOSURES, ONE WITH SEAM, ONE WITHOUT SEAM

The present use of continuous welds in Naval construction eliminates both of these mechanisms. Thus, the designer need not consider penetration via seams.

5.3.4 Corners

We have shown that cubic and rectangular enclosures may be modeled as spheres or cylinders with satisfactory results. These solutions, however, do not apply in the vicinity of corners where the field penetration is significantly greater than that predicted for the center of the enclosure.

Figure 5.11 gives H_c/H_1 as a function of Γ/a. H_c/H_1 is the ratio of the magnetic field near the corner to the magnetic field near the center of the enclosure. The ratio Γ/a is the ratio of the distance from the corner, Γ, to the half width of the enclosure, a.

The magnetic field increases rapidly as the corner is approached, although the effect does not become significant until Γ/a is down to about 0.2.

The most simple means of protecting against this problem is to locate the more sensitive equipments away from the compartment corners.

5.3.5 Apertures

5.3.5.1 Analysis

Several shield discontinuities will be discussed under the topic of apertures, including windows, doors, hatches and air vents.

The penetration of EMP through a circular aperture in an infinite plane shield is considered in reference 9. This analysis will be pursued here for the sake of completeness, as well as to illustrate the threat imposed by unprotected openings.

The fields penetrating such holes will have the same time dependence as the external fields. The field magnitudes, however, will diminish with distance from the aperture.

Figure 5.12 illustrates the problem. The EMP is assumed to be propagating in a direction parallel to the shielding plane. The electric field is normal to the plane and the magnetic field is parallel. If $a < \lambda/2\pi$, when λ is the shortest wavelength of importance in the EMP spectrum, and when the distance, r, into the enclosure from the center of the aperture satisfies the constraint $a<r<\lambda/2\pi$, then the following formulae hold:

$$E_r = 2/3\pi \left(\frac{a}{r}\right)^3 E_o \cos\theta \qquad (5.14)$$

$$E_\theta = \frac{1}{3\pi} \left(\frac{a}{r}\right)^3 E_o \sin\theta \qquad (5.15)$$

$$E_\phi = 0 \qquad (5.16)$$

$$H_r = \frac{4}{3\pi} \left(\frac{a}{r}\right)^3 H_o \sin\phi \sin\theta \qquad (5.17)$$

$$H_\phi = \frac{2}{3\pi} \left(\frac{a}{r}\right)^3 H_o \cos\phi \qquad (5.18)$$

$$H_\theta = \frac{2}{3\pi} \left(\frac{a}{r}\right)^3 H_o \sin\phi \cos\theta \qquad (5.19)$$

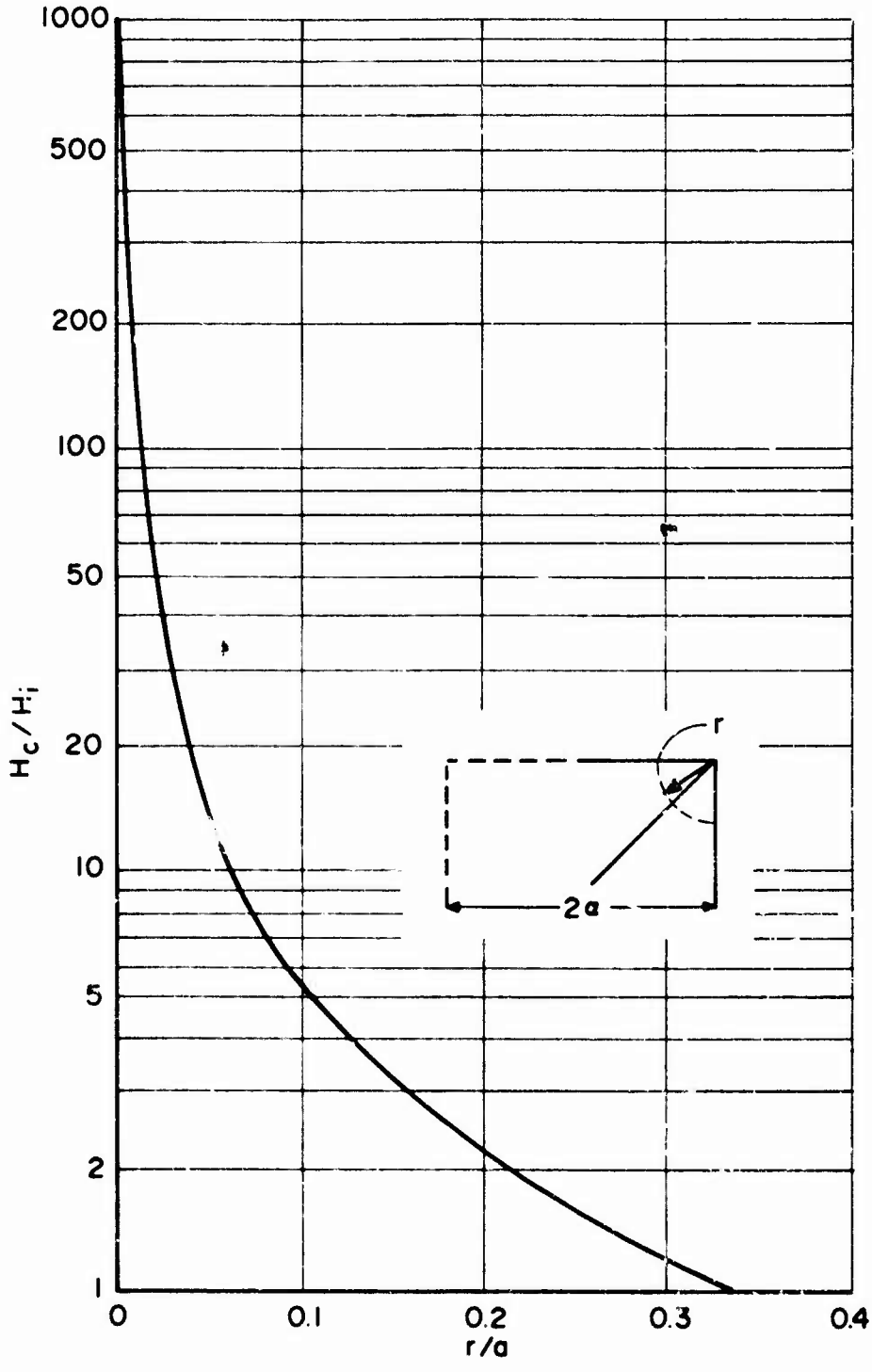

Fig. 5.11 INCREASE OF MAGNETIC FIELD STRENGTH WHEN APPROACHING THE CORNER OF A SHIELDED SPACE (REF. 6)

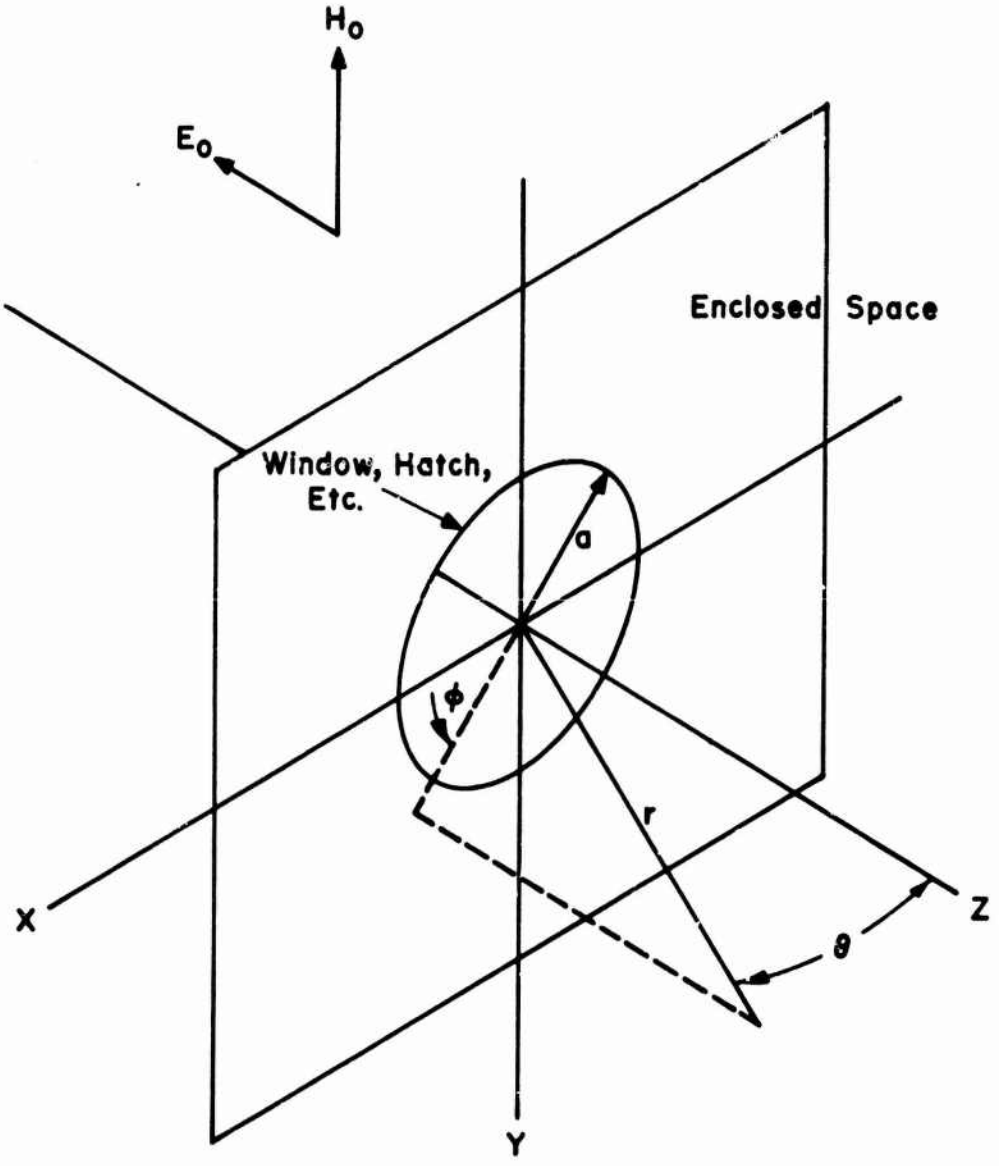

Fig. 5.12 PENETRATION OF ELECTRIC AND MAGNETIC FIELDS THROUGH A CIRCULAR HOLE (REF. 6)

where

E_ϕ, E_r, E_θ = Internal electric field components in spherical coordinates.

H_ϕ, H_r, H_θ = Internal magnetic field components in spherical coordinates.

a = radius of the aperture. In analysis of non-circular apertures, "a" should be set equal to 1/2 the largest dimension of the opening under consideration.

r = radial distance from the point in the enclosure at which the field strengths are to be determined to the center of the hole.

It is desirable to consider only the case describing the most adverse direction of EMP penetration. From the point of view of circuit coupling, this occurs when the sines and/or cosines in one of the above equations are of unit value. In such a situation, the entire magnetic field is in one direction since the other two components must be zero. Since the expression for H_r, Equation 5.17, has the greatest coefficient $(4/3\pi)$, our analysis may be confined to Equation 5.17. Thus, the most extreme EMP penetration may be expressed as:

$$H_r = \frac{4}{3\pi} \left(\frac{a}{r}\right)^3 H_o \tag{5.20}$$

or

$$\frac{H_r}{H_o} = -\frac{4}{3\pi} \left(\frac{a}{r}\right)^3 \tag{5.21}$$

Consider a compartment having a large aperture, perhaps a door or hatch. This opening can be conservatively modeled as a circular hole with a radius of 1.0m. Consider also, that it is necessary to locate a piece of electronic equipment in this compartment about 3 meters from the aperture. Thus:

$$\frac{H_r(\omega)}{H_o(\omega)} = \frac{4}{3\pi} \left(\frac{a}{r}\right)^3 = 0.57 \times 10^{-2} \tag{5.22}$$

Because the field penetrating the door has the same time dependence as the external EMP fields, one may determine the internal loop pickup by merely multiplying the attenuation factors of Equation 5.22 by any previously determined values for external loop pickup.

For the sake of completeness and example, we will illustrate such a calculation here. Baird and Frigo[6] have determined some representative values for loop pickup, and Chapter 3 of this manual discusses pickup mechanisms in detail. It will suffice here to state the necessary results, describing maximum open circuit voltage and short circuit current for external loop pickup.

The radius of the loop is 2 ft.

$$V_{oc,\ max} = 49\ kV \tag{5.23}$$

$$I_{ss,\ max} = 41.6A \tag{5.24}$$

where

$V_{oc,\ max}$ = Maximum open circuit voltage developed in the circuit loop

$I_{ss,\ max}$ = Maximum short circuit current developed in the circuit loop

A loop, illuminated by EMP penetrating a door or hatch, can collect enough energy to damage or upset electronic equipment. Thus, in EMP-critical areas, the number and size of apertures should be kept to a minimum and all should be protected.

5.3.5.2 Hardening

Hardening techniques for air vents will be considered first. These concepts may be applied equally to vents penetrating ship bulkheads or equipment cabinets. Figure 5.13 illustrates one hardening scheme utilizing wire screening as a shield. Note that paint, oil, etc. must be removed from all mating surfaces prior to assembly. Also note the use of a molded RF gasket; if the assembly is ever taken apart, this gasket should be replaced.

Figure 5.14 illustrates the use of honeycomb shielding material. This is similar to metal screen except that the honeycomb protrudes into the duct. As shown in Figure 5.14, the molded gasket may be eliminated if the metal retaining plate is welded rather than bolted to the enclosure. Honeycomb tubes act as waveguides below cutoff and offer several advantages over screening.

Figure 5.15 graphs the shielding effectiveness of several honeycomb materials. Steel and cadmium-plated aluminum provide the best performance.

Figure 5.16 compares the attenuation of wire mesh to honeycomb. Honeycomb and very fine screening are best. Note, however, that for equal shielding effectiveness, the honeycomb presents much less resistance to air flow.

The treatment of windows is similar. Wire screen may be used either internally or externally to the glass, or conductive coatings may be deposited on the glass. In either instance, the conductive medium must make good electrical contact with the bulkhead of the ship, and a molded RF gasket must be used. Typical commercially available conductive coatings on glass or transparent substrates can provide 90-100 dB of attenuation for electric (E) fields over a frequency range of 10 kHz to 100 MHz. Magnetic (H) fields below 100 kHz are only attenuated 15 to 20 dB. Visibility through these coatings may be between 65% to 90%[10]. In general, the coatings are stable, will not oxidize and are not sensitive to light or water. If better visibility is required, sensitive equipment must be hardened or located elsewhere.

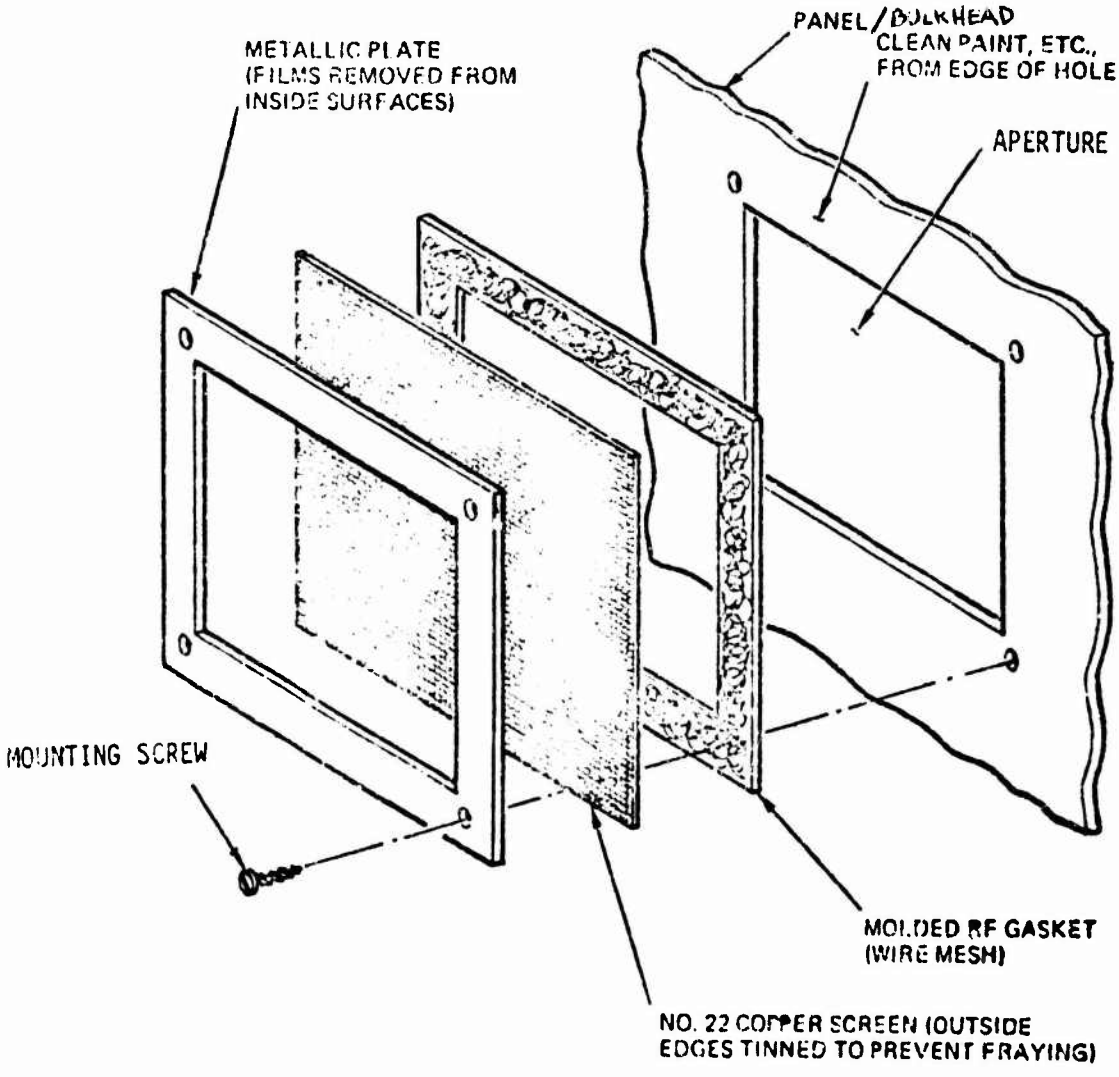

Fig. 3.13 METHOD OF MOUNTING WIRE SCREEN OVER AN APERTURE (REF. 5)

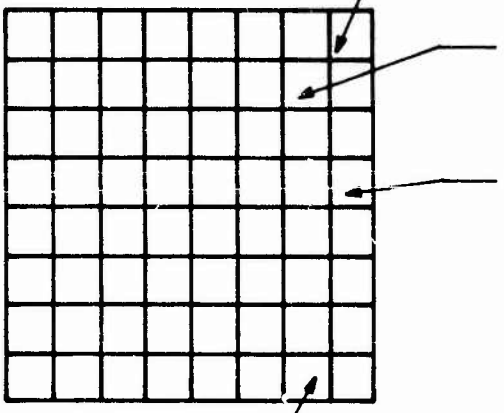

Metal Partitions Welded, Brazed Or Soldered At Each Intersection

Closed Cells (Square Or Hexagonal)

Maximum Cell Opening < $\lambda/3$ Of Highest Frequency (Shortest Wavelength) To Be Attenuated

Depth Of Closed Cell Depends On Ratio Of Operating Frequency To Cut Off Frequency Of Cell & Attenuation Required. Nominal Depth Is 5 Times Largest Opening For 100db Attenuation.

Typical Element

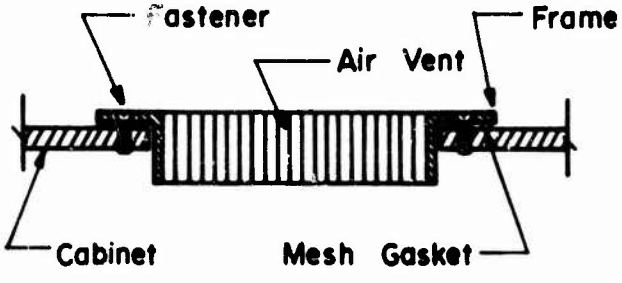

a) Bolted Installation On Cabinet

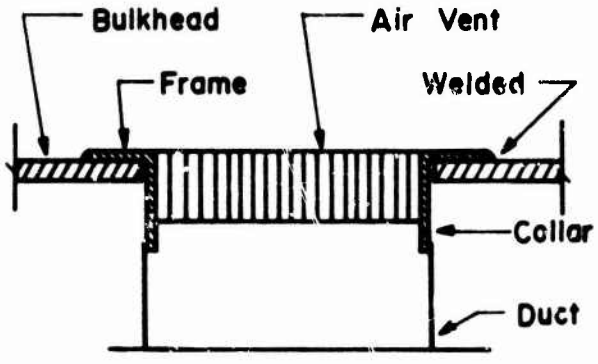

b) Welded Installation On Bulkhead

Fig. 5.14 USE OF HONEYCOMB MATERIAL FOR SHIELDING AIR VENTS (REF. 7)

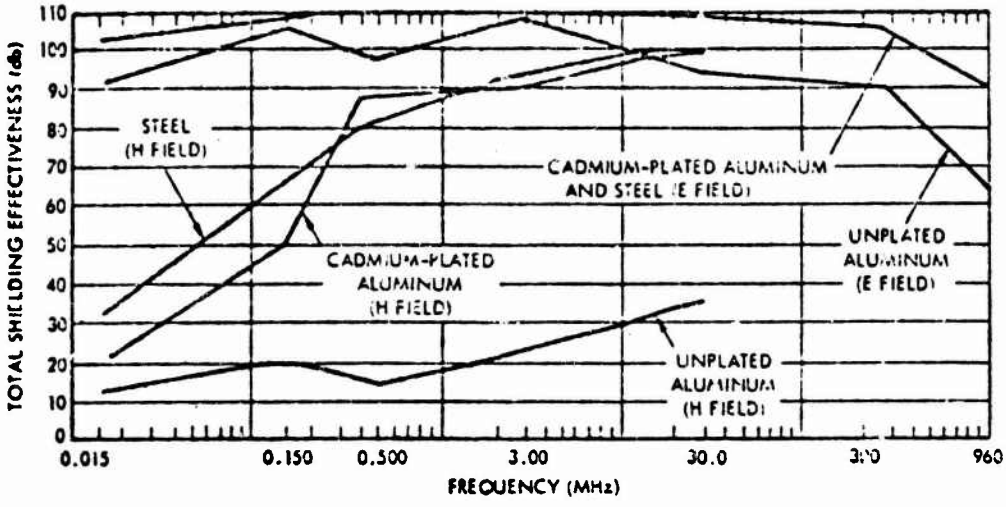

Figure 5.15 TYPICAL SHIELDING EFFECTIVENESS VERSUS FREQUENCY FOR HONEYCOMB (HONEYCOMB THICKNESS = 1/2 INCH, CELL WIDTH = 1/3 INCH) (Ref. 5)

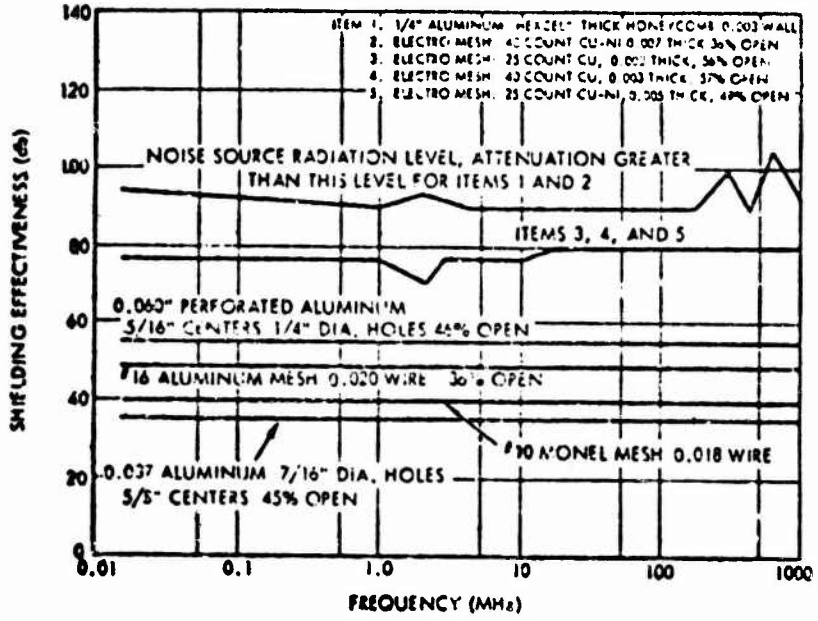

Figure 5.16 ATTENUATION OF VARIOUS SCREENING MATERIALS

Hatches, doors and scuttles should be kept to a minimum in the vicinity of a hardened area. Escape scuttles penetrating the peripheral wall of the area should be fitted with conductive gaskets and be securely bolted closed. Whenever the scuttles are opened, the gaskets should be replaced. Naturally all paint, grease, etc. must be removed from the mating surfaces before installation.

The number of entries to a critical equipment area should be kept to a minimum, preferably one. Since these entries will see frequent use, conductive gaskets will not be adequate. The utilization of a double door hallway entrance as illustrated in Figure 5.17 is strongly recommended. The double doors provide redundant shielding and should be closed at all times. The hallway also acts as a waveguide below cutoff. That is, it will act as a waveguide that attenuates the low frequency portion of the EMP spectrum. Figure 5.18 shows the amount of attenuation the EMP will encounter in traveling the length of the hallway. In this figure, "L" represents the length of the hallway and "D" is the height or width of the aperture, whichever is larger. As can be seen, a hall which is approximately 18 feet long would provide about 80 dB of attenuation for a "D" of about 6 feet.

Elevator shafts and stairwells present a major breach in structural shielding. Such openings should be located as far as possible from areas containing critical equipment.

5.4 System Grounding Plan

Within a ship there are, essentially, two ground systems. One is the personnel safety ground system and the other is the electronic signal ground system. The purposes and implementation of these systems are often in direct conflict.

For safety ground, the outermost metallic surface of all equipments connected to the ship's electrical power, and exposed to personnel touch, should be bonded per MIL-STD-1310C to the bench/deck/bulkhead where it is located. The purpose of this bonding is to insure that no electrical potential may be developed between the metal enclosure and the surrounding metallic structures. It is not important if the absolute potential of "ground" is different in different areas of the ship; it is only necessary to guarantee that hazardous voltages cannot exist between surfaces exposed to personnel.

The purpose of signal ground, on the other hand, is to provide a reference level between interconnected electronic equipments. Digital systems, such as NTDS, are especially level-sensitive. Thus, it is important that the absolute potential of this ground be the same throughout its extent. It should be obvious that the safety ground and the signal ground may be at widely differing potentials. This will be important later.

A "Christmas Tree" or Fishbone configuration should be utilized for the ship's ground system as illustrated in Figure 5.19. This is to avoid the creation of ground loops.

A digital equipment signal ground system should be installed in all major, digital equipment spaces. In general, these spaces would be in an EMP hardened area. This ground system should connect to all units of the digital system and

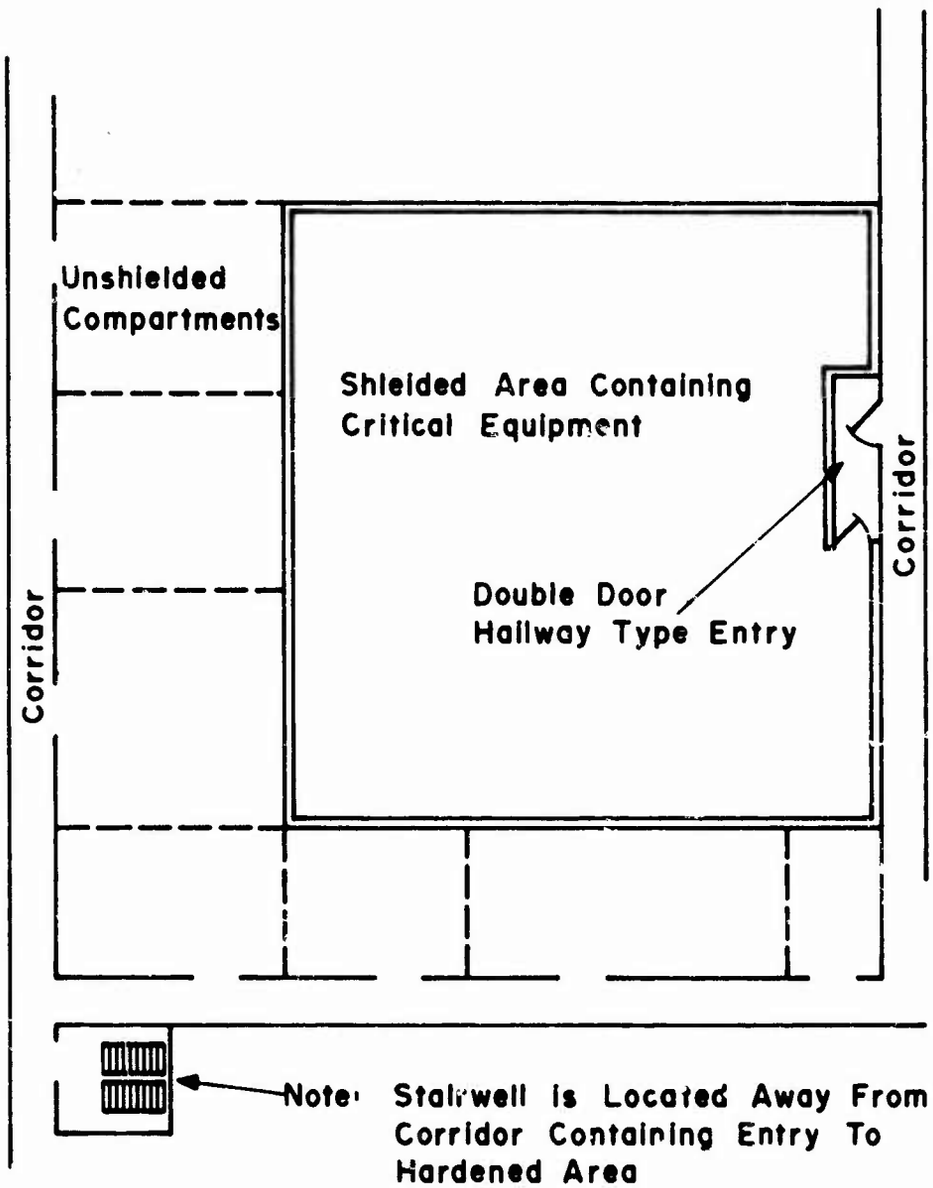

Fig. 5.17 DOUBLE DOOR HALLWAY TYPE ENTRY TO HARDENED AREA

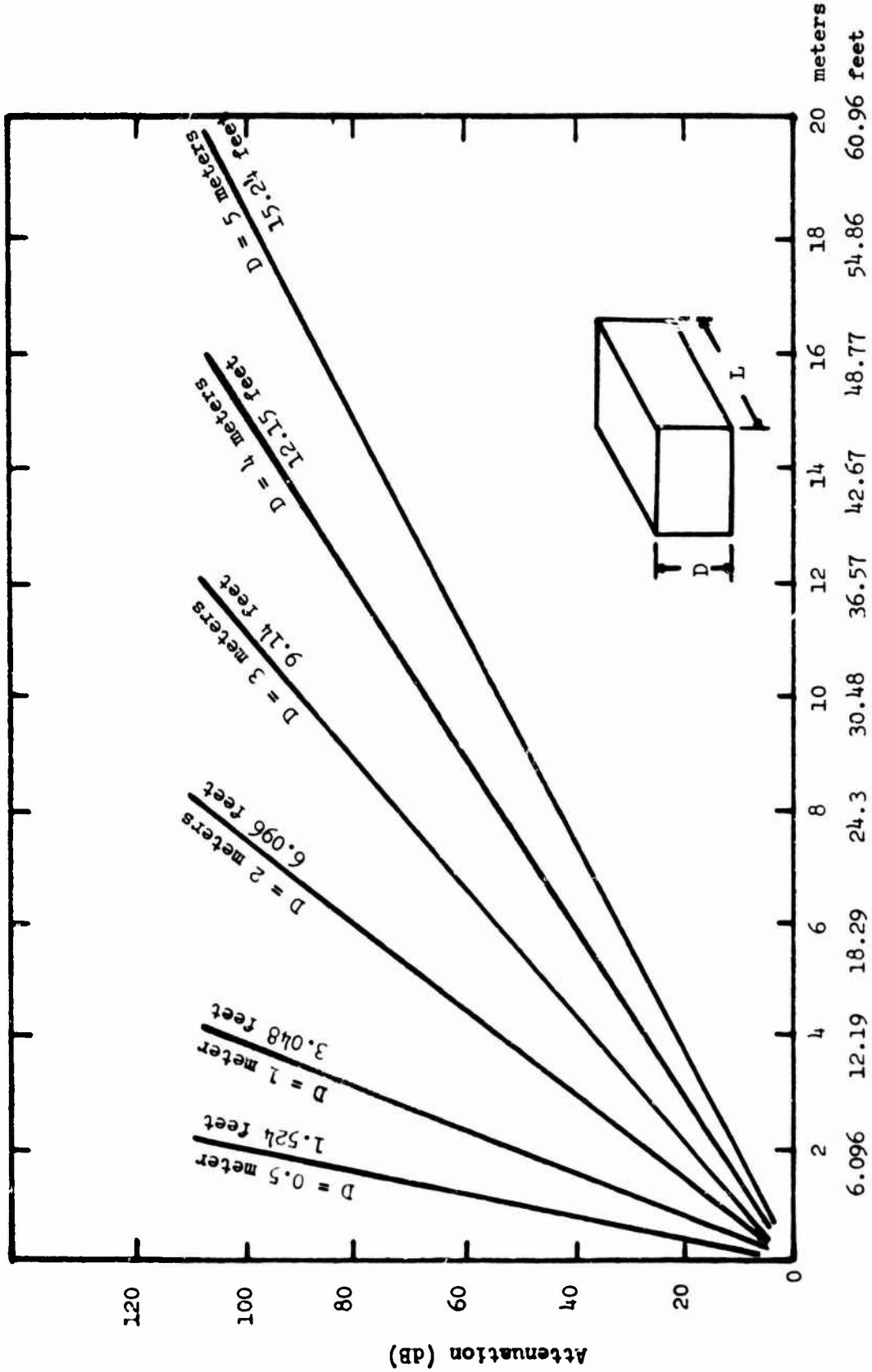

FIGURE 5.18 Wave-guide attenuation as a function of wave-guide dimensions.

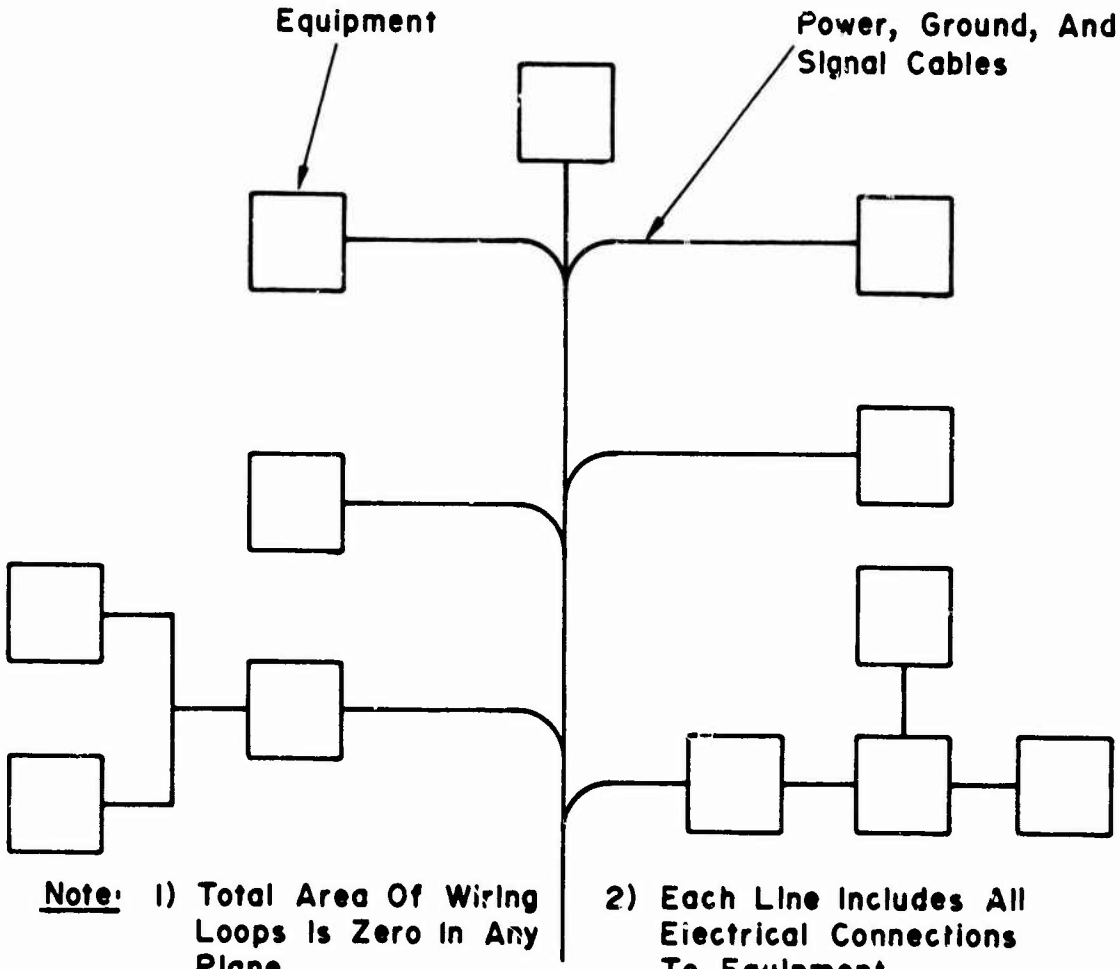

Fig. 5.19 "TREE" WIRING SYSTEM

extend to and include the first digital-to-analog and analog-to-digital converters. These converters should be located within the hardened space if possible. Analog input and output to the shielded space should have balanced terminations, as discussed in Chapter 3. Thus, the ground system does not extend to remotely located ancillary equipments. Motor generators and RF equipments should not connect to this ground system.

The main ground cable should be run in and between all major digital equipment spaces, such as computer control areas and combat information centers. Except for a one-point ground connection (or where signal ground is common to cabinet ground), the main ground cable should be electrically isolated from the ship structures. This one-point ground connection should be in the vicinity of the single point entry for cables and pipes, and should be in good electrical contact with the hull/bulkhead ground. Branch ground cables should connect the individual equipments to the main ground cable. Cable sizes and connections should be in accordance with MIL-STD-1310C, Section 5, and MIL-C-915/28.

If more than one system is located in a single shielded space, all may utilize one signal ground system, subject to the previously mentioned restrictions.

While MIL-STD-1310C requires such a signal ground system only for digital equipments, it is good EMP practice to provide such a system for each shielded space, if more than one is constructed.

Figure 5.20 illustrates the type of equipment connection required on any apparatus located external to the shielded space. In this case, the cabinet (safety) ground must be isolated from the signal ground. Such a configuration should be avoided, if possible, by relocating the equipment internal to the shielded space or by utilizing balanced signal terminations which eliminate the need for the extended ground.

Figure 5.20 shows the type of connection which is acceptable within the shielded areas. Safety and electrical power grounding should be in accordance with MIL-STD-1310C.

5.5 Conclusions

The most cost-effective approach to EMP hardening is, in general, to locate as much sensitive, mission-critical equipment in hardened areas as possible. This approach saves money during initial outfitting and increases the flexibility of the ship since future equipments may also take advantage of the shielded area(s). The following is a summary of recommendations concerning the location and construction of hardened areas.

- Steel is superior to aluminum as a shield, thus, hardened areas should be located below decks when possible.
- The shielded area should be located approximately mid ship.
- These areas should be situated as far as possible from elevator shafts and stairwells.
- The present continuously welded steel construction used on Naval

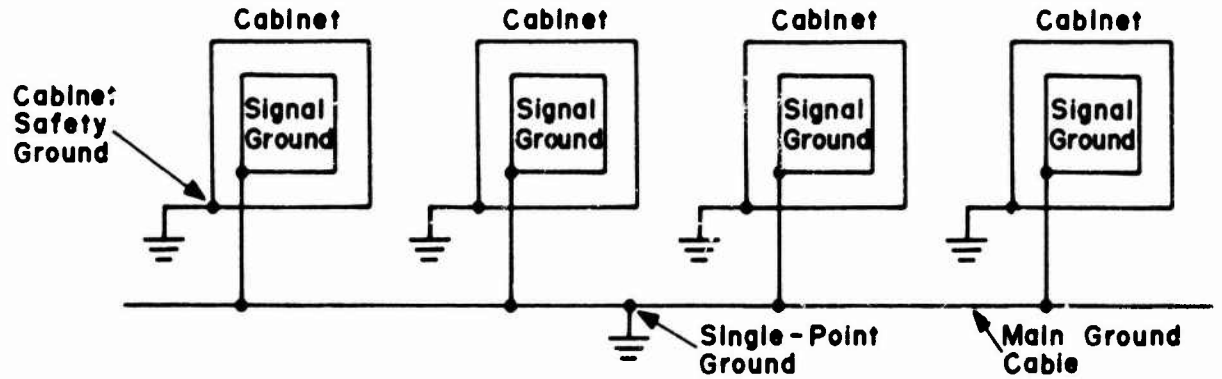

a) Signal Ground Isolated From Cabinet Ground

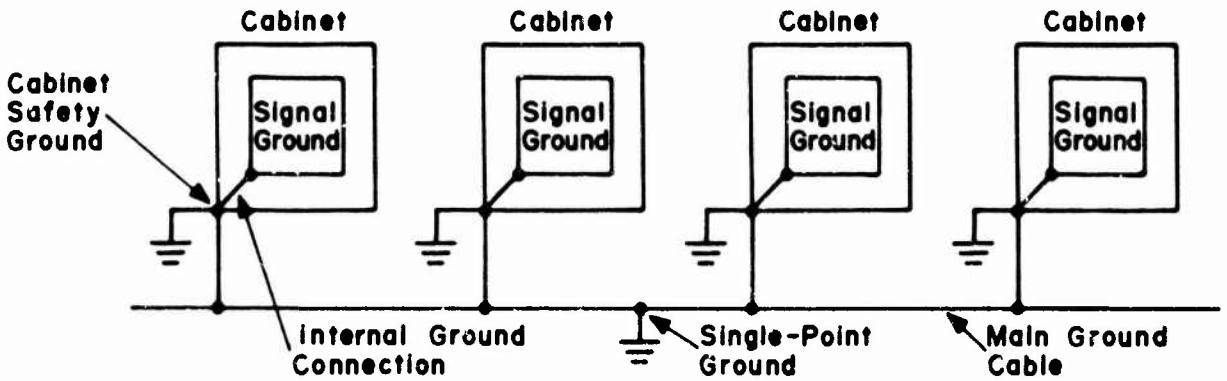

b) Signal Ground Common To Cabinet Ground

Fig. 5.20 GROUND SYSTEM FOR CRITICAL EQUIPMENT

ships will allow no significant direct EMP penetration. Thus, the ship designer may concentrate his attention on hardening apertures and cable/pipe entries.

- Perimeter walls and decks of the hardened area must be a minimum of 1/4" steel.

- Pipes, conduits, cables and air ducts not terminating in the shielded space should not be routed through it.

- Access to the space should be via a double-door entry. Preferably an interlock system should be provided to prevent the opening of both doors simultaneously.

- Escape scuttles in the peripheral walls of the area must be hardened.

- It is recommended that the hardened area be provided with a separate blower system, drawing and exhausting ventilation from an adjacent corridor. This would eliminate the need to penetrate the peripheral walls with ducts.

- Intake and exhaust vents opening onto the adjacent corridor should be protected with honeycomb material.

- A low impedance single point ground system should be provided in each hardened area for electronic equipment.

- All pipes, conduits and cables entering the shielded area should do so via a single point entry. For a small shielded area, a heavy metal cabinet which is continuously welded to the outside of a peripheral wall will be adequate. For a large space, a small adjacent compartment must be allocated to serve as a cable vault. The cabinet/vault must be large enough to accommodate protective devices for every penetrating conductor.

- Access to the vault/cabinet should not be through the peripheral wall of the hardened area.

- No apertures, other than those discussed above, may penetrate the boundary walls/decks of the hardened area. Thus, expansion joints, holes or perforations may not be placed in these structures.

REFERENCES

1. King, L.Y.,"Electromagnetic Shielding at Radio Frequencies", Philo Mag. VII, Vol. 15, p. 201-223, February, 1933.

2. Miller, D.A., and Bridges, J.E., "Review of Circuit Approach to Calculate Shielding Effectiveness", IEEE Transactions on Electromagnetic Compatibility, Vol. EMC-10, No. 1, p. 52-62, March, 1968.

3. Perala, R.A., and Ezell, T.F., "Engineering Design Guidelines for EMP Hardening of Naval Missiles and Airplanes", Mission Research Corp., Albuquerque New Mexico, December, 1973.

4. United States Army Material Command, "Engineering Design Handbook, Hardening Weapon Systems Against RF Energy", AMCP 706-235, February, 1972.

5. Margan, G.E., and Erba, J.C., et.al, "Design Guidelines for EMP Hardening of Aeronautical Systems", Autonetics Report, No. C72-451/201, August, 1974.

6. Baird, J.K., and Frigo, N.J., "Effects of Electromagnetic Pulse (EMP) on the Supervisory Control Equipment of a Power System", Oak Ridge National Laboratory, ORNL-4899, October, 1973.

7. Defense Civil Preparedness Agency, "EMP Protection for Emergency Operating Centers", TR-61A, July, 1972.

8. Joliff, J.V., Cdr., USN, "Improvements in Ship Construction Techniques to Reduce Electromagnetic Interference", Naval Engineers Journal, April, 1974.

9. DASA EMP (Electromagnetic Pulse) Handbook, DASA-2114-1, DASA Information and Analysis Center, General Electric Co., TEMPO, Santa Barabara, Calif. September, 1968.

10. "Concept Design Recommendations for EMP Hardening of CVA Class Aircraft Carriers", IITRI Report No. E6299, IIT Research Institute, Chicago, Illinois, 60616.

CHAPTER 6

RETROFIT HARDENING

6.1 Susceptibility Classification

The application of EMP hardening techniques is more difficult for a ship which is already in service than for one which is in the design stage. This is due to the constraints imposed by structure, space, equipment location and cable routing. To maintain the cost of retrofit hardening at a reasonable level, it is imperative that a systematic approach be used. This requires the compilation of a Centers and Systems Ranking table as discussed in Section 2.2 of this manual. The information contained in the ranking table spotlights those centers and systems which require attention.

The decision to harden a particular system is based not only on need, but also on cost. The costs involved in retrofit hardening are generally greater than those incurred if hardening is included in initial design. Cost reductions which also result in protection level reductions may be a waste of the total money invested in the hardening, since a system which is "almost safe" will likely fail during an EMP event. If the cost to harden all of the systems which are selected from the ranking table is prohibitive, a priority ranking on mission criticality may be necessary.

6.2 Applicable Hardening Techniques

6.2.1 Shielding

As discussed in Chapter 5, the basic construction of a ship provides a considerable amount of natural shielding. The violations of this shielding occur due to apertures (hatches, windows, ducts, etc.) and conducting path penetrations (cables, pipes, etc.). Free field levels in a compartment are augmented by direct penetration through apertures and by reradiation from conducting energy paths.

The treatment of apertures in retrofit is similar to initial design procedures. Windows which are in critical areas should be covered with a transparent conducting film or a wire mesh. This conductive covering must make good contact with the bulkhead around the entire periphery of the window. Escape hatches should be fitted with a conductive gasketing around the entire periphery. This conductive gasketing may also be utilized on doors. However, frequent inspection is required of gasketing used on doors due to degradation caused by opening and closing of the door.

A better procedure for increasing the shielding effectiveness of doorways is to use a double door system. Obviously, space limitations may eliminate this method from consideration. To obtain greatest effectiveness from this procedure, the doors should not be located opposite one another.

The insertion of a conducting honeycomb is recommended to minimize field penetrations through duct openings. The honeycomb acts as a waveguide below cutoff for the frequency range in which most of the EMP energy occurs and provides a large amount of attenuation of this energy.

In some cases, the most cost effective solution to the improvement of shielding effectiveness is to construct a shielded enclosure within a compartment and place critical equipment within this enclosure. Only those cables and power lines associated with the equipment would enter the enclosure via a single point entry, with cable and power line shields well grounded at the entry.

6.2.2 Conducting Energy Paths

Cables and cable-like structures such as water, sewage and fuel pipes, provide a conducting path for energy flow. Energy which is coupled to these paths may be applied directly to input circuits of equipment via the signal conductor or may be reradiated in the equipment area via sheath current. As in the case of initial design, the most effective solution to the problem of EMP energy on conducting paths is to reduce the exposure.

Cable runs which are located above the main deck receive the greatest exposure and, therefore, must be given first consideration. All such cables should be routed within an electromagnetic shield such as the mast, the superstructre, solid conduit, or raceways. The use of raceways to protect cables which are not within any other shielding structure is probably the most viable retrofit procedure when compared to the cost and time required for rerouting within the superstructure or adding solid conduit. To provide intended protection levels, the entire length of the raceway must be properly welded to the structure along which the cable is routed (mast, bulkhead, deck, etc.).

At the points where cables enter the superstructure or the main deck, it is recommended that a cable vault be constructed to accomplish proper grounding of sheath currents. In addition, protective devices such as surge arrestors and filters can be installed on the terminal board within the vault to reduce transmitted EMP energy on the cable and power leads. Conducting cable-like structures should be peripherally welded at their points of entry.

The energy which appears on cable conductors originates on the cable shield or on antennas. Enclosing the cables in a shielding structure, as previously discussed, will minimize the energy on the cable shield. To minimize energy transfer from antennas to equipment areas, it is recommended that a relay system be installed to disconnect the feed cable at the antenna base when the antenna is not being used for transmission or reception.

Reradiation, which increases the free field strength, and cable interaction, which couples energy between cables, are the major problems in internal areas of the ship. Cables which have picked up EMP energy on their sheaths will reradiate a portion of this energy in the form of free fields or will directly transfer a portion of the energy if contact is made to another conductor. The radiated fields may couple into equipment in compartments or may couple into other cables. Contact between armor sheaths of cables in the same bundle allows direct transfer of energy between cables.

Both reradiation and direct transfer between cables are problems associated with cable routing. It is not possible to eliminate reradiation. However, if cables which have been exposed to EMP energy are not routed through compartments containing susceptible equipment, the reradiated fields will not produce detrimental effects. Similarly, if cables which have been exposed to EMP energy are routed in bundles which are separate from those cables which have not been exposed, energy transfer to the unexposed cables via coupling and direct sheath contact will be minimized.

When modifications are made, it is not realistic to assume that a complete cable system rerouting can be performed. However, it should be possible to reroute some cables around compartments which contain critical equipment. In addition, the separation of exposed and unexposed cables and the containment of reradiated fields may be accomplished by the construction of raceways around the separated cable bundles. These raceways are of particular importance in critical areas.

6.2.3 Grounding

The grounding scheme which is recommended for EMP energy control is the single point ground. As in the case of cable routing, a complete change in ground plan in a retrofit situation to conform to recommended practice for new construction is neither realistic nor advisable. In a complex system it is all too easy to overlook or incorrectly predict ground paths when changes are made, with the result that equipment is more susceptible or possibly does not even operate correctly after the changes have been made.

The best procedure for retrofit treatment of grounds is to provide proper grounds where they were required in the initial construction and installation. This involves such items as replacement of connectors which do not provide peripheral shield contact, replacement of ground straps which have become corroded, are too long, or are too narrow, and replacement of main or branch ground cables which have deteriorated.

6.2.4 Equipment

In dealing with electrical equipment there are three approaches which may be used for decreasing the vulnerability to an EMP transient.

- Redundancy
- Replacement
- Relocation

These methods may be applied separately or in combination.

The simplest procedure is to provide redundancy by carrying spare equipment as backup for equipment which may be damaged by the EMP energy or by any other electrical or mechanical transient. This method provides protection in the sense that the ship may remain on active duty after sustaining equipment damage, but continuity of full capability is interrupted for the length of time required to perform equipment interchange.

A second method for decreasing vulnerability is to replace original apparatus with equipment which has been specifically designed to withstand EMP environments. Such equipment utilizes built-in protection devices, components which have high damage thresholds, circuit designs which are not prone to upset, and have proper shielding incorporated in the housing.

Another method for obtaining EMP hardness is to relocate equipment from an area of high EMP exposure to areas where EMP energy is less prevalent, such as below the main deck or in specially shielded compartments. However, because of the cost and redesign effort necessary to interface the relocated equipment with its associated auxiliary systems, strong justification must be made before this approach can be implemented as a retrofit effort. The decision as to which equipments or systems should be relocated in a retrofit hardening effort depends on many factors which include but are not necessarily limited to the following:

- EMP susceptibility
- Criticality to ship's mission
- Redesign and reconfiguration necessary
- Availability of alternative locations aboard ship
- Effort and cost to relocate equipment being displaced.

Apparatus which requires adjustment or tuning such as transmitters and receivers, and apparatus which provide visual display or audio output of information are generally located in accordance with the battle station which they serve and cannot be moved for strategic reasons. However, support equipment such as computers are prime candidates for relocation if their present location is an area where high energy levels could result.

The movement of equipment will require rerouting of cables and, possibly, additional cables. It is important that these new cable runs be well shielded using conduit or raceways so that energy levels are not increased in previously "safe" areas.

6.2.5 Protective Devices

The use of protective devices (filters and breakdown devices) for retrofit hardening is a relatively simple procedure. These devices should be installed at external locations such as antenna bases and cable entry points (cable vaults) to shunt and reflect energy before it reaches internal areas. Correct installation practice is discussed in Sections 4.2.4 and 4.3.3.

It must be kept in mind that protective devices act to limit conducted energy of the cable core. However, the energy contained in direct field penetrations through apertures, and that contained on poorly shielded and grounded cable sheaths, can easily exceed the conducted core energy. Therefore, the use of protective devices alone will generally not provide the required level of EMP retrofit hardness.

GLOSSARY OF ACRONYMS AND ABBREVIATIONS

AC	Alternating Current
DC	Direct Current
EMC	Electromagnetic Compatibility
EMI	Electromagnetic Interference
EMP	Electromagnetic Pulse
EMPRESS	Electromagnetic Pulse Radiation Environment System Simulator
FTM	Fourier Transform Method
HERO	Hazards of Electromagnetic Radiation to Ordnance
HF	High Frequency (3 to 30 MHz)
LF	Low Frequency (30 to 300 kHz)
LPN	Lumped Parameter Network
MF	Medium Frequency (.3 to 3 MHz)
MIL-STD	Military Standard
NACSEM	National Comsec/Emsec
NSWC	Naval Surface Weapons Center
RF	Radio Frequency
RFI	Radio Frequency Interference
SEM	Singularity Expansion Method
TEMPEST	Designation for Compromising Emanations
VHF	Very High Frequency (30 to 300 MHz)

INDEX

INDEX (CONTINUED)

APPENDIX A

ROUGH ESTIMATES OF PEAK CURRENTS USING PROCEDURES BASED ON LANDT'S METHOD

The following are rough estimates of peak currents for six different typical antennas and antenna-like structures. The calculations used to obtain these estimates are based on the method developed by Landt, which was described in Section 3.2.1.4 of this text. Note that in Example 1 below, the unit vector, $\bar{k}$, denotes the direction of wave propagation.

Example 1

Antenna Geometry

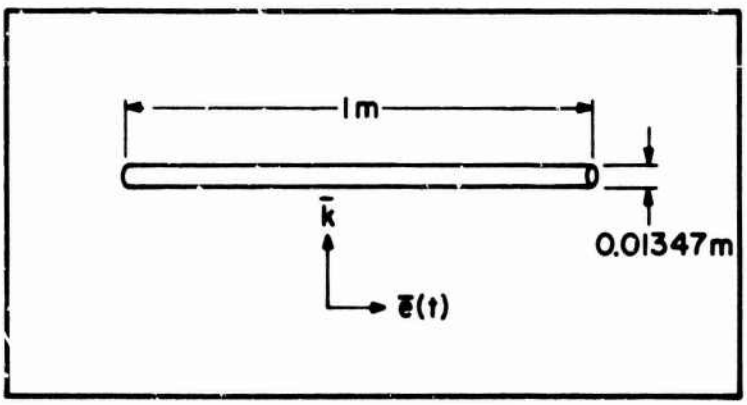

Waveform Of Incident Field

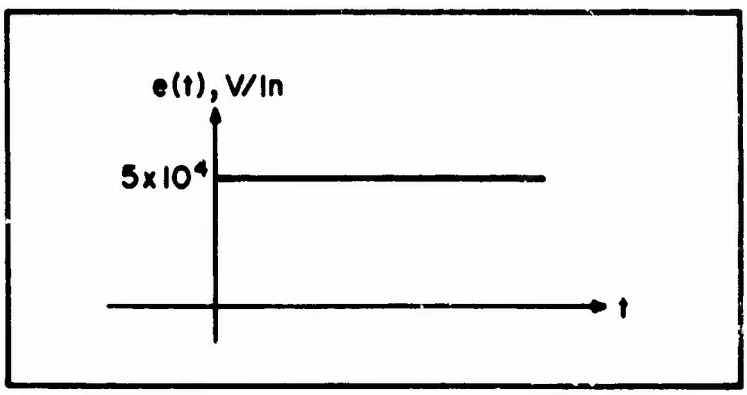

Steps of Calculation

(1) Wire radius a = 0.00674

(2) Wire length ℓ = 1.0

(3) Time of reflection $t_2 = \ell/2c = 1.67 \times 10^{-9}$

(4) Rise time $t_1 = 0$

(5) Write $\tau = \frac{t_2 - t_1}{2} = 0.833 \times 10^{-9}$

(6) Estimate $\int_0^{t_2} e(t)dt = 8.35 \times 10^{-5}$

(7) Calculate $\frac{c\tau}{a} = 37.1$

(8) From Figure A.1, find $h(\frac{c\tau}{a}) \approx 1.06 \times 10^{6}$

(9) Obtain peak current $I_{peak} = h\,(\frac{c\tau}{a}) \int_0^{t_2} e(t)\,dt = 88.5$ amps

Example 2

Antenna Geometry

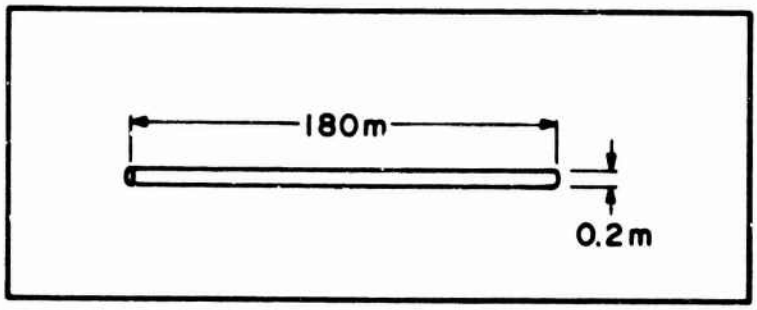

Waveform Of Incident Field

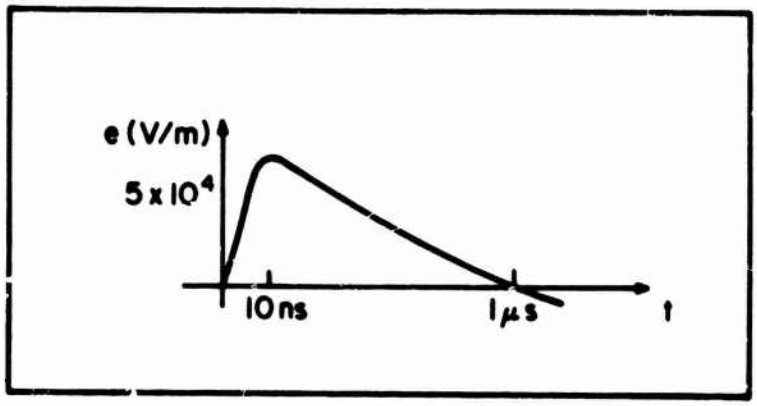

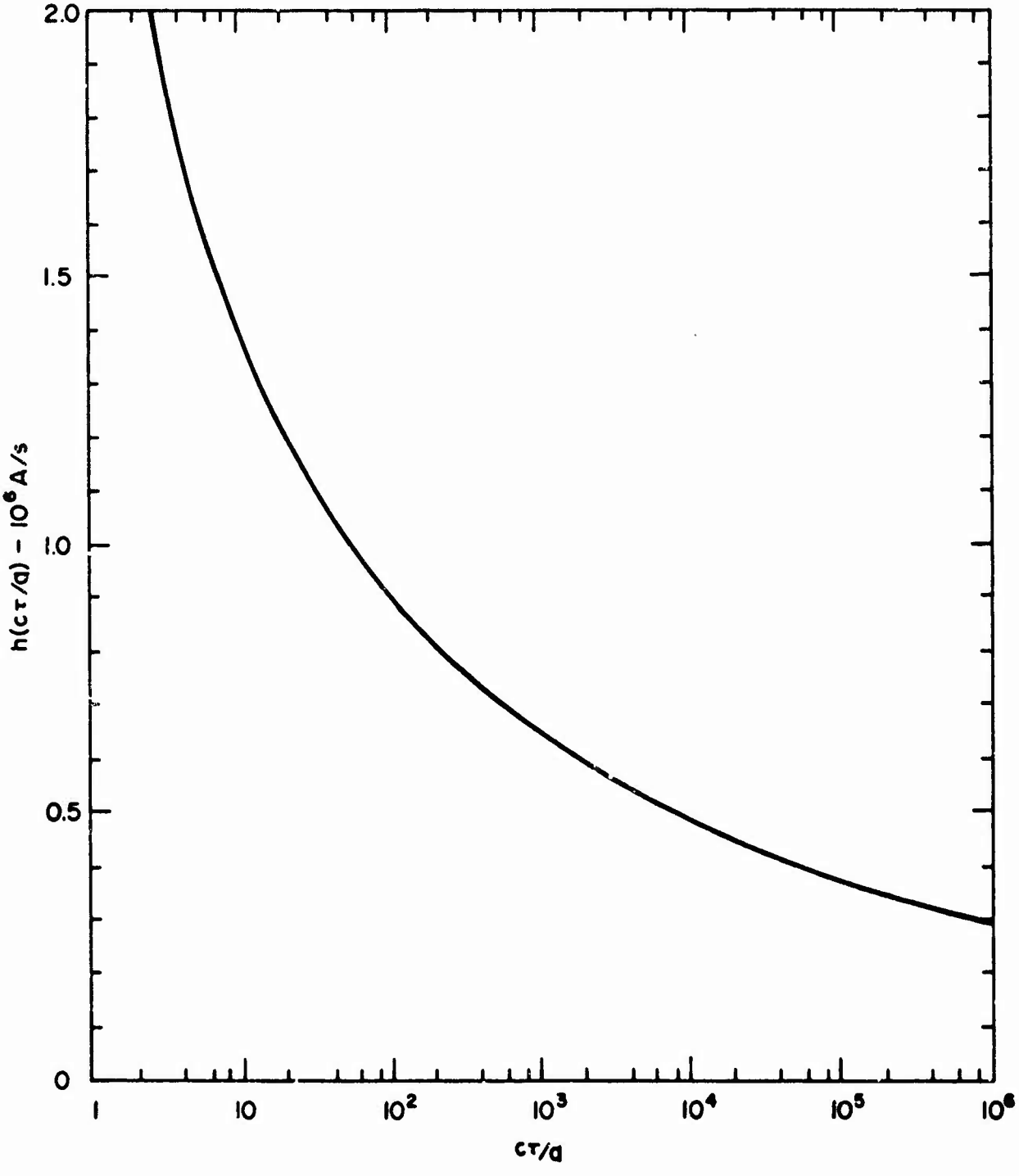

Figure A.1 IMPULSE RESPONSE OF THE CURRENT ON AN INFINITE WIRE WHEN ILLUMINATED FROM BROADSIDE BY A PLANE WAVE

Steps of Calculation

(1) Wire radius a = 0.1

(2) Wire length ℓ = 180.

(3) Time of reflection $t_2 = \frac{\ell}{2c}$ 3.0×10^{-7}

(4) Sketch the approximate incident waveform

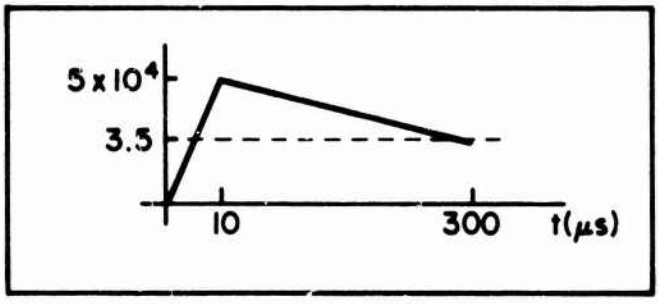

(5) Rise time $t_1 = 10^{-8}$

(6) Estimate $\int_0^{t_2} e(t)\,dt = 1.28 \times 10^{-2}$

(7) $\tau = \frac{t_2 - t_1}{2} = 1.45 \times 10^{-7}$

(8) $\frac{c\tau}{a} = 435$

(9) From Figure A.1, $h(\frac{c\tau}{a}) = 0.73 \times 10^{6}$

(10) $I_{peak} = h(\frac{c\tau}{a}) \int_0^{t_2} e(t)\,dt = 9400$ A

Example 3

Geometry Of Antenna-Like Structure

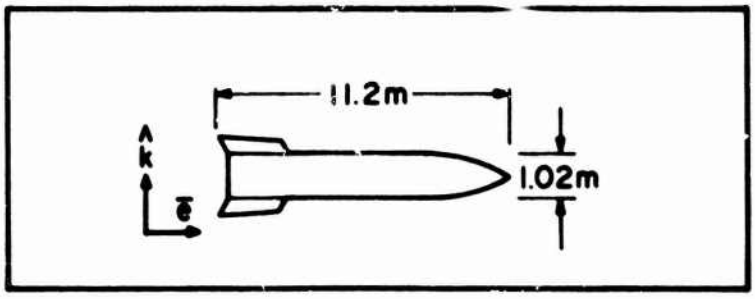

Waveform Of Incident Field

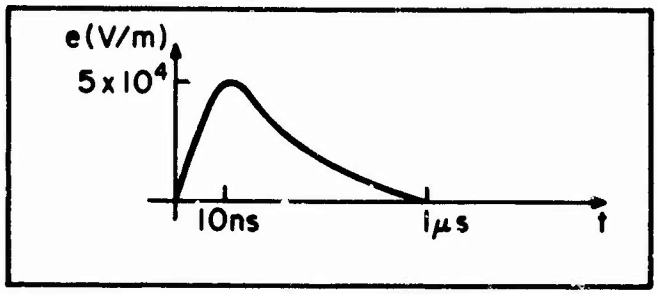

Steps of Calculation

(1) Sketch the approximate antenna model

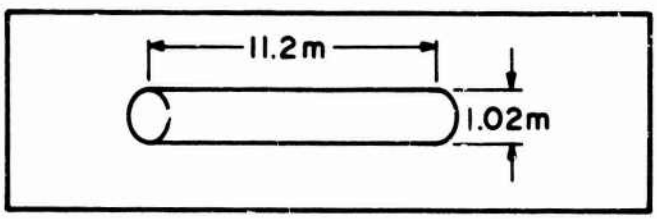

(2) Wire radius $a = 0.51$

(3) Wire length $\ell = 11.2$

(4) Sketch the approximate incident waveform

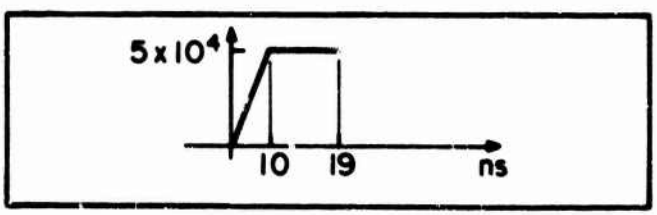

(5) Time of reflection $t_2 = \frac{\ell}{2c} \approx 1.9\times10^{-8}$

(6) Rise time $t_i = 10^{-8}$

(7) $\tau = \frac{t_2 - t_i}{2} = 0.45\times10^{-8}$

(8) $\frac{c\tau}{a} = 2.65$

(9) From Figure A.1, $h(\frac{c\tau}{a}) = 2.1\times10^{6}$

(10) Estimate $\int_0^{t_2} e(t)\,dt = 7.0\times10^{-4}$

(11) $I_{peak} = h(\frac{cT}{a}) \int_0^{t_2} e(t)\,dt = 1470$ A

Example 4

Geometry Of Structure

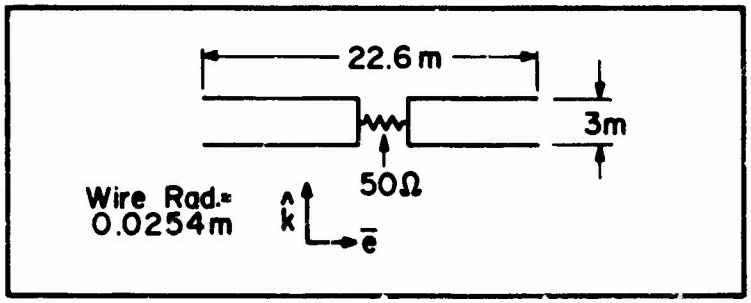

Waveform Of Incident Field

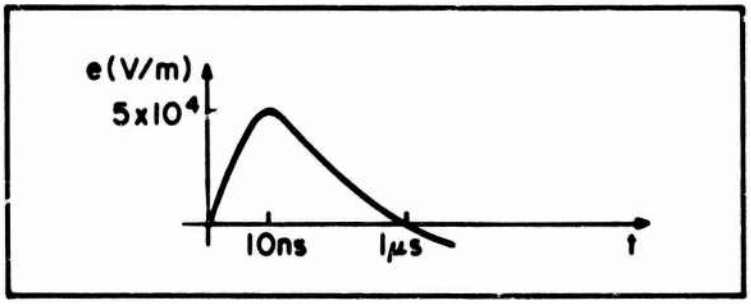

Steps of Calculation

(1) Sketch Approximate Antenna Model

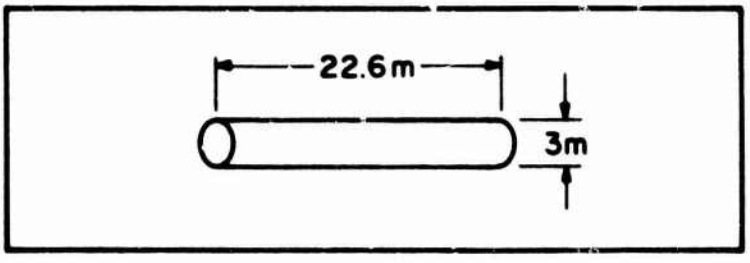

(2) Wire radius a = 1.5

(3) Wire length ℓ = 22.6

(4) Time of reflection $t_2 = \ell/2c = 3.76 \times 10^{-8}$

(5) Sketch the apprcximate incident waveform

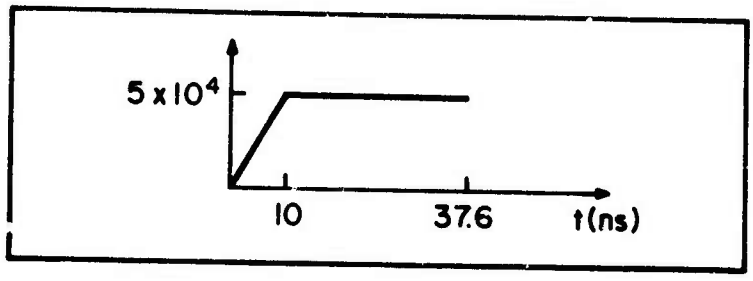

(6) Rise time $t_1 = 10^{-8}$

(7) $\tau = \frac{t_2 - t_1}{2} = 1.38 \times 10^{-8}$

(8) $\frac{c\tau}{a} = 2.76$

(9) From Figure A.1, $h(\frac{c\tau}{a}) = 2.0 \times 10^{6}$

(10) Estimate $\int_0^{t_2} e(t)\, dt = 1.63 \times 10^{-3}$

(11) $I_{peak} = h(\frac{c\tau}{a}) \int_0^{t_2} e(t)\, dt = 3260$ A

(12) Loading $G_L = \frac{1}{Z_L} = 20 \times 10^{-3}$

(13) Calculate $G_{eff} = \frac{I_{peak}}{c\int_0^{\tau} e(t)\, dt} = 6.7 \times 10^{-3}$

(14) Calculate the load current

$$I_L = \frac{G_L}{G_L + G_{eff}} I_{peak} = 2440 \text{ A}$$

Example 5

Geometry Of Antenna-Like Structure

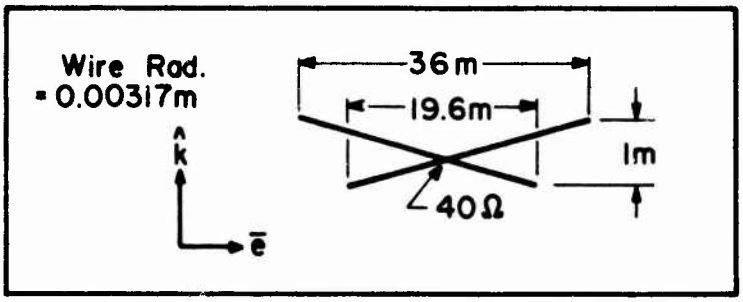

Waveform Of Incident Field

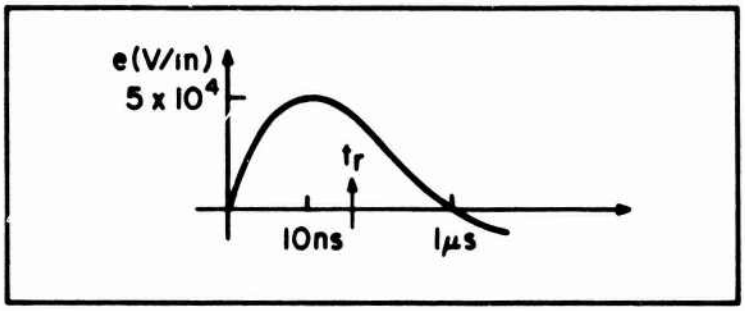

Steps of Calculation

(1) Sketch the approximate antenna model

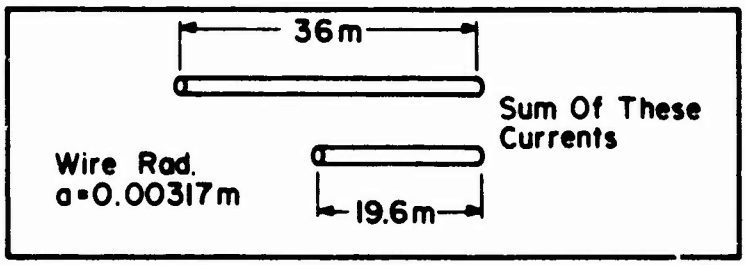

(2) Wire radius a = 0.00317

(3) Wire length ℓ = 36, 19.6

(4) Sketch the approximate incident waveform

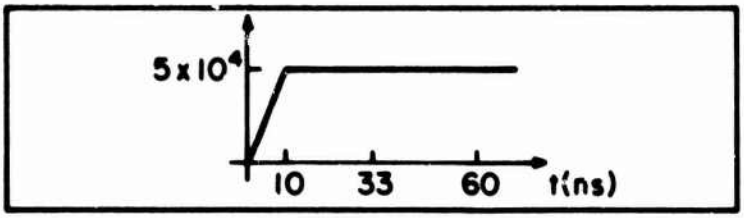

(5) Time of reflection $t_2 = \frac{\ell}{2c} = 6\text{x}10^{-8}, \ 3.3\text{x}10^{-8}$

(6) Rise time $t_1 = 10^{-8}$

(7) $\tau = \frac{t_2 - t_1}{2} = 2.5\text{x}10^{-8}, 1.65\text{x}10^{-8}$

(8) $\frac{c\tau}{a} = 2366, 1562$

(9) Estimate $\int_0^{t_2} e(t)\,dt = 2.75\text{x}10^{-3}, 1.4\text{x}10^{-3}$

(10) From Figure A.1, $h(\frac{c\tau}{a}) = 0.58\text{x}10^{6}, 0.63\text{x}10^{6}$

(11) $I_{peak} = h(\frac{c\tau}{a}) \int_0^{t_2} e(t)\,dt = 1595 + 882$

(12) Loading $G_L = \frac{1}{Z_L} = 25\text{x}10^{-3}$

(13) Calculate $G_{eff} = \frac{I_{peak}}{c \int_0^{t_2} e(t)\,dt} = 1.98\text{x}10^{-3}$

(14) $I_L = \frac{G_L}{G_L + G_{eff}} I_{peak} = 2295$ A

Example 6

Geometry Of Antenna-Like Structure

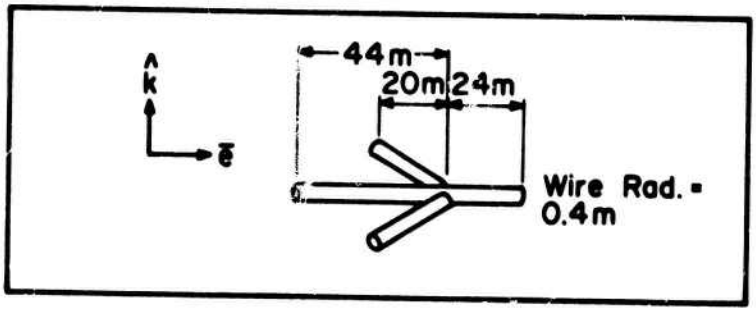

Waveform Of Incident Field

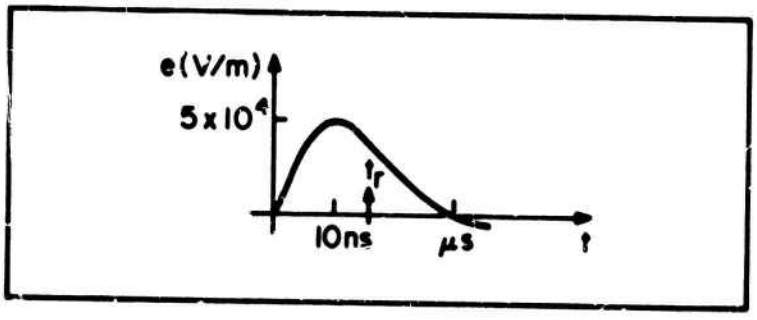

Steps of Calculation

(1) Sketch the approximate antenna model

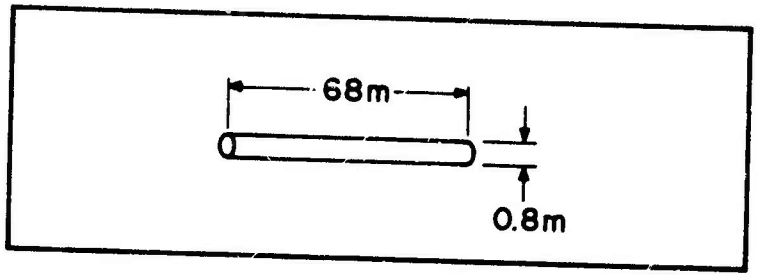

(2) Wire radius a = 0.4

(3) Wire length ℓ = 68

(4) Sketch the approximate incident waveform

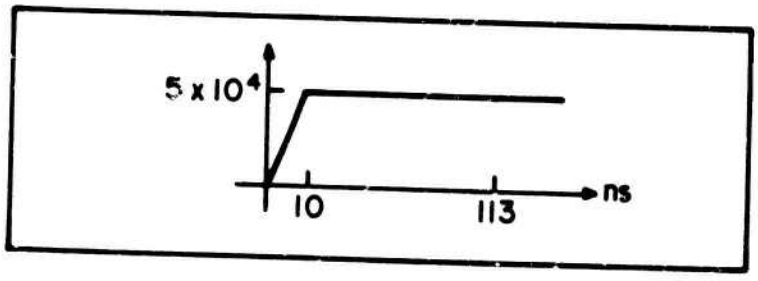

(5) Time of reflection $t_2 = \frac{\ell}{2c} = 1.13 \times 10^{-7}$

(6) Rise time $t_1 = 10^{-8}$

(7) $\tau = \frac{t_2 - t_1}{2} = 5.15 \times 10^{-8}$

(8) $\frac{c\tau}{a} = 39$

(9) Estimate $\int_0^{t_2} e(t)\,dt = 5.4 \times 10^{-3}$

(10) From Figure A.1, $h(\frac{c\tau}{a}) = 1.05 \times 10^{6}$

(11) $I_{peak} = h(\frac{c\tau}{a}) \int_0^{t_2} e(t)\,dt = 5670$ A

APPENDIX B

NUMERICALLY RIGOROUS CALCULATIONS OF EMP PICKUP BY HORIZONTAL CABLES

In this Appendix, the load currents for both the shield and the inner conductor at $x = 0$ and $x = \ell$ are calculated for the model of the horizontal cable shown in Figure B.1. In order to determine sensitivities to the major parameters (length, height, load and diameter), currents are calculated for several parametric variations.

The conductive plane considered here which could be the deck of a ship or other highly conducting metal structure associated with the cable system is assumed to be a perfectly conducting plane. The conductivities of most metals such as aluminum and mild steel are high in the range of 10^6 to 10^7 ohms/m. Hence, the assumption that the plane beneath the cable is a perfectly conducting plane is not too unrealistic for a ship.

To facilitate the analysis of coupling and/or penetration of the EMP on cable systems, it is convenient to represent the waveform given in Figure B.2 mathematically by a double exponential of the form:

$$E(t) = E_o\{e^{-\alpha t} - e^{-\beta t}\} \quad \text{(volts/meter)} \tag{B.1}$$

where

t = time in seconds

$\alpha = 1.5 \times 10^6$ (sec^{-1})

$\beta = 2.6 \times 10^8$ (sec^{-1})

and the electric field intensity E_o is normalized to unity for convenience, and the magnetic field intensity is given as:

$$H(t) = \frac{E(t)}{\eta_o} \quad \text{(amps/meter)} \tag{B.2}$$

where η_o is the intrinsic impedance (377 Ω) of free space.

The rise time, t_r, of the EMP pulse in this expression is on the order of 10 ns and the fall time, t_f, is about 2 μsec.

The EMP amplitude spectrum covers an extremely broad frequency range extending from very low to microwave frequencies. The rate of attenuation of the amplitude

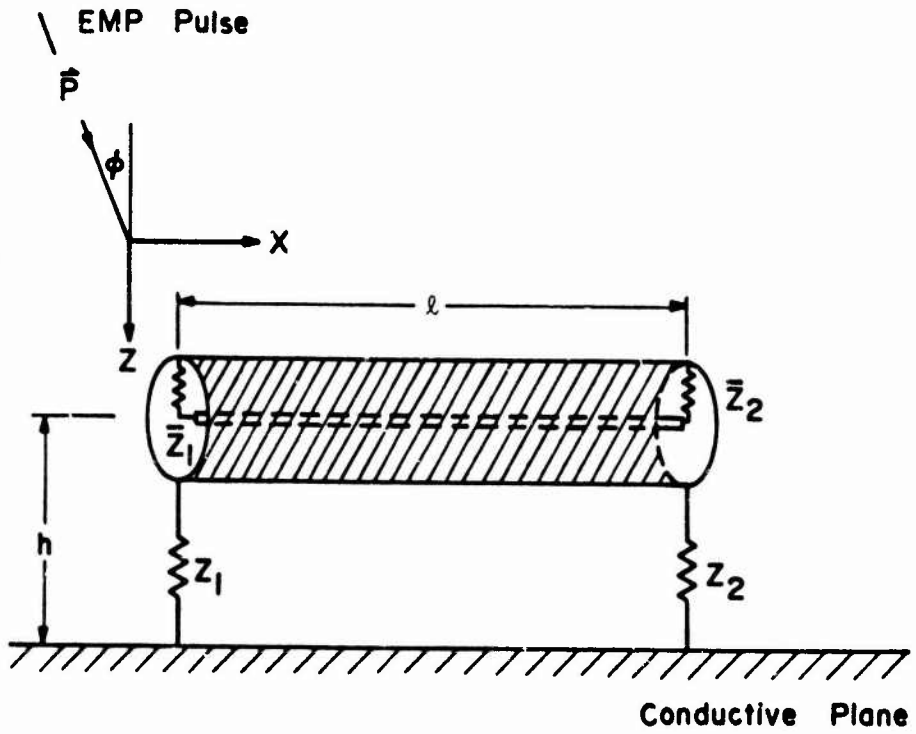

Figure B.1 HORIZONTAL CABLE MODEL

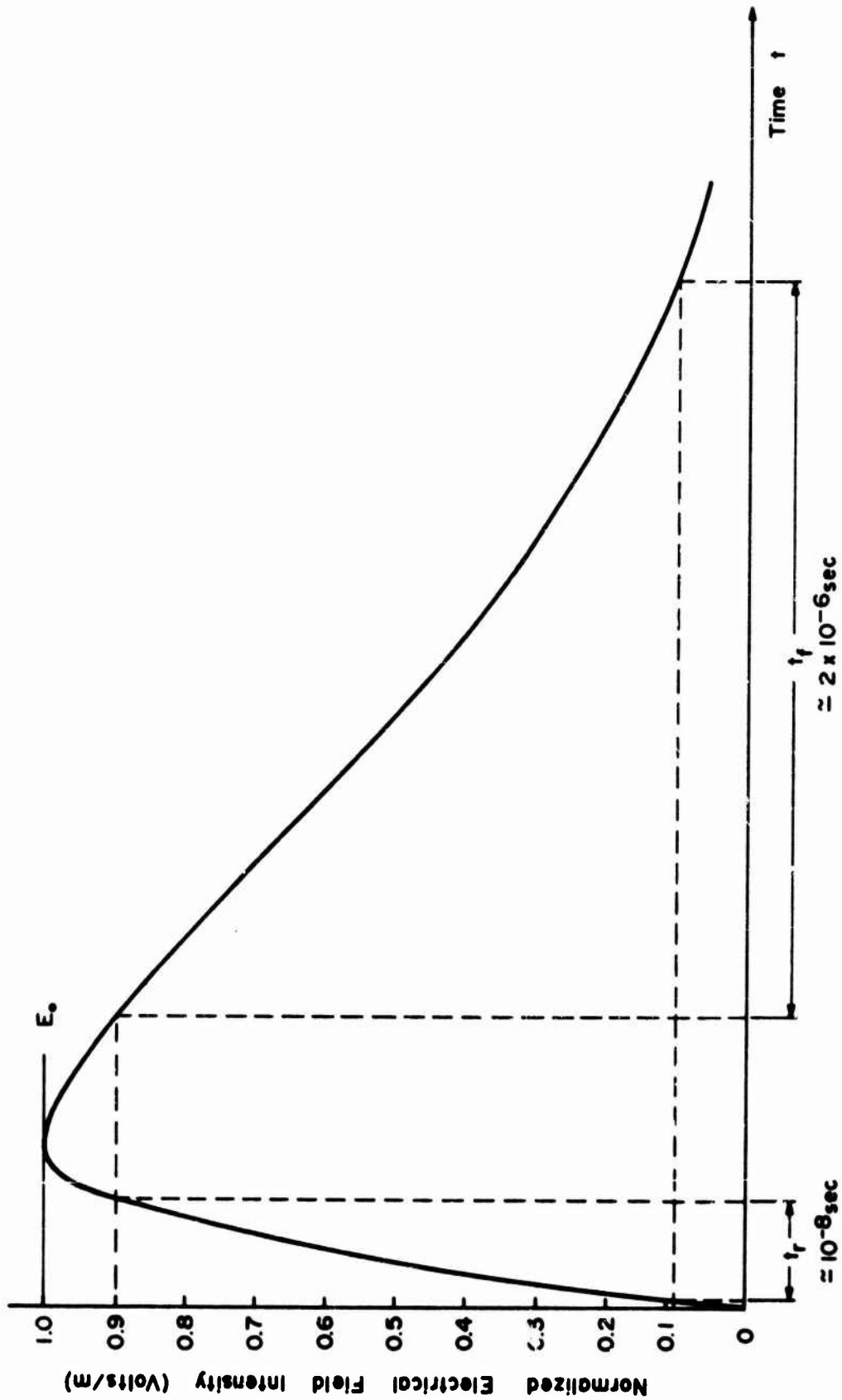

Fig. B.2 REPRESENTATIVE EMP WAVEFORM FOR HIGH-ALTITUDE BURST (ELECTRIC FIELD)

spectrum is shown in the plot of Figure B.3, where the break frequencies are determined by the time constants of the EMP waveform given in Equation (B.1). This plot is obtained from the log-magnitude of the Fourier transform expression of Equation (B.1).

It is important to note that the spectrum obtained is almost constant below the HF range. From the standpoint of equipment, this means that EMP is difficult to filter and can couple into electronic circuitry over a wide range of frequencies.

B.1 Sheath Current

Calculations of the transient response to the EMP of Figure B.2 for various important cable parameters have been performed by IITRI with the aid of a digital computer. In the calculation, the cable is considered to be an RG-8A/U coaxial cable and cable losses are included. Some of the results are presented below:

Cable Length

Figure B.4 shows the effect of the length of an RG-8A/U coaxial cable on the sheath current for the case of broadside incidence and matched conditions, i.e., $Z_1 = Z_2 = Z_0$. The cable considered is 15.24 cm (6 inches) above the perfect conducting plane which corresponds to a cable-plane characteristic impedance of about 203 ohms.

As indicated in the figure, the magnitude of peak current increases as the cable length increases. However, the increase of peak current is not linear with respect to the cable length. In fact, the peak current tends to saturate at about 0.7 mA when the cable length is longer than 200 meters. In using this figure, it must be remembered that the incident EMP electric field is normalized to unity as compared to the nominal EMP threat of 50 kV/m. Thus, currents of about 35 amps can be expected for a horizontal cable of 200 meters.

For matched conditions, the sheath currents at both ends of the cable, $x = 0$ and $x = \ell$, are found to be identical. From a physical point of view, this is expected because of the symmetric properties of the cable configuration and the external excitation.

The shape of the current waveform would be expected to depend on the cable resonance characteristics. As indicated in Figure B.5, the pulse duration, which is defined here as the time of the current's first zero crossing, is given by the relation $t_d = \ell/c$, where ℓ is the cable length.

In order to provide the reader with the details of the transient characteristics in addition to the peak current values, computer results of all the current responses are presented in Figures B.6, 7, 8 and 9 for ℓ = 25, 50, 100 and 200 meters, respectively.

Height

As shown in Figure B.10, the peak magnitude of the sheath current increases monotonically, as the height, h, increases. This is true because the loop, consisting of the cable and the conductive plane, becomes bigger as h increases. This, in turn, increases the magnetic field pickup. The results of Figure B.10 are valid for broadside incidence only. This, however, would represent the maximum cable pickup.

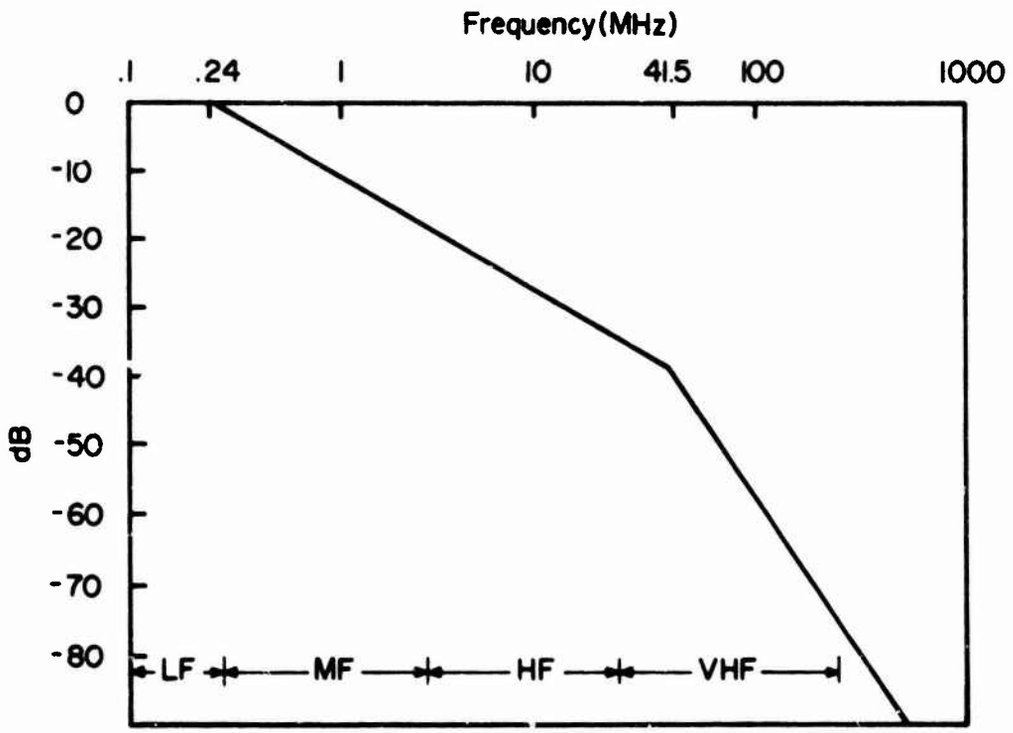

Fig. B.3 FREQUENCY SPECTRUM OF EMP PULSE

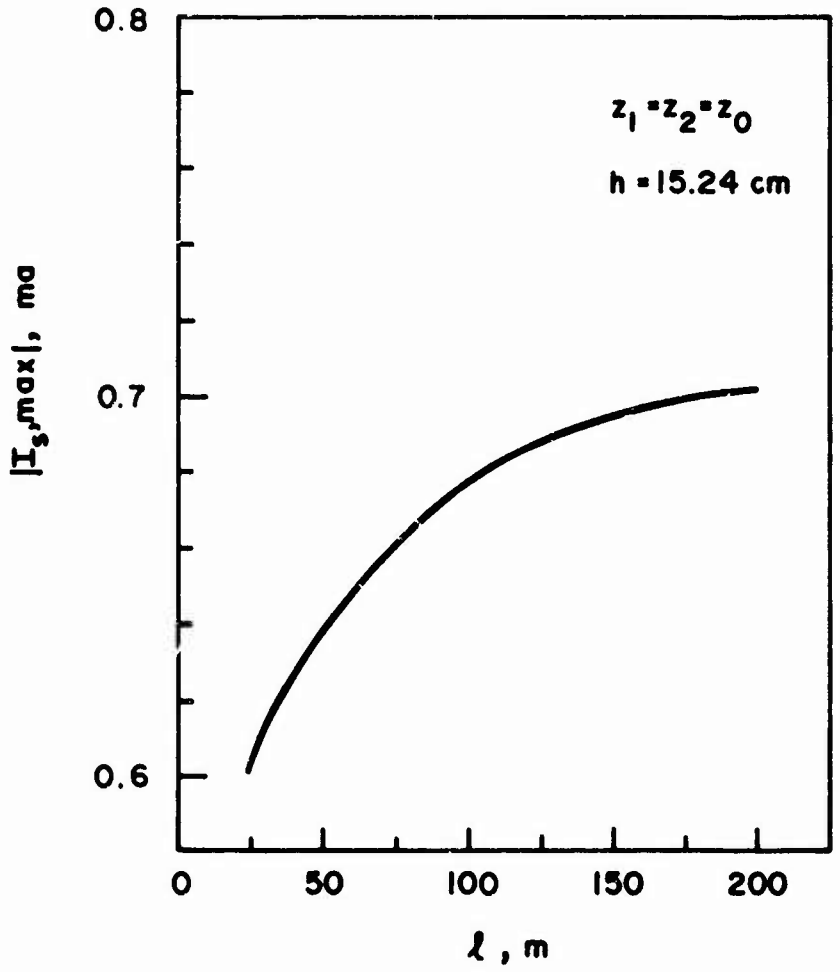

Fig. B.4 PEAK SHEATH CURRENT AS A FUNCTION OF CABLE LENGTH FOR A HORIZONTAL CABLE

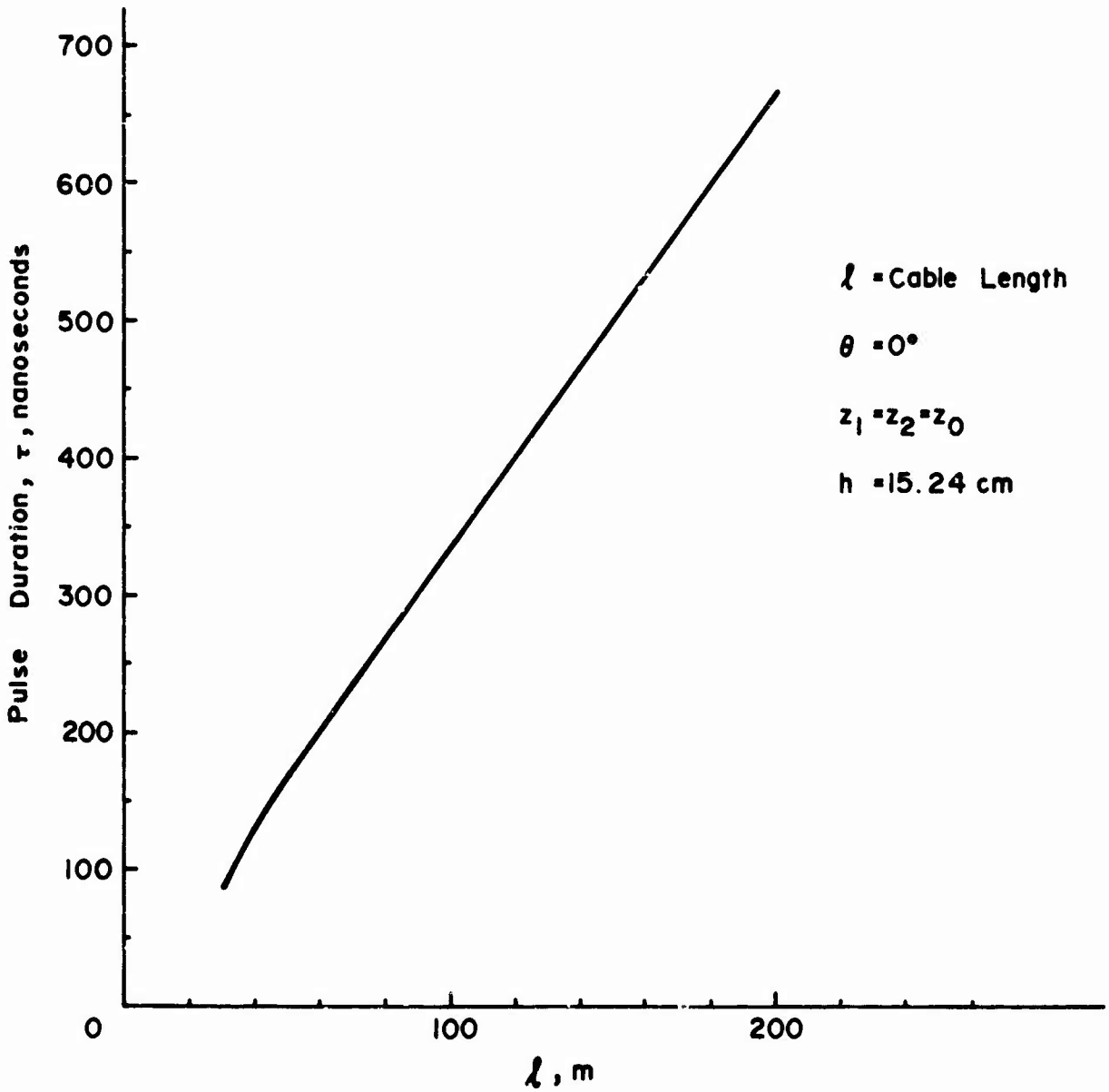

Fig. B.5 PULSE DURATION AS A FUNCTION OF CABLE LENGTH FOR A HORIZONTAL CABLE

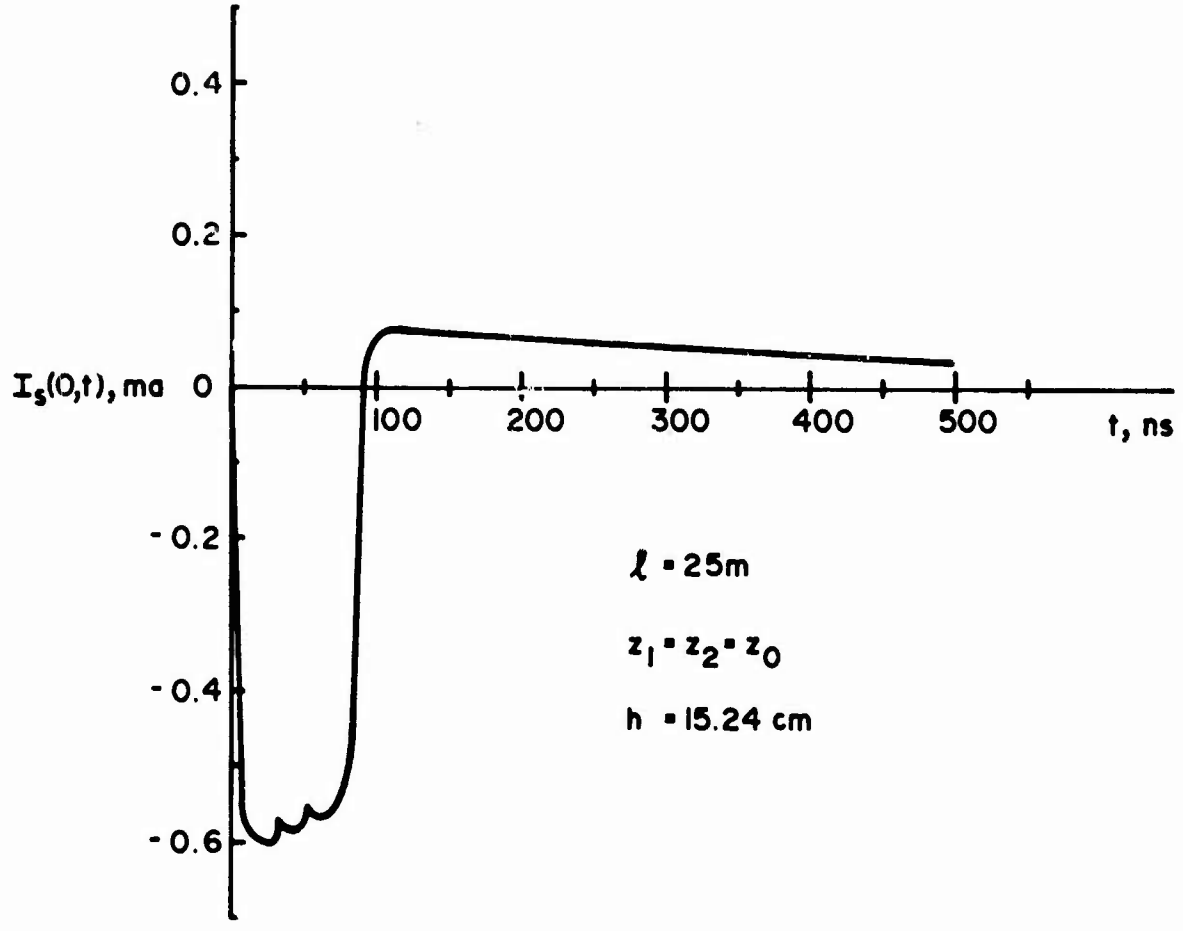

Fig. B.6 TRANSIENT SHEATH CURRENT FOR A 25 METER HORIZONTAL CABLE

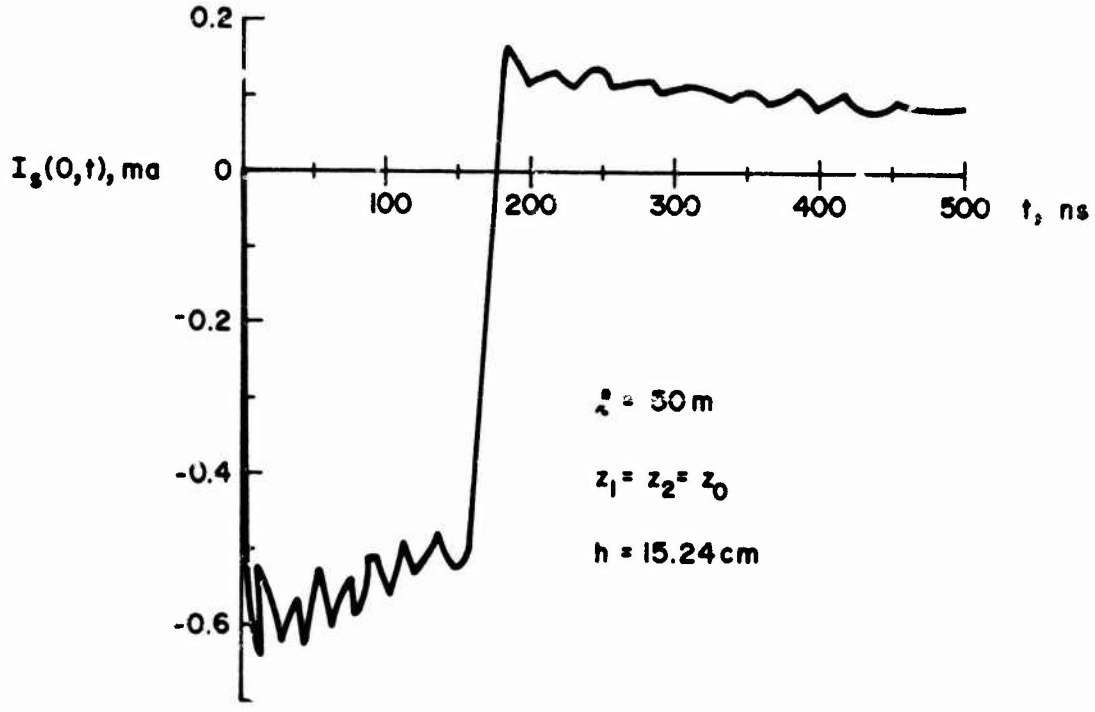

Fig. B.7 TRANSIENT SHEATH CURRENT FOR A 50 METER HORIZONTAL CABLE

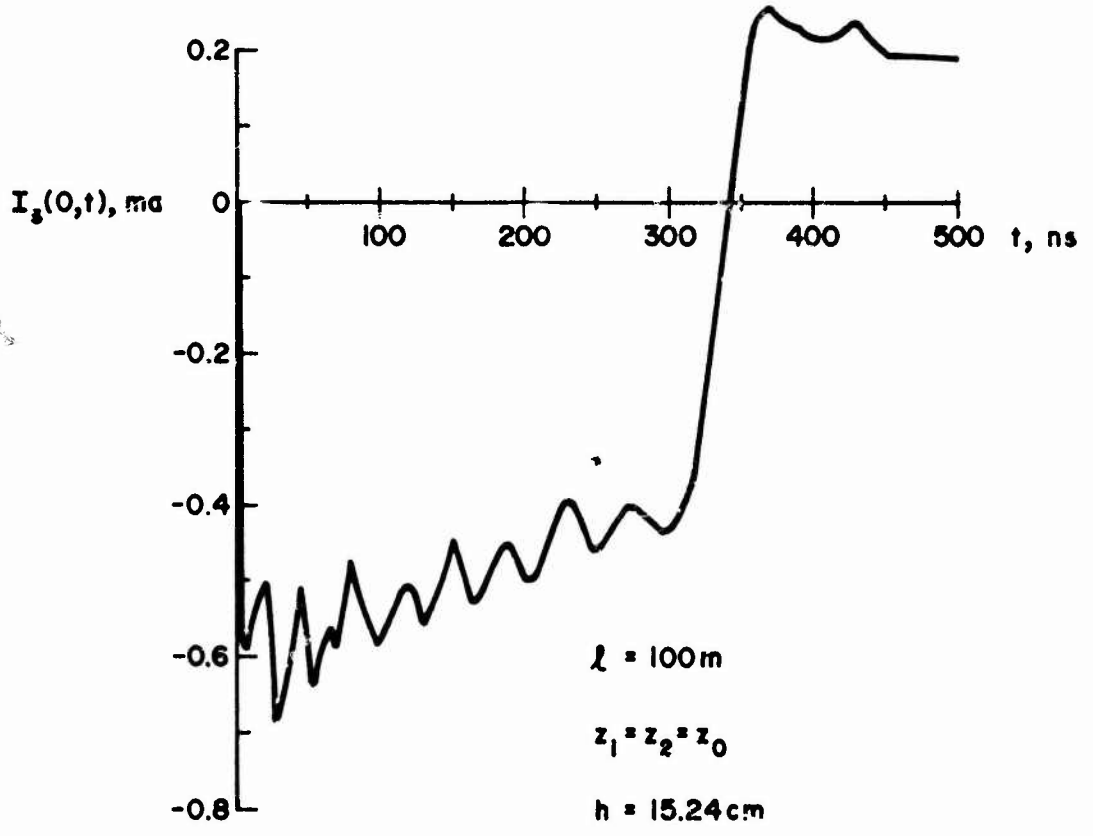

Fig. B.8 TRANSIENT SHEATH CURRENT FOR A 100 METER HORIZONTAL CABLE

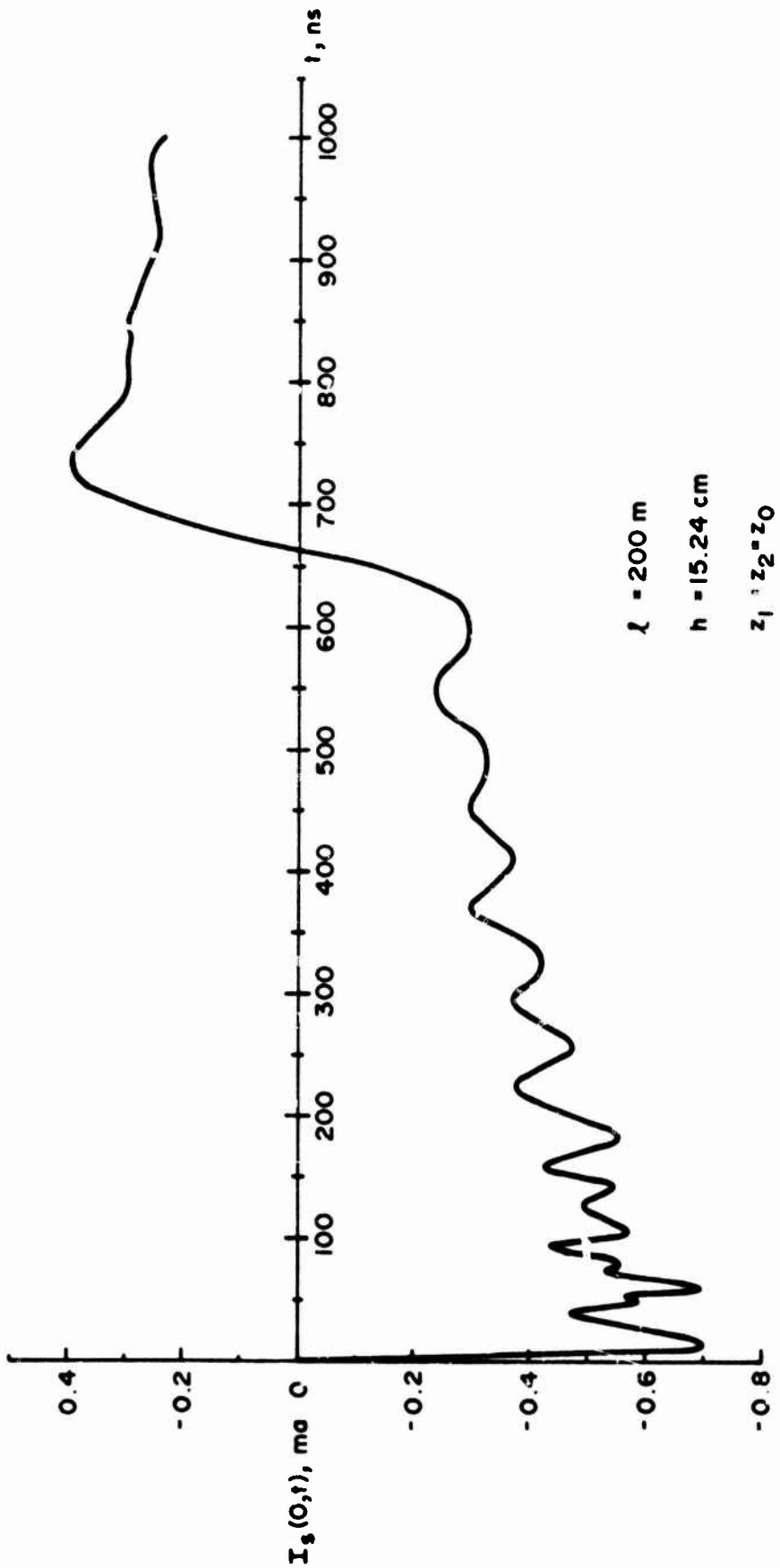

Fig. B.9 TRANSIENT SHEATH CURRENT FOR A 200 METER HORIZONTAL CABLE

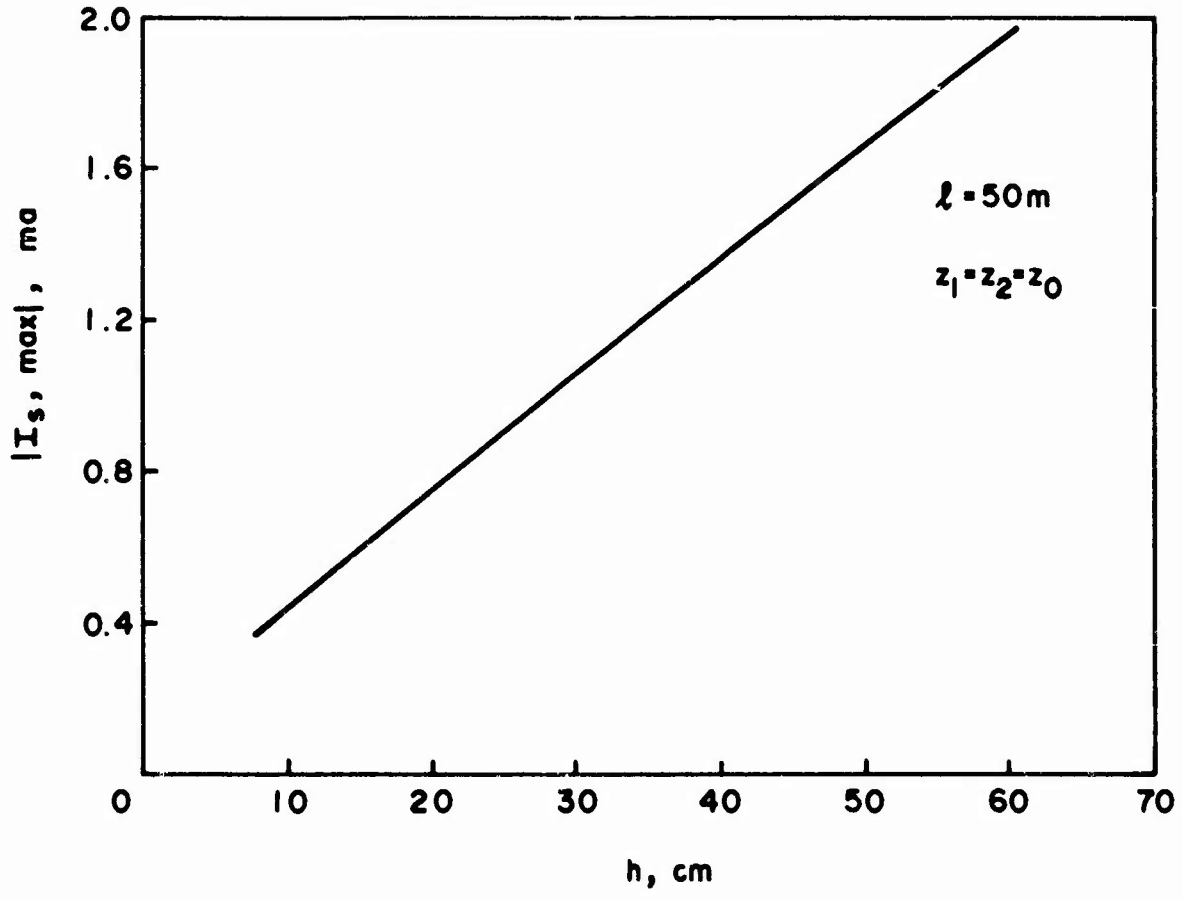

Fig. B.10 PEAK SHEATH CURRENT AS A FUNCTION OF HEIGHT FOR A HORIZONTAL CABLE

Load Impedance

The effect of load impedance on the sheath current is plotted in Figure B.11 as a function of Z_1, the load impedance for the sheath at x = 0, when the impedance Z_2 at x = ℓ is matched to the characteristic impedance and ℓ = 50 meters. The currents at x = 0 and x = ℓ are not equal unless $Z_1 = Z_0$. For $Z_1 \neq Z_2$, the entire cable configuration is not symmetric, although the symmetric property of excitation still exists for broadside incidence.

The results obtained reveal that the sheath current at x = 0 decreases as Z_1 increases. Increasing Z_1 by a factor of five causes a decrease in the load current at x = 0, as evidenced by Figure B.11, by a factor of approximately 1.5. However, the change of the load current at x = ℓ, which is also shown in the figure by a dotted curve, becomes less marked as Z_1 is changed. The fact that a decrease in load impedance Z_1 results in an increase in the load current at x = 0 implies that, for cables terminated by matched impedance at x = ℓ, the short-circuit condition at the other end of the cable (x = 0) will draw the largest current. In this case, an EMP threat of 50 kV/m, for example, would produce a peak sheath current of about 64 amps.

In connection with transient waveforms, the details of cable responses for Z_1 = 0 and Z_1 = 123 Ω, shown in Figures B.12 and B.13, respectively, are presented here for comparison. In either case, the cable is considered to be illuminated by a broadside EMP.

Cable Diameter

The calculation of sheath currents for increasing cable diameters exhibits an increase of peak sheath currents. This fact is clearly illustrated by comparing Figure B.4 to Figure B.14 which is a plot of peak sheath current versus cable length when the cable diameter is twice that of an RG-8A/U coaxial cable. For example, increasing the cable diameter by a factor of two would cause the peak sheath current to increase from 35 amps to 42 amps, if the cable is 200 meters long and the incident EMP is scaled to 50 kV/m.

B.2 Core Current

This section presents calculated results for an RG-8A/U coaxial cable. Because of the wide scope of cables and their shielding, the data presented might be considered illustrative rather than a firm description applicable to all conditions on a ship.

Cable Length

The effect of cable length on the core current is shown in Figure B.15. Results are obtained for an RG-8A/U cable suspended at a height of 15.24 cm (6 inches) above the deck of a ship. The cable shields are assumed to be shorted at the ends, and the core-to-inner shield terminal is assumed to be matched to the characteristic impedance of the cable, i.e., $\bar{Z}_1 = \bar{Z}_2 = \bar{Z}_0$ where $\bar{Z}_0$ is approximately 50 ohms for RG-8A/U cable. The transfer impedance is determined from results of tests performed at IITRI using a triaxial tester.

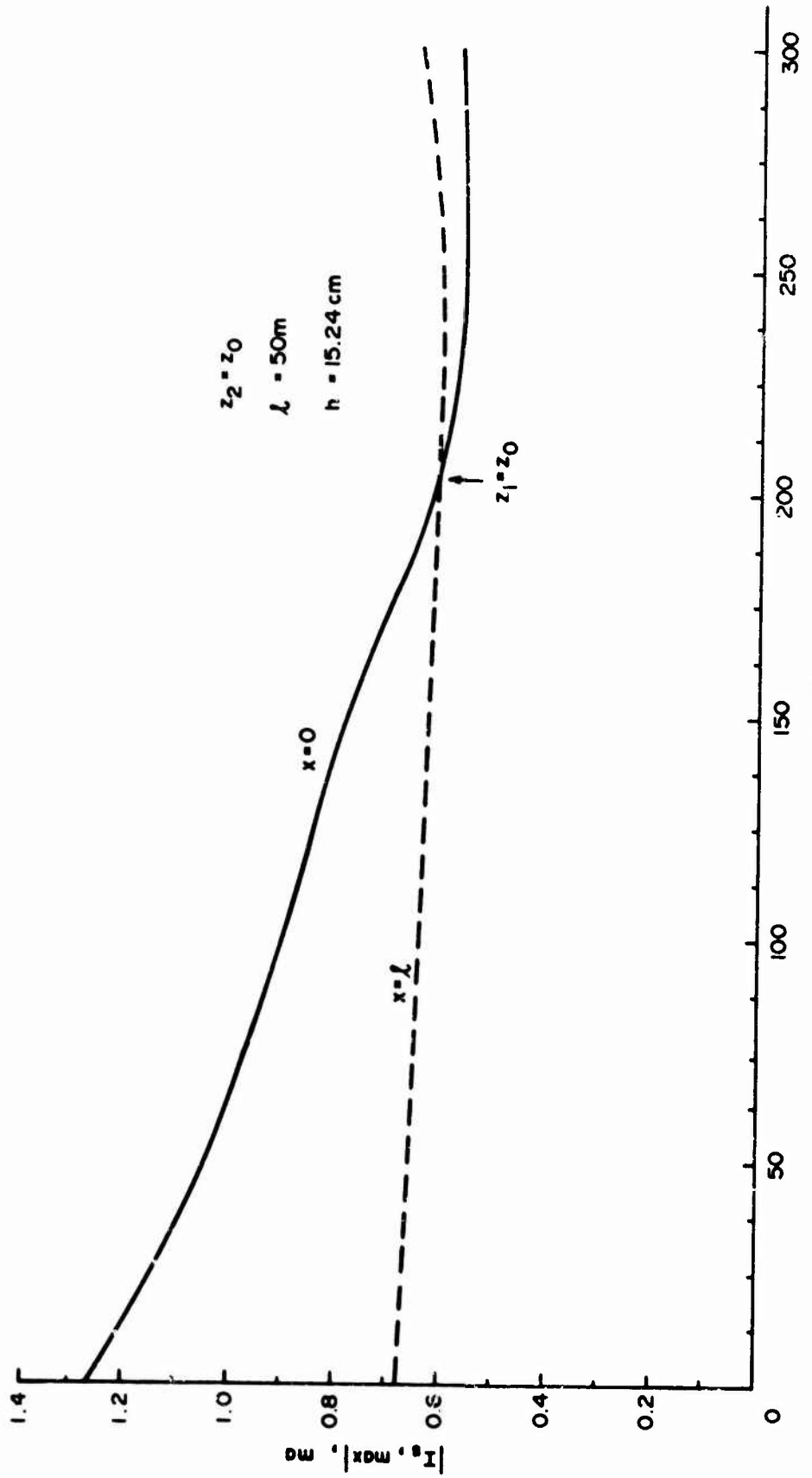

Fig. B.11 PEAK SHEATH CURRENT AS A FUNCTION OF THE LOAD IMPEDANCE, Z_1, FOR A HORIZONTAL CABLE

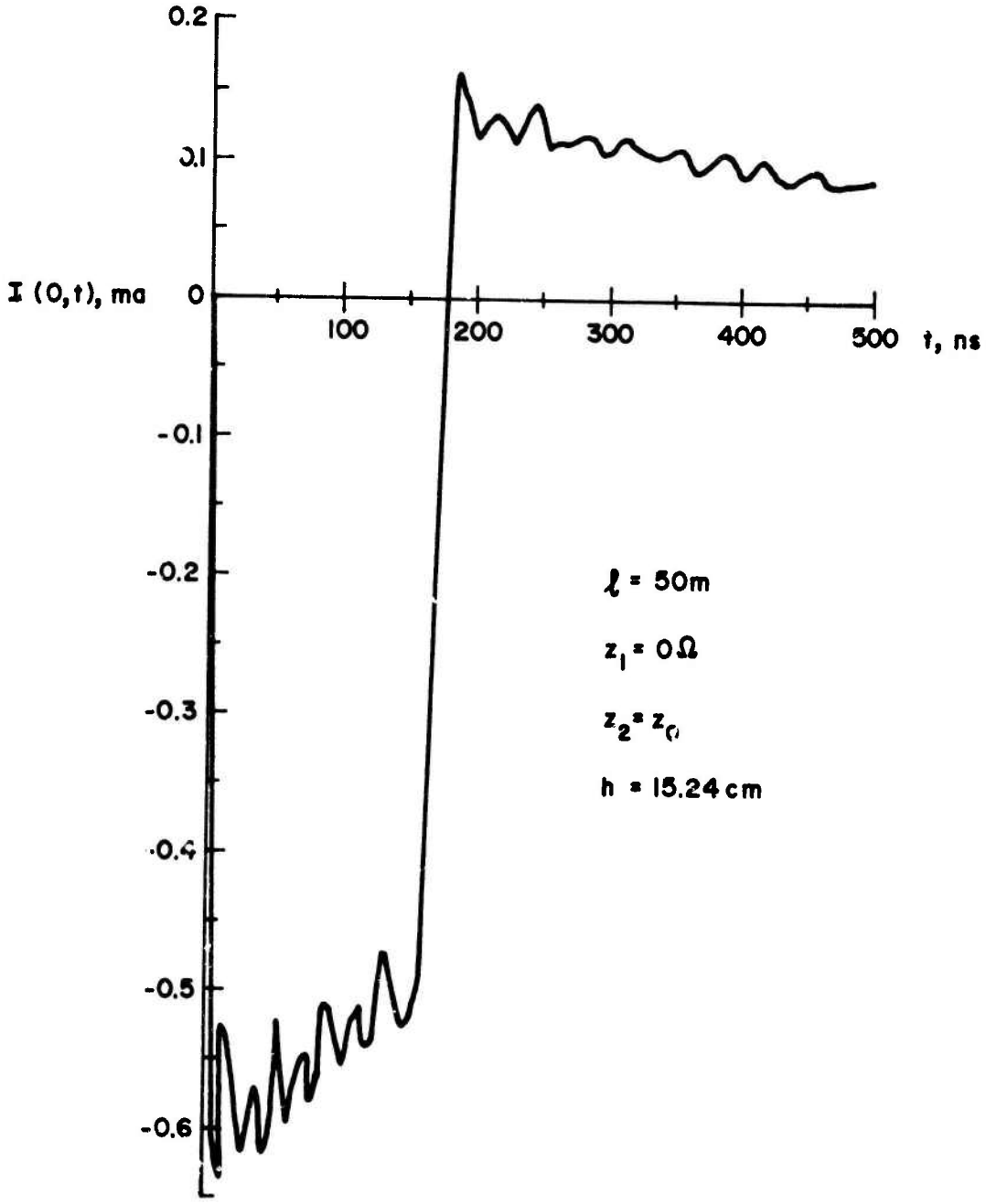

Fig. B.12 TRANSIENT WAVEFORM WHEN SHEATH LOADING IS NOT MATCHED (Z_1=0)

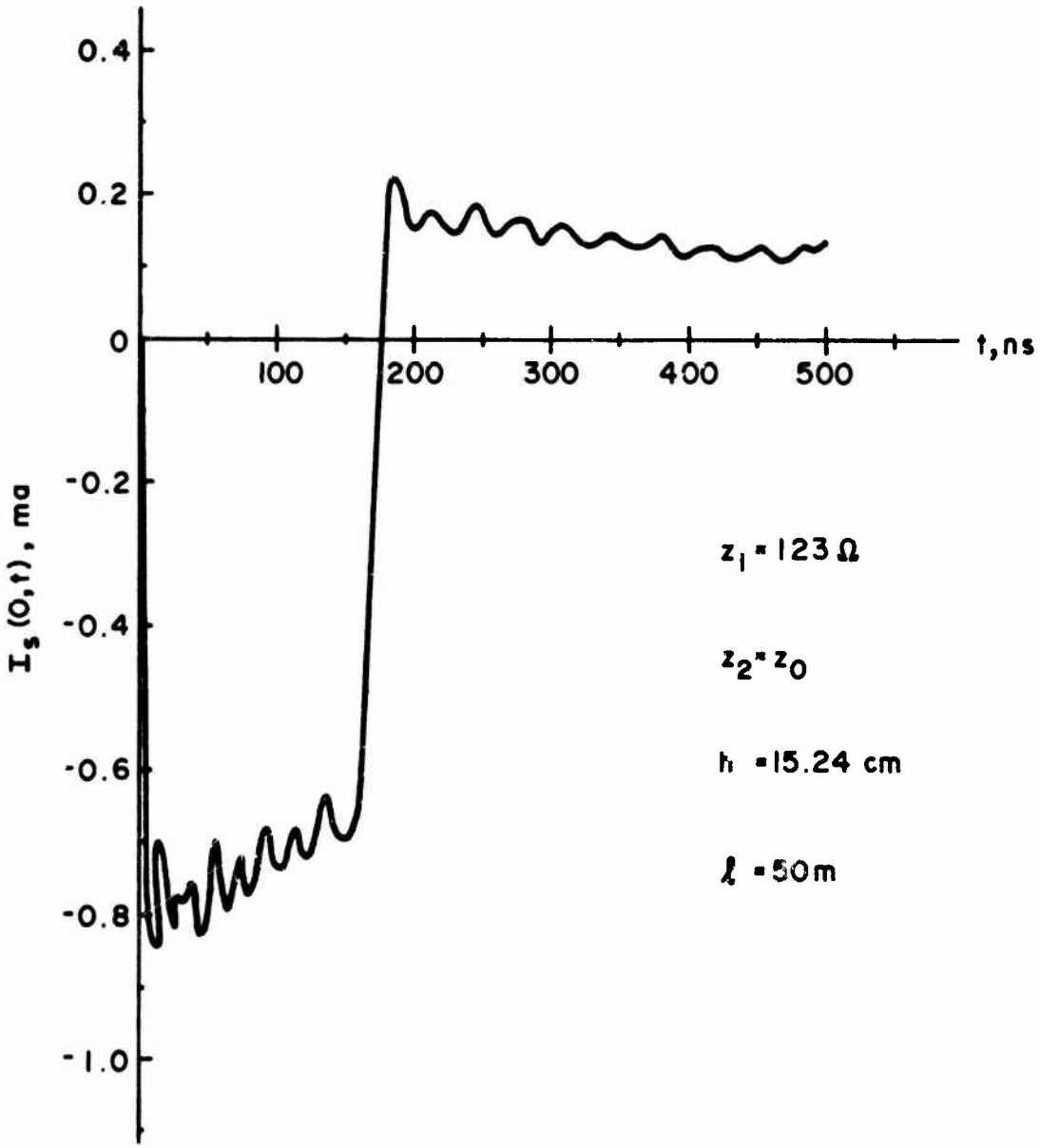

Fig. B.13 TRANSIENT WAVEFORM WHEN SHEATH LOADING IS NOT MATCHED ($z_1 = 123\ \Omega$)

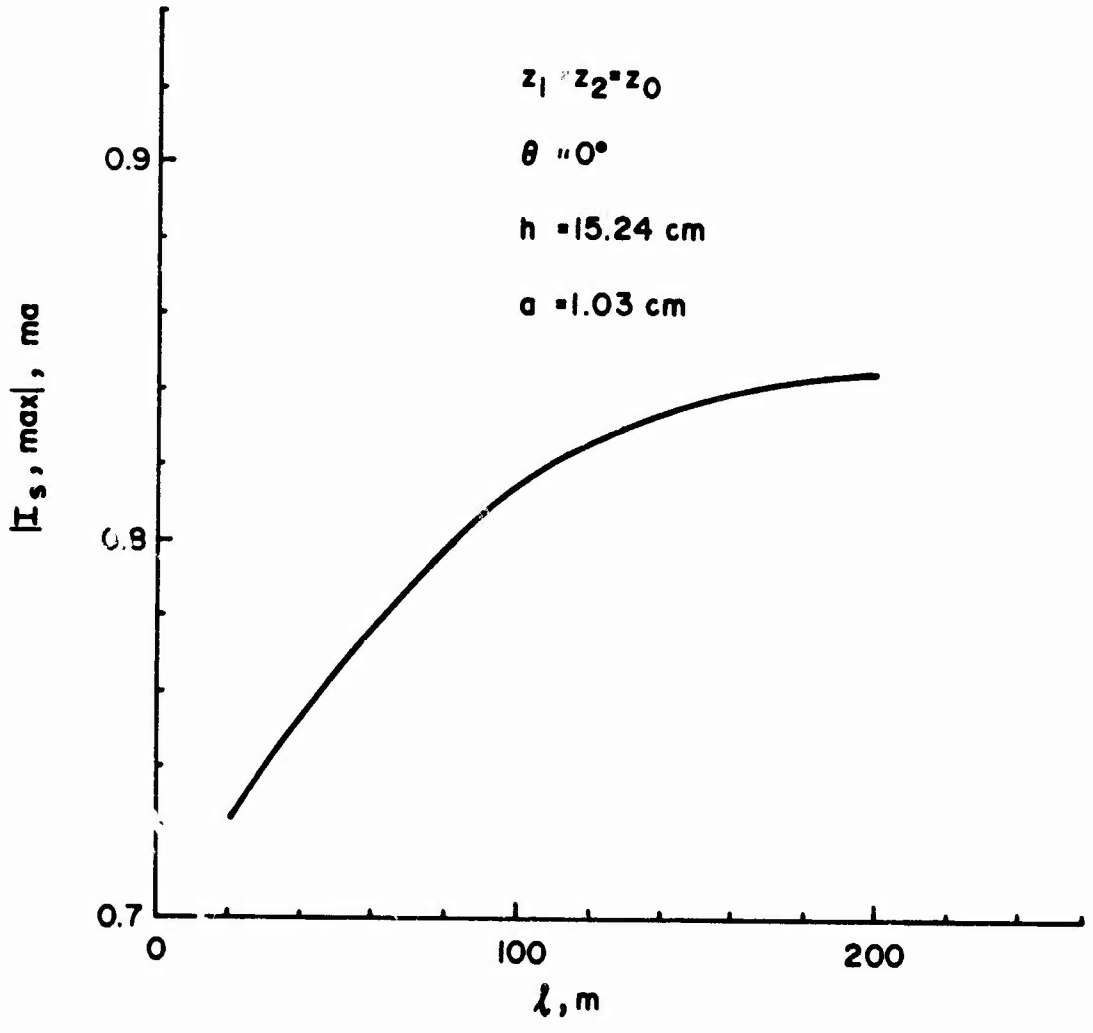

Fig. B.14 EFFECT OF LARGER DIAMETER ON PEAK SHEATH CURRENT

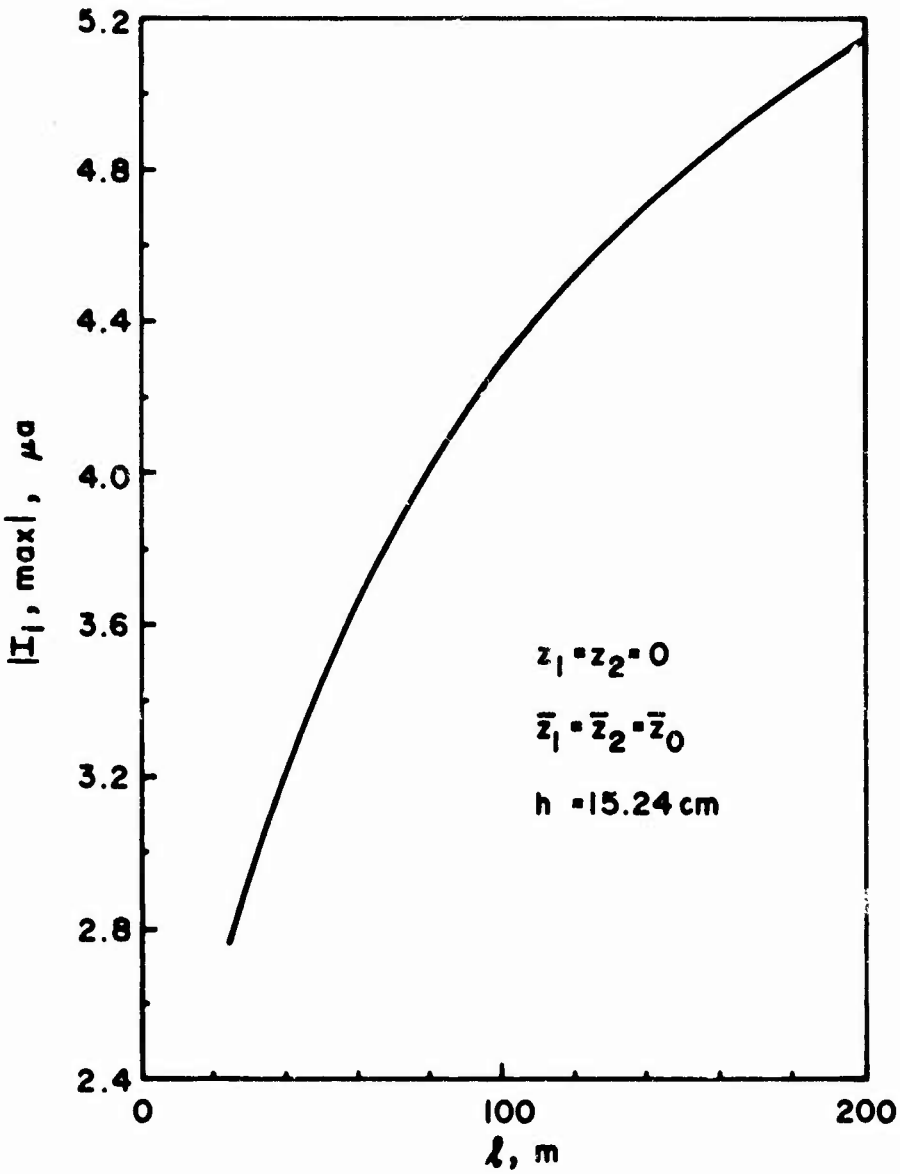

Fig. B.15 PEAK CORE CURRENT AS A FUNCTION OF CABLE LENGTH FOR A HORIZONTAL CABLE

Like the sheath current, the core current increases as the cable length increases. However, it should be noted that the entire waveform of the core current is much different from that of the sheath current. Plotted in Figures B.16 and B.17 are the responses of the core current for cable lengths of 25 and 50 meters respectively. It is interesting to see that the pulse waveform exhibits no zero-crossing until the very late time, as indicated in the figures.

Height

Figure B.18 shows the core current at $x = 0$, as a function of cable height, which would result from a cable with core-to-inner shield load impedances matched at $x = \ell$ and shorted at $x = 0$. The cable shields are assumed to be matched at both ends, and the cable length is taken to be 50 meters long. As would be expected, the core current increases linearly with respect to the height. The response waveforms in this case do show a zero crossing at about 265 nanoseconds in the early time, as shown in Figures B.19 and B.20. The reason for the difference in waveforms between Figures B.17 and B.19 is most probably due to the multiple reflections from the different loads used in the calculations.

Load Impedances

Shown in Figure B.21 are the peak core current plots as a function of the core-to-inner shield load, $\overline{Z}_2$, at $x = \ell$, when the load at the other end of the cable $\overline{Z}_1$ is shorted. Both core currents at $x = 0$ and $x = \ell$ are shown in the figure. In either case, the 50 ohm cable suspended at a height of 15.24 cm above the conducting plane is taken to be 50 meters in length and the outer shield-to-ground impedances, Z_1 and Z_2, are shorted.

The peak current plots of Figure B.21 show an increase in core current at $x = \ell$, as the core-to-inner shield load $\overline{Z}_2$ is decreased. The peak core current at $x = 0$, however, shows only a slight change as $\overline{Z}_2$ is changed. Examination of the calculated results also reveals that the response waveform, in general, is sensitive to a change in load impedance, $\overline{Z}_2$. This is clearly shown in the plots of core currents at $x = 0$ in Figures B.22 and B.23.

The current in a matched load at one end of a cable is greater if the other end of the cable is terminated in a short circuit, as in Figure B.21, than if the other end is also terminated in a matched load, as in Figure B.15.

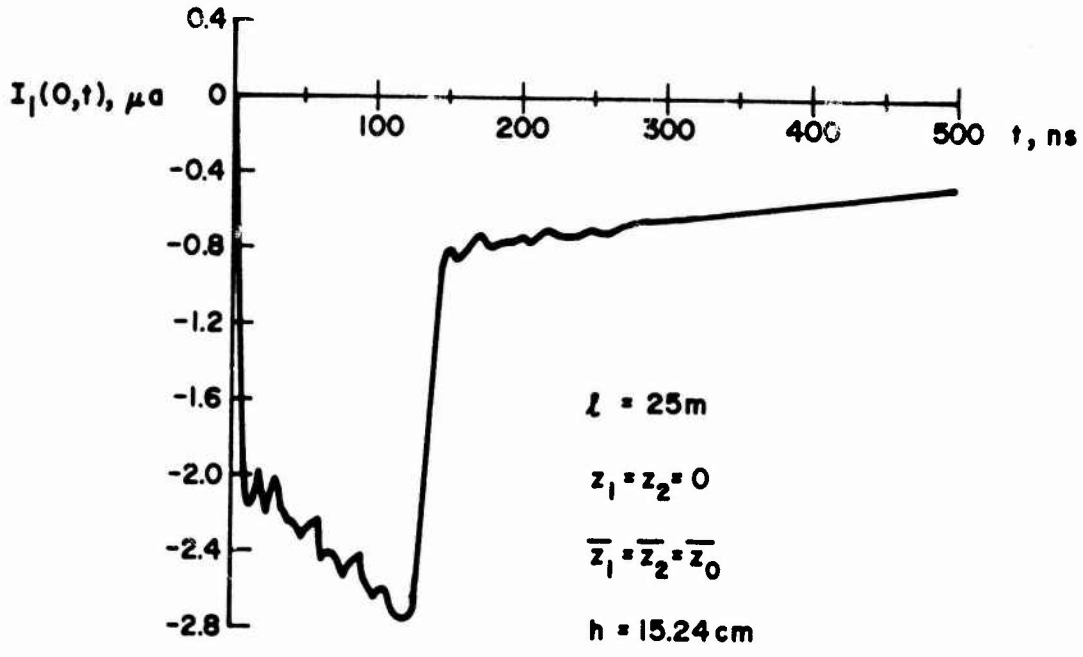

Fig. B.16 TRANSIENT CORE CURRENT FOR A 25 METER HORIZONTAL CABLE

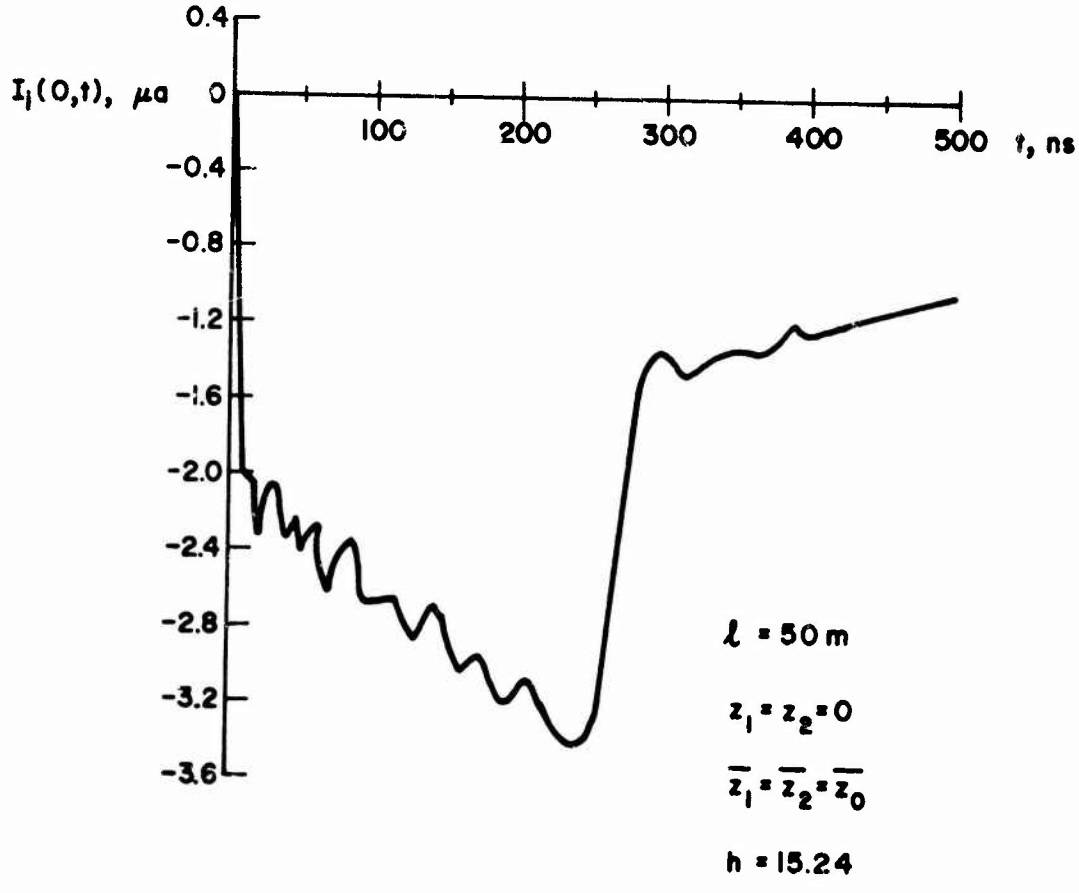

Fig. B.17 TRANSIENT CORE CURRENT FOR A 50 METER HORIZONTAL CABLE

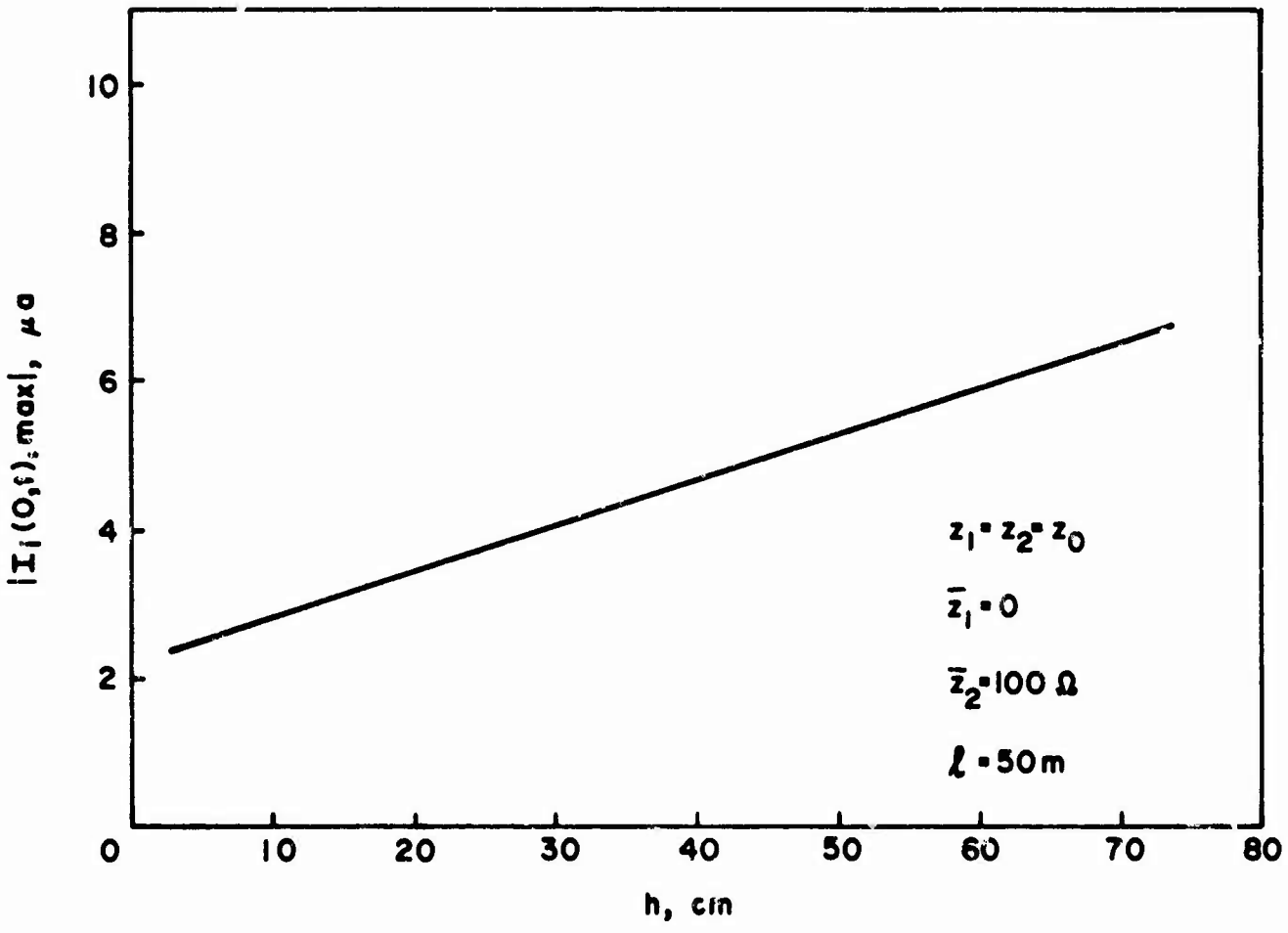

Fig. B.18 PEAK CORE CURRENT AS A FUNCTION OF HEIGHT FOR A HORIZONTAL CABLE

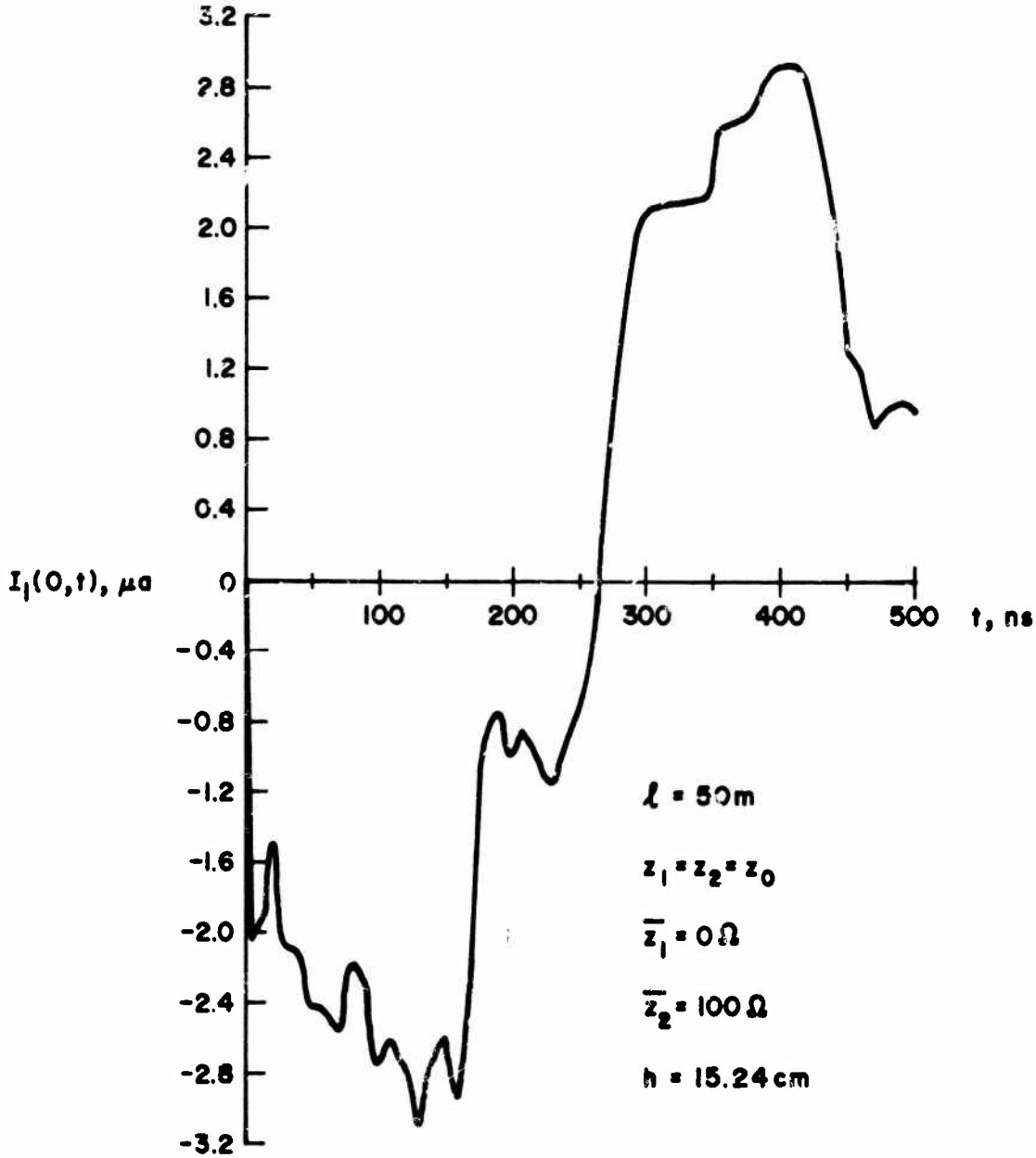

Fig. B.10 CORE CURRENT WAVEFORM FOR A HORIZONTAL CABLE 6 INCHES ABOVE A CONDUCTING PLANE

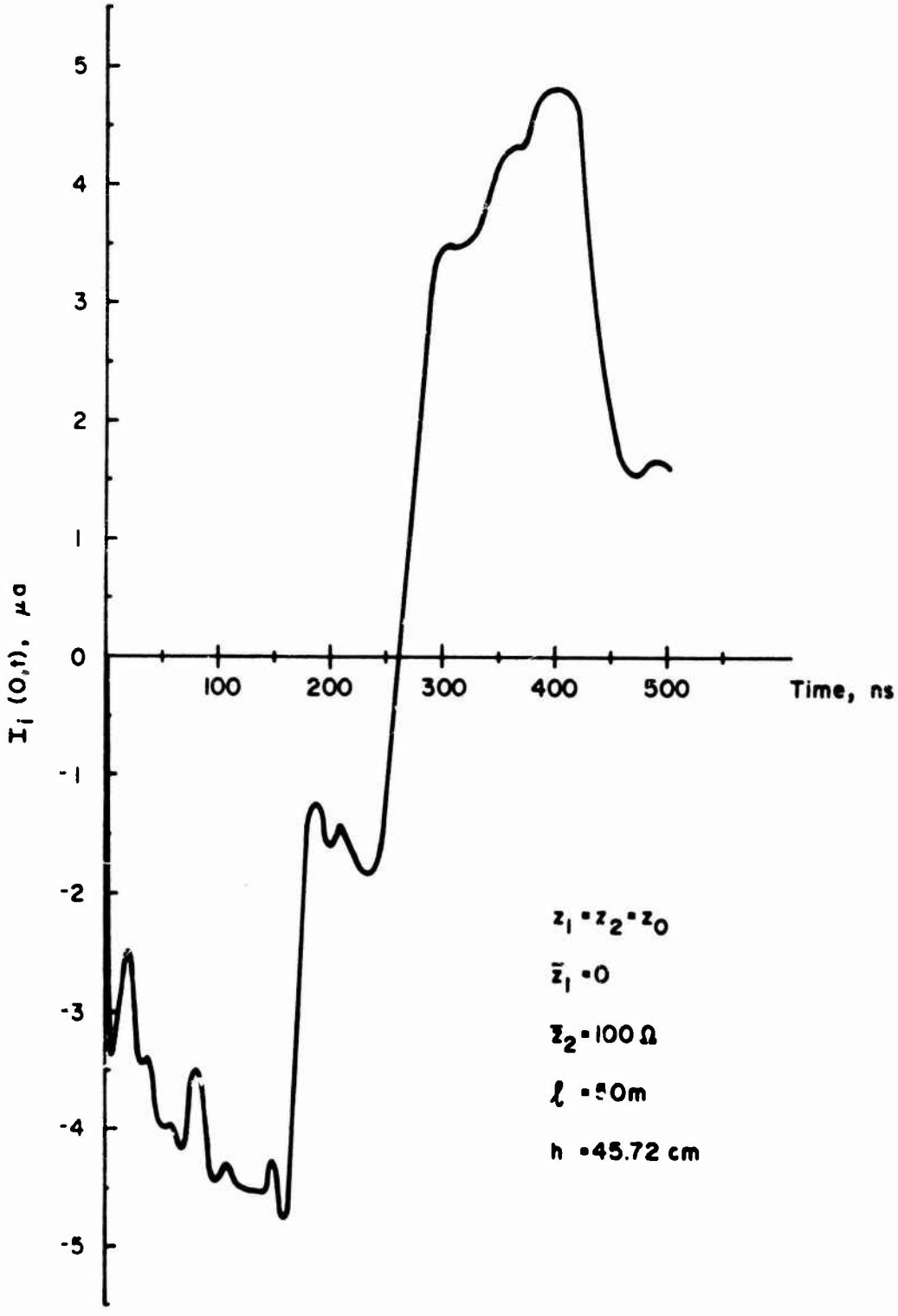

Fig. B.20 CORE CURRENT WAVEFORM FOR A HORIZONTAL CABLE 12 INCHES ABOVE A CONDUCTING PLANE

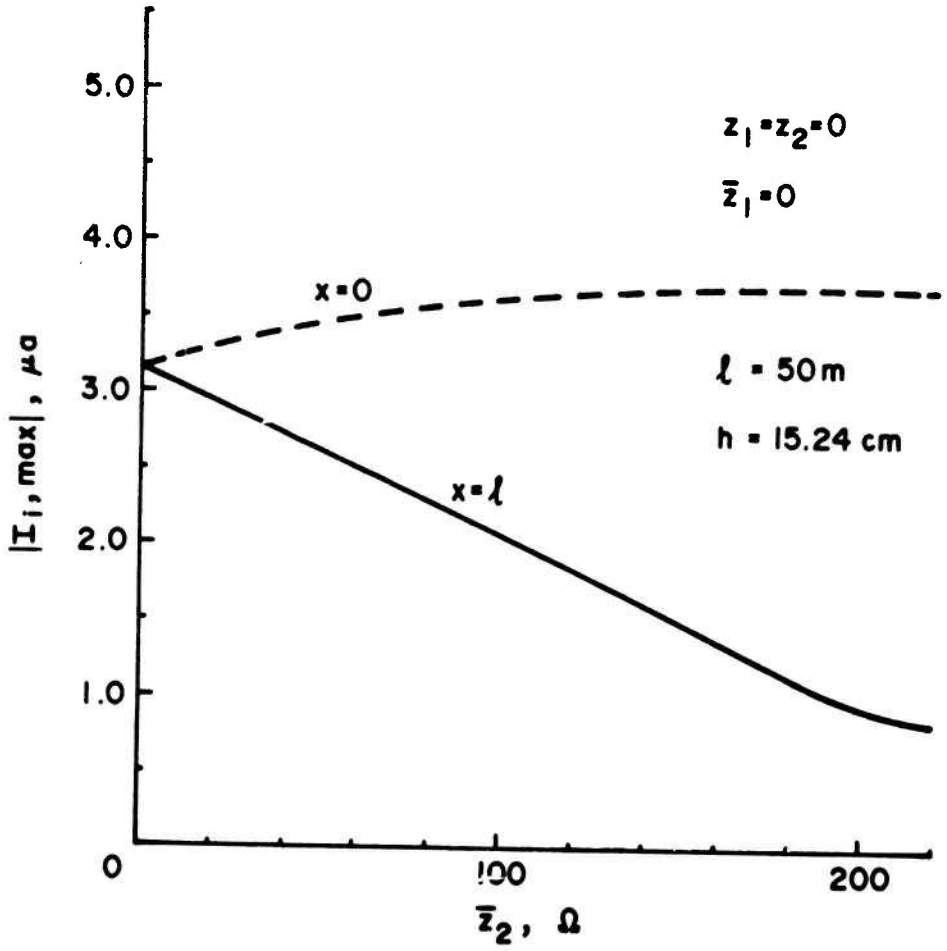

Fig. B.21 PEAK CORE CURRENT AS A FUNCTION OF LOAD IMPEDANCE FOR A HORIZONTAL CABLE

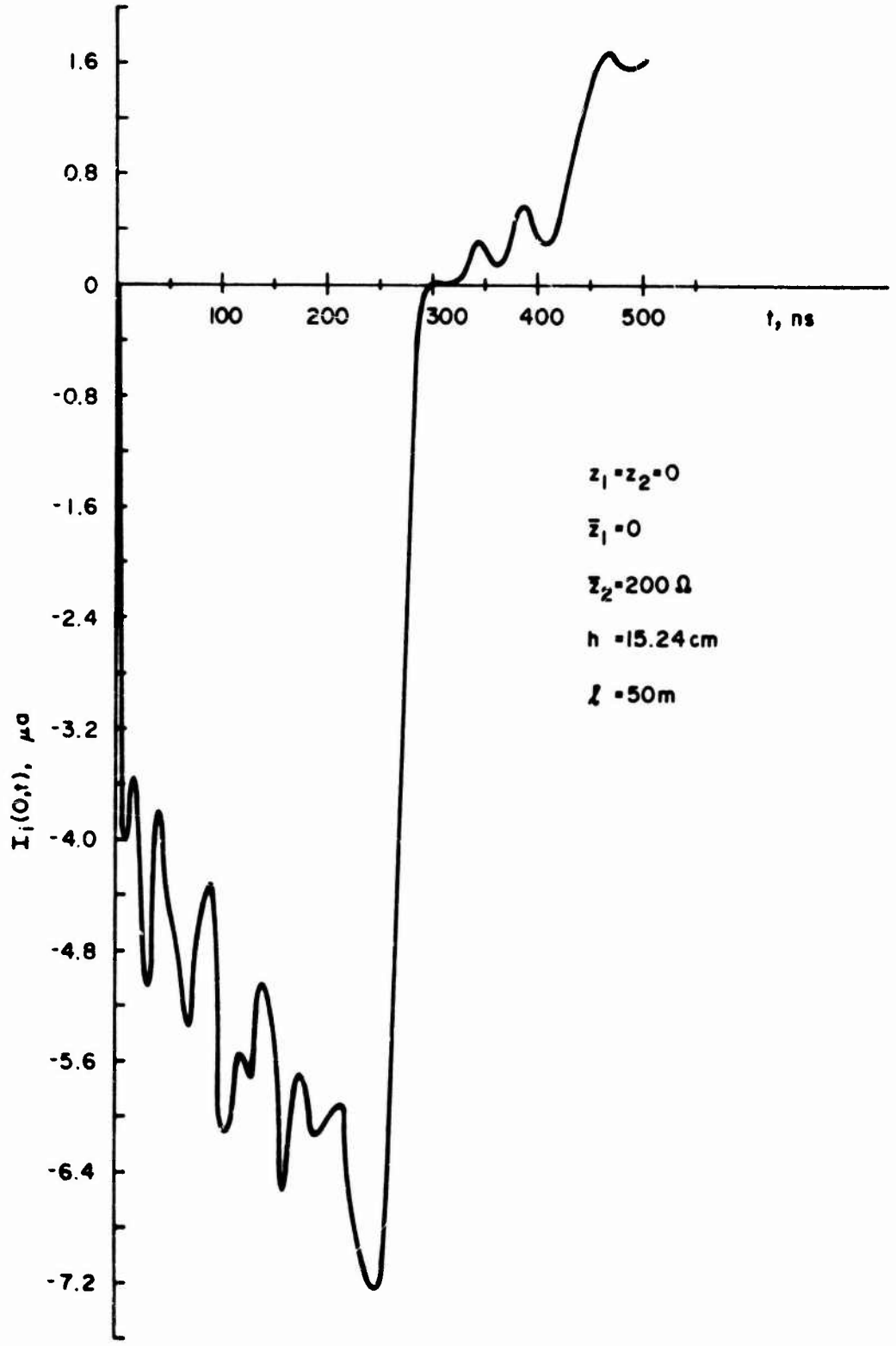

Fig. B.22 CORE CURRENT WAVEFORM FOR A LOAD GREATER THAN THE CHARACTERISTIC IMPEDANCE

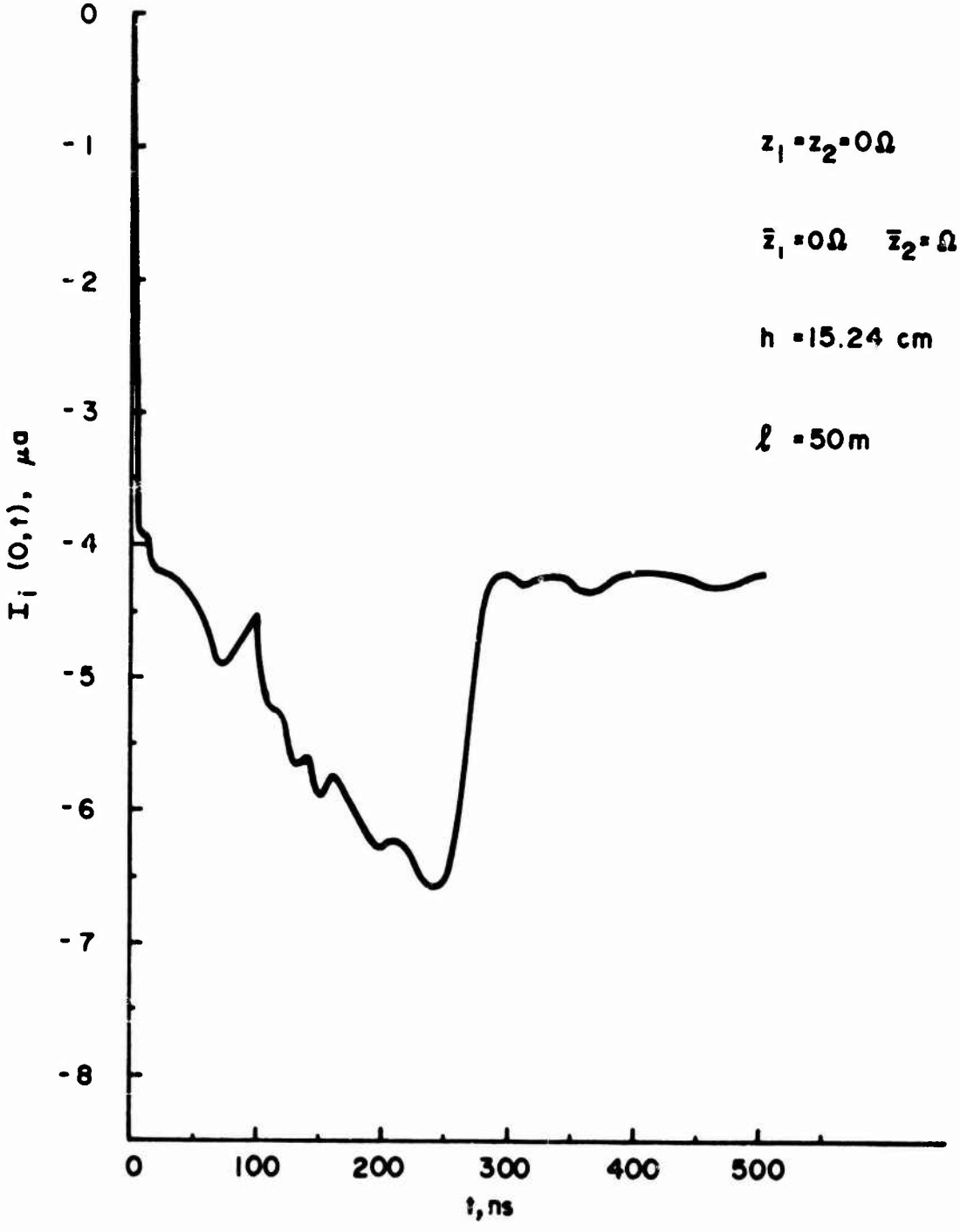

Fig. B.23 CORE CURRENT WAVEFORM FOR A LOAD LESS THAN THE CHARACTERISTIC IMPEDANCE

DISTRIBUTION

Copies

Director
Telecommunications & Command & Control
Systems
Washington, D. C. 20301
ATTN: Dep. Dir. (Command & Control)

Assistant to the Secretary of Defense
(Atomic Energy)
Washington, D. C. 20301
ATTN: Document Control

Commander in Chief, Pacific, JCS
Pentagon, Room 2E873
Washington, D. C. 20310
ATTN: J30S, Box 13

Director
Defense Advanced Research Projects Agency
Architect Building
1400 Wilson Boulevard
Arlington, Virginia 22209
ATTN: Dr. G. H. Heilmeir

Director
Defense Civil Preparedness Agency
Washington, D. C. 20301
ATTN: TS(AED), Room 1C 535

Science Advisor
Third Fleet
FPO San Francisco, California 96610
ATTN: Mr. M. Baldwin

Defense Communication Engineer Center
1860 Wiehele Avenue
Reston, Virginia 22070
ATTN: H620, Mr. A. L. Izzo

1

	Copies
Director Defense Communications Agency Washington, D. C. 20305 ATTN: Asst. to Ch. Scientist for Survivability	
Defense Documentation Center Cameron Station Alexandria, Virginia 22314 ATTN: TC	12
Director Defense Intelligence Agency Washington, D. C. 20301 ATTN: DI-7D, Mr. Edward O'Farrell	
Director Defense Nuclear Agency Washington, D. C. 20305 ATTN: APTL, Technical Library ATTN: Dep. Dir. for Science & Technology; Robert Poll ATTN: Radiation Dir., COL Richard S. Numbers ATTN: Vulnerability Dir., Eugene C. LaVier	2
Director of Defense Research & Engineering Washington, D. C. 20301 ATTN: Dep. Dir. (Res. & Adv. Tech.) John L. Allen ATTN: Dep. Dir. (Tactical Warfare Programs) Mr. C. Robert Wieser ATTN: Dep. Dir. (Strategic & Space Systems) ATTN: Dep. Dir. (Test & Evaluation)	
Commander Field Command Defense Nuclear Agency Kirtland Air Force Base Albuquerque, New Mexico 87115 ATTN: FCTA-E ATTN: FCSM-A	
Interservice Nuclear Weapons School Kirtland Air Force Base Albuquerque, New Mexico 87115 ATTN: Document Control	

Copies

Director
Joint Strategic Target Planning Staff, JCS
Offutt Air Force Base
Omaha, Nebraska 68113
ATTN: JSAS, Major Baran

Chief
Livermore Division, Field Command, DNA
Lawrence Livermore Laboratory
Box 808
Livermore, California 94550
ATTN: Document Control for L-395

National Communications System
Office of the Manager
Washington, D. C. 20305
ATTN: NCS-TS, Mr. Dennis Bodson

Director
National Security Agency
Fort Meade, Maryland 20755
ATTN: O. O. Van Gunten, R-425

Chairman
Office of Joint Chiefs of Staff
Washington, D. C. 20301
ATTN: Director J-6 (Communications - Electronics)
ATTN: J-5, Plans & Policy, R&D Division

Weapons Systems Evaluation Group
400 Army-Navy Drive
Washington, D. C. 20305
ATTN: Document Control

Director
Ballistic Missile Defense Program Office
1300 Wilson Boulevard
Arlington, Virginia 22209
ATTN: CRDABM-NE, Dr. John Jamison

Assistant Chief of Staff for Communications-Electronics
Department of the Army
Washington, D. C. 20314
ATTN: CEEO-7, Mr. Wesley T. Heath, Jr.

Copies

Chief of Research & Development
Department of the Army
Washington, D. C. 20310
ATTN: DARD-DDM-N, LTCOL J. P. Goncz

Commander
Frankford Arsenal
Bridge and Tacony Streets
Philadelphia, Pennsylvania 19137
ATTN: N5000, Marvin Elnick

Commander
Harry Diamond Laboratories
Washington, D. C. 20438
ATTN: AMXDO-EM, Mr. Ron Bostak,
Chief Lab 1000
ATTN: AMXDO-NP, Mr. F. Wimenitz,
Chief, NWEPO
ATTN: AMXDO-TI, Technical Library
ATTN: AMXDO-RB, Dr. E. E. Conrad,
Chief Lab 200

Commander
Picatinny Arsenal
Dover, New Jersey 07801
ATTN: SMUPA-ND-C-S, Dr. Amina Nordio

Commander
Safeguard Communications Agency
Special Scientific Activities Directorate
Fort Huachuca, Arizona 85613
ATTN: ACCX-SAT-EMP

Commander
U.S. Army Aberdeen Research & Development Center
Aberdeen Proving Ground, Maryland 21005
ATTN: AMXRD-XSE for AMXRD-BVL, J. H. McNeilly

Director
Ballistic Missile Defense Advanced Technology
Center
P. O. Box 1500
Huntsville, Alabama 35807
ATTN: Chris H. Horgen

Commander
U.S. Army Communications Command
Combat Development Division
Fort Huachuca, Arizona 85613
ATTN: USACC-EF-C, EMP

Copies

Commander
U.S. Army Computer Systems Command
Fort Belvoir, Virginia 22060
ATTN: CSCS-TME-R, Mr. E. T. Parker

Commander
U.S. Army Electronics Command
Fort Monmouth, New Jersey 07703
ATTN: AMSEL-TL-IR, Dr. Edwin T. Hunter
ATTN: AMSEL-TN-N, Dr. E. Both
ATTN: AMSEL-TL-NS, R. Freiberg

Commander
U.S. Army Electronics Proving Ground
Fort Huachuca, Arizona 85613
ATTN: STEEP-MT-M, Mr. Durbin

Commander
U.S. Army Foreign Science & Technology Center
220 7th Street, N.E.
Charlottesville, Virginia 22901
ATTN: AMXST-TDI, Dr. P. A. Crowley

Commander
U.S. Army Mobility Equipment R&D Center
Fort Belvoir, Virginia 22060
ATTN: STSFB-RN, D. B. Dinger

Commander
U.S. Army Nuclear Agency
Fort Bliss, Texas 79916
ATTN: ATCN-W

Commander
U.S. Army Strategic Communications Command
Fort Huachuca, Arizona 85613
ATTN: Safeguard Communications Agency, J. McAdoo

Project Manager
U.S. Army Tactical Data Systems, AMC
Fort Monmouth, New Jersey 07703
ATTN: AMCPN-TDS-TF

Assistant Secretary of the Navy
(Research & Development)
Washington, D. C. 20301
ATTN: H. Sonnemann (Spec. Asst. - Electronics)
ATTN: Dr. S. Koslov (Spec. Asst. - Research)
ATTN: Dr. P. Waterman (Spec. Asst. - Systems)

Copies

Commander
White Sands Missile Range
White Sands, New Mexico 88002
ATTN: STEWS-TE-NT, Mr. Marvin P. Squires

Chief of Naval Operations
Department of the Navy
Washington, D. C. 20350
ATTN: OP-622C, Robert Piacesi
ATTN: OP-985F, CAPT L. Warner
OP-985F, LCDR N. Gee

Chief of Naval Research
Department of the Navy
800 North Quincy Street
Arlington, Virginia 22217
ATTN: Code 418, Dr. T. P. Quinn

Commander
Naval Air Systems Command
Headquarters
Washington, D. C. 20360
ATTN: AIR 360G
ATTN: AIR 350
ATTN: AIR 52023
ATTN: AIR 52022
ATTN: AIR 533D3
ATTN: Technical Library

Commanding Officer
Naval Ammunition Depot
Crane, Indiana 47522
ATTN: Code 7024, Mr. James L. Ramsey

Chief of Naval Material
Department of the Navy
Washington, D. C. 20360
ATTN: NMAT 0323
ATTN: NMAT 03L
ATTN: NMAT 0312
ATTN: CNM-PM-20-3

Commander
Naval Communications Command
Naval Communications Command Headquarters
4401 Massachusetts Avenue, N.W.
Washington, D. C. 20390
ATTN: N-7, LCDR Hall

Copies

Commander
Naval Electronic Systems Command
Headquarters
Washington, D. C. 20360
ATTN: ELEX 095
ATTN: PME 117-215A, Dr. Brunhart
ATTN: ELEX 304, J. Cauffman
ATTN: Code 530
ATTN: PME 117-21
ATTN: PME 106, R. Dyson
ATTN: ELEX 5032
ATTN: ELEX 501
ATTN: ELEX 510133
ATTN: Technical Library

Commander
Naval Electronics Laboratory Center
San Diego, California 92152
ATTN: Technical Library
ATTN: Leo Johnson

Commanding Officer
Naval Intelligence Support Center
4301 Suitland Road
Washington, D. C. 20390
ATTN: Dr. P. Alexander
ATTN: NISC-30
ATTN: Technical Library

Superintendent
Naval Postgraduate School
Monterey, California 93940
ATTN: Code 2124, Technical Reports Librarian

Director
Naval Research Laboratory
Washington, D. C. 20390
ATTN: Code 4004, Dr. E. L. Brancato
ATTN: Dr. G. Seigel
ATTN: Technical Library

Commander
Naval Ship Engineering Center
Hyattsville, Maryland 20782
ATTN: Code 6174D, Edward F. Duffy
ATTN: Code 6105D, Robert E. Fuss
ATTN: Technical Library

Copies

Commander
Naval Sea Systems Command
Washington, D. C. 20362
ATTN: Code SEA 06T
ATTN: Code SEA 0333
ATTN: Code SEA 9931
ATTN: Code SEA 030
ATTN: Code SEA 03412
ATTN: Code SEA 09G32

Commander
Naval Weapons Center
China Lake, California 93555
ATTN: Code 753, Technical Library

Commanding Officer
Naval Weapons Evaluation Facility
Albuquerque, New Mexico 87117
ATTN: L. Oliver

Commanding Officer
Navy Astronautics Group
Box 30
Point Mugu, California 93042
ATTN: Mr. T. Smith

Commanding Officer
Naval Missile Center
Point Mugu, California 93042
ATTN: Norbert Tackman

Director
Strategic Systems Project Office
Department of the Navy
Washington, D. C. 20390
ATTN: SP-234, R. Coleman
ATTN: NSP-27201, LCDR L. Stoessl
ATTN: SP-2701, Mr. John W. Pitsenberger, Br. Eng.

Commander-in-Chief
U.S. Atlantic Fleet
Norfolk, Virginia 23511
ATTN: Document Control

Copies

Naval Weapons Engineering Support Activity
Washington Navy Yard
Washington, D. C. 20390
ATTN: E.S.A. 70

Commander
U.S. Naval Coastal Systems Laboratory
Panama City, Florida 32401
ATTN: Code 771, Mr. E. T. Parker

Commander-in-Chief
U.S. Pacific Fleet
FPO San Francisco, California 96610
ATTN: Document Control, 303

AF Cambridge Research Laboratories, AFSC
Hanscom Field
Bedford, Massachusetts 01730
ATTN: LQD, Mr. Russel P. Dolan, Jr.

Commanding Officer
Nuclear Weapons Training Center, Pacific
Naval Air Station, North Island
San Diego, California 92135
ATTN: Code 50

AF Weapons Laboratory, AFSC
Kirtland Air Force Base
New Mexico 87117
ATTN: SUL, Technical Library
ATTN: DYX, Dr. Donald C. Wunsch

Air Force Avionics Laboratory, AFSC
Wright-Patterson Air Force Base
Ohio 45433
ATTN: AFAL, TEA, Mr. Robert Conklin

Headquarters
Electronic Systems Division, AFSC
L. G. Hanscom Field
Bedford, Massachusetts 01730
ATTN: XRE, Survivability

Commander
Rome Air Development Center, AFSC
Griffiss Air Force Base, New York 13440
ATTN: RBRP, Mr. J. S. Smith

Space & Missile Systems Organization
Box 92960 WWPC
Los Angeles, California 90009
ATTN: SKT, Peter H. Stadler

Copies

Assistant General Manager for Military Application
Energy Research Development Agency
U. S. Atomic Energy Commission
Washington, D. C. 20545
ATTN: LTCOL Donald C. Little

Los Alamos Scientific Laboratory
P. O. Box 1663
Los Alamos, New Mexico 87544
ATTN: Document Control for J-8

Sandia Laboratories
Kirtland Air Force Base
New Mexico 87115
ATTN: Document Control for Technical Library

Sandia Laboratories
Livermore Laboratory
Box 969
Livermore, California 94550
ATTN: J. A. Mogford, Div. 8341

Union Carbide Corporation
Oak Ridge National Laboratory
P. O. Box X
Oak Ridge, Tennessee 37830
ATTN: Dr. D. B. Nelson

University of California
P. O. Box 808
Livermore, California 94551
ATTN: L-3, Technical Information Department

Central Intelligence Agency
Washington, D. C. 20505
ATTN: Dr. Carl Miller

Department of Commerce
National Bureau of Standards
Washington, D. C. 20234
ATTN: Judson C. French, Chief, Electron Tech. Div.

Aerojet Electro-Systems Co. Div.
Aerojet-General Corporation
Box 296
Azusa, California 91702
ATTN: Thomas D. Hanscome, B170, D6711

Copies

Aerojet Energy Conversion Company
Aerojet Liquid Rocket Compa
Box 13222
Sacramento, California 95813
ATTN: Technical Information Center

Aerospace Corporation
P. O. Box 92957
Los Angeles, California 90009
ATTN: Library

Agbabian Jacobsen Associates
8939 South Sepulveda Boulevard
Los Angeles, California 90045
ATTN: Mary Casey

Analog Technology Corporation
3410 East Foothill Boulevard
Pasadena, California 91107
ATTN: John Joseph Baum

Avco
Government Products Group
201 Lowell Street
Willington, Massachusetts 01887
ATTN: Research Library, A680, Rm. 2201

Battelle Memorial Institute
505 King Avenue
Columbus, Ohio 43201
ATTN: Richard K. Thatcher

Bell Aerospace Company
Division of Textron, Inc.
Box 1
Buffalo, New York 14240
ATTN: Carl B. Schoch, Wpns. Effects, M.S. I-85

Bell Telephone Laboratories, Inc.
Mountain Avenue
Murray Hill, New Jersey 07974
ATTN: E. C. Snyder, Rm. WH-2B-170

The Bendix Corporation
Communication Division
Joppa Road
Baltimore, Maryland 21204
ATTN: Document Control

Copies

The Bendix Corporation
Research Laboratories Division
Bendix Center
Southfield, Michigan 48075
ATTN: Manager, Program Development

Bechtel Power Corporation
P. O. Box 60860
Los Angeles, California 90060
ATTN: Proj. Mgr., Gov. Projects,
H. L. Dietz

The Bendix Corporation
Navigation & Control Division
Teterboro, New Jersey 07608
ATTN: Dr. E. O. Stoll, Dept. 7111

The Bendix Corporation
Aerospace Systems Division
3300 Plymouth Road
Ann Arbor, Michigan 48017

Booz-Allen & Hamilton, Inc.
4733 Bethesda Avenue
Bethesda, Maryland 20014
ATTN: R. W. Shrader

The Boeing Company
P. O. Box 3999
Seattle, Washington 98124
ATTN: Aerospace Library

Booz-Allen & Hamilton, Inc.
106 Apple Street
New Shrewsbury, New Jersey 07724
ATTN: R. J. Chrisner

Braddock, Dunn & McDonald, Inc.
P. O. Box 8441
Albuquerque, New Mexico 87108
ATTN: Robert B. Buchanan

Brown Engineering Company, Inc.
Huntsville, Alabama 35807
ATTN: Tech. Library, M.S. 12, P. Shelton

Burroughs Corporation
Federal & Special Systems Group
Box 517
Paoli, Pennsylvania 29301
ATTN: S. E. Gluck

Copies

Charles Stark Draper Laboratory, Inc.
68 Albany Street
Cambridge, Massachusetts 01239
ATTN: Dr. Richard G. Haltmaier

Cincinnati Electronics Corporation
26309 Glendale-Milford Road
Cincinnati, Ohio 45241
ATTN: Lois Hammond

Collins Radio Company
5225 C Avenue, N.W.
Cedar Rapids, Iowa 52406
ATTN: M. Lahr, Librarian, Bldg. 106-216

Communications Satellite Corporation
950 L'Enfant Plaza South, S.W.
Washington, D. C. 20024
ATTN: Richard A. Arndt

Computer Sciences Corporation
P. O. Box 530
Falls Church, Virginia 22046
ATTN: Peter K. Carleston

Cutler-Hammer, Inc.
AIL Division
Comac Road
Deer Park, New York 11729
ATTN: Central Technical Files, Anne Anthony

The Dikewood Corporation
1009 Bradbury Drive, S.E.
Albuquerque, New Mexico 87106
ATTN: L. Wayne Davis

E-Systems, Inc.
Greenville Division
Major Field, Box 1056
Greenville, Texas 75401
ATTN: Library 8-51910

Effects Technology, Inc.
3383 Helister Avenue
Santa Barbara, California 93105
ATTN: Edward John Steele

EG&G, Inc.
Albuquerque Division
Box 4339
Albuquerque, New Mexico 87106
ATTN: Hilda H. Hoffman

Copies

Electronic Communications, Inc.
Subsidiary of NCR
Box 12248
Saint Petersburg, Florida 33733
ATTN: J. T. Daniel, M.S. 9

Energy Sciences, Inc.
111 Terrace Hall Avenue
Burlington, Massachusetts 01803
ATTN: Dr. Sam V. Nablo

Fairchild Camera & Instrument Corporation
464 Elles Street
Mountain View, California 94040
ATTN: Security Dept. for 2-233, Mr. David K. Myers

Fairchild Industries, Inc.
Sherman Fairchild Technology Center
Fairchild Drive
Germantown, Maryland 20767
ATTN: William Metzger

The Franklin Institute
20th Parkway
Philadelphia, Pennsylvania 19103
ATTN: Ramie H. Thompson

Garrett Corporation
9851 Sepulveda Boulevard
Los Angeles, California 90009
ATTN: Robert Weir, Dept. 93-9

General Dynamics Corp.
Electronics Division
Box 80877
San Diego, California 92138
ATTN: 7-11, Space Electronics Design, R. E. Fixsen

General Electric Company
816 State Street
Santa Barbara, California 93102
ATTN: DASIAC, W. Alfonte

General Electric Company
Re-Entry & Environmental Systems Division
P. O. Box 7722
Philadelphia, Pennsylvania 19101
ATTN: Robert V. Benedict

Copies

General Physics Corporation
1000 Century Plaza Building
Columbia, Maryland 21043
ATTN: Robert W. Deutsch

General Research Corporation
1501 Wilson Boulevard
Arlington, Virginia 22209
ATTN: Paul J. Kramer

Georgia Institute of Technology
Office of Research Administration
Atlanta, Georgia 30332
ATTN: Res. & Sec. Coordinator for Mr. Hugh Denny

Goodyear Aerospace Corporation
Arizona Division
Litchfield Park, Arizona 85340
ATTN: Mr. B. Manning

GTE Sylvania, Inc.
Electronics Systems Group, Eastern Division
77 A Street
Needham, Massachusetts 02194
ATTN: Librarian, Mr. C. Thornhill

Harris Corporation
Electronic Systems Division
P. O. Box 37
Melbourne, Florida 32902
ATTN: A. M. Gowen

Hazeltine Corporation
Pulaski Road
Greenlawn, New York 11740
ATTN: J. B. Colombo

Honeywell Incorporated
Aerospace Division
13350 U. S. Highway 19
St. Petersburg, Florida 33733
ATTN: Harrison H. Noble, Staff Engineer, M.S. 725-5A

Honeywell Incorporated
Radiation Center
2 Forbes Road
Lexington, Massachusetts 02174
ATTN: Technical Library

Copies

Hughes Aircraft Company
Centinela Avenue and Teale Streets
Culver City, California 90230
ATTN: R&D Div., Dr. John Singletary, M.S. D157

Illinois Institute of Technology
Chicago, Illinois 60616
ATTN: Professor E. Weber

IIT Research Institute
10 West 35th Street
Chicago, Illinois 60616
ATTN: Mr. Jack E. Bridges
ATTN: I. Mindel
ATTN: T. Martin 6

IIT Research Institute
Electromagnetic Compatability Analysis Center
North Severn-Ecac Building
Annapolis, Maryland 21402
ATTN: ACOAT

Institute for Defense Analyses
400 Army-Navy Drive
Arlington, Virginia 22202
ATTN: Classified Library

Intelcom Rad Tech
P.O. Box 80817
San Diego, California 92117
ATTN: James A. Naber
ATTN: Eric Wenaas

International Business Machines Corporation
Route 170
Owego, New York 13827
ATTN: Mr. Fred C. Tietze, Dept. L 99, Bldg. 002A

International Telephone & Telegraph Corporation
492 River Road
Nutley, New Jersey 07110
ATTN: Defense Space Group, SMTS, Frank Johnson
ATTN: Defense Space Group, J. Gulack
ATTN: Avionic Division, Alexander Richardson

ION Physics Corporation
South Bedford Street
Burlington, Massachusetts 01803
ATTN: Dr. H. Milde

Copies

Johns Hopkins University
Applied Physics Laboratory
8621 Georgia Avenue
Silver Spring, Maryland 20910
ATTN: Leroy Walters, Jr.

Kaman Sciences Corporation
1700 Garden of the Gods Road
Colorado Springs, Colorado 80907
ATTN: Dr. W. Ware

Litton Systems, Inc.
5500 Conoga Avenue
Los Angeles, California 91364
ATTN: Mr. Sam Sternbach, Data Systems Division

Litton Systems, Inc.
8000 Woodley Avenue
Van Nuys, California 91409
ATTN: Dr. Val J. Ashby, Bldg. 31, M.S. 67
ATTN: J. F. Fischer, Jr., Data Systems Division

Litton Systems, Inc.
Electron Tube Division
1035 Westminster Drive
Williamsport, Pennsylvania 17701
ATTN: Frank J. McCarthy

Litton Systems, Inc.
AMECOM Division
5115 Calvert Road
College Park, Maryland 20740
ATTN: David Segerson

Lockheed Missiles & Space Company, Inc.
3257 Hanover Street
Palo Alto, California 94304
ATTN: G. F. Heath, D/81-14 B/154
ATTN: Dr. Clarence F. Kooi, Dept. 52-11, Bldg. 204, LMSCPA

LTV Aerospace Corporation
Vought Systems Division
Box 6267
Dallas, Texas 75222
ATTN: Technical Data Center

LTV Aerospace Corporation
Michigan Division
Box 909
Warren, Michigan 48090
ATTN: Mr. T. M. Rozelle

Copies

M.I.T. Lincoln Laboratory
P. O. Box 73
Lexington, Massachusetts 02173
ATTN: Leona Loughlin, Librarian

Martin Marietta Aerospace
Orlando Division
P. O. Box 5837
Orlando, Florida 32805
ATTN: Eng. Library, Mrs. Mona C. Griffith, Lib., MP-30

Martin Marietta Corporation
Denver Division
Box 179
Denver, Colorado 80201
ATTN: Research Library, 6617, J. R. McKee

Maxwell Laboratories, Inc.
9244 Balboa Avenue
San Diego, California 92123
ATTN: Dr. A. Kolb
ATTN: Dr. V. Fargo

McDonnell Douglas Corporation
P. O. Box 516
St. Louis, Missouri 63166
ATTN: John Cummings

McDonnell Douglas Astronautics Company
5301 Bolsa Avenue
Huntington Beach, California 92647
ATTN: Dr. Donald L. Mykannen

Mission Research Corporation
P. O. Drawer 719
Santa Barbara, California 93102
ATTN: Dr. Conrad L. Longmire

Mission Research Corporation
P. O. Box 1886
Albuquerque, New Mexico 87103
ATTN: David E. Merewether

The Mitre Corporation
P. O. Box 208
Bedford, Massachusetts 01730
ATTN: Library

Copies

Motorola, Inc.
Government Electronics Division
8201 E. McDowell Road
Scottsdale, Arizona 85252
ATTN: Technical Inf. Center, A. J. Kordalewski

Northop Corporation
Northop Research & Technology Center
3401 West Broadway
Hawthorne, California 90250
ATTN: Mr. James P. Raymond
ATTN: Library

Perkin-Elmer Corporation
Maine Avenue
Norwalk, Connecticut 06852
ATTN: Thomas D. Jones, Jr.

Philco-Ford Corporation
Aerospace & Communications Operations
Aeronutronic Division
Ford and Jamboree Roads
Newport Beach, California 92663
ATTN: Dr. L. H. Linder

Physics International Company
2700 Mercer Street
San Leandro, California 94577
ATTN: Document Control for B. Bernstein

Power Physics Corporation
Industrial Way West
Box 626
Eatontown, New Jersey 07724
ATTN: Mitchell Baker

Puget Sound Naval Shipyard
Bremerton, Washington 98314
ATTN: R. V. Carstensen, Code 270.3
ATTN: H. O. Debolt, Code 260
ATTN: G. Campbell, Code 240

Pulsar Associates, Inc.
7911 Hershal Avenue
Suite 400
La Jolla, California 92037
ATTN: Carleton Jones

R&D Associates
Box 3580
Santa Monica, California 90403
ATTN: Dr. William R. Graham

Copies

Raytheon Company
Hartwell Road
Bedford, Massachusetts 01730
ATTN: Gajanan Joshi, Radar Systems Lab.

Raytheon Company
528 Boston Post Lane
Sudbury, Massachusetts 01776
ATTN: Harold L. Flescher

RCA Corporation
Government & Commercial Systems
Missile & Surface Radar Division
Moorestown, New Jersey 08057
ATTN: Mr. A. L. Warren

Procedyne Corporation
221 Somerset Street
New Brunswick, New Jersey 08903
ATTN: Peter Horowitz

Raymond Engineering, Inc.
217 Smith Street
Middleton, Connecticut 06457
ATTN: Mrs. Loretta Aber

RCA Corporation
P. O. Box 591
Somerville, New Jersey 08876
ATTN: R. W. Rostrom

RCA Corporation
Government & Commercial Systems
Astro Electronics Division
P. O. Box 800
Princeton, New Jersey 08540
ATTN: Dr. George Brucker

Research Triangle Institute
P. O. Box 12194
Research Triangle Park
Washington, D. C. 27709
ATTN: Eng. Div.,
Dr. Mayrant Simons, Jr.

Rockwell International Corporation
3370 Mirolama Avenue
Anaheim, California 92803
ATTN: J. Bell, HA 10

Copies

Rockwell International Corporation
4701 West Imperial Highway
Los Angeles, California 90009
ATTN: Donald J. Stevens, BB33

Sanders Associates, Inc.
95 Canal Street
Nashua, New Hampshire 03060
ATTN: M. L. Aitel

Science Applications, Inc.
Suite 908
1701 North Fort Myer Drive
Arlington, Virginia 22209
ATTN: William L. Chadsey

Simulation Physics, Inc.
41 B Street
Burlington, Massachusetts 01803
ATTN: Mr. Roger G. Little

The Singer Company
1151 McBridge Avenue
Little Falls, New Jersey 07424
ATTN: Irwin Goldman, Eng. Management 5710
Plant 10

Sperry Microwave Electronics Division
Sperry Rand Corporation
P. O. Box 4648
Clearwater, Florida 33517
ATTN: Mr. R. E. Lazarchik

Sperry Rand Corporation
Univac Division
Defense Systems Division
P. O. Box 3525
St. Paul, Minnesota 55101
ATTN: Mr. J. A. Inda, M.S. 5451

Stanford Research Institute
333 Ravenswood Avenue
Menlo Park, California 94025
ATTN: Mr. Arthur Lee Whitson

Systems, Science & Software
Box 1620
La Jolla, California 92307
ATTN: Alan F. Klein

Copies

Systron-Donner Corporation
200 San Miguel Road
Concord, California 92037
ATTN: Harold D. Morris

Texas Instruments, Inc.
Box 5474
Dallas, Texas 75222
ATTN: R&D Proj. Man., Dr. Donald J. Manus,
M.S. 72

Texas Tech University
Box 5404 North College Station
Lubbock, Texas 79409
ATTN: Travis L. Simpson

TRW Systems Group
1 Space Park
Redondo Beach, California 90278
ATTN: Technical Information Center, S-1930

United Aircraft Corporation
Norden Division
Helen Street
Norwalk, Connecticut 06851
ATTN: Conrad Corda

United Aircraft Corporation
Hamilton Standard Division
Bradley International Airport
Windsor Locks, Connecticut 06069
ATTN: Raymond G. Gignere

University of Denver
Colorado Seminary
Denver Research Institute
University Park
Denver, Colorado 80210
ATTN: Fred P. Venditti

Westinghouse Electric Corporation
Astronuclear Laboratory
P. O. Box 10864
Pittsburgh, Pennsylvania 15236
ATTN: P. W. Dickson

Westinghouse Electric Corporation
Research & Development Center
1310 Beulah Road
Pittsburgh, Pennsylvania 15235
ATTN: William E. Newell

Copies

Don White Consultants, Inc.
14800 Springfield Road
Germantown, Maryland 20767

Commander
Foreign Technology Division, AFSC
Wright-Patterson Air Force Base
Ohio 45433
ATTN: XRE, Mr. Ballard

Telecommunications Industries, Inc.
1375 Akron Street
Copiague, N.Y. 11726

ATTN: John W. Kent

NDW-NSWC(W)-5605/1 (Rev. 1-75)

TO AID IN UPDATING THE DISTRIBUTION LIST FOR NAVAL SURFACE WEAPONS CENTER, WHITE OAK LABORATORY TECHNICAL REPORTS PLEASE COMPLETE THE FORM BELOW:

TO ALL HOLDERS OF NSWC/WOL/TR 75-193

DO NOT RETURN THIS FORM IF ALL INFORMATION IS CURRENT

A. FACILITY NAME AND ADDRESS *(OLD) (Show Zip Code)*

NEW ADDRESS *(Show Zip Code)*

B. ATTENTION LINE ADDRESSES:

C.

☐ REMOVE THIS FACILITY FROM THE DISTRIBUTION LIST FOR TECHNICAL REPORTS ON THIS SUBJECT.

D.
NUMBER OF COPIES DESIRED

GPO 885-870